USGS
science for a changing world

Prepared in cooperation with the U.S. Nuclear Regulatory Commission

Flood-Frequency Estimation for Very Low Annual Exceedance Probabilities Using Historical, Paleoflood, and Regional Information with Consideration of Nonstationarity

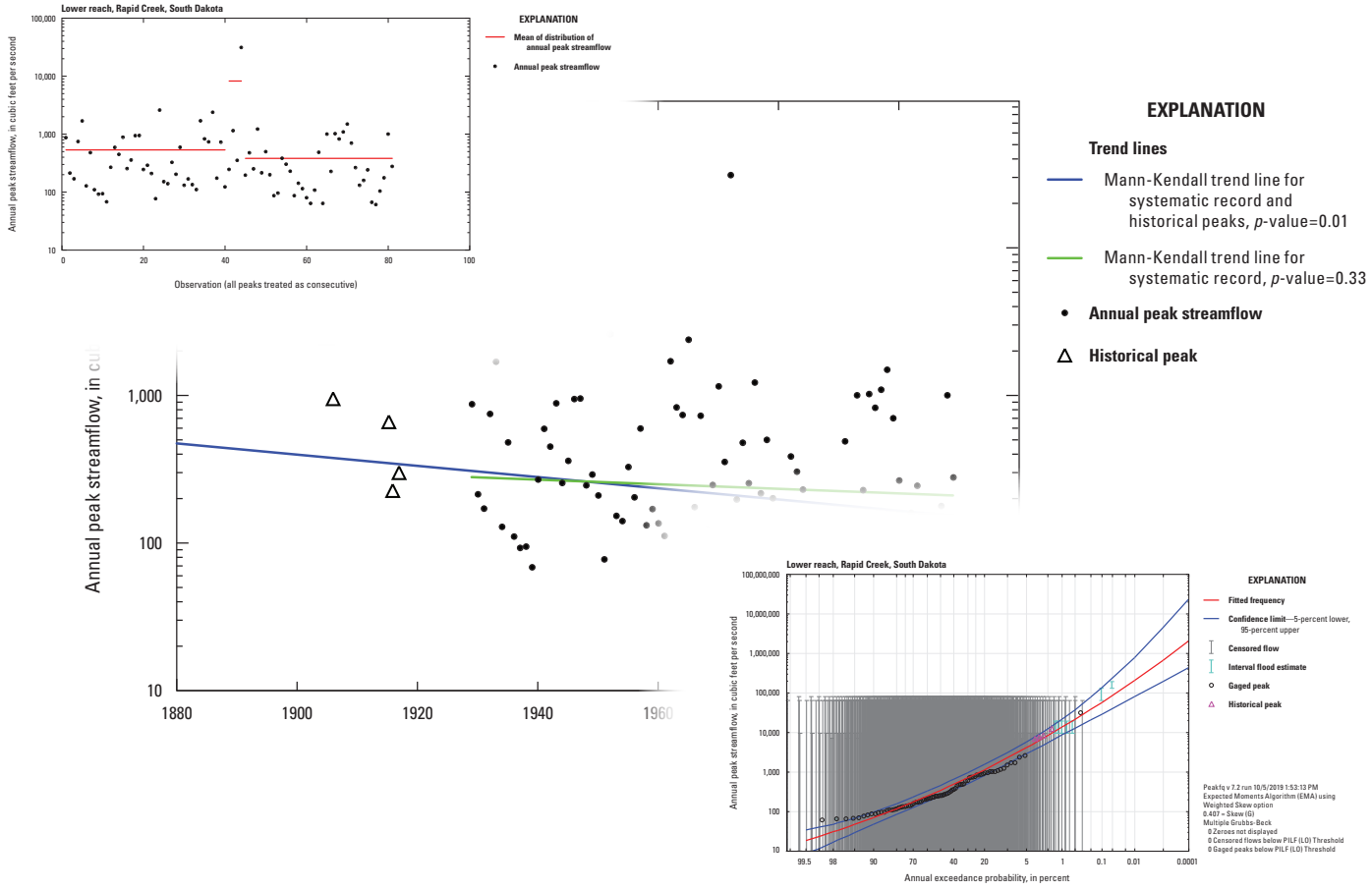

Scientific Investigations Report 2020–5065

U.S. Department of the Interior
U.S. Geological Survey

Cover. Upper left to bottom right, figures 21, 22, and 24.

Flood-Frequency Estimation for Very Low Annual Exceedance Probabilities Using Historical, Paleoflood, and Regional Information with Consideration of Nonstationarity

By Karen R. Ryberg, Kelsey A. Kolars, Julie E. Kiang, and Meredith L. Carr

Prepared in cooperation with the U.S. Nuclear Regulatory Commission

Scientific Investigations Report 2020–5065

U.S. Department of the Interior
U.S. Geological Survey

U.S. Department of the Interior
DAVID BERNHARDT, Secretary

U.S. Geological Survey
James F. Reilly II, Director

U.S. Geological Survey, Reston, Virginia: 2020

For more information on the USGS—the Federal source for science about the Earth, its natural and living resources, natural hazards, and the environment—visit https://www.usgs.gov or call 1–888–ASK–USGS.

For an overview of USGS information products, including maps, imagery, and publications, visit https://store.usgs.gov/.

Suggested citation:
Ryberg, K.R., Kolars, K.A., Kiang, J.E., and Carr, M.L., 2020, Flood-frequency estimation for very low annual exceedance probabilities using historical, paleoflood, and regional information with consideration of nonstationarity: U.S. Geological Survey Scientific Investigations Report 2020–5065, 89 p., https://doi.org/10.3133/sir20205065.

Associated data for this publication:
U.S. Geological Survey, 2017, USGS water data for the Nation: U.S. Geological Survey National Water Information System database, https://doi.org/10.5066/F7P55KJN.

ISSN 2328-0328 (online)

Author Roles and Acknowledgments

Robert R. Mason, Jr. and Timothy A. Cohn of the U.S. Geological Survey (USGS) and Joseph Kanney of the U.S. Nuclear Regulatory Commission (NRC) developed the project scope. The NRC also developed the Statement of Work and actively participated in the design of the study. Karen R. Ryberg (USGS) provided most of the draft text, including contributions to the literature review section, and completed the initial data analysis and flood-frequency analyses. Kelsey A. Kolars (USGS) completed most of the literature review on flood-frequency estimation in consideration of stationary and nonstationary systems. Julie E. Kiang (USGS) contributed to the introduction, report structure, and revisions. Harry Jenter assisted with project scoping and oversight. Ryberg, Kolars, Kiang, and Meredith L. Carr (NRC) compiled the report; all authors contributed to addressing review comments. Steven K. Sando (USGS) and William H. Asquith (USGS) provided technical reviews of all material, and Tara Williams-Sether (USGS) provided an additional technical review of methods for including regional information. The NRC also contributed technical comments. This work was funded by the U.S. Nuclear Regulatory Commission (NRC–HQ–60–15–I–0006) with Carr acting as the Commission project manager.

The authors acknowledge the USGS Water Mission Area Nonstationarity Workgroup (of which the USGS authors are members) for their in compiling a database of citations related to floods under nonstationary conditions before the start of this project. Many of those citations were used for this report.

Contents

Author Roles and Acknowledgments iii
Abstract 1
Introduction 2
Purpose and Scope 3
Limitations of Analysis 3
Literature Review of Stationary and Nonstationary Flood-Frequency Analysis 3
Flood-Frequency Analysis Background 3
Nonstationarity Detection 4
Analysis Tools 5
U.S. Army Corps of Engineers Nonstationarity Detection Tool 5
The TREND Tool 5
R Packages for Nonstationary Detection 6
Factors that Contribute to Nonstationarity 7
Regulation 7
Land-Use Change 8
Climate Variability and Change 8
Long-Term Climate and Land Changes 9
Including External Information 9
Historical and Paleoflood Data 9
Historical Data 10
Paleoflood Data 10
Use of Thresholds in Historical and Paleoflood Data 11
Regional Data 12
Regional and Weighted Skew 12
Regression Methods 13
Regional Transfer 13
Index Flood 13
Region-of-Influence Approach 14
Methods and Tools for Examining Peak-Flow Series Characteristics and Associated Statistical Assumptions 14
Nonstationary Detection Methods 15
Regional Analysis Tools 18
Sites Selected for Case Studies 18
Red River of the North at Winnipeg, Manitoba, Canada 20
Lower reach, Rapid Creek, South Dakota 20
Spring Creek, South Dakota 21
Cherry Creek near Melvin, Colorado 21
Escalante River near Escalante, Utah 21
Data and Methods Used for Case Studies 21
Data 22
Initial Data Analysis 22
Autocorrelation 22
Change-Point Analysis 22
Monotonic Trend Analysis 23

Flood-Frequency Analysis 23
Statistical Distribution Used 24
Method for Estimating Distribution Parameters 24
Potentially Influential Low Floods 24
Case Study Results and Discussion 24
Red River of the North at Winnipeg, Manitoba, Canada 25
Autocorrelation 26
Change-Point Analysis 26
Trend Analysis 27
Flood-Frequency Analysis 27
Comparisons to Other Flood-Frequency Methods 32
Summary 36
Lower reach, Rapid Creek, South Dakota 40
Initial Data Analysis 40
Flood-Frequency Analysis 40
Comparisons to Other Flood-Frequency Methods 42
Summary 42
Spring Creek, South Dakota 46
Initial Data Analysis 46
Flood-Frequency Analysis 46
Comparisons to Other Flood-Frequency Methods 50
Summary 52
Cherry Creek near Melvin, Colorado 54
Initial Data Analysis 54
Flood-Frequency Analysis 54
Comparisons to Other Flood-Frequency Methods 56
Summary 58
Escalante River near Escalante, Utah 63
Initial Data Analysis 63
Flood-Frequency Analysis 63
Comparisons to Other Flood-Frequency Methods 68
Summary 72
Summary 74
References Cited 76
Appendix 1. Data, Settings, and Output for Each Site and Scenario 89

Figures

1. Map showing sites selected for detailed analysis of the peak-flow record and for flood-frequency analysis 19
2. Graph showing systematic, historical, and paleoflood peaks and historical intervals for streamgage station 05OJ015 25
3. Graph showing the autocorrelation for peaks in the systematic period of record for streamgage station 05OJ015 26

4. Graph showing change point in mean and variance for peaks in the systematic period of record for streamgage station 05OJ015....27
5. Graph showing Mann-Kendall test for trend in the annual peak-streamflow record for streamgage station 05OJ015....28
6. Graph showing peaks and thresholds used as input for flood-frequency analysis scenarios 1 and 2 for streamgage station 05OJ015....30
7. Graph showing annual exceedance probability plot and fitted distribution for streamgage station 05OJ015....30
8. Graph showing systematic and historical peaks, paleo-derived peaks, and historical and paleo-derived thresholds used for flood-frequency analysis scenarios 9 and 10 for streamgage station 05OJ015....31
9. Graph showing annual exceedance probabilities for streamgage station 05OJ015 with the input data depicted in figure 8 and at-site skew (scenario 9)....31
10. Graph showing annual exceedance probabilities for streamgage station 05OJ015 with the input data depicted in figure 8 and weighted skew (scenario 10)....32
11. Graph showing point and interval estimates for streamgage station 05OJ015 floods with annual exceedance probability of 0.10, calculated using U.S. Geological Survey PeakFQ software version 7.2 under 10 different scenarios....33
12. Graph showing point and interval estimates for streamgage station 05OJ015 floods with annual exceedance probability of 0.01, calculated using U.S. Geological Survey PeakFQ software version 7.2 under 10 different scenarios and 13 additional point estimates from other flood-frequency studies....33
13. Graph showing point and interval estimates for streamgage station 05OJ015 floods with annual exceedance probability of 1×10^{-3}, calculated using U.S. Geological Survey PeakFQ software version 7.2 under 10 different scenarios....34
14. Graph showing point and interval estimates for streamgage station 05OJ015 floods with annual exceedance probability of 1×10^{-4}....34
15. Graph showing point and interval estimates for streamgage station 05OJ015 floods with annual exceedance probability of 1×10^{-5}....35
16. Graph showing point and interval estimates for streamgage station 05OJ015 floods with annual exceedance probability of 1×10^{-6}....35
17. Graphs showing point and interval estimates for a range of annual exceedance probabilities for streamgage station 05OJ015 floods, calculated using U.S. Geological Survey PeakFQ software version 7.2, with at-site and weighted skew and the systematic record only....38
18. Graphs showing point and interval estimates for a range of annual exceedance probabilities for streamgage station 05OJ015 floods, calculated using U.S. Geological Survey PeakFQ software version 7.2 with at-site and weighted skew and the systematic record plus historical peaks and thresholds and paleo-derived peaks and paleo-derived thresholds....39
19. Graph showing systematic peaks and historical peaks for lower reach, Rapid Creek, South Dakota....40
20. Graph showing the autocorrelation for peaks in systematic period of record for lower reach, Rapid Creek, South Dakota....41
21. Graph showing change points in mean and variance for peaks in systematic period of record for lower reach, Rapid Creek, South Dakota....41
22. Graph showing Mann-Kendall test for trend in the peak-streamflow record for lower reach, Rapid Creek, South Dakota....42

23. Graph showing systematic and historical peaks, paleo-derived interval peaks, and historical and paleo-derived thresholds used as input for flood-frequency analysis with weighted skew, lower reach, Rapid Creek, South Dakota 43
24. Graph showing annual exceedance probability plot and fitted distribution for lower reach of Rapid Creek, South Dakota, using the input data depicted in figure 23 and weighted skew 43
25. Graph showing point estimates and confidence bounds for scenarios using U.S. Geological Survey PeakFQ software version 7.2 for lower reach of Rapid Creek, South Dakota, for floods with annual exceedance probability of 0.01 44
26. Graphs showing point and interval estimates for a range of annual exceedance probabilities for lower reach of Rapid Creek, South Dakota, floods, calculated using U.S. Geological Survey PeakFQ software version 7.2 with weighted skew and systematic data and with systematic plus historical data 45
27. Graph showing point and interval estimates for a range of annual exceedance probabilities for lower reach of Rapid Creek, South Dakota, floods, calculated using U.S. Geological Survey PeakFQ software version 7.2, with weighted skew and systematic, historical, and paleoflood data 46
28. Graph showing the autocorrelation for peaks in systematic period of record for Spring Creek, South Dakota 47
29. Graph showing change points in mean and variance for peaks in systematic period of record for Spring Creek, South Dakota 47
30. Graph showing Mann Kendall test for trend in the peak-streamflow record for Spring Creek, South Dakota 48
31. Graph showing systematic and paleo-derived interval peaks and thresholds used as input for flood-frequency analysis with weighted skew, Spring Creek, South Dakota 49
32. Graph showing annual exceedance probability plot and fitted distribution for Spring Creek, South Dakota 49
33. Graph showing interval peaks predicted from lower reach Rapid Creek, thresholds, and systematic data 50
34. Graph showing annual exceedance probability plot and fitted distribution for Spring Creek, South Dakota 51
35. Graph showing point estimates and confidence bounds for PeakFQ scenarios for Spring Creek, South Dakota, for floods with annual exceedance probability of 0.01 51
36. Graphs showing point and interval estimates for a range of annual exceedance probabilities for Spring Creek, South Dakota, floods, calculated using U.S. Geological Survey PeakFQ software version 7.2, with weighted skew and systematic data and with systematic plus paleoflood data 53
37. Graph showing point and interval estimates for a range of annual exceedance probabilities for Spring Creek, South Dakota, floods, calculated using U.S. Geological Survey PeakFQ software version 7.2, with weighted skew and systematic, historical, and predicted paleoflood data 54
38. Graph showing the autocorrelation for peaks in systematic period of record for streamgage station 06712500 55
39. Graph showing change points in mean and variance for peaks in systematic period of record for streamgage station 06712500 55
40. Graph showing Mann-Kendall test for trend in the peak-streamflow record for streamgage station 06712500 56

41. Graph showing annual exceedance probability plot and fitted distribution for streamgage station 06712500 using systematic data only and weighted skew.....57
42. Graph showing annual exceedance probability plot and fitted distribution for streamgage station 06712500 using systematic and paleoflood data with weighted skew.....57
43. Graph showing point estimates for streamgage station 06712500 flood with annual exceedance probability of 0.10.....58
44. Graph showing point estimates for streamgage station 06712500 flood with annual exceedance probability of 0.01.....59
45. Graphs showing point estimates for streamgage station 06712500 flood with annual exceedance probability of 1×10^{-3}.....59
46. Graph showing point estimates for streamgage station 06712500 flood with annual exceedance probability of 1×10^{-4}.....60
47. Graph showing point estimates for streamgage station 06712500 flood with annual exceedance probability of 1×10^{-5}.....60
48. Graph showing point estimates for streamflow-gaging station 06712500 flood with annual exceedance probability of 1×10^{-6}.....61
49. Graphs showing point and interval estimates for a range of annual exceedance probabilities for streamgage station, calculated using U.S. Geological Survey PeakFQ software version 7.2, with weighted skew and no paleoflood data and with weighted skew and systematic and paleoflood data.....62
50. Graph showing the autocorrelation for peaks in systematic period of record for streamgage station 09337500, 1943–55.....64
51. Graph showing the autocorrelation for peaks in systematic period of record for streamgage station 09337500, 1972–2015.....64
52. Graph showing change points in mean and variance for peaks in systematic period of record for streamgage station 09337500, 1943–55.....65
53. Graph showing change points in mean and variance for peaks in systematic period of record for streamgage station 09337500, 1972–2015.....65
54. Graph showing Mann Kendall test for trend in the peak-streamflow record for streamgage station 09337500.....66
55. Graph showing peaks and thresholds for flood-frequency analysis, streamgage station 09337500.....66
56. Graph showing annual exceedance probabilities for streamgage station 09337500 using the systematic peaks only.....67
57. Graph showing annual exceedance probabilities for streamgage station 09337500 using the input data depicted in figure 55.....67
58. Graph showing annual exceedance probabilities for streamgage station 09337500 using systematic, historical, and paleoflood peaks and thresholds.....68
59. Graph showing point estimates and confidence bounds for streamgage station 09337500 floods with annual exceedance probability of 0.10, calculated under three different scenarios using U.S. Geological Survey PeakFQ software version 7.2.....69
60. Graph showing point estimates and confidence bounds for streamgage station 09337500 floods with annual exceedance probability of 0.01, calculated under three different scenarios using U.S. Geological Survey PeakFQ software version 7.2 compared to five point estimates from other studies.....69
61. Graph showing point estimates and confidence bounds for streamgage station 09337500 floods with annual exceedance probability of 1×10^{-3}.....70

62. Graph showing point estimates and confidence bounds for streamgage station 09337500 floods with annual exceedance probability of 1×10^{-4} 70
63. Graph showing point estimates and confidence bounds for streamgage station 09337500 floods with annual exceedance probability of 1×10^{-5} 71
64. Graph showing point estimates and confidence bounds for streamgage station 09337500 floods with annual exceedance probability of 1×10^{-6} 71
65. Graphs showing point and interval estimates for a range of annual exceedance probabilities for streamgage station 09337500 floods, calculated using U.S. Geological Survey PeakFQ version 7.2, with weighted skew and systematic data and with weighted skew systematic plus historical data 73
66. Graph showing point and interval estimates for a range of annual exceedance probabilities for streamgage station 09337500 floods, calculated using U.S. Geological Survey PeakFQ version 7.2, with weighted skew and systematic, historical, and paleoflood data 74

Tables

1. Parametric and nonparametric approaches for detection of abrupt and gradual nonstationarity 16
2. Sites selected for flood-frequency analysis 20
3. Trend results for streamgage station 05OJ015, 1907–2016, using modifications of the Mann-Kendall test for trend 29
4. Streamflow estimates for selected annual exceedance probabilities and associated confidence intervals (lower and upper) and variance estimates for flood-frequency analysis under 10 different scenarios using U.S. Geological Survey PeakFQ software (Veilleux and others, 2014) version 7.2 for streamgage station 05OJ015 as well as results from flood-frequency studies by Burn and Goel (2001) and Harden (1999) 29
5. Streamflow estimates for selected annual exceedance probabilities and associated confidence intervals (lower and upper) and variance estimates for flood-frequency analysis under three different scenarios using U.S. Geological Survey PeakFQ software version 7.2 for the lower reach of Rapid Creek, South Dakota, with comparisons to Harden and others (2011) 40
6. Streamflow estimates for selected annual exceedance probabilities and associated confidence intervals (lower and upper) and variance estimates for flood-frequency analysis under three different scenarios using U.S. Geological Survey PeakFQ software version 7.2 for Spring Creek, South Dakota, with comparisons to Harden and others (2011) 46
7. Streamflow estimates for selected annual exceedance probabilities and associated confidence intervals (lower and upper) and variance estimates for flood-frequency analysis under two different scenarios using U.S. Geological Survey PeakFQ software version 7.2 for streamgage station 06712500 with comparisons to other distributions and fitting methods 56
8. Streamflow estimates for selected annual exceedance probabilities and associated confidence intervals (lower and upper) and variance estimates for flood-frequency analysis under three different scenarios using U.S. Geological Survey PeakFQ software version 7.2 for streamgage station 09337500 with comparisons to Webb and others (1988), Webb and Rathburn (1988), and Kenney and others (2008) 63

Conversion Factors

U.S. customary units to International System of Units

Multiply	By	To obtain
	Length	
foot (ft)	0.3048	meter (m)
mile (mi)	1.609	kilometer (km)
	Area	
square mile (mi^2)	2.590	square kilometer (km^2)
	Volume	
acre-foot (acre-ft)	1,233	cubic meter (m^3)
	Flow rate	
cubic foot per second (ft^3/s)	0.02832	cubic meter per second (m^3/s)

International System of Units to U.S. customary units

Multiply	By	To obtain
	Length	
meter (m)	3.281	foot (ft)
kilometer (km)	0.6214	mile (mi)
	Area	
square kilometer (km^2)	0.3861	square mile (mi^2)
	Volume	
cubic meter (m^3)	35.31	cubic foot (ft^3)
	Flow rate	
cubic meter per second (m^3/s)	35.31	cubic foot per second (ft^3/s)

Abbreviations

acf	autocorrelation function
AEP	annual exceedance probability
EMA	Expected Moments Algorithm
H	Hurst exponent coefficient
LTP	long-term persistence
Ma	megaanum or million years
MBIC	modified Bayes information criterion
MKT	Mann-Kendall test for monotonic trend
MLE	maximum likelihood estimation
MOVE	maintenance of variance extension
MOVE.3	Maintenance of Variance Extension Type III
NRC	U.S. Nuclear Regulatory Commission
PE3	Pearson type III distribution (three-parameter probability distribution)
PFF	peak-flow file
PILF	potentially influential low flood
PMF	probable maximum flood
PREC	probabilistic regional envelope curve
Q	streamflow
ROI	region of influence
STP	short-term persistence
USACE	U.S. Army Corps of Engineers
USGS	U.S. Geological Survey

Flood-Frequency Estimation for Very Low Annual Exceedance Probabilities Using Historical, Paleoflood, and Regional Information with Consideration of Nonstationarity

By Karen R. Ryberg,[1] Kelsey A. Kolars,[1] Julie E. Kiang,[1] and Meredith L. Carr[2]

Abstract

Streamflow estimates for floods with an annual exceedance probability of 0.001 or lower are needed to accurately portray risks to critical infrastructure, such as nuclear power-plants and large dams. However, extrapolating flood-frequency curves developed from at-site systematic streamflow records to very low annual exceedance probabilities (less than 0.001) results in large uncertainties in the streamflow estimates. Traditionally, methods for statistically estimating flood frequency have relied on the systematic streamflow record, which provides a time series of annual maximum flood peaks, often including some historical peaks. However, most peak-flow records are less than 100 years, and uncertainties are large when trying to extrapolate magnitudes of very low annual exceedance probability events.

Other data may be available that extend the record beyond the systematic dataset. Historical data are defined as data from outside the period of systematic records but within the period of human records. Examples of historical information include flood estimates from other agencies and newspaper accounts that can be translated to flood magnitude point estimates, interval estimates, or perception thresholds (such as a statement that an 1880 flood was the largest since 1869). Paleoflood data, which may also extend the dataset, include a broad range of information about flood occurrence or magnitude from sources like sediment deposits or tree rings.

Several assumptions are made in flood-frequency analysis, and an understanding of whether the data conform to these assumptions is desired. A particularly difficult assumption to evaluate for flood-frequency analysis is the underlying assumption that the flood series is stationary—the assumption that a time series of peak flow varies around a constant mean within a particular range of values (constant variance). As the hydrologic community's understanding of natural systems and anthropogenic effects on streamflows has evolved, the community has come to understand that many surface-water systems exhibit one or more forms of nonstationarity, and thus the stationarity assumption is often violated to some degree. However, there is currently (2020) no consensus among hydrologists regarding the most appropriate flood-frequency-analysis methods for nonstationary systems, and this topic remains an active area of research.

A literature review was completed to summarize the state of the science of flood frequency. The literature review highlights tools available to detect nonstationarities and identifies approaches that include external information to inform flood-frequency analysis. To demonstrate methods for initial data analysis and for incorporating historical and paleoflood information in flood-frequency analysis, five sites were selected: the Red River of the North at James Avenue Pumping Station, Winnipeg, Manitoba, Canada; lower reach, Rapid Creek, South Dakota; Spring Creek, South Dakota; Cherry Creek near Melvin, Colorado; and Escalante River near Escalante, Utah. The sites were chosen for the availability of published historical and paleoflood data and for their geographic diversity and unique characteristics, which highlighted issues such as autocorrelation, change points, trends, outlier peaks, or short periods of record.

An initial data analysis that involved examining records for autocorrelation, change points, and trends was completed for all sites. The flood-frequency analysis completed for this study used version 7.2 of the U.S. Geological Survey PeakFQ program. Multiple analyses were done on each site documenting the change in the flood-frequency curve when additional historical or paleoflood data were added. When other flood-frequency studies were available, their results were compared to the results here. The comparisons in some cases simply show the effect of additional years of data, whereas other comparisons show results from probability distributions or fitting methods other than those used in PeakFQ.

For the Red River of the North, flood-frequency analysis shows that paleoflood data appear necessary to reasonably estimate very low annual exceedance probabilities. For the analysis of the lower reach of Rapid Creek and Spring Creek, paleoflood information helped put a high outlier from

[1]U.S. Geological Survey.

[2]U.S. Nuclear Regulatory Commission.

the systematic period in context; however, very low annual exceedance probabilities at these sites still had extraordinarily large confidence bounds. These sites also showed that paleoflood information might be transferred from one site to another, with the caveat that this is a case where we had existing paleoflood data to test the transfer of paleoflood information—this is not the case at many sites, and transferring paleoflood information requires assumptions about the comparability of floods at the sites. The Cherry Creek analysis affirmed the result of an earlier study that showed that the generalized Pareto distribution was not a good distribution for estimating very low annual exceedance probabilities. The Escalante River analysis showed that adding paleoflood information might increase uncertainty for very low annual exceedance probabilities, compared to analysis with the systematic period of record information only, when the paleoflood peaks are of much larger magnitudes than the systematic record.

Introduction

The U.S. Geological Survey (USGS), with cooperation and funding from the U.S. Nuclear Regulatory Commission (NRC), has investigated the application of statistical analysis methods and tools for probabilistic flood hazard assessment, focusing on low probability floods. Estimating the frequency and magnitude of low probability floods is needed to quantify flood risks for critical infrastructure, such as nuclear powerplants and large dams. These floods are defined as events having "very low" annual exceedance probabilities (AEPs), less than 0.001 (as in Asquith and others, 2017); scientific notation is used to represent these very low AEPs, such as 1×10^{-3} for 0.001. Although floods with an AEP of 1×10^{-4} might be considered exceptionally rare from a hydrological perspective, they are not exceptionally rare from a nuclear powerplant safety perspective. In fact, nuclear powerplant design-basis events hazards (for example, large break loss of coolant accidents) often have a frequency in the range of 1×10^{-5} per year and lower (Tregoning and others, 2008).

Standard flood-frequency analysis approaches rely on a time series of annual maximum streamflow (hereinafter referred to as "peak flow"), derived from the at-site systematic record. The time series is fit to a statistical distribution to estimate flood quantiles, and the analysis requires several assumptions about the data. A concern for flood-frequency analysis is the underlying assumption that the peak-flow series is stationary. A stationary peak-flow series has been recorded within a consistent (albeit potentially highly variable) hydroclimatic system with long-term consistency in the fundamental flood-generating processes. Statistically, a stationary peak-flow series varies around a constant mean within a particular range of values according to a defined variance (spread of the distribution). As the hydrologic community's understanding of natural systems and anthropogenic effects on streamflows has evolved, the community has come to understand that many surface-water systems exhibit one or more forms of nonstationarity, and thus the stationarity assumption is often violated to some degree. Nonstationarity is a statistical property of a peak-flow series such that the long-term distributional properties (the mean, variance, or skew) change one or more times either gradually or abruptly through time. Individual nonstationarities may be attributed to one source (for example, either regulation, land-use change, or climate) but often are the result of a mixture of those sources (Vogel and others, 2011), making detection and attribution of nonstationarities challenging. However, detection and attribution can inform flood-frequency analysis. Currently, there is no consensus among hydrologists regarding the most appropriate frequency-analysis methods to use for nonstationary systems, and this topic remains an active area of research.

An additional concern in fitting the flood-frequency curve is the availability of data. The systematic streamflow records that form the basis of the analysis are typically short (the oldest USGS streamflow records start in the late 1800s, and records exceeding 100 years in length are scarce), and large uncertainties remain when trying to extrapolate to very low AEPs.

Other data may be available that extend the period of record beyond the systematic dataset. Historical data are defined as data from outside the period of systematic records, yet within the period of human records, such as newspaper accounts that can be used to calculate to flood magnitude point estimates, interval estimates, or perception thresholds (such as a statement that an 1880 flood was the largest since 1869).

Paleoflood data, which may also extend the dataset, include a broad range of information about flood occurrence or magnitude from sources like sediment deposits or tree rings. Paleoflood data are generally not available in the USGS peak-flow file (PFF) or the streamflow databases of other agencies but are published in paleoflood studies.

The purpose of this work was to complete some of the tasks in a work plan the NRC and USGS developed to investigate the state of practice for using and characterizing the uncertainties of statistical analytical tools for assessing very low AEPs (less than 0.001, that is floods that have an average recurrence interval of less than 1,000 years, see Holmes and Dinicola [2010] for more information). Asquith and others (2017) completed the first task of the plan, which was to better understand the uncertainty of flood-frequency estimates when they are determined from peaks collected as part of a regular program of streamflow collection to produce systematic records of peak flow. The later tasks, which are the focus of this work, were to explore methods used to identify and characterize nonstationarities and to investigate the possible usage of additional sources of information (especially historical and paleoflood data and regionalization) that may extend the record and affect the uncertainty of flood-frequency estimates for very low AEPs.

The first goal of this work is to explore how to identify if a hydrologic system may be changing over time (nonstationarity). Tools available to detect nonstationarities are discussed,

possible attributing factors are identified, and efforts to include external information for detection of nonstationarities are reviewed. Additionally, the work contributes to the understanding of underlying causes of nonstationarities and potential ways to address nonstationarities, while showing that the problem is not easy to address.

The second goal of this work is to describe and demonstrate how information about peak flows outside the systematic record can be incorporated into statistical flood-frequency analysis to improve flood-frequency estimates and accurately characterize and quantify uncertainty through the incorporation of historical, paleoflood, and regional information. Historical, paleoflood, and regional information are reviewed, and methods and tools to incorporate this information into flood-frequency analysis are described and tested.

Purpose and Scope

The purpose of this report is to describe methods for flood-frequency estimation for very low AEPs using historical, paleoflood, and regional information with consideration of nonstationarity. This report has two main sections. The first section discusses methods to detect nonstationarities and reviews some suggested methods for dealing with nonstationarities. The second section demonstrates the use of historical and paleoflood data and of regional information to extend or inform the record. Together, this report and Asquith and others (2017) are intended to serve as a resource for NRC technical staff, collaborators, and other parties interested in studying the exposure of critical infrastructure, such as nuclear powerplants and large dams. Conventions established in Asquith and others (2017) are continued in this report.

For this work, five sites were selected to demonstrate methods for initial data analysis and to incorporate historical, paleoflood, and regional information into flood-frequency analyses. The sites were chosen because published historical or paleoflood data were available for them and because of their geographic diversity and unique characteristics, some of which highlighted issues such as autocorrelation, change points, trends, outlier peaks, or short periods of record.

Limitations of Analysis

This report describes methods and illustrates their use through their application to selected sites. Some subjectivity is inherent in assessing the validity of historical and paleoflood data and in incorporating thresholds for missing periods during the systematic record and for paleo periods. Local or regional experts might make different choices when assessing these sites. In addition, flood-frequency analysis under nonstationary conditions is an active area of research, and many suggested methods are not yet able to be incorporated into currently available software or cannot incorporate historical or paleoflood data. Therefore, the flood-frequency results reported here should not be considered definitive for design purposes at any of these sites. The flood-frequency results are described as case studies to indicate that these studies are examples of using state of practice techniques to assess nonstationarity and to better characterize very low AEPs.

Literature Review of Stationary and Nonstationary Flood-Frequency Analysis

An important consideration for any flood-frequency analysis is whether a hydrologic system meets the assumption of stationarity underpinning flood-frequency analysis. Stationarity is a statistical concept meaning the underlying distribution of a process does not change when shifted in time. In the context of streamflow, stationarity means that flows vary within a particular window of variability around a long-term mean.

Milly and others (2008) concluded that the assumption of stationarity in water resources is “dead” because of anthropogenic changes to Earth’s climate and has long been compromised because of anthropogenic disturbance to the landscape. However, Villarini and others (2009, p. 1) stated that it is “easier to proclaim the demise of stationarity of flood peaks than to prove it through analyses of annual flood peak data.” The stationarity issue is not limited to anthropogenic change though. A system can exhibit long-term “excursions,” such as a multidecadal drought that may be part of the system’s natural variation about a mean, but that excursion may be difficult to distinguish from an anthropogenic change that altered the system (Cohn and Lins, 2005). Methods have been developed to treat hydrologic time series with these excursions as scaled stochastic processes (Hamed, 2008; Koutsoyiannis, 2003; Koutsoyiannis, 2006). In other cases, it has been shown through tree-ring proxy records that some hydrologic regimes have likely never been stationary and that many records of hydrologic observation are too short to be representative of the long-term properties of the systems (Razavi and others, 2015). Flood-frequency analysis of nonstationary peak flows is an area of active research without a clear path forward if one declares the stationarity assumption cannot be used. The following literature review discusses tools available to detect individual nonstationarities, identifies possible attributing factors, and reviews efforts to include external information for detection of nonstationarities. The review contributes to the understanding of underlying causes of nonstationarity and potential ways to address nonstationarities, while showing that the problem is not easy to address.

Flood-Frequency Analysis Background

Around the late 1800s, the United States began to establish an extensive streamgaging network, today (2020) known as the USGS Streamgaging Network, with the first

gaging station constructed in 1889 along the Rio Grande (U.S. Geological Survey, 2014). As the accumulation of streamflow data grew, so did the need for a nationwide standard for analyzing the data and determining flood frequencies. Fuller (1914) published the first method to estimate flood frequencies nationwide. It was an innovative approach in that it used principles of probability; however, the method assumed flood frequencies could be calculated from short peak-flow records provided one had records from several streams (Rumsey, 2015). Fuller's work was improved upon by Hazen (1930) with technical refinements and a discussion of how flood-frequency analysis could be applied to understanding the risk associated with flood protection, such as levees (Rumsey, 2015). Initially, flood-frequency analysis was completed by private entities, but the Government increasingly became involved in flood protection and floodplain management and, therefore, had a growing interest in flood frequency. The USGS published a Water Supply Paper on flood magnitude and frequency in 1936 (Jarvis, 1936). Over the next 30 years, there was a growing interest in flood insurance and flood-loss control (Rumsey, 2015). In a 1966 U.S. Government report by the U.S. Task Force on Federal Flood Control Policy, President Lyndon Johnson's letter of transmittal to the U.S. House of Representatives stated, "… a Great Society cannot rest on the achievements of the past. It must constantly strive to develop new means to meet the needs of the people… The task force report lays stress on actions which can and should be immediately undertaken—To improve basic knowledge about the flood hazard…" (U.S. Task Force on Federal Control Policy, 1966, p. III–IV). To improve flood hazard knowledge, the report recommended specific actions, including that "a uniform technique of determining flood frequency should be developed by a panel of the Water Resources Council" (U.S. Task Force on Federal Control Policy, 1966, p. 1). The Water Resources Council Hydrology Committee's work resulted in a 1967 publication of a report titled "A Uniform Technique for Determining Flood Frequencies," known as "Bulletin 15" (Water Resources Council, 1967). Since then, this Bulletin has been revised several times (Bulletin 17, U.S. Water Resources Council, 1977; Bulletin 17A, U.S. Water Resources Council, 1976; Bulletin 17B, Interagency Advisory Committee on Water Data, 1982; and Bulletin 17C, England and others, 2019), and software has been developed to assist with analysis (England and others, 2019; Flynn and others, 2006). In the most recent Bulletin (Bulletin 17C; England and others, 2019), as with the previous bulletins, the flood-frequency methods rely on the assumption that the data are stationary, independent and identically distributed, and lack any short- or long-term persistence (STP or LTP; serial or autocorrelation of values in the time series with lags greater than 1 year). For some basins, these assumptions hold true, and the methods suggested in Bulletin 17C are sufficient; for others, the methods suggested in Bulletin 17C may result in incorrect conclusions. As more information becomes available through historical and paleoflood records, there have been questions about whether the hydrologic system ever was stationary and if some apparent nonstationarities are simply the result of LTP or autocorrelation (Cohn and Lins, 2005).

Nonstationarity, as discussed in this report, refers to peak-flow distributions with either gradual or abrupt changes in mean, variance, or both. Individual nonstationarities may be attributed to one source (for example, either regulation, land-use change, or climate) but often are the result of a mixture of those sources (Vogel and others, 2011), making detection difficult.

The difficulties associated with detection and attribution of nonstationarities have prompted much research. Review papers and workshop discussions are available and serve as guides to help determine the best methods for detecting nonstationarities and to offer suggestions on potential causes for nonstationarities detected (Kundzewicz and Robson, 2000, 2004; Olsen and others, 2010; Working Group 4 Flood Frequency Estimation Methods and Environmental Change, 2013). Software tools have been created that incorporate several well-known tests used for determining abrupt or gradual changes that make detecting nonstationarities quicker, easier, and more consistent. These software tools are publicly available, such as the U.S. Army Corps of Engineers (USACE) Nonstationarity Tool (Friedman and others, 2016; U.S. Army Corps of Engineers, 2016), TREND software (Chiew and Siriwardena, 2005), and change-point analysis add-on packages for the statistical analysis software R (R Core Team, 2019), such as changepoint (Killick and Eckley, 2014), ecp (James and Matteson, 2014), and cpm (Ross, 2015). Other resources, such as websites like The Changepoint Repository (Killick and others, 2012b), have been created to aid analysts in locating references to techniques and methods related to nonstationarity. These are just some of the many resources available to those inquiring about nonstationarities in their streamflow records and how to deal with them.

Nonstationarity Detection

Consideration of nonstationarity in flood-frequency analysis starts with selecting an appropriate nonstationarity-detection method and determining the cause of detected nonstationarities. Selecting an appropriate detection method involves a thorough understanding of the data being analyzed; this understanding is gained by examining the data for autocorrelation, LTP, seasonality, independence, or non-normalities (such as skew; Kundzewicz and Robson, 2004). Method selection also requires a clear understanding of the type of nonstationarity of interest, whether looking for a nonstationarity in the mean, median, variance, or other parameter defining the peak-flow distribution, or attempting to locate a nonstationarity in the form of a gradual trend. Specifically, a detected nonstationarity in the underlying distribution could be the result of a change in the distributional parameters or of changing

from one distribution to another (Friedman and others, 2016). Even with a variety of available detection methods, it can be difficult to detect nonstationarity in peak-flow series.

Traditionally, nonstationarity-detection methods have tested time series for trends, abrupt changes in the mean or variance, or changes in frequency (He and others, 2013). Tests for abrupt changes in higher-order statistics, or higher moments, of statistical distributions (such as skew, the third moment about the mean, or kurtosis, the fourth moment about the mean) exist (He and others, 2013) but are less apt to be examined because changes in the mean are sensitive to changes in skew and skew and kurtosis are functions of both mean and variance (Abramowitz and Stegun, 1965). Many change-point methods that identify abrupt nonstationarities search for a change in the mean (Friedman and others, 2016, 2018; Ryberg and others, 2020). These generally do not work well for peak flow because of skew in the data, and change-point tests for changes in the median can be more successful (Ryberg and others, 2020).

The relation between streamflow and certain climatic factors (temperature and precipitation) can further complicate analysis because nonstationarities detected in temperature or precipitation may not be reflected in the peak-flow series (Hirsch, 2011). Extreme caution is advised when reporting on or using detected nonstationarities without a clear understanding of what caused the nonstationarity. Attributing a nonstationarity to regulation or land-use changes may be easier than climate and even easier than attributing it to a mixture of regulation and land-use change with climate.

Autocorrelated (or serially correlated) peak-flow series have persistence or memory in that each peak is not a random process but is related to one or more of the previous peaks. Change points, or step trends, are abrupt changes in distributional parameters of a time series defined by a particular statistical distribution or are abrupt changes in median or scale in a series of unknown statistical distribution. Trends are gradual increases (or decreases) in peak flow over time and are a violation of the assumption of independent identically distributed observations. Flood-frequency analysis is based on the assumption of independent, identically distributed observations. Autocorrelated series, series with change points and series with trends, violate this assumption and are therefore nonstationarities.

Analysis Tools

Publicly available tools to assist with detecting nonstationarities in time series datasets include the USACE Nonstationarity Detection Tool (U.S. Army Corps of Engineers, 2016), TREND software (Chiew and Siriwardena, 2005), and a series of R packages and functions. These tools ensure methods for detecting nonstationarities remain consistent at differing locations and with different datasets. Each tool implements a variety of nonstationarity-detection methods to aid the user, but each tool also requires that the data satisfy certain assumptions. Findings of a statistical nonstationarity should be supported by documented changes to the hydrologic system such as regulation, land-use change, or significant climatic events.

U.S. Army Corps of Engineers Nonstationarity Detection Tool

The USACE Nonstationarity Detection Tool is intended to aid users in assessing the stationarity of streamflow records in support of planning and engineering decision making (Friedman and others, 2016, 2018). The tool has been designed to produce consistent results across different locations and to be more convenient to apply than the TREND Tool or R packages (although the Nonstationarity Detection Tool itself is based on underlying R packages). The USACE Nonstationarity Detection Tool does not require the user to input time-series data (the user selects from a preset menu of individual USGS streamgages). Application of the tool is restricted to streamgages with at least 30 years of peak-flow records (the tool will automatically identify streamgages with sufficient record length). These features may make the tool convenient for novice users but also make the tool restrictive to specified USGS streamgage locations. The tool implements 12 statistical methods for nonstationarity detection that include parametric (based on estimates of distributions parameters) and nonparametric (making no assumptions about a particular distribution) approaches, gradual changes or abrupt change points, single/multiple change points, change points in the mean/variance/distribution, and a test for serial correlation that, depending on the result, further limits the options available (Friedman and others, 2016). The restrictions associated with the USACE Nonstationarity Detection Tool enforce consistent nonstationarity detection at different locations and support acceptance of the tool as meeting the guidelines for certain Federal agencies (Friedman and others, 2016).

The TREND Tool

The TREND Tool was developed in Australia for use by hydrologists, scientists, and consultants to aid in detecting trends, change points, and randomness in the data. The TREND Tool not only detects trends, as the name implies, but also detects abrupt changes in annual streamflow and precipitation and includes a test for serial correlation. The TREND Tool implements methods from Grayson and others (1996) and Kundzewicz and Robson (2000). Like the USACE Nonstationarity Detection Tool, the TREND Tool provides methods for detecting nonstationarities. The TREND Tool can be considered more flexible than the USACE Nonstationarity Detection Tool because it allows the user to input their own time-series data. Allowing user data requires more preprocessing, but also allows greater flexibility in the locations analyzed and input data type. However, allowing the user to input time-series data requires an understanding of the minimum length of record and continuity of record required for each method. Like the USACE Nonstationarity Detection Tool, the TREND Tool includes parametric and nonparametric approaches for

detecting gradual/abrupt nonstationarity in either the mean or variance. The TREND Tool tests for detecting a gradual nonstationarity are like those of the USACE Nonstationarity Detection Tool, but tests for detecting an abrupt nonstationarity differ between the two. The TREND Tool implements more parametric tests than nonparametric tests for abrupt changes compared to the USACE Nonstationarity Detection Tool. The TREND Tool can optionally resample the data (that is, randomly select a subsample of user-specified size) and report the associated test statistic and critical values after resampling. Resampling is beneficial when working with skewed data, as annual maximum streamflow data are often skewed. However, the added flexibility of resampling the data requires the user to understand how to interpret the reported results. In addition, the last update for TREND was February 2005, meaning the tool's methods are no longer maintained or updated, which may eventually make the tool obsolete.

R Packages for Nonstationary Detection

R is an open-source programming language and environment for statistical computing and graphics (R Core Team, 2019). R packages are groupings of R functions (a piece of code that are capable of accepting user-defined arguments/parameters and returning one or more values), compiled code, and sometimes data. Source code and precompiled binaries for the R environment, as well as many contributed packages, are freely available. Using R packages and functions related to detecting nonstationarities requires the user to be familiar with R and the characteristics of the data because it is up to the user to select an appropriate R package and function. The variety of R packages and functions available, as well as the choice of argument/parameters input to the functions, makes their use more flexible than the USACE Nonstationarity Detection Tool and the TREND Tool but also requires the user to have a better understanding of the different requirements and assumptions of each method (R package or R function) used. For example, the USACE Nonstationarity Detection Tool and the TREND Tool have a finite list of methods (with predefined arguments or parameters), so the user can identify properties of the data and then eliminate those methods that do not fit the properties, whereas with R packages and functions there is a larger set of methods available.

Some R packages used to detect nonstationarities include changepoint, ecp, cpm, and bcp. The changepoint package uses a series of computationally intensive algorithms (binary segmentation, segment neighborhood, and pruned exact linear time algorithms) that provide the user flexibility in selecting the type of change point (such as mean or variance), number of change points (single or multiple), and type of test statistic (assumed distribution, parametric, or distribution-free, nonparametric, method) (Killick and Eckley, 2014). The changepoint package is applicable to independent observations (an assumption sometimes violated by peak-flow series); however, the theory behind the implementation can allow for some types of serial dependence (James and Matteson, 2014; Killick and others, 2012a). The ecp package detects any type of distributional change in univariate or multivariate time series, also operating under an assumption that observations are independent over time (James and Matteson, 2014). The distributional changes detected by the ecp package include changes in distribution parameters and the actual probability distribution form (mathematical definition). The cpm package (Ross, 2015) provides "computationally efficient" methods for detecting single or multiple change points in the mean or variance of univariate, independent identically distributed sequences (conditional on the change points). The bcp package (Erdman and Emerson, 2007) accomplishes the Bayesian change-point analysis implementing methods of Barry and Hartigan (1993). Frequentist methods for change-point analysis estimate one or more specific locations for change points in a series, and this Bayesian method provides the distribution of the probability of a change point at each location in the series (Erdman and Emerson, 2007). This method assumes that the probability of a change point at a specific position, i, is independent at each i (Barry and Hartigan, 1993; Erdman and Emerson, 2007).

Many of these R packages assume the data are independent. Autocorrelated peak-flow series have persistence or memory, and this violates the assumption of independent identically distributed observations. How much correlation is too much is difficult to define; however, the degree of autocorrelation at a site is an important part of understanding the hydrology of a site and a part of the initial data analysis that should precede any flood-frequency analysis. The autocorrelation function (acf) in R (R Core Team, 2019) computes lagged correlations and generates plots that indicate, if present, autocorrelation and lags. The R package randtests (Caeiro and Mateus, 2014) provides functionality for several hypothesis-based tests for randomness in data.

A series of packages and functions are also available to test for monotonic trends in peak-flow time series. Trends can be detected using a variety of methods, including the Mann-Kendall test for monotonic trend (MKT), a nonparametric test of a monotonic trend based on Kendall's tau (Kendall, 1938), implemented in the R package EnvStats (Millard, 2013). If a series is autocorrelated or contains change points, this is a violation of the assumptions of independence and identical distribution underlying the MKT. The variance of the MKT statistic increases with increased autocorrelation (Yue and others, 2002), and the p-value (attained significance level) calculated is not correct if the underlying assumptions are violated. Many extensions of the MKT have been implemented to adjust for STP or LTP in trend analysis. The function mkTrend in the fume package (Santander Meteorology Group, 2012) implements a modified MKT with variance correction based on Hamed and Rao (1998) and adjusted for effective sample size on the basis of Yue and Wang (2004). The function zyp.trend.vector in the zyp package (Bronaugh and Werner, 2013) can accomplish modified-MKT analysis using two different prewhitening methods (methods that filter the data to make it free of autocorrelation; Zhang's method described in Wang and Swail [2001] or the method of Yue and others [2002]). The

MannKendallLTP function of the HKprocess package (Tyralis, 2016) applies the MKT under the scaling hypothesis (a way of modeling climatic variability; Hamed, 2008). The TheilSen function in the openair package (Carslaw and Ropkins, 2012) has an option to consider autocorrelated data using block bootstrap simulations (Kunsch, 1989).

The availability of tools such as R packages, the USACE Nonstationarity Detection Tool, and the TREND Tool assists the user by providing a more consistent framework for nonstationarity analysis, as well as reducing computational demands on the user. The statistical detection of a nonstationarity, however, does not imply one exists, but that there is merely evidence one may exist. Evidence of a nonstationarity can be supported by documented changes to the hydrologic system such as regulation, land-use change, or climatic events.

Factors that Contribute to Nonstationarity

Determining the cause of a detected nonstationarity is a way to validate it exists and increases the reliability of extending flood-frequency estimates to extreme flooding events. Broadly, nonstationarities have been attributed to regulation, land-use change, and climate variability and change. Ryberg and others (2020) test the ability of change-point methods to detect known changes in regulation; however, they also show that change-point methods can detect statistical anomalies in randomly generated data.

Regulation

Attributing nonstationarity to regulation tends to be easier than attributing it to land-use or climate change because the construction and completion dates and location of the regulation structure(s) can be clearly identified. Oftentimes nonstationarity, resulting from regulation, can be detected through data analysis because regulation tends to dampen the streamflow record, reducing the variability in annual streamflow events (Asquith, 2001). This dampening effect on the streamflow record affects the flood-frequency distribution. However, estimating this flood-frequency distribution can be difficult because the frequency of inflows is not directly related to the frequency of flow downstream from the reservoir because downstream flows are determined by reservoir and outlet structure size, time of flood wave arrival, release capacity and outlet structures, and operation guidelines (Ayalew and others, 2013).

The extent to which a stream is regulated can vary from small agricultural dams to major structures intended to moderate downstream flows and protect downstream communities. In a study by Ayalew and others (2017), the effect of 133 small dams (storage capacities ranging from 19 to 12,640 acre-feet) throughout a 255-square-mile drainage basin in Iowa reduced peak flow (compared to unregulated peak flow) for AEPs between 0.5 and 0.001. This result indicates that the effect of small dams on flood frequencies can be significant even at lower AEPs. Specifically, when looking at reservoirs, Ayalew and others (2013) determined that reservoirs have the potential to reduce peak flow for low AEP events up to a point, and at this point, differences in regulated and unregulated streamflow become negligible. For larger structures, such as those built to accommodate low AEP floods, the effects of regulation on streamflow statistics are much more visible. Oftentimes, large regulation structures reduce the magnitude of floods, resulting in a decreased AEP for a particular flood magnitude. A study comparing preregulated and postregulated flood frequencies at four streamgages in the Delaware and North Branch Susquehanna River Basins showed annual maximum postregulation streamflows for a flood with an AEP of 0.01 had been reduced by 20 and 60 percent at two streamgages, whereas negligible increases or decreases occurred at the other two streamgages (Roland and Stuckey, 2007). The lack of change in two of the streamgages was attributed to the attenuation of a series of smaller upstream regulation structures and the short period of record used for analysis (Roland and Stuckey, 2007). Similarly, when looking at regulation effects on the 100-year flood (AEP of 0.01), the Howard Hanson Dam constructed on the Green River decreased the magnitude of the 100-year flood from around 28,000 cubic feet per second (ft^3/s) to around 14,500 ft^3/s (Dinicola, 1996).

Not all regulation structures are designed to handle a 100-year flood, and consideration needs to be given to the design capacities and operating criteria of different structures when analyzing flood frequencies. Once a dam (or regulation structure) is breached, the flood-frequency curve is assumed to follow the curve of the natural streamflow regime (before regulation); however, given the lack of such large flooding events, it is difficult to provide evidence for this. Flows large enough to cause failure are rare, given most major structures have been designed over the last century and have yet to see a flood near the probable maximum flood (PMF, a hypothetical flood generated by the probable maximum precipitation event for drainage area upstream from a site; Prasad and others, 2011). However, a few notable dam breaks in the United States include the South Fork Dam in Pennsylvania (1889), a tailings dam in West Virginia (1972), Teton Dam in Idaho (1976), Kelly Barnes Dam in Georgia (1977), and more recently the Lake Delhi Dam breach in Iowa (2010) (FEMA, 2016). These dam breaks remind those downstream from the dams of the devastating effects a large flood event (or degrading dam structure) can have on downstream communities (FEMA, 2016). Ideally, the use of two flood-frequency curves would be used for regulated streams, one for regulation (up to designed flood protection) and one for natural flow (once flows have exceeded design criteria). To more accurately assess the probability of large flooding, Greenbaum and others (2014) used only the unregulated portion of the recorded streamflow data, along with historical and paleoflood data, thus eliminating the effects of regulation and land-use change.

In general, for commonly reported AEPs (great than or equal to 0.01), the effects of regulation may be quite visible in a flood-frequency analysis completed for a series of peaks with preregulated and postregulation peaks. However, for

lower-frequency (AEPs less than 0.01) floods in a series of peaks with lower AEP preregulated and postregulation peaks, the effects of regulation may not appear to make a difference in the AEP estimates of interest because the regulation structures may not be able to detain a very low AEP flood.

Land-Use Change

For low AEP events, the effects of land-use change on peak flows may not be as apparent as regulation effects because the effect of land cover on peak flows for large floods is reduced. Relating land-use changes to changes in flood frequency can be much more difficult than relating regulation changes to changes in flood frequency because the exact location, extent, and timing of land-use change may not be clear. Additionally, land-use change can take on multiple forms such as urbanization, agricultural drainage, municipal water-use changes, or other vegetation changes. When looking at changes that are not as direct as regulation, but instead may involve gradual change such as land-use changes or atmospheric processes, attribution to regional land-use or climate changes may more appropriately reflect an apparent nonstationarity (Viglione and others, 2016). Recently, the National Land Cover Database covering the conterminous United States has been used to analyze land-cover changes over 10 years at a 30-meter resolution (Homer and others, 2015). Over the 10-year period (2001–11) land cover changed by 2.96 percent, of which 0.3 percent was an increase in urban area (an additional 20,296 square kilometers; Homer and others, 2015). Notable changes in land-use presented through the National Land Cover Database emphasize how rapidly various vegetative covers change and provide valuable data for flood-frequency analyses that consider land-use effects on streamflow.

Besides being able to quantify the extent of a land-use change, it also is important to understand how that a specific land-use change (such as reforestation, conversion of grassland to cropland, or urbanization) interacts with the hydrologic system. A study of the Ganaraska River Basin in southern Ontario, Canada, by Buttle (2011) found that changes in basin vegetation, such as reforestation of an area, potentially altered the extent or size of the peak flows more than the timing of peak flows. A study looking at the effects of urbanization on streamflow trends in the Milwaukee, Wisconsin, metropolitan region found that a complex mix of global and regional climate and land-use changes (urbanization), resulted in changes in streamflow trends (Yang and others, 2013). A study of streamflow trends in the Tarim River Basin in Xinjian, China, found that irrigation and domestic water use led to a downward trend in streamflow even when considering the effects of climate variability (Tao and others, 2011).

It may be difficult to distinguish between streamflow changes occurring because of land-use change from those occurring because of climate variability or a combination of both. Therefore, to assess land-use change and its effect on streamflow, studies often include a control basin with little to no land-use change and compare it with a similar (nearby) basin that has experienced notable land-use changes. An analysis of 145 long-term streamgage records (greater than 50 years) across Canada showed that basins with notable land-use change tended to have more abrupt changes in peak flow than basins with minimal regulation, minimal land-use change, or both (Tan and Gan, 2014), indicating that land-use changes played a bigger role than climate change. Vogel and others (2011) looked at decadal flood magnification factors (ratio of T-year flood in a decade to the T-year flood today, where T is the threshold return period) for sites classified as pristine, that is with minimal anthropogenic effects, and found that the magnification factors were much lower in pristine sites compared to regulated and unregulated sites. Results from the Vogel and others (2011) study indicate the current 100-year flood may become more prevalent because of a variety of factors inducing nonstationarity in the streamflow regime (land-use change in combination with regulation, water use, and climate variation.

Climate Variability and Change

Despite the general associations between climate and streamflow, attributing nonstationarities to climate effects for specific locations and periods can be challenging. Natural climate variability can encompass highly variable conditions, nonstationarities, and long-term climatic persistence (Vecchia, 2008; Ryberg and others, 2014, 2016; Razavi and others, 2015; Kolars and others, 2016), whereas climate change is driven by anthropogenic forcing of the climate, such as intensification of the hydrologic cycle or increases in temperature. Detecting a climate signal in a set of streamflow data can be difficult given the detected change could be the result of a combination of natural climate variability and various anthropogenic causes. In addition, the lack of long streamflow records (greater than 100 years) reduces the ability to relate nonstationarities detected in the streamflow record to climate (Villarini and Smith, 2010; Dutta and others, 2015). Kundzewicz and Robson (2004) suggested a minimum record of 50 years be used when attempting to look at nonstationarities in streamflow attributed or partly attributed to climate. Grouping nearby streamgages may help compensate for a short record and help examine the extent of a climate signal because a group of streamflow records all exhibiting a similar nonstationarity further supports climate as the main driver compared to other anthropogenic affects (Kundzewicz and Robson, 2004).

Several studies over portions of North America found an abrupt change in climate or streamflow around the 1970s (McCabe and Wolock, 2002; Villarini and others, 2009; Armstrong and others, 2012; Mazouz and others, 2012; Sagarika and others, 2014; Tan and Gan, 2014; Kolars and others, 2016; Ryberg and others, 2020). Studies noting an abrupt change in climate could provide validation for detected nonstationarities in streamflow. Certain climate patterns such as the Pacific Decadal Oscillation and El Niño Southern

Oscillation have also been related to changes in flood frequency and magnitude (Redmond and others, 2002; Benito and others, 2004; Wirth and others, 2013; Merz and others, 2014; Nazemi and others, 2017). A study looking at 20th century streamflow patterns over the Canadian Prairies found a relation between Pacific Decadal Oscillation and annual mean streamflow (Nazemi and others, 2017). Another study looking at 20th century streamflow patterns over North America and Europe found that for major flood events (25–100-year return period; AEPs of 0.04–0.01) there was a significant relation between the frequency of annual floods and the Atlantic Multidecadal Oscillation (Hodgkins and others, 2017).

Natural long-term hydroclimatic persistence in association with anthropogenic changes can further complicate clear attribution of detected nonstationarities in the streamflow record to climate. Villarini and others (2009) found that LTP, identified through the Hurst parameter (a measure of LTP), could be detected as a nonstationarity, but upon closer inspection, they found many of those sites flagged as having LTP were actually affected by noted human influences. Villarini and Smith (2010) found that human-induced climate change was not related to increased peak flows. A study by Lang and others (2006) examined 192 streamflow records, each with a minimum record of 40 years, and found no clear relation between climate change and streamflow frequencies, whereas Mallakpour and Villarini (2015) suggested the increased frequency of flood peaks were the result of changes in seasonal rainfall and temperature across the United States.

Long-Term Climate and Land Changes

Similar to the lack of effect that regulation and land-use change may have on low AEP floods, apparent variability in climate (and associated nonstationarities) may also fade out when considered over a much longer period because climate trends may be part of a much longer cycle (Razavi and others, 2015; Stoa, 2015). In addition, by looking beyond the century-scale analysis of extreme events, a more accurate estimate can be made about what extremes the hydrologic system is capable of (as intended to be indicated by the PMF) and the climatic conditions (for example, transitions between cool and warmer climates) that tend to produce extreme events. When looking at climate variability over the last few million years, (Quaternary Period, 2.58 million years, or 2.58 megaanum [Ma] to present [2020]), there have been multiple ice ages resulting in glaciation of large areas of North America (Fulton, 1989).

Specifically, over the last 0.78 Ma known as the Brunhes Chron (a polarity chron or a subdivision of geological time based on constant polarity of the geomagnetic field) (Allaby, 2008), two large glaciations (Wisconsin, 0.09–0.01 Ma and Illinois, 0.32–0.13 Ma) are presumed to have covered most (if not all) of Canada, extending into portions of the United States and potentially resulting in the maximum extent of glaciation during the Quaternary Period (Barendregt and Irving, 1998; Fulton, 1989). In between these two glaciations was a glacier-free period (Sangamonian, 0.13–0.09 Ma), emphasizing the extent of climatic variability during the Brunhes Chron (Barendregt and Irving, 1998; Fulton, 1989; Rocky Mountain National Park, [n.d.]). Even though it is speculated that the largest extent of glacier coverage during the Quaternary Period was within the Brunhes Chron, there is still evidence of a series of smaller glaciers covering disjoint portions of North America dating back to 2.58 Ma (Matuyama Chron, 2.58–0.78 Ma), showing the dynamic formation, ascent, and retreat of glacier coverage over North America in response to climatic variability (Barendregt and Irving, 1998).

Consequences of this dynamic glaciation are changes in topography (creating features like the flat Red River of the North "Valley" of the north-central United States, which is actually the bed of a glacial lake; U.S. Environmental Protection Agency, 2013), soil structure (loess, coarse, and fertile farmland), hydrology (new waterbodies, new riverways, and potentially different directions of flow; for example, rivers that tended to flow north may flow south), and vegetation. Glaciation wipes the slate clean and reworks the land and, in turn, its hydrology to form an entirely new system that behaves differently but still experiences seasonal periods of warming and cooling in response to Earth's tilt and orbit. The extent of this warming and cooling can be extreme when looking at the past million years, and the cause is not well understood; at best, it can be attributed to climate variability. Hence, nonstationarity in the climate over the last million years is evident, but determining shifts in the climate (nonstationarities) at much smaller scales can prove challenging. Flood-frequency estimates based on a static record typical of what is available to analysts may be in a constant state of change, whether the change is gradual (taking place over thousands of years) or abrupt (change points).

Including External Information

One possible way to better estimate the distribution parameters for a flood-frequency distribution and improve estimates of confidence intervals for the tails of the distribution is to extend the systematic record used for flood-frequency analysis to include historical or paleoflood peaks or regional information (England and others, 2019). Each type of additional information has special characteristics because the way they are collected or calculated. The implications of the addition of this information need to be understood to make decisions about whether or not to include them and to understand their effect on AEP estimates.

Historical and Paleoflood Data

Historical denotes data that were collected at the time the event was occurring through human observation, whereas paleoflood data are based on geologic and physical evidence such as geomorphic, sedimentologic, stratigraphic, and dendrochronologic (tree-ring evidence; England and others, 2019; Redmond and others, 2002). The longer the period of record,

the more robust the flood-frequency curve; however, most extensions of a streamflow record are not continuous and tend to capture only extreme events such as large floods or droughts (Razavi and others, 2015).

When considering longer streamflow records (even with large gaps), detected nonstationarities, whether gradual or abrupt, may change or cease to exist. In addition, the extent with which to extend the streamflow record (100-year, 1,000-year, or 10,000-year record) for the purpose of developing a comprehensive flood-frequency curve that considers every extreme of the system (maximum flood or droughts) is unknown (Razavi and others, 2015). Given that historical and paleoflood data are sparse, the general attitude is to use what is available; therefore, historical and paleoflood peaks used in a single study may come from a variety of sources. Incorporating such data can be difficult given the wide variety of forms the data come in (point and interval estimates, threshold values, or censored values) and the uncertainty associated with each record.

Some of the more common methods for incorporating historical and paleoflood data are maximum likelihood estimators, the Expected Moments Algorithm (EMA), and Bayesian methods (O'Connell and others, 2002). Guidelines to incorporate historical, paleoflood, and regional data into flood-frequency analysis in the United States have been standardized through Bulletin 17C (England and others, 2019), using EMA, which had the same power as the maximum likelihood estimation method without the numerical estimation challenges related to the maximum likelihood function (Benito and others, 2004; Filliben and Heckert, 2012). Bulletin 17C EMA methods have been implemented in the flood-frequency analysis software PeakFQ (Flynn and others, 2006; Veilleux and others, 2014) and the USACE Hydrologic Engineering Center's Statistical Software Package (HEC–SSP; Bartles and others, 2016). Software such as FLDFRQ3 and PeakfqSA can incorporate historical and paleoflood data into their flood-frequency analysis (Harden and others, 2011). FLDFRQ3 makes use of Bayesian and maximum likelihood estimation (MLE) methods, whereas PeakfqSA uses EMA and has the added capability of "top fitting," which is an option to help reduce the effects of low flows and may create a more robust flood-frequency curve (Harden and others, 2011). FLDFRQ3 and PeakfqSA allow perception thresholds (Harden and others, 2011). The Bureau of Reclamation uses FLDFRQ3 in their flood-frequency analyses (O'Connor and others, 2014), whereas other Federal agencies such as the USGS use PeakFQ, which uses EMA (Veilleux and others, 2014).

Historical Data

A common source of historical data is the USGS PFF database that is available as part of the USGS National Water Information System at https://nwis.waterdata.usgs.gov/usa/nwis/peak (U.S. Geological Survey, 2017). Historical peaks are qualified with a peak qualification code of 7. Some code 7 peaks are used in this study. The use of code 7 to qualify peaks has not been consistent over time; therefore, some clarification is provided in the following paragraph.

The official definition for code 7 is that the "discharge is an historic peak" (Ryberg and others, 2017, p. 8; U.S. Geological Survey, 2017). This definition has caused some confusion over time in that "historic" means "famous or important in history," such as a historic occasion, whereas historical means "concerning history or historical events," such as in historical evidence (Oxford University Press, 2017). (A secondary issue in the USGS definition is that historic and historical both should be preceded by "a" rather than "an" because the "h" in historic is pronounced.) Thus, historical peak-flow data that should be qualified with a code 7 are those that provide historical evidence and are outside the systematic period of record. However, some USGS staff responsible for applying the qualification codes interpreted the "discharge is an historic peak" literally and coded the largest peak in the PFF as a code 7, historic, regardless of where it fell in the record, and nonsystematic peaks that should have been qualified with a code 7 were not. There has been an ongoing effort to correct these misinterpretations for all sites in the PFF; however, the official definition still uses the term "historic" (Ryberg, 2008; Ryberg and others, 2017). Throughout this report, we refer to the nonsystematic peaks as "historical" unless we are specifically mentioning their designation as "historic" peaks in the PFF or in flood-frequency analysis software that interprets those codes.

Paleoflood Data

Large floods can leave a mark on the landscape, and this evidence can persist for many thousands of years. Techniques have been developed to identify geologic and botanical evidence of previous floods and estimate their associated magnitudes and dates. Where robust paleoflood information is available, assessment of the uncertainty in flood-frequency estimates for extreme events can be substantially improved. O'Connor and others (2014) reviewed inundation hazards and approaches to geologic assessment for riverine floods, tsunamis, and storm surges and indicated that layered sedimentary deposits can provide records for large floods that may be preserved for hundreds to thousands of years, depending on the environment. Harden and others (2015) found evidence for three long-term flooding episodes in the stratigraphic record over the last 2,000 years in the Black Hills of South Dakota. Harden and others (2011) used the Black Hills stratigraphic record to incorporate paleoflood data into flood-frequency analysis and to provide better information about the physical basis for low-probability floods. Harden and O'Connor (2017), through stratigraphic analysis, found records of Tennessee River floods that extend back as far as 9,000 years ago. Recently updated Federal guidelines for determining flood frequency, known as Bulletin 17C, describe the incorporation of paleoflood and botanical information into flood-frequency analysis (England and others, 2019).

Use of Thresholds in Historical and Paleoflood Data

For years with missing data within the systematic record or for historical or paleo periods in which some flood information is known, perception thresholds may contribute to additional information about the frequency of large floods. These thresholds are used to describe knowledge about a particular year or series of years for which a streamflow value, *Q*, would have been observed or recorded if it has occurred. The lower bound of a perception threshold represents the smallest peak flow that would result in a recorded flow. For example, analysis of a source of paleoflood information, compared to the systematic record, may conclude that the source will reflect floods of a minimum magnitude; floods below the minimum magnitude may not be observable in the source. The upper bound of the threshold represents the largest peak flow that could be observed or recorded. Oftentimes, the upper bound is set to infinity because the upper bound may not be definitively known. Much greater detail about perception thresholds is provided in England and others (2019), including appendix 9, which has examples with data from streamgages and paleoflood estimates. As pointed out by Sando and McCarthy (2018), most peak-flow data have not been collected within a perception threshold framework, and specific protocols for defining and applying perception thresholds typically were not in place at the time the peak flows were recorded and electronically stored in a database. As a result, determining the appropriate thresholds for ungaged periods associated with some historical peaks can require considerable judgment (Parrett and others, 2011). When dealing with large historical peaks, one often sets the lower perception threshold for an ungaged period to the magnitude of the lowest historical peak within that period. Some peak flows, with a code of 7, indicate historical peaks might not satisfy the requirement for reasonable confidence of nonexceedance during an ungaged period; such peaks might be considered "opportunistic" peaks (collected for some opportunistic reason other than the fact that they were particularly large; Sando and McCarthy, 2018). If the peak is an opportunistic peak, it is not clear that its magnitude should be the lower perception threshold; therefore, the peaks should be excluded from the frequency analysis.

Extended records (using either historical or paleoflood data or both) do not always increase the flood magnitudes for the flood with an AEP of 0.01 or 0.002 but can instead offer a way to refine the flood-frequency distribution. A study on a portion of the Colorado River near Moab, Utah, showed that 0.01- and 0.002-AEP floods, estimated from the systematic record (unaffected by regulation and minimal land-use change), would produce flows of 2,730 and 3,185 cubic meters per second (m^3/s), respectively, whereas estimates of the 0.01- and 0.002-AEP floods, considering paleoflood data (dating back about 2,000 years), increased the 0.01- and 0.002-AEP floods by about 70–80 percent and 110–130 percent, respectively (Greenbaum and others, 2014). This difference became even larger when looking at the 0.0002-AEP flood, where the peak-flow estimate increased 180 percent using a gaged record and paleoflood data compared to only using the gaged record (Greenbaum and others, 2014). In addition, the paleoflood data revealed there were two extreme floods that exceeded the PMF (Greenbaum and others, 2014). Similarly, historical and paleoflood data for specific study locations in western South Dakota revealed much larger streamflow estimates for the 0.01- and 0.002-AEP events, with increases of as much as 130 and 140 percent, respectively (Harden and others, 2011). To highlight the complexity of hydrologic systems, six of the study sites considered in the western South Dakota study were within 30 miles of each other; four of the study sites had increases in the 0.01- and 0.002-AEP flood estimates when historical and paleoflood data were considered; and the other two sites reported decreases of as much as 62 and 76 percent for 0.01- and 0.002-AEP floods, respectively (Harden and others, 2011). Additionally, several paleofloods considered in the study by Harden and others (2011) exceeded the bound of the regional envelope curve (where a regional envelope curve summarizes the limits of extreme floods in a region; Castellarin and others, 2005) developed by Crippen and Bue (1977), but none exceeded the bound of the national envelope curve. Another study over the Colorado River Basin in Arizona and southern Utah considered several thousand years' worth of paleoflood data and found the upper bound of the regional envelope curve did not change (Enzel and others, 1993).

In a report published by the Bureau of Reclamation, it was noted that analysis of the Holocene Epoch (last 10,000 years) may be all that is needed to estimate a flood probability that that most resembles the present climate state (Swain and others, 2004). Several studies have pointed to a potential link between increased frequency in flooding and atmospheric global circulation patterns over portions of the Holocene Epoch, with one of the more well studied relations being drawn between the contemporary El Niño Southern Oscillation and flooding (Benito and others, 2004; Merz and others, 2014; Nazemi and others, 2017; Redmond and others, 2002; Wirth and others, 2013).

Including historical and paleoflood data can help establish if a site or region exhibits any nonstationarity in the streamflow record. Tree-ring analyses over the Canadian Prairie Provinces (dating back to the 1000s and 1300s) indicated the hydrologic system might have never been stationary and that what are often considered long records, about 100 years, may still fail to record long-term patterns in the hydrology of a stream or a region (Razavi and others, 2015). Overall, inclusion of historical and paleoflood data can refine the tails of the frequency distribution; potentially assist with the detection of nonstationarities; and validate any proposed PMF, envelope curve, or existing extrapolations of the systematic flood record.

Regional Data

Besides using historical and paleoflood data to extend hydrologic records, regional data can also be used with the intention of substituting space for time (Eslamian, 2014). When flood-frequency analysis is needed for a site with a short period of record or when very low AEPs are desired, it may be possible to transfer regional information to improve flood-frequency analysis.

Statistical methods for regional transfer are often used by Federal agencies (such as maintenance of variance extension [MOVE] and regional skew) and tend to assume a stationary system (Dawdy and others, 2012; England and others, 2019). When combining regional data with at-site streamflow data, the Bureau of Reclamation suggests the typical reliability of the AEP increases from 0.01 to 0.002 (Swain and others, 2004). A combination of regional and paleoflood data was noted to have a typical reliability of an AEP of 6.67×10^{-5}, and the addition of other regional datasets can increase the typical reliability of an AEP to 2.5×10^{-5} (Swain and others, 2004).

Historical or paleoflood data can be used in at-site flood-frequency analysis, but extension of these data to sites in adjacent or nearby basins may require a better understanding of catchment characteristics. Harden and others (2011) analyzed paleoflood records from three different catchments within a 30 x 30-mile area and found there were vast differences in the extent and number of large paleofloods from adjacent catchments. Suggesting transfer of paleoflood data, regionally, may require knowledge of catchment characteristics and responses to hydrologic events, as adjacent catchments may not experience the same flood event. Merz and others (2014) noted the relation between climate and flooding in one catchment does not imply a similar relation with other catchments in the same region. Similarly, Martínez-Goytre and others (1994) found that basin orientation and location in mountainous regions played an important role when relating paleofloods along the same mountain range (within a roughly 30 x 30-kilometer area) to flooding extent/streamflow. A careful consideration and understanding of catchment characteristics is needed when relating paleoflood data regionally.

Regional and Weighted Skew

At-site skew can be affected by outliers, and regional skew information can be used to adjust the shape of the distribution or to transfer specific flood or regional information to the site (see figs. 10–2 and 10–3 of England and others 2019). Efforts to incorporate regional data using regional skew can be seen through the initial development of a regional skew map in Bulletin 17 (plate 1, U.S. Water Resources Council, 1976) and its inclusion in updated Bulletins (up to Bulletin 17B; Interagency Advisory Committee on Water Data, 1982). The regional skew estimates provided through this map were intended to modify at-site skew estimates and, as a result, improve at-site flood-frequency distributions. However, these skewness estimates have been shown to be extremely sensitive to sampling error. Given sampling error increases with reduced record length, and because the equivalent record length of data used to develop the regional skew map was 17 years, there has been skepticism as to the accuracy of the map (Parrett and others, 2011). Bulletin 17C suggests that the Interagency Advisory Committee on Water Data's regional skew map, originally published in 1976 (U.S. Water Resources Council), should not be used; however, a new, national map is not available. If the user cannot find regional skew data for an area, it is suggested that the user either substitute the regional skew with a value of zero or estimate a new value with methods suggested in the Bulletin 17C. Stedinger and Griffis (2008) provide a review of Bulletin 17B's guidelines for skewness estimation and a summary of recent research on the topic. Once an appropriate regional skew estimate is found or calculated, Bulletin 17C recommends use of a weighted skew coefficient (weighted mean of at-site skew and regional skew) and a Bayesian Weighted Least Squares or a Bayesian Generalized Least Squares procedure as described by Veilleux and others (2011).

Efforts to update regional skew estimates have been made on a state-by-state basis, but there is a lack of consistency in the type of data and methods used. A study looking at sites in Alaska and associated basins in Canada developed two new regional skew areas with a requirement that there be at least 25 years of streamflow data recorded for the streamgages used to define the areas (Curran and others, 2016). A study looking at sites in Arizona made use of two methods for estimating regional skew, one following methods in the USGS Water Supply Paper 2433 (Thomas and others, 1997) and another determined through a Bayesian generalized least squares analysis (Paretti and others, 2014). A similar study in Arizona developed a regional skew value for 1-, 3-, 7-, 15-, and 30-day daily mean streamflow nonexceedance probabilities (durations) using a hybrid weighted least squares/generalized least squares method and used a constant skew value for the entire state, which was unique to each of the nonexceedance probabilities (Kennedy and others, 2014). A study in California looked at updating regional skew values on the basis of Bayesian generalized least squares regression using streamflow records of 30 years or longer. The study also examined at-site skew and used EMA to fit the log-Pearson type III flood-frequency distribution (Parrett and others, 2011). The new methodology introduced in Parrett and others' (2011) study identified a nonlinear function relating regional skew to mean basin elevation, reflecting the interaction of snow with rain. Regional generalized skew estimates were estimated from a variety of selection criterion (more than 25, 50, and 60 years of record) in an area encompassing portions of Massachusetts, Connecticut, and Rhode Island (Zarriello and others, 2012). Determining regional skew is a challenge; however, it is worth exploring in flood-frequency analysis because at-site flood-frequency analysis may be affected by outliers.

Regression Methods

Using regression methods (relating short-term peak-flow records to nearby long-term records) has also been suggested when incorporating regional data into flood-frequency analysis. In their simplest form, regression methods could be used to develop a prediction equation to predict one peak-flow record on the basis of another record. More advanced methods exist; specifically, Bulletin 17C suggests using the Maintenance of Variance Extension type III (MOVE.3) technique (Hirsch, 1982; Vogel and Stedinger, 1985), which is one of the several MOVE techniques that improve upon ordinary least squares by maintaining the variance of estimated data (Hirsch, 1982). The two main requirements when using the MOVE methods are having at least 10 years of concurrent data and a correlation coefficient, which exceeds a critical high value. An assumption of MOVE methods is a linear or log-linear relation between the short and long records over the entire record range of peak flows; often, this assumption holds true for streamgages in proximity (several miles) on the same reach, but can cause error when applied to gages not in proximity on the same reach or on different reaches where streamflow generation properties may vary (Eng and others, 2011). Zarriello and others (2012) noted that application of MOVE methods to multiple short-term streamgages in an area can improve regional skew estimates but may increase inter-streamgage correlation. A study looking at the entire United States found MOVE methods were just as useful as multiple linear regression methods for extending short streamflow records when it came to analyzing low flows (Eng and others, 2011).

MOVE methods have not been developed to address specific issues related to historical floods and paleofloods. With the development of EMA using the log Pearson Type III distribution (EMA–PE3) and its incorporation into readily available software, MOVE estimates should be expressed as interval estimates, not point estimates, because of the greater uncertainty associated with MOVE estimates as compared to gaged estimates of streamflow. However, development of MOVE methods has focused on producing point estimates (see appendix 8 of England and others, 2019, and appendix A of Parrett and others, 2011) because that is what could historically be incorporated into flood-frequency analysis. In addition, regression-based MOVE estimates assume that the explanatory (predictor) variable (the observed flood at a site) is known without error (this is one of the assumptions of regression analysis; Neter and others, 1996). Fuzzy regression, where uncertainty can be incorporated in the explanatory and response variables (Buckley and Jowers, 2008), could be used to develop MOVE estimates from historical flood or paleoflood interval estimates, but that methods development, including the subsequent estimation of prediction intervals, has not been done yet. The Australian Rainfall and Runoff guidelines also use statistical methods for regional transfer and suggest the use of Bayesian generalized least squares regression, specifically looking at quantile or parameter regression techniques (Haddad and Rahman, 2012).

Regional Transfer

When flood-frequency analysis is needed for a site with limited information or when very low AEPs are desired, it may be possible to transfer regional information to that site to improve flood-frequency analysis. Statistical methods, such as regression methods discussed in the previous section, for regional transfer are often used by Federal agencies (MOVE, regional skew) and tend to assume a stationary system (Dawdy and others, 2012; England and others, 2019). A study by Lang and others (2006) found a bootstrap-based procedure described in Douglas and others (2000) worked best when it came to testing regionally meaningful change. Dawdy and others (2012) provided a brief review of regional flood-frequency methods that consider physical mechanisms, which produce floods such as the use of spatial power-law statistics (scaling). Merz and Blöschl (2005) looked at various flood-frequency regionalization methods and found that spatial proximity was a better predictor of regional flood frequencies than catchment attributes and that a method combining spatial and catchment attributes gave the best results.

Index Flood

The index-flood method, introduced by Dalrymple (1960), is one of the first regional flood-estimation methods implemented and has been used for a long time. The index-flood method is used to develop a frequency curve for catchments that lack enough streamflow data or are ungaged. The index-flood method is based upon the assumption that flood flows in a hydrologically similar region, when standardized by an appropriate index flood, are identically distributed. The "index flood," usually the mean annual flood, scales the curve (Kjeldsen and Rosbjerg, 2002), and the method pools the data from stations within a defined region to estimate parameters for a dimensionless flood-frequency curve (Grover and others, 2002). The index-flood method was used for most of the regional flood-frequency analyses made by the USGS before 1965 (Riggs, 1982).

The index-flood method contains two major parts. The first is the development of a basic dimensionless frequency curve representing the ratio of the flood of any frequency to an index flood (the mean annual flood). The second is the development of relations between geomorphologic characteristics of drainage areas and the mean annual flood by which the mean annual flood is predicted at any point within the region. By combining the mean annual flood with the basic dimensionless frequency curve, a regional frequency curve is produced (Malekinezhad and others, 2011).

The index-flood method achieves the general purposes of a regionalization by relating the position of the frequency curve on the streamflow scale to basin size and by averaging the shapes of the individual curves. The method provides

satisfactory results in many regions and is simple to implement. The results are easy to apply to ungaged areas because usually only drainage areas need be measured (Riggs, 1982). It has been noted in Dawdy and others (2012) that the index-flood method does not work well for larger drainage areas and that a single nondimensional flood-frequency relation does not generalize well to such drainages. The index-flood method is still used as noted in Brath and others (2001), Grover and others (2002), Javelle and others (2002), Malekinezhad and others (2011), Portela and Dias (2005), and Smith and others (2015).

A new method termed a probabilistic regional envelope curve (PREC) is based on the index-flood method (Dalrymple, 1960) and requires the method to be used over a homogeneous region (Castellarin and others, 2005). A study over parts of Australia found that when records were reasonably long (greater than 60 years), there was little difference between traditional flood-frequency analysis and PREC methods when estimating a 100-year flood. However, in this same study, 60–74 percent of streamgages showed a significant change in the 100- and 1,000-year flood when comparing traditional and PREC flood-frequency analysis. Others have used the PREC methods to modify distribution functions and, as a result, improve at-site flood-frequency analysis.

Although there may be difficulties using historical or paleoflood information regionally, the additional information is valuable when it comes to developing regional index flood distributions (Jin and Stedinger, 1989). A study analyzing regional flood frequency in Slovakia and the South of France found inclusion of historical data, using a likelihood formulation combined with a Bayesian Markov Chain Monte Carlo algorithm for determining regional distribution parameters, significantly reduced the confidence intervals of regional flood quantiles (Gaume and others, 2010). The extension of paleoflood data (specifically tree scarring) to regional analysis was also found to be a promising approach for some regions (Ballesteros Cánovas and others, 2011). Hosking and Wallis (1986) found that paleoflood information was useful for at-site flood-frequency analysis, but when incorporated into a regional flood-frequency analysis, the effect was minimal.

Region-of-Influence Approach

The region of influence (ROI) approach is an alternative methodology for using information transfer from surrounding stations to inform the at-site estimation of extreme flows. This method, proposed by Burn (1990 a, b), used concepts suggested by Acreman and Wiltshire (1987) that involve nonfixed regions. It is considered a homogenous region delineation method (Gado and Nguyen, 2016).

Traditionally, the delineation of regions relied on geographic, political, administrative, or physiographic boundaries. The resulting regions were assumed to be homogeneous in terms of hydrologic response, but this cannot in general be guaranteed, particularly if the spatial variability of the physiographic and hydrologic characteristics is large (Zrinji and Burn, 1996).

With the application of the ROI method, unique equations are developed for each ungaged site and AEP flood of interest. The method uses a search routine to select stations with basin characteristics that are like those at the ungaged site and performs OLS regression using data only from the selected stations. The unique region composed of the stations selected for a site-specific regression is termed the region of influence (Burn, 1990a, b).

The ROI method offers several advantages over the traditional geographic regional regression methods. The method is a logical approach in which estimation data includes only stations with characteristics (such as drainage area, slope, or elevation) like the ungaged site. Therefore, predictions tend to be made near the center of the space of the explanatory variables, and the extrapolation errors area is reduced. Any violation of the assumption of linearity for the regression is less likely to cause problems (Tasker and others, 1996). Each site can be considered to have its own region, which consists of the collection of stations that compose the ROI for that site. Regions can overlap from site to site (Zrinji and Burn, 1994). According to Eng and others (2005), the ROI can be applied to broader areas and need not be restricted to approaches that use predictor-variable space to define hydrologic similarity.

Three approaches are used for defining hydrologic similarity among basins when using the ROI method. These are the independent or predictor-variable space, geographic space, and a combination of predictor-variable and geographic spaces (a hybrid) developed by Eng and others (2007). All three of these methods can be found in the USGS weighted-multiple-linear regression program developed by Eng and others (2009).

It has been noted by Pope and Tasker (1999) and Law and Tasker (2003) that little difference was found in mean predictive abilities between traditional regional regression equations and the ROI method. Eng and others (2007) concluded that the hybrid ROI method yielded lower estimation errors and produced fewer extreme errors than the predictor-variable or geographic methods. The ROI method is usually considered an alternative method of determining flood frequency.

Methods and Tools for Examining Peak-Flow Series Characteristics and Associated Statistical Assumptions

Many statistical methods and tools can be used to perform the initial data analysis described in Bulletin 17C (England and others, 2019) that determines if the series is stationary or violates underlying assumptions of flood-frequency analysis. This is an evolving area of research both in the field of hydrology and in the field of statistics. Therefore, the scope of this section was narrowed to those methods that have been reported on hydrology.

Nonstationary Detection Methods

Autocorrelated peak-flow series have persistence or memory, indicating that individual peaks are not independent events. Many statistical methods assume independent, identically distributed observations, and autocorrelated series violate this assumption. To examine autocorrelation, an analyst can use the acf function (R Core Team, 2019). Lagged correlations are computed up to a user-defined limit or $n-1$, where n is the number of peaks in the series (R Core Team, 2019). The acf function uses point estimates only, so historical or paleoflood peaks with interval estimates cannot be included in the correlation analysis. The acf function has a method for plotting that will produce a subsequent autocorrelation plot with a confidence interval to help the analyst determine when correlation might be statistically significant and at what lag(s) (R Core Team, 2019). How much correlation is too much is difficult to define; however, the degree of autocorrelation at a site is an important part of understanding the hydrology of a site and a part of the initial data analysis before flood-frequency analysis.

A variety of detection methods can be used to identify additional nonstationarities in a peak-flow series. Generally, these detection methods can be categorized into two types: gradual and abrupt (Kundzewicz and Robson, 2004; Friedman and others, 2016, 2018). Gradual detection methods look at the entire record to assess the significance of change and determine if there is a trend. Abrupt methods look for specific points in the series when there is a significant change in a selected statistic (such as the mean or variance for parametric tests and location and scale for nonparametric tests) and these changes are often referred to as change points or step trends. However, the type of nonstationarity detected by either a gradual or abrupt method may be unclear (Rougé and others, 2013). For instance, an abrupt method may identify the center of a gradual linear trend as a change point. Similarly, a gradual method may identify a trend when the data series exhibits a change point. Whether a series contains a change point, a monotonic trend, or both, such features are a violation of the independent and identically distributed data assumption for flood-frequency analysis. Preferred detection methods do not rely on the assumptions that the data conform to a particular probability distribution (parametric methods), are independent, and are not autocorrelated because streamflow data often violate these assumptions (Kundzewicz and Robson, 2004). A list of some detection methods, the type of nonstationarity targeted (gradual or abrupt), and the analytical approach used (parametric or nonparametric) is presented in table 1.

Many methods exist for detecting change points depending on whether or not one wants to detect a single change point or multiple change points, and there are many methods for penalizing the number of change points detected, depending on the detection method and the desired sensitivity for change detection (Barry and Hartigan, 1993; Zeileis and others, 2002; Erdman and Emerson, 2007; James and Matteson, 2014; Killick and Eckley, 2014; Ross, 2015). The ideal method may not be the same for every site and application and depends on the type of change point desired. Some methods find only one change point that may work if one is looking for the most extreme change in a series. Methods that detect more than one change point are more realistic because some sites alternate between relatively lower flow and relatively higher flow periods or periods of relatively more or less variability. However, these multiple change-point detection methods have higher false-positive rates than those that find only one point (Ryberg and others, 2020). Change-point detection is sensitive to individual outliers (which one may or may not want to consider as a change point) and to back-to-back peaks of similar magnitude (short periods of low variability, which can take place at random or because of short-term climate persistence). Change-point methodology has not incorporated interval estimates; therefore, paleoflood peaks were not incorporated into the efforts to determine change points.

For gradual trends, nonparametric tests may be preferable to parametric methods, such as linear regression, because nonparametric methods are less affected by outliers. Nonparametric does not mean, however, that one does not have to be concerned about properties of the data. The nonparametric nature of the MKT test means that it is not dependent on parameter estimates of a particular statistical distribution, such as the normal distribution; however, the MKT still has underlying assumptions about the data, specifically that the time series is independent and does not have STP or LTP. If a time series is autocorrelated or contains change points, the assumptions of independence and identical distribution underlying the MKT are violated. The variance of the MKT statistic increases with increased autocorrelation (Yue and others, 2002), and the p-value calculated is not correct if the underlying assumptions are violated. In cases of assumption violation, various compensating procedures are available and were used in this study to improve the MKT results.

Discussions of trend analysis that mention STP and LTP often do not clearly define or state the difference between STP and LTP, in part because the difference is relative, and the perception of long term can vary depending on one's experience. In the United States, a hydrologic time series of 125 years is long term (Hirsch and Ryberg, 2012), whereas Beran (1994) published annual minimum water levels of the Nile River for the years A.D. 622 to 1284 (663 observations). Koutsoyiannis and Montanari (2007, p. 2) provide an informative discussion of the definition and difference of STP and LTP:

> "The Markovian dependence (also known as autoregressive of order 1, or AR (1)) is the most typical and simple example of the so-called short-term persistence (STP, also known as short-term dependence). STP is contrasted with LTP (also known as Hurst phenomenon, Joseph effect, long memory, long-range dependence, scaling behavior, and multiscale fluctuation). From a practical point of view, LTP indicates that the process is compatible with the presence of fluctuations on a range of timescales, which may reflect the long-term variability of several factors

Table 1. Parametric and nonparametric approaches for detection of abrupt and gradual nonstationarity.

Aspect of distribution analyzed	Method	Remarks and reference
Abrupt nonstationarity—Parametric method		
Mean	Bayesian changepoint analysis	Provides the distribution with the probability of a change point at each location in the series; method may not work well with short time series or small changes in magnitude (Barry and Hartigan, 1993; Erdman and Emerson, 2007; Wang and others, 2015; U.S. Army Corps of Engineers, 2016; Friedman and others, 2018).
Mean	Student's *t*-test	This is a common statistical test that can be used to detect a difference in the mean between two groups of normal data; the analyst would choose a known time for the change point and test the difference in means (Helsel and Hirsch, 1992; Kundzewicz and Robson, 2004).
Mean, variance, or mean and variance	At most, one change	At most, one change point in mean, variance, or mean and variance (Killick and Eckley, 2014).
Mean, variance, or mean and variance	Binary segmentation	Can find multiple change points in mean, variance, or mean and variance; arguably the most widely used multiple change-point search method (Scott and Knott, 1974; Sen and Srivastava, 1975; Killick and Eckley, 2014).
Mean, variance, or mean and variance	Pruned exact linear time	Can find multiple change points in mean, variance, or mean and variance; similar to the segment neighborhood algorithm but more computationally efficient (Killick and others, 2012a; Killick and Eckley, 2014).
Mean, variance, or mean and variance	Segment neighborhoods	Can find multiple change points in mean, variance, or mean and variance (Auger and Lawrence, 1989; Killick and Eckley, 2014).
Mean, variance, or mean and variance	Wild binary segmentation	Can find multiple change points in mean (Fryzlewicz, 2014; Baranowski and Fryzlewicz, 2015; Sharma and others, 2016).
Abrupt nonstationarity—Nonparametric method		
Distribution	Cramer-von-Mises	Can find multiple change points in the distribution of the data; is more likely to detect changes in the tails of the distribution (extremes) than it is at detecting changes in the location (center) of the distribution (U.S. Army Corps of Engineers, 2016; Friedman and others, 2018).
Distribution	Energy-based divisive	Can find multiple change points in the distribution of the data (U.S. Army Corps of Engineers, 2016; Friedman and others, 2018).
Distribution	Kolmogorov-Smirnov	Can find multiple change points in the distribution of the data; is more likely to find a nonstationarity in the center of the distribution than in the tails (U.S. Army Corps of Engineers, 2016; Friedman and others, 2018).
Distribution	Kruskal-Wallis	This is a common nonparametric statistical test for differences in distribution among two or more groups; the analyst would choose a known time or times for the change point(s) and test the differences (Helsel and Hirsch, 1992; Higgins, 2003; Kundzewicz and Robson, 2004).
Distribution	LePage	Can find multiple change points in the distribution of the data (U.S. Army Corps of Engineers, 2016; Friedman and others, 2018).
Median	Cumulative sums (CUSUM)	Can find a change point in median (location of distribution); successive observations are compared with the median of the series, and the statistic is the maximum cumulative sum of the signs of the difference from the median starting from the beginning of the series (McGilchrist and Woodyer, 1975; Chiew and McMahon, 1993; Kundzewicz and Robson, 2004).

Table 1. Parametric and nonparametric approaches for detection of abrupt and gradual nonstationarity.—Continued

Aspect of distribution analyzed	Method	Remarks and reference
Median	Pettitt	Can find a change point in median (location of distribution); finds one change point; one of the most widely used tests in hydroclimatic studies; can be sensitive to trends and serial correlation; when looking for a single change point, it has proved better than many other methods that have larger false-positive rates (Pettitt, 1979; Busuioc and von Storch, 1996; Kundzewicz and Robson, 2004; Villarini and others, 2009; Mallakpour and Villarini, 2015; U.S. Army Corps of Engineers, 2016; Pohlert, 2018; Ryberg and others, 2020).
Median	Wilcoxon-Mann-Whitney	Can find a change point in median (location of distribution); some implementations can find multiple change points (Mann and Whitney, 1947; Kundzewicz and Robson, 2004; Ross and others, 2011; Ross, 2015; U.S. Army Corps of Engineers, 2016).
Scale	Mood	Can find a change in scale (spread of distribution); some implementations can find more than one change point (Mood, 1954; Ross and others, 2011; Ross, 2015; U.S. Army Corps of Engineers, 2016).
Gradual nonstationarity—Parametric method		
Linear trend	Linear regression and test of significant slope	Tests for a trend with a linear form and assumes the residuals are independent, normally distributed, with constant variance (Helsel and Hirsch, 1992; Kundzewicz and Robson, 2004).
Gradual nonstationarity—Nonparametric method		
Monotonic trend	Mann-Kendall test for trend and Sen's slope estimate (original method and modifications)	Tests for a monotonic trend and does not have distributional assumptions about the residuals; robust to outliers but can be affected by autocorrelation. Several modifications have been proposed to deal with autocorrelation. The trend test tests the null hypothesis of no trend and Sen's slope estimates the magnitude of the trend (Kendall, 1938; Sen and Srivastava, 1975; Kunsch, 1989; Hamed and Rao, 1998; Wang and Swail, 2001; Yue and others, 2002; Kundzewicz and Robson, 2004; Yue and Wang, 2004; Hamed, 2008; Villarini and others, 2009; Carslaw and Ropkins, 2012; Santander Meteorology Group, 2012; Bronaugh and Werner, 2013; Millard, 2013; Tyralis, 2016; Hodgkins and others, 2019).
Monotonic trend	Spearman test for trend	Similar to Mann-Kendall test for trend and based on a rank-based correlation (Kundzewicz and Robson, 2004; Villarini and others, 2009; Pohlert, 2018).
Smooth transition in the median	Lombard Wilcoxon	Can be used to detect a single smooth change in the median of the distribution; does not work well for short series or for small magnitude changes (Lombard, 1987; Quessy and others, 2011; U.S. Army Corps of Engineers, 2016).
Smooth transition in the variance	Lombard Mood	Can be used to detect a single smooth change in the scale of the distribution; does not work well for short series or for small magnitude changes (Lombard, 1987; Quessy and others, 2011; U.S. Army Corps of Engineers, 2016).

such as solar forcing, volcanic activity and so forth. LTP can be also conceptualized as a tendency of clustering in time of similar events (droughts, floods, etc.)…In stochastic terms, STP and LTP are conceptualized in terms of conditional probabilities for the future given past observations. Thus, in a Markovian process the future is not influenced by the past when the present (a time instant) is known whereas in a process exhibiting LTP the influence of the past (the entire history) never ceases."

If series are autocorrelated, this is a violation of the assumptions of independence and identical distribution underlying the MKT. With STP, or short-term autocorrelation, the type I error, rejecting the null hypothesis when there is no trend, is inflated, which can result in the detection of trends that are not significant. In other words, the existence of serial correlation in the time series would increase the chance of finding a statistically significant result, even in the absence of a trend (Cox and Stuart, 1955; Cohn and Lins, 2005). With LTP, the same increase in the type I error rate can increase,

depending on the portion of a record with LTP that one has observed; statistical uncertainty can also dramatically increase in LTP (Koutsoyiannis and Montanari, 2007), and statistically significant positive and negative trends on multidecadal scales exist for the same rivers within their period of record (Hamed, 2008; Khaliq and others, 2009; Hodgkins and Dudley, 2011). STP is easier to deal with than LTP. STP can be dealt with by "removing serial correlation from the data before applying trend tests (prewhitening) or by modifying trend tests to account for the serial correlation [Hamed, 2008]…The presence of LTP is difficult to prove with the generally short (less than 50–100 years) records available [Vogel et al., 1998; Khaliq et al., 2009]. However, LTP-like patterns (such as multidecadal droughts) are seen in longer hydroclimatic records [Koutsoyiannis, 2002; Cohn and Lins, 2005; Koutsoyiannis, 2006; Hamed, 2008]" (Hodgkins and Dudley, 2011, p. 6).

Many modifications of MKT have been proposed to deal with STP, including prewhitening, trend-free prewhitening, and variance correction, and to deal with LTP, including block bootstrap and Hurst scaling (Hamed and Rao, 1998; Bayazit and Önöz, 2007; Önöz and Bayazit, 2012; Bayazit, 2015). Many modifications of the MKT are available in several R packages with varying degrees of documentation.

Regional Analysis Tools

Like the tools developed for nonstationarity detection (USACE Nonstationarity Tool, TREND, R-package) and estimation of at-site flood-frequency distributions (PeakFQ, FLDFRQ3), tools are available to assist with regional analysis of peak-flow data. One of these tools is provided through the Government of Australia and is known as the Regional Flood Frequency Estimation model. The Regional Flood Frequency Estimation model follows methods provided in the Australian Rainfall and Runoff guidelines and is based on information from 853 streamgages (Rahman and others, 2016). The model uses a variety of methods for regional analysis such as predefined regions in conjunction with the ROI approach, Bayesian generalized least squares regression to regionalize distribution parameters (log-Pearson type III), and an index method in some locations (Rahman and others, 2016). Recent investigations of the ROI approach (in combination with Bayesian least squares regression) have found it outperforms fixed-region approaches (Haddad and Rahman, 2012; Haddad and others, 2015). Limitations of the model include its applicability to only one country/continent (Australia) and its difficulty compensating for urbanization, regulation, and severe land-use changes (Rahman and others, 2016). The USACE has created a regional analysis tool for precipitation data, the International Center for Integrated Water Resources Management–Regional Analysis of Frequency Tool, to estimate the intensity and frequency of certain duration precipitation events (U.S. Army Corps of Engineers, 2013). The methodology in the International Center for Integrated Water Resources Management–Regional Analysis of Frequency Tool model mostly stems from a monograph by Hosking and Wallis (2005) with a focus on L-moments (Asquith, 2011, 2017; U.S. Army Corps of Engineers, 2013; Asquith and others, 2017). Another tool for regional analysis is the R package nsRFA for nonsupervised regional frequency analysis (Viglione and others, 2014). The nsRFA package is based on the index-value method and assists with regionalizing the index value, grouping similar regions with similar growth curves and fitting distribution functions to regional growth curves (Viglione and others, 2014). The methods contained within the nsRFA package can be used with historical, paleoflood, or both types of data to assist with refining the tails of the distribution (Gaume and others, 2010; Ballesteros Cánovas and others, 2017).

Sites Selected for Case Studies

Several sites around the United States with paleoflood information were examined for diversity in geography, hydrology, and type of paleoflood information, as well as the existence of a systematic (instrumental) record of peak flows. In addition, a site in Manitoba, Canada, was also considered because of several types of historical data and tree-ring based paleoflood information. An initial list of sites was explored for potential flood-frequency analysis challenges and the availability of paleoflood information. For example, the streamflow record upstream from the Canadian site is known to be nonstationary (Hirsch and Ryberg, 2012; Ryberg and others, 2014; Ryberg and others; 2020) and, therefore, challenging for flood-frequency analysis.

While examining potential sites, some paleo information had more utility than others. For example, the Little Tennessee River near Prentiss, North Carolina, was the subject of a paleoflood study (Wang and Leigh, 2012) that found two periods in the last 2,000 years with large floods and no severe droughts; however, flood magnitudes were not estimated in the study and, therefore, this study does not have sufficient information for incorporation into flood-frequency analysis. Information on flood-rich or flood-poor periods contributes to a better understanding of past climate but is not able to be incorporated into current flood-frequency analysis methodologies that require some information about magnitudes (even if the information consists of intervals or thresholds). Finally, another site considered, the Lower Deschutes River near Axford, Oregon, had paleoflood data and was the subject of a paleoflood study (Hosman and others, 2003) but the analysis was done by multiplying the gaged record from a downstream regulated site by a constant and making assumptions about dam storage during large floods. To complete the analysis including more recent streamgage data, one would have to examine the potential flood storage for each peak, incorporate methods used by Hosman and others (2003), and reevaluate the use of the downstream streamgage. Such regulation assessments were beyond the scope of this work.

Five sites, shown in figure 1, were selected for detailed analysis of the peak-flow record and of the challenges presented by the sites for flood-frequency analysis and the estimation of very low AEPs. The period of record and amount of historical and paleoflood data vary among the sites. The sites were not selected to develop definitive peak-streamflow frequencies for design considerations at these streamgages; instead, the sites are examples used for purposes of illustration. Peak-flow data included data collected by the USGS as part of its network of streamgaging sites (U.S. Geological Survey, 2017) and data collected by the streamgaging network in Manitoba, Canada; for the USGS data, see appendix 1 of Asquith and others (2017) for a primer on streamgage operation and determination of peak flow. The sites are listed in table 2 and a description of each site follows.

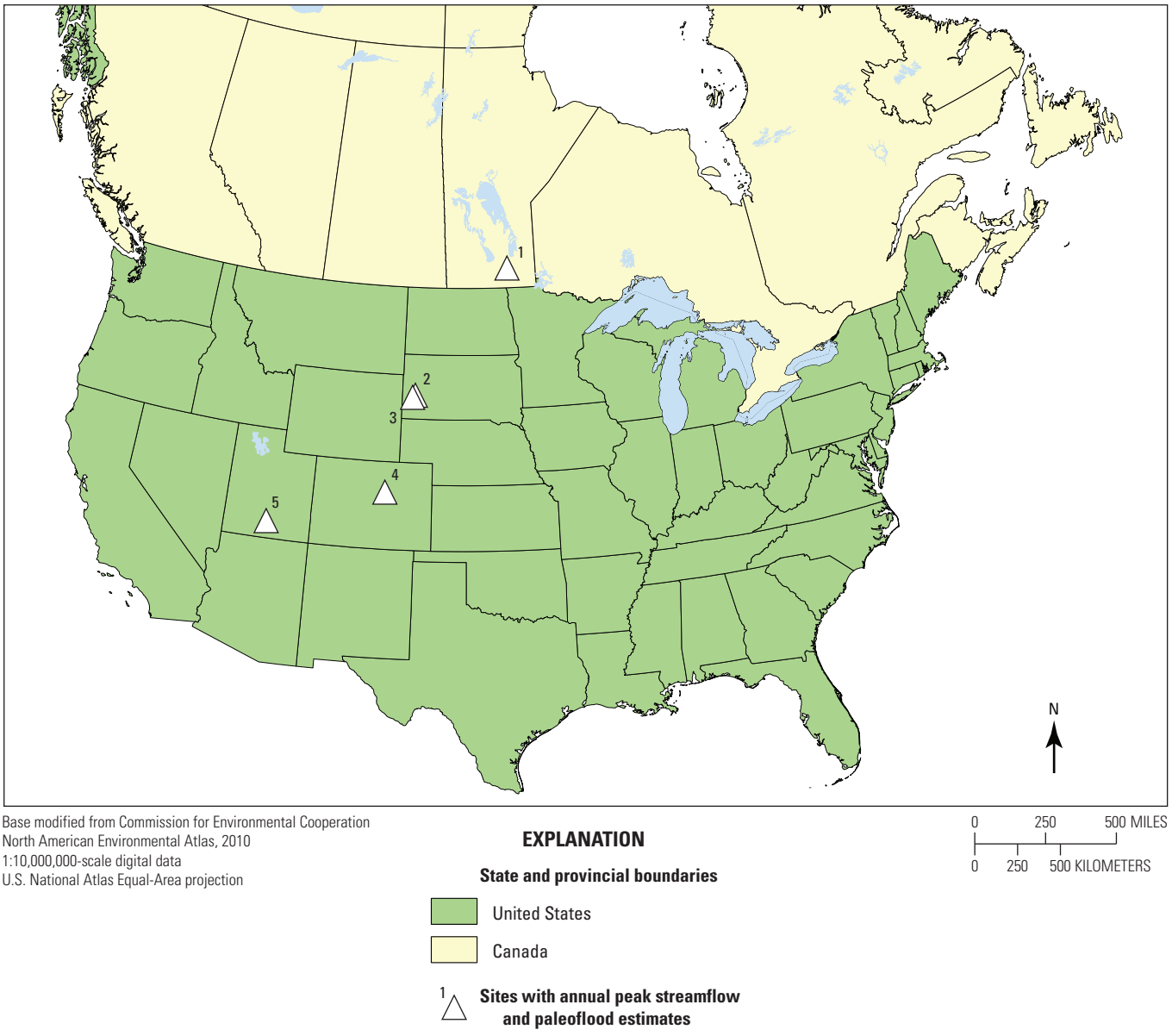

Figure 1. Sites selected for detailed analysis of the peak-flow record and for flood-frequency analysis, including the estimation of very low annual exceedance probabilities.

Table 2. Sites selected for flood-frequency analysis.

Site number	Site identifier	Site name	Drainage area, in square miles (and data source)
1	05OJ015	Red River of the North at James Avenue Pumping Station, Winnipeg, Manitoba, Canada	110,039 (Government of Canada, 2019)
2	Based on multiple gage records (Harden and others, 2011)	Lower reach, Rapid Creek, South Dakota	375 (Harden and others, 2011)
3	Based on multiple gage records (Harden and others, 2011)	Spring Creek, South Dakota	171 (Harden and others, 2011)
4	06712500	Cherry Creek near Melvin, Colorado	360 (U.S. Geological Survey, 2017)
5	09337500	Escalante River near Escalante, Utah	5,670 (U.S. Geological Survey, 2017)

Red River of the North at Winnipeg, Manitoba, Canada

The Red River of the North (Red River; site 1 in fig. 1) begins at the confluence of the Bois de Sioux and Ottertail Rivers on the North Dakota-Minnesota border near Wahpeton, North Dakota. It flows north to Winnipeg, Manitoba, Canada, and continues north where it flows into Lake Winnipeg. Research has shown that the Red River Basin and surrounding areas in the north-central United States and southern Manitoba experience distinct periods of hydroclimatic persistence, alternating between wet and dry periods (Burn and Goel, 2001; St. George and Nielsen, 2002; Vecchia, 2008; Ryberg and others, 2014; Ryberg, 2015; Kolars and others, 2016; Ryberg and others, 2016) that are visible in the sediments of Devils Lake, North Dakota, for the past 4,000 years (Bluemle, 1996). The Red River Basin stands out in national flood magnitude trend studies as an area of increasing flood magnitude with time (Hirsch and Ryberg, 2012; Peterson and others, 2013); however, the trend may only represent LTP of the wet period in the last few decades of the record.

The Red River at Winnipeg was selected because it represents an opportunity for studying flood frequency at a site with LTP because of long-term monitoring and a rich set of historical point estimates, historical interval estimates, and tree-ring-based estimates. The peak-flow data were provided by Mark Lee of Manitoba Conservation and Water Stewardship (written commun., August 20, 2014, and September 26, 2016). These peaks are considered the natural flow (adjusted to unregulated conditions) at Winnipeg downstream from the confluence with the Assiniboine River. Peaks outside the period of systematic record have been quantified with point estimates and with interval estimates by Rannie (1998) and the Canada Department of Resources and Development (1953). Tree-ring based flood estimates and thresholds were determined by St. George and Nielsen (2002, 2003). The tree-ring based proxy flood record extends back to A.D. 1648 and indicates episodes of frequent flooding that occurred in the mid-1700s, early to mid-1800s, and the latter half of the 20th century, with the largest flood in 350 years occurring in 1826 (St. George, 2010).

Lower reach, Rapid Creek, South Dakota

The peak-flow record for the lower reach of Rapid Creek (site 2 in fig. 1) was selected because of the existence of paleoflood estimates and previous flood-frequency analyses that could be compared to this study (Harden and others, 2011). The geographic setting of Rapid Creek, the Black Hills, creates the potential for especially large floods because of steep topography that concentrates flow and for limited flood peak attenuation because of narrow canyons in some reaches (Sando and others, 2008; Harden and others, 2011). Rapid Creek was one of the creeks investigated by Harden and others (2011) because the geology of the area is conducive to flood deposition and preservation of slack-water deposits.

The peak-flow record for the lower reach of Rapid Creek is based on streamflow records from multiple sites that were modeled (by compilation and adjustment) to be comparable with a paleoflood chronology developed for this reach (Harden and others, 2011). “Long-term flood chronologies primarily were derived from stratigraphic and geochronologic analysis of paleoflood deposits...The modern peak-flow chronology for the lower Rapid Creek study reach...was developed to estimate pre-regulation conditions [before the development of Pactola Dam], which is consistent with the paleoflood chronology obtained for the reach” (Harden and others, 2011, p. 8 and 44). The multisite-based synthetic record contains peaks designated as historical peaks, systematic or gaged peaks, and paleo-derived interval estimates and thresholds.

Notable at this site, and others in the Black Hills, is a high outlier flood within the systematic period of record. This flood occurred in 1972 and for many sites it is a high outlier, exceeding the next largest peak flow by a factor of 10 or more (Harden and others, 2011). This outlier is extremely influential when attempting to estimate flood magnitudes for very low AEPs. Harden and others (2011) found that floods as large or

larger than the 1972 flood have affected the Black Hills and that incorporating paleoflood data can reduce the effect of this individual large flood on the flood-frequency curve.

Spring Creek, South Dakota

Spring Creek (site 3, fig. 1) is another site studied by Harden and others (2011). The peak-flow record for Spring Creek also is based on streamflow records from multiple sites that were modeled to be comparable with a paleoflood chronology developed for this reach. Long-term flood chronologies were derived from stratigraphic and geochronologic analysis of paleoflood deposits as described in the lower reach, Rapid Creek section above and in Harden and others (2011). The multisite-based synthetic record contains estimated peaks outside a systematic period, systematic peaks, and paleo-derived interval estimates and thresholds. The 1972 outlier flood is evident in this record.

This site was selected, in part, to be the subject of an experiment in transferring paleoflood information from one site to another. Martínez-Goytre and others (1994), Harden and others (2011), and Merz and others (2014) cautioned that it is not always appropriate to transfer paleoflood data to a nearby site. However, that type of transfer was included here as an experiment. Spring Creek initially was analyzed using the at-site paleoflood data; then Spring Creek was analyzed using paleoflood estimates based on the lower reach of Rapid Creek, and the results were compared to explore the effects for regional transfer for paleoflood information.

Cherry Creek near Melvin, Colorado

Cherry Creek's headwaters are on the Palmer Divide (a ridge in central Colorado that separates the Arkansas and South Platte drainage basins), and Cherry Creek (site 4, fig. 1) flows northerly to the South Platte in Denver, Colorado (Jarrett, 2000). This site was selected in consultation with USGS hydrologist Michael Kohn on the basis of the availability of systematic record (albeit short 1940–69), a nonsystematic (historical) flood peak, and a paleoflood estimate. This site has been the subject of other paleoflood studies to help refine the PMF for a downstream dam (Jarrett, 2000) and has been part of a larger effort to improve peak-flow regional regression equations for eastern Colorado (Kohn and others, 2016).

Because this site has a fairly short period of record, it was also chosen to compare PeakFQ methods EMA–PE3, with and without paleoflood information, to methods described in Asquith and others (2017) that use different probability distributions and fitting methods but do not incorporate paleoflood data. The resulting comparisons are made to determine whether any of the alternative distribution and fitting methods improve upon EMA–PE3 analysis with systematic data only and provide estimates comparable to EMA–PE3 analysis with the extended record available with paleoflood data.

Escalante River near Escalante, Utah

The Escalante River near Escalante, Utah, in the Southwestern United States (site 5, fig. 1) represents a site that receives sporadic but intense rainfall, and the rock shelters and alcoves along the river's bedrock canyon are conducive to deposition of flood sediments (Webb and others, 1988). This site was selected because evidence exists for four historical and nine prehistoric floods dated using radiocarbon and tree-ring chronologies (Webb and others, 1988). In addition, previous flood-frequency studies provide methodological comparisons (Webb and others, 1988; Webb and Rathburn, 1988; Kenney and others, 2008).

Data and Methods Used for Case Studies

There are many considerations for the acquisition of data, initial data analysis; and flood-frequency analysis. This bulleted list provides a general list of considerations that were followed for the analyses presented.

- Inspect and review data:
  - Are historical and paleoflood peaks well documented?
  - Can the historical and paleoflood peaks be included as interval estimates (preferable) rather than point estimates?
- Initial data analysis:
  - Check for autocorrelation.
  - Carry out change-point analysis and, if necessary, review ancillary climatic, land-use, or regulation data that may explain the change points and inform subsequent analyses.
  - Complete trend analysis, modified for autocorrelation, if needed.
- Flood-frequency analysis:
  - Consider distribution choice. (PE3 was the only option in this study, but methodologies may become available that allow for the use other distributions with interval estimates.)
  - Consider fitting method. (EMA was the only option in this study, but methodology may become available allowing other fitting methods with interval estimates to be used.)
  - Consider low outliers. The Multiple Grubbs-Beck Test was used in this study to identify and censor potentially influential low floods (PILFs).

- Consider whether to use at-site skew or regionally weighted skew. (This may entail comparing analyses with different skews.)
- Compare with existing studies, if available.

The following sections provide details about the initial data analysis methods and the flood-frequency analysis methods used for sites in this study (table 2).

Data

The data used consist of peak-flow series from gaged sites, historical peaks, and paleoflood peaks. The data represent water years, where a water year is the period from October 1 to September 30 and is designated by the year in which it ends; for example, water year 2015 was from October 1, 2014, to September 30, 2015. All historical and paleoflood data came from the USGS PFF database that is available as part of the USGS National Water Information System at https://nwis.waterdata.usgs.gov/usa/nwis/peak (U.S. Geological Survey, 2017) or from literature cited in the case studies. The historical and paleoflood peaks were assumed to be accurate, and no additional systematic, historical, or paleoflood peak data were collected for this this study.

Initial Data Analysis

The data series used for flood-frequency analysis were subject to data analysis described in appendix 4 "Initial Data Analysis" of Bulletin 17C (England and others, 2019). This included examining autocorrelation in the systematic period of record, testing for trends with and without historical peaks, and examining the systematic record for change points in mean and variance.

Three types of peak-flow information were used. The first were peaks that are part of a systematic data collection effort at a site. In the case of the Red River site in Canada, the systematic peaks represent naturalized flows. In the case of the peaks in South Dakota, the systematic record consists of annual, modeled peaks based on several nearby sites (Harden and others, 2011). The second type was historical peaks. Most of the case studies have peaks qualified with a code of 7 indicating that they were collected outside the period of systematic record and there is reasonable confidence that they were not exceeded during a specified ungaged period outside of the period of systematic record. Historical peaks are qualified because they represent nonrandom sampling and are biased in favor of larger peak flows. Typically, the reason a historical peak was determined was because there was above normal flooding. In some cases, peaks that were not qualified with a code of 7 in the USGS PFF were qualified for this analysis (such peaks are identified in the text). The third type are paleoflood peaks determined from previously published studies.

The existence of one type of stationarity may affect the results of another detection method. However, the order in which the three possible nonstationarities are investigated does not necessarily matter. Some of these analyses could be combined, for example, an analyst could use a method that adjusts monotonic trends for autocorrelation by default. Examining the results should include plots that allow one to consider the autocorrelation, trends, and change points together with additional gage characteristics, such as climate information and the extent of regulation.

Autocorrelation

To examine autocorrelation at each site, the acf function in R was used to calculate lagged correlations with the number of lags being the default, $10\times\log_{10}(n)$, where n is the number of peaks. The user can adjust up to $n-1$, where the n is the number of peaks in the series. The argument "na.action" was set to "na.pass" because some series did have missing values within the systematic period of record. This means the autocorrelation function passes through the missing values and computes correlations from complete cases (rather than deleting missing values and assuming a time step of 1 year between observations that had missing years between them). Notably, the acf function uses point estimates only, so paleoflood peaks with interval estimates are not included in the correlation analysis. The subsequent autocorrelation plots show a 95-percent confidence interval for correlation (on the basis of an uncorrelated series; R Core Team, 2019). If the line representing a lag crosses the upper or lower confidence bound, that lag is correlated and statistically significant at the 0.05 significance level.

Change-Point Analysis

Change points in the mean and variance of the peak-flow series were determined using the changepoint package for R (Killick and Eckley, 2014; Killick and others, 2016). The change-point detection method used is the pruned exact linear time (Killick and others, 2012a), a compromise method in terms of algorithm complexity and computational speed. Pruned exact linear times also is a compromise method in terms of outliers and short periods of variability in that one can set a minimum segment length to eliminate outliers or 2-year periods being identified as change points. However, this means outliers are grouped with the peaks near them that may not be similar. The method minimizes a cost function of possible pruned locations of change points. The penalty used to determine change points was the package default, the modified Bayes information criterion (MBIC; Zhang and Siegmund, 2007), one of several standard penalties for change-point analysis. The method does not return p-values for the change points, which means that inferences based on statistical significance are not possible. The change-point detections presented here could be modified to detect more or fewer change points,

depending on the degree of concern one has about change points, by adjusting the minimum segment length, relaxing or further constraining the maximum number of change points, or changing the penalty method (Killick and others, 2016). Initially viewing a larger number of change points highlights outliers and periods of low or high variability. Pruned exact linear time was constrained to find at most 10 change points with a minimum segment length of 4.

Monotonic Trend Analysis

Peak-flow series, with and without historical peaks, were analyzed for trends in each case study using the MKT, the kendallTrendTest function in the R package EnvStats (Millard, 2013). This is a nonparametric test of a monotonic trend, based on Kendall's tau (Kendall, 1938). The trend line is plotted using the Theil-Sen estimator (Sen, 1968; Theil, 1992) for the slope and the Conover equation (Conover, 1999) for the intercept. The confidence interval for the slope uses Gilbert's modification of the Theil-Sen method (Gilbert, 1987). Additional adjustments of the MKT test were used for the first case study to compare the different methods. Considerations made for the MKT and a description of the additional adjustment methods follow.

For the site with autocorrelation, the Red River of the North, modifications to MKT were compared. The function mkTrend in the fume package carries out a modified MKT with variance correction (variance is inflated with positive autocorrelation) on the basis of Hamed and Rao (1998) and returns a corrected *p*-value after accounting for "temporal pseudoreplication" (Santander Meteorology Group, 2012). The variance correction approach reduces the type I error (rejection of the null hypothesis when there is no trend or a false positive) but decreases the power to detect actual trends (more false negatives, or type II errors; Önöz and Bayazit, 2012; Yue and Wang, 2004).

The function zyp.trend.vector with method argument equal to "yuepilon" in the zyp package (Bronaugh and Werner, 2013) performs a modified MKT that first detrends the series, then uses the estimated lag-one autocorrelation coefficient of the detrended series to remove, or prewhiten, the serial correlation, then the estimated trend is added back and the MKT is applied (Yue and others, 2002; Önöz and Bayazit, 2012). This method reduces the type I error and does a better job of maintaining power than does simply prewhitening (Önöz and Bayazit, 2012). Yue and others (2002) found that trend-free prewhitening had larger power than prewhitening or variance correction. The "sig" value is the *p*-value computed for the final detrended series.

The function zyp.trend.vector with method argument equal to "zhang" in the zyp package (Bronaugh and Werner, 2013) carries out a modified MKT that first detrends the series if the trend is significant, and then computes the autocorrelation. "This process is continued until the differences in the estimates of the slope and the AR (1) in two consecutive iterations are smaller than 1 percent. The MKT is then run on the resulting time series" (Bronaugh and Werner, 2013, unpaginated). This method is described in Wang and Swail (2001).

The MannKendallLTP of the HKprocess package (Tyralis, 2016) applies the MKT under the scaling hypothesis for the data (Hamed 2008). The scaling approach acknowledges that trends can exist normally in natural time series. The stochastic process can be expressed as a scaling stochastic process in which the standard deviation of the random variable being investigated is scaled as a function of the Hurst exponent coefficient, *H*, a measure of LTP or the Hurst phenomenon (Hurst, 1951). One can calculate *H* on a scale of 0 to 1, and if *H* is approximately equal to 0.5, the data are random with zero correlation at nonzero lags, and the series can be analyzed with classical statistical techniques (Beran, 1994; Hamed, 2008; Koutsoyiannis, 2003; Koutsoyiannis, 2006). *H* greater than 0.5 indicates the autocorrelation function has a slow decay compared to short memory processes, such as an autoregressive or autoregressive-moving mean, and that modified statistics should be used to adjust for a scaled stochastic process (Hamed, 2008). A problem of attribution for *H* remains. We know such persistence can be normal; however, Villarini and others (2009) showed that *H* can be sensitive to anthropogenic changes. Attribution requires additional data to investigate the mechanisms generating the persistence, and these data are not always available.

An analyst can also use the regular MKT with block bootstrap resampling to correct for serial correlation (Önöz and Bayazit, 2012). The resampling is done by blocks, of fixed or varying lengths, which preserves short-term correlation among observations. These blocks are repeatedly assembled in random order, the MKT is performed, and a series of these trends is used to develop a distribution and obtain a confidence interval for the observed trend by comparing the observed series to the distribution of randomized series with STP. The block bootstrap method has comparable power for detecting trends to variance correction methods, and block bootstrap has a smaller type I error (false-positive rate) than trend-free prewhitening (Önöz and Bayazit, 2012).

The methods to determine trends and scaling do not incorporate the ability to include interval estimates. Therefore, paleoflood peaks were not included in the checks for monotonic trends. Historical peaks with point estimates, however, can be included in monotonic trend estimation.

Flood-Frequency Analysis

As Lins and Cohn (2011, p. 475) stated, nonstationarities are not easily addressed and "[i]n such circumstances, humility may be more important than physics; a simple model with well-understood flaws may be preferable to a sophisticated model whose correspondence to reality is uncertain." The literature highlights many suggestions for improved flood-frequency analysis with nonstationarities. However, some of

them are not practical to implement, are not prudent for very low AEPs (an estimate of a large, rare flood based on the most recent 30 years of record ignores a great deal of information about the variability of a system), or have not been extended to accommodate the inclusion of paleoflood data. In the interest of using a well-understood model with known limitations that has the capability of extending the flood record with historical and paleoflood data, the flood-frequency analysis followed the procedures described in England and others (2019) and used version 7.2.22429 of PeakFQ of the USGS (Veilleux and others, 2014). See appendix 1 for specific PeakFQ settings used in the analyses in this report.

Statistical Distribution Used

The EMA–PE3 method incorporated in PeakFQ analyzes the peak-flow series under the assumption that the series follows a log-Pearson type III distribution. This distribution is sometimes called an "LPIII distribution," but it is referred to as PE3 in this report for consistency with Asquith and others (2017). The PE3 distribution is widely used in hydrology, particularly in the United States, where it is used as a guideline for Federal agencies in determining flood-flow frequencies (Water Resources Council, 1967; Interagency Advisory Committee on Water Data, 1982; England and others, 2019). Applications of the PE3 distribution use systematically collected and historical peak-streamflow values to define a frequency distribution based on the sample mean (location of the distribution), the standard deviation (scale of the distribution), and the skew (shape of the distribution).

Skew is an important consideration because determines the shape of the PE3 distribution, which affects the frequency of large floods in the right tail of the distribution. Skews determined using the peak data at a particular site, at-site skew, can have large uncertainty depending on the site and the length of the systematic peak record and the skew estimate is sensitive to extreme events (Interagency Advisory Committee on Water Data, 1982; Griffis and Stedinger, 2007). The accuracy of a skew estimate can be improved by weighting the station skew with a generalized skew estimated by pooling nearby sites, thereby creating a regional skew estimate. Bulletin 17B outlined a method for determining a generalized skew for detailed flood-frequency studies and provided a generalized skew map for the United States in plate I as an alternative for use in studies that did not develop generalized skews (U.S. Water Resources Council, 1976). Bulletin 17B also provided equations to determine the weighted skew coefficient and to estimate the mean-square error of station skew (eqs. 5 and 6 of U.S. Water Resources Council, 1976).

The understanding of skew estimates has evolved since Bulletin 17B, and Bulletin 17C (England and others, 2019) recommended using Bayesian weighted least squares/generalized least squares to develop better regional skew estimates (Veilleux and others, 2011). Developing regional skew estimates for the hydrologically and geographically diverse sites in this study is beyond the scope of this work. Therefore, efforts were made to find updated regional skew estimates in other USGS studies and, if an updated study could not be found, the regional skew from plate 1 of Bulletin 17B was used to demonstrate the use of regional information.

Method for Estimating Distribution Parameters

This study estimates distribution parameters using EMA (Cohn and others, 1997). Nonstandard flood data may be used with EMA, including flood-interval estimates, as opposed to the standard point estimates and flood thresholds. Asquith and others (2017) compared the PE3 distribution and EMA to other probability distributions and fitting methods amenable to flood-frequency analysis; however, historical and paleoflood data are currently difficult to incorporate into those methods. The mathematics of the PE3 distribution are further described in appendix 5 of Asquith and others (2017).

Potentially Influential Low Floods

An important feature of EMA–PE3 is that it allows one to identify PILFs. Small floods may be the result of a different hydrologic process than the larger floods with low AEPs and they can have a large effect on distribution fitting procedure (Cohn and others, 2013; England and others, 2019), hence the name PILFs. PeakFQ incorporates the Multiple Grubbs Beck Test to detect PILFs (Cohn and others, 2013). Within PeakFQ, those peaks identified as PILFs are recoded as less than a threshold streamflow and treated as interval data in EMA because PILFs do not convey meaningful information about the magnitude of floods with very low AEPs, but they do contribute information about the frequency of very low AEP floods. See appendix 7 of Bulletin 17C (England and others, 2019) for more information on the treatment of PILFs in EMA computations.

Case Study Results and Discussion

Analyses were performed under different scenarios, depending on available data, such as flood-frequency analysis with the systematic peaks only, followed by more complex analyses with systematic peaks plus historical peaks, and with systematic and historical peaks plus paleoflood information. Because of the different types of data available at the sites, and the differing challenges for flood-frequency analysis, a different set of plots is presented for each site.

Regional information was taken into consideration by comparing results determined with an at-site skew and a weighted skew, computed from the at-site skew and regional skew. Additionally, in one test case, Spring Creek, paleoflood information collected at a site was transferred to a nearby site to investigate the effect of paleoflood information.

Consideration was also given to some suggested methods for dealing with climate nonstationarity, such as separate wet and dry period flood-frequency estimates, using the most recent 30-year period because it is the period most likely (by some theories) to represent future climate, or adjusting past periods defined by step changes to match other periods. When other flood-frequency studies were available, their results were compared to the results here. Most of the studies compared to this work reported the 100-year flood (or AEP of 0.01) as the lowest frequency flood, so very low AEPs are not directly compared. The comparisons in some cases simply show the effect of additional years of data, whereas other comparisons show results from methods other than PeakFQ's EMA–PE3 approach (that is, different distributions or fitting methods).

Red River of the North at Winnipeg, Manitoba, Canada

Though snowmelt dominated, the Red River may have a peak-flow record representing a mixed population from snowmelt, rain on snow, and rainfall. If one could segregate the peaks into two or more distinct and independent populations, separate frequency curves could be calculated and combined into a joint probability distribution (Morris, 1982). However, Bulletin 17C lacks guidance as to how to segregate the peaks based on physical processes and states that "additional efforts are needed to provide guidance on the identification and treatment of mixed distributions" (England and others, 2019, p. 22). In addition, if the peak-flow record was divided into two or more distinct populations, it would be unclear which population could be analyzed with the addition of paleoflood data. Therefore, the Red River was treated as a record coming from one population, as were other sites in this study.

The systematic, historical, and paleoflood peaks are shown in figure 2. The first two point-estimate peaks are paleoflood peaks determined by St. George and Nielsen (2003) from tree rings representing the period 1648–1999. They also determined that the 1826 flood was the largest in this period and that the threshold for flood signatures in the tree-ring record was 106,000 ft^3/s. The next three-point estimates in the 1800s, including the 1826 peak, were determined by the Canada Department of Resources and Development (1953). The historical interval estimates were determined by Rannie (1998) based on a compilation of Manitoba Provincial archival materials representing the period 1793 to 1870, Canadian and United States Government entities, historical and scientific research articles, and other entities.

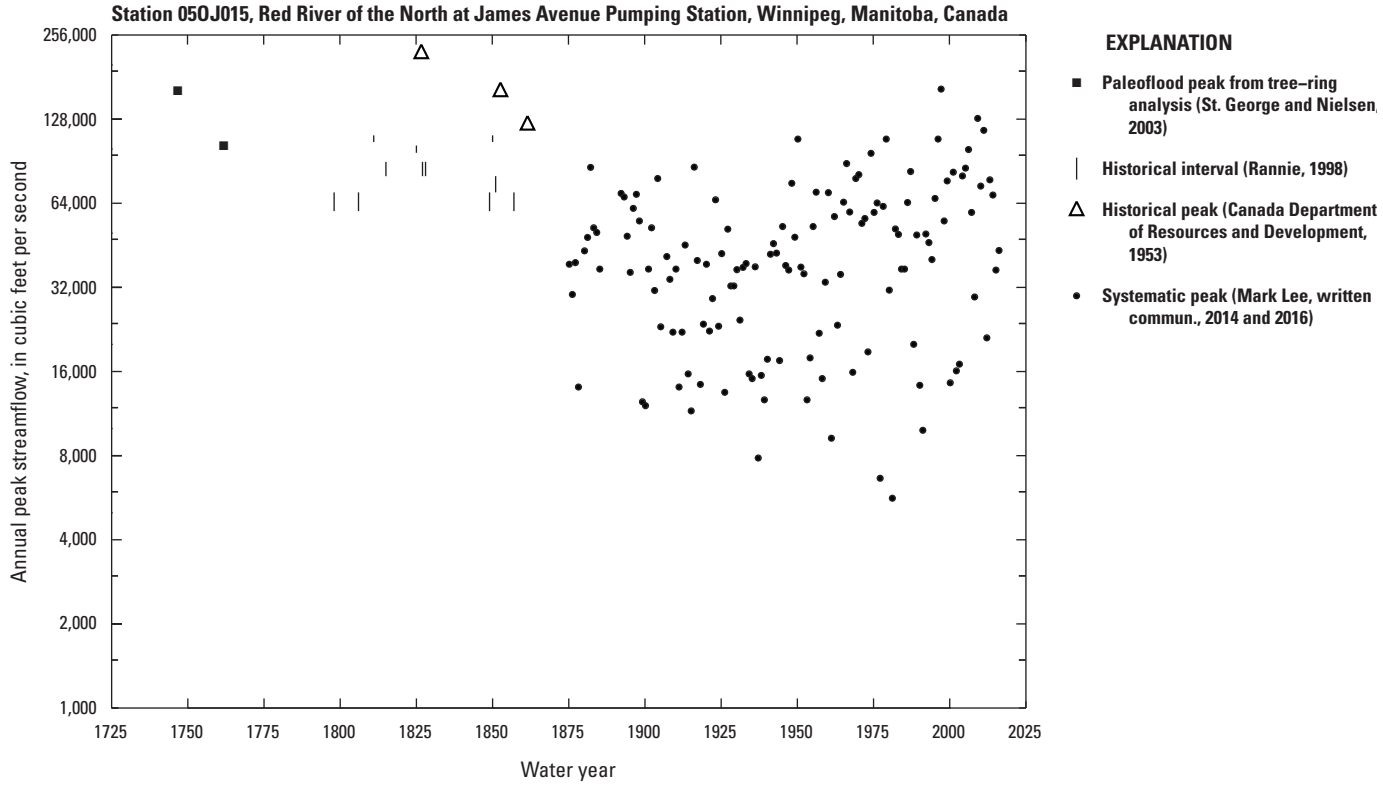

Figure 2. Systematic, historical, and paleoflood peaks and historical intervals for streamgage station 05OJ015, Red River of the North at James Avenue Pumping Station, Winnipeg, Manitoba, Canada.

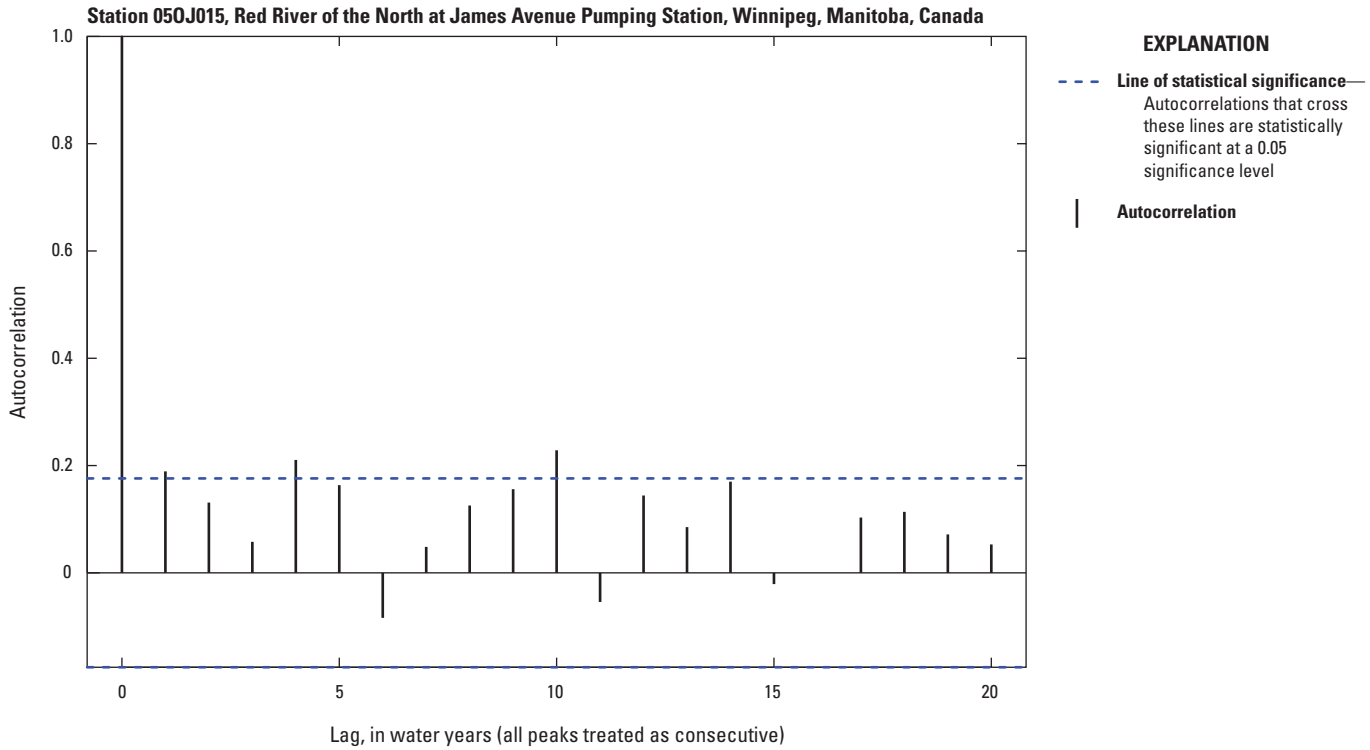

Figure 3. The autocorrelation for peaks in the systematic period of record for streamgage station 05OJ015, Red River of the North at James Avenue Pumping Station, Winnipeg, Manitoba, Canada.

Autocorrelation

The systematic peaks only (without historical or paleoflood peaks) were examined for autocorrelation from 1892 through 2016. The result was that the series contains statistically significant autocorrelation on the scale of 1 year up to 14 years (fig. 3), likely a feature of climatic persistence. (Because of the scale of the figure, line weights, the dashed line, and precision issues, the lag at year 14 does not appear to cross the dashed line, but numerical investigation shows that the lag correlation is greater than the upper confidence bound.) Autocorrelation is a violation of the assumptions of independent identically distributed peaks necessary for trend and frequency analysis. Many such analyses have some degree of assumption violation, and how much autocorrelation is too much is not clear. One implication is that the effective length of the record is not as long as it appears: that is, there is redundancy in the information. The redundant information can increase the uncertainty in the estimates of flood magnitude. This increase in uncertainty was shown by Burn and Goel (2001) in an analysis of 117 years of record for this site. They determined that the 117 years of record was equivalent to an independent record of 45 years. They also showed the increased uncertainty in boxplots (fig. 2 of Burn and Goel, 2001) that compare estimates for floods with AEPs of 0.01, 0.02, and 0.005 under a mixed-noise model (Booy and Lye, 1989; 5,000 sequences of 115 years with correlation structure in the data) and an independent model (5,000 independent sequences of 115 years).

Change-Point Analysis

Only the systematic peaks were examined for change points from 1892 through 2016. The change point algorithm assumes all peaks are consecutive (that is why the historical and paleoflood point estimates were not included) and the algorithm relabels the observations 1 to n, where n is the number of values in the series. There is a distinct change in the mean and variance defining two periods (fig. 4). This provides evidence of the persistent two-state climate system documented in parts of the basin with relatively higher flow periods and relatively lower flow periods (Vecchia, 2008; Kolars and others, 2016).

This change point is a violation of the independent and identically distributed data assumption for flood-frequency analysis. However, PeakFQ can identify PILFs, small values that would have a considerable effect on the fit of the flood-frequency distribution (Cohn and others, 2013), and then focus on the larger floods for fitting the flood-frequency distribution. At least some of the floods from the period of relatively lower flows may be identified as PILFs, decreasing the effect of this period in the flood-frequency analysis.

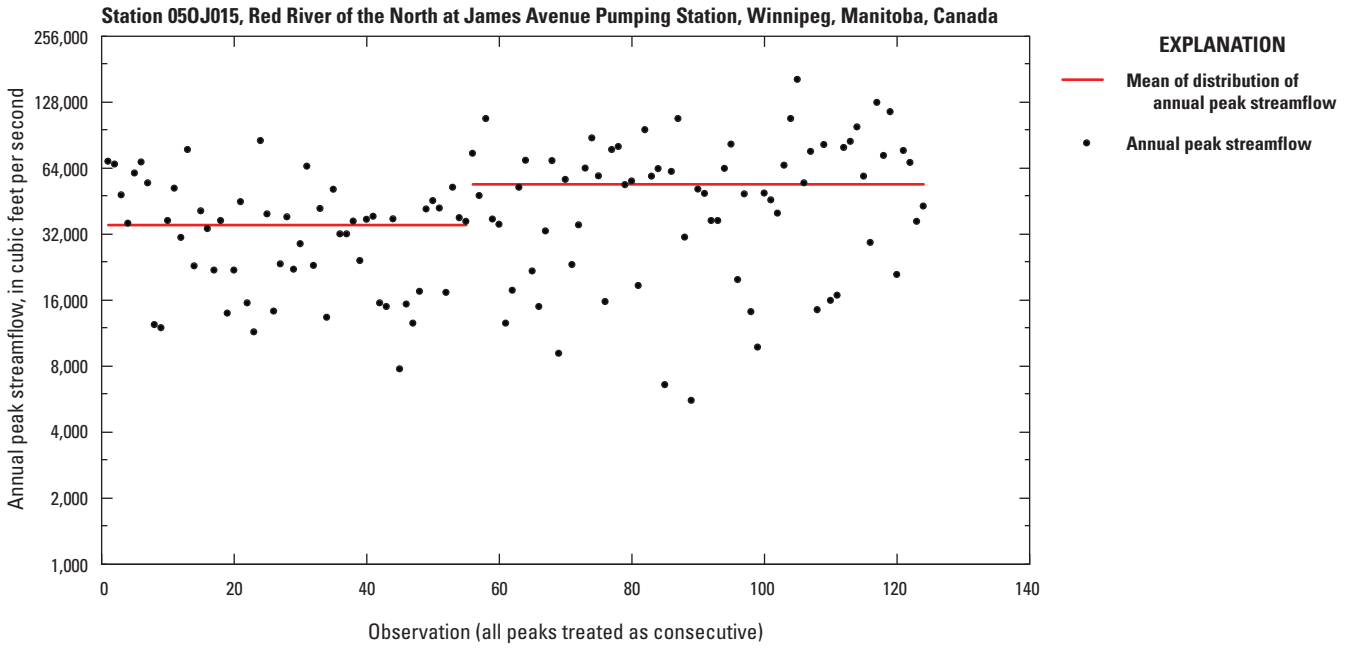

Figure 4. Change point in mean and variance for peaks in the systematic period of record for streamgage station 05OJ015, Red River of the North at James Avenue Pumping Station, Winnipeg, Manitoba, Canada.

Trend Analysis

The existence of autocorrelation and change points in the mean and variance violates assumptions of the MKT, indicating the *p*-value would likely be incorrect. For consistency with the other sites in this study, the unadjusted MKT was done and plotted (fig. 5) for three periods: one that includes the historical peaks, one that includes the systematic peaks, and one with the systematics peaks from 1907 to 2016 (a period with no missing values). The plot shows that the large historical peaks do not have a great deal of leverage on the trend line, but it does show that the choice of trend period affects the slope.

Next, a variety of adjustments to MKT (described in the methods section) were used to explore the issues of STP and LTP in this peak-flow record. The results of the adjusted MKT are shown in table 3, except for the MKT modified for LTP, which requires more explanation. Results indicate that this site has a statistically significant trend, *p*-value less than 0.05, using all modified methods. Among the various methods, trend estimates ranged from 336 to 350 ft^3/s per year. Most methods provide confidence intervals, which are also reported in table 3.

The results of MannKendallLTP of the HKprocess package are not as straight forward to present. The results for the Red River indicate a trend based on the original test statistic (as shown in fig. 5). The Hurst coefficient, *H,* calculated before any detrending using the MLE method, was 0.64, indicating scaling may be an issue. After detrending and adjusting *H*, the result is less than 0.5 and not statistically significant; therefore, the original trend is considered significant and not a product of LTP (Hamed, 2008).

The many methods for modifying the MKT make little difference in quantifying the trend. The block bootstrap with a geometric mean of the blocks equal to 25 had the narrowest confidence intervals. The bootstrap confidence intervals tended to be shifted slightly larger in magnitude, with the largest blocks (25) of fixed and mean length having the narrowest confidence intervals. The many adjustments make little difference in estimation of the trend magnitude, indicating that the MKT may be robust to assumption violations. Additional testing on other sites with serial correlation would be informative but is beyond the scope of this work.

Flood-Frequency Analysis

Flood-frequency analysis was completed under a variety of scenarios for the Red River because of the rich dataset available for this site. At-site skew was used unless otherwise indicated, and the systematic record does have some missing years in which perception thresholds were estimated. When regional skew was incorporated, a regional skew of −0.509 and a regional skew standard error of 0.368 were used (from table 2, zone A, which included the Red River Basin upstream from Winnipeg, in Williams-Sether [2015]). The scenarios analyzed included flood-frequency analyses with the following information series:

1. systematic peaks and at-site skew (standard at-site analysis);

2. systematic peaks and weighted skew;

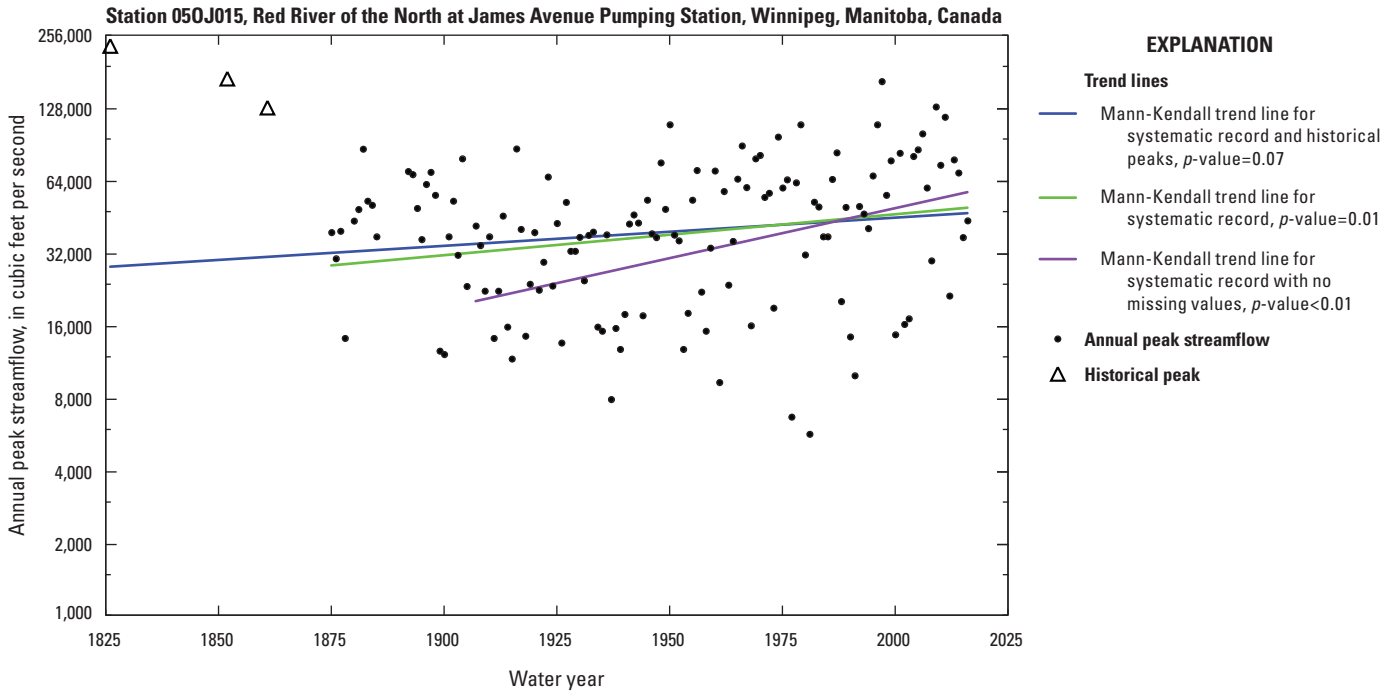

Figure 5. Mann-Kendall test for trend in the annual peak-streamflow record for streamgage station 05OJ015, Red River of the North at James Avenue Pumping Station, Winnipeg, Manitoba, Canada.

3. dry period of 1899–1947, based on the change-point analysis;

4. wet period of 1948–2016, based on the change-point analysis;

5. most recent 30 years of data;

6. systematic peaks with the dry period, 1899–1947, shifted up by the difference in mean between the wet and dry period;

7. systematic peaks plus historical peaks;

8. systematic and historical peaks and interval estimates;

9. systematic and historical peaks, historical and paleo-derived estimates, and paleo-derived thresholds;

10. systematic and historical peaks, historical and paleo-derived estimates, and paleo-derived thresholds, with weighted skew; and

11–23. in addition to the analyses performed for this study, estimates were obtained from other flood-frequency studies that compared flood-frequency analysis with and without historical data (Burn and Goel, 2001; Harden, 1999). Those peaks were called scenarios as well and are listed as scenarios 11–23 in results for comparison of the floods with an AEP of 0.01. See table 4 (available for download at https://doi.org/10.3133/sir20205065) for more information.

The input data for flood-frequency analysis in scenarios 1–2 are shown in figure 6. There are some missing years in the dataset and on the basis of examining the distribution of the peaks and the work of Rannie (1998), an assumption was made that if the peaks had been greater than 60,000 ft^3/s, they likely would have been estimated; therefore, there are perception thresholds set at 60,000 ft^3/s to infinity for the missing years. The years with missing data but a perception threshold are indicated as censored flow by peakFQ. In this case, the censoring interval indicates peak flow in the missing years was between 0 and 60,000 ft^3/s.

The resulting flood-frequency curve for scenario 1 is shown in figure 7. The figure indicates that there were 39 PILFs. The PILFs were identified using the Multiple Grubbs-Beck Test in PeakFQ, and they were censored at 29,000 ft^3/s in the analysis so that the fit was focused on the higher flows. Streamflow estimates for those AEPs used in Asquith and others (2017; 0.10, 0.01, 1×10^{-3}, 1×10^{-4}, 1×10^{-5}, and 1×10^{-6}) and their associated confidence intervals are shown in table 4.

Scenarios 2–8 were also analyzed; however, the input data plots are not shown because all the additional historical and paleoflood information is ultimately combined under scenarios 9 and 10 and shown in figure 8. The frequency curves are not shown; however, the flood estimates for selected AEPs are shown in table 4.

The input data for the flood-frequency analyses completed under scenarios 9 and 10 using systematic and historical peaks, historical and paleo-derived estimates, and paleo-derived thresholds are shown in figure 8. The same assumption

Table 3. Trend results for streamgage station 05OJ015 Red River of the North at James Avenue Pumping Station, Winnipeg, Manitoba, Canada, 1907–2016, using modifications of the Mann-Kendall test for trend.

[Bootstrap trend results are the median from the bootstrap replicates and 95-percent confidence intervals calculated using the bootstrap percentile method (Davison and Hinkley, 1997). <, less than; MKT, Mann-Kendall test for monotonic trend]

Method	Trend estimate (upper and lower confidence bounds)	*p*-value (upper and lower confidence bounds)	Comment
kendallTrendTest EnvStats, Theil-Sen Estimator	339 (158, 509)	0.0001	Unmodified trend test. 95-percent confidence interval using Gilbert's modification of Theil-Sen method.
mkTrend in the fume package	350	<0.0001	Modified Mann-Kendall trend test with variance correction.
zyp.trend.vector with method argument equal to "yuepilon" in the zyp package	339 (158, 508)	0.0001	Trend-free prewhitening variation; this should have larger power to detect a trend than the variance correction method.
zyp.trend.vector with method argument equal to "zhang" in the zyp package	346 (165, 526)	0.0001	Trend-free prewhitening variation; this should have larger power to detect a trend than the variance correction method.
Block-bootstrapping MKT, fixed block size=5	337 (152, 517)	0.0002 (0.0000, 0.0504)	5,000 bootstrap replicates.
Block-bootstrapping MKT, fixed block size=10	338 (176, 530)	0.0002 (0.0000, 0.0642)	5,000 bootstrap replicates.
Block-bootstrapping MKT, fixed block size=15	339 (171, 543)	0.0003 (0.0000, 0.1216)	5,000 bootstrap replicates.
Block-bootstrapping MKT, fixed block size=20	336 (161, 544)	0.0004 (0.0000, 0.1514)	5,000 bootstrap replicates.
Block-bootstrapping MKT, fixed block size=25	338 (171, 528)	0.0004 (0.0000, 0.2043)	5,000 bootstrap replicates.
Block-bootstrapping MKT, geometric mean of block size=5	338 (158, 535)	0.0002 (0.0000, 0.0732)	5,000 bootstrap replicates.
Block-bootstrapping MKT, geometric mean of block size=10	336 (170, 533)	0.0003 (0.0000, 0.0982)	5,000 bootstrap replicates.
Block-bootstrapping MKT, geometric mean of block size=15	338 (167, 525)	0.0003 (0.0000, 0.1247)	5,000 bootstrap replicates.
Block-bootstrapping MKT, geometric mean of block size=20	338 (171, 520)	0.0003 (0.0000, 0.1528)	5,000 bootstrap replicates.
Block-bootstrapping MKT, geometric mean of block size=25	337 (173, 511)	0.0004 (0.0000, 0.2043)	5,000 bootstrap replicates.

as scenario 1 was made for missing years within the systematic period of record (perception thresholds set at 60,000 ft^3/s to infinity for the missing years).

The resulting flood-frequency curve for scenario 9, at-site station skew, is shown in figure 9, and the flood-frequency curve for scenario 10, weighted skew, is shown in figure 10. Both analyses again indicated that there were 39 PILFs. Streamflow estimates for selected AEPs and their associated confidence intervals are shown in table 4.

The use of at-site skew (fig. 9) appears to fit the largest four peaks better than the use of weighted skew (fig. 10). The confidence bounds for an AEP of 1×10^{-4} are much narrower when the weighted skew is used. The upper confidence bound is more than two times larger with at-site skew than with weighted skew. There appears to be a tradeoff between precision and accuracy, with regional skew providing a more precise estimate, but the at-site skew may be more accurate in that the largest peak shown fits within the flood-frequency curve best when using at-site skew. Regional skew may not

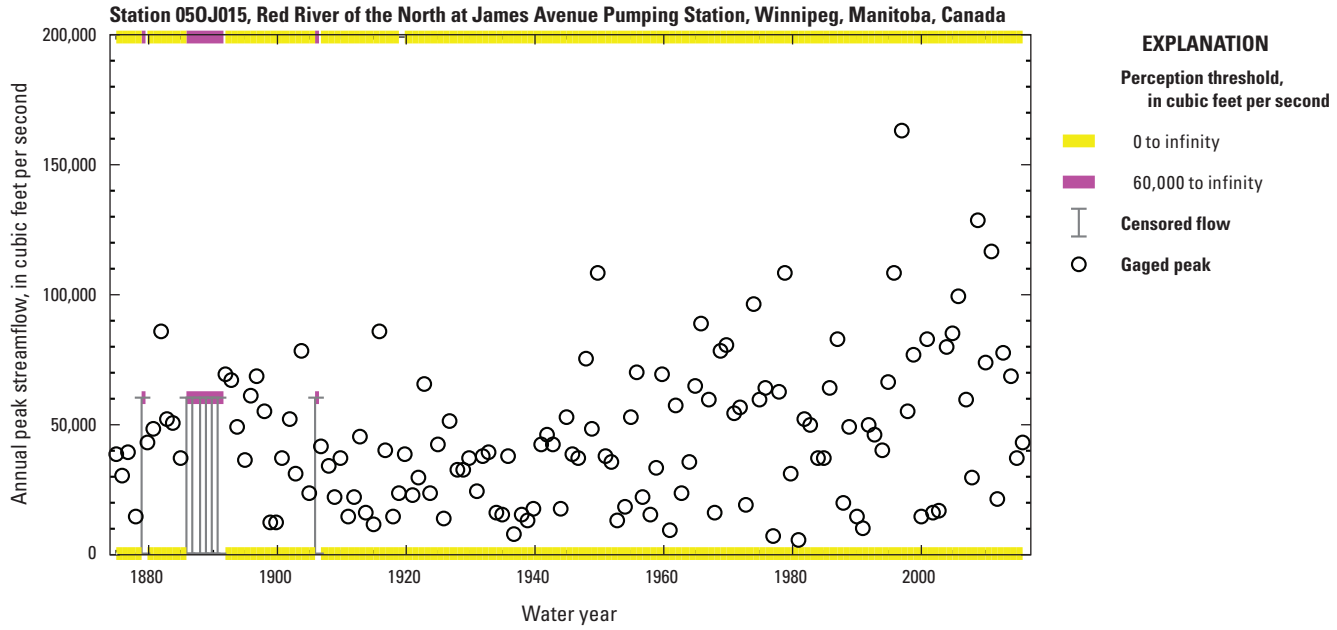

Figure 6. Peaks and thresholds used as input for flood-frequency analysis scenarios 1 and 2 (systematic record) for streamgage station 05OJ015, Red River of the North at James Avenue Pumping Station, Winnipeg, Manitoba, Canada.

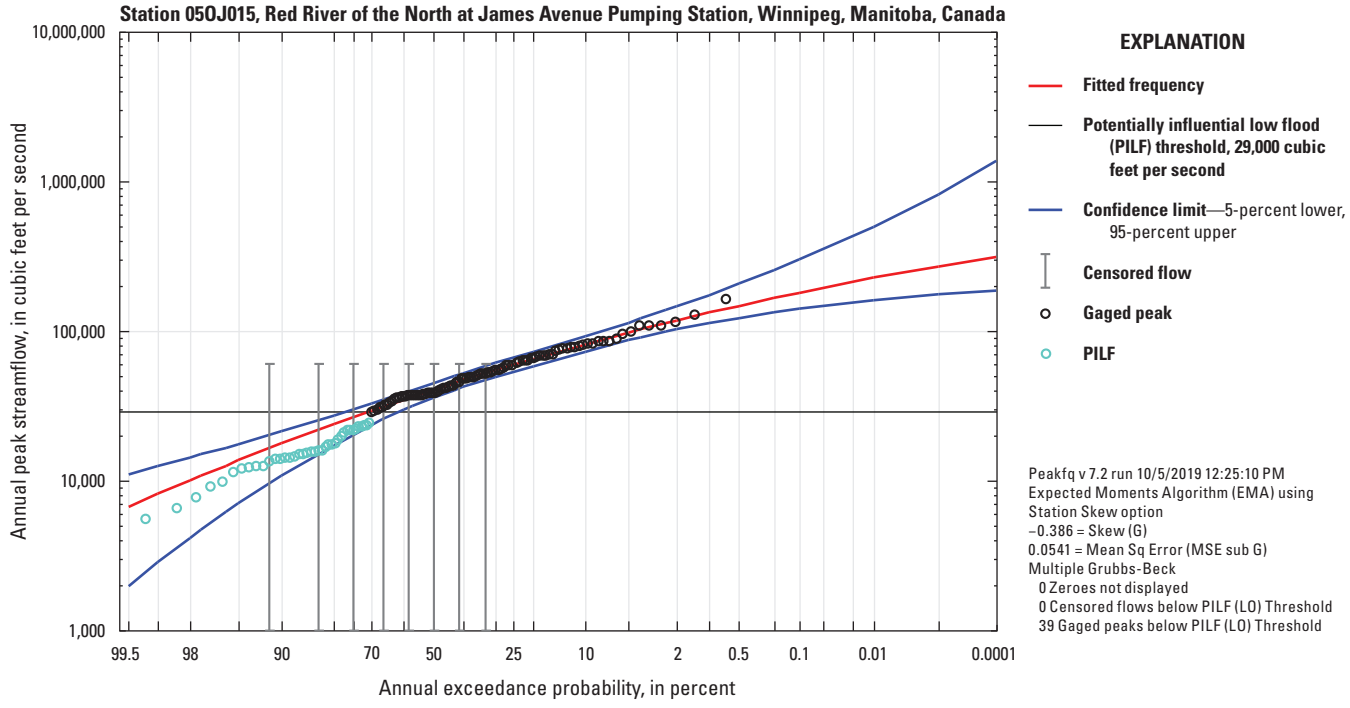

Figure 7. Annual exceedance probability plot and fitted distribution for streamgage station 05OJ015 with the input data shown in figure 6 and at-site skew (scenario 1).

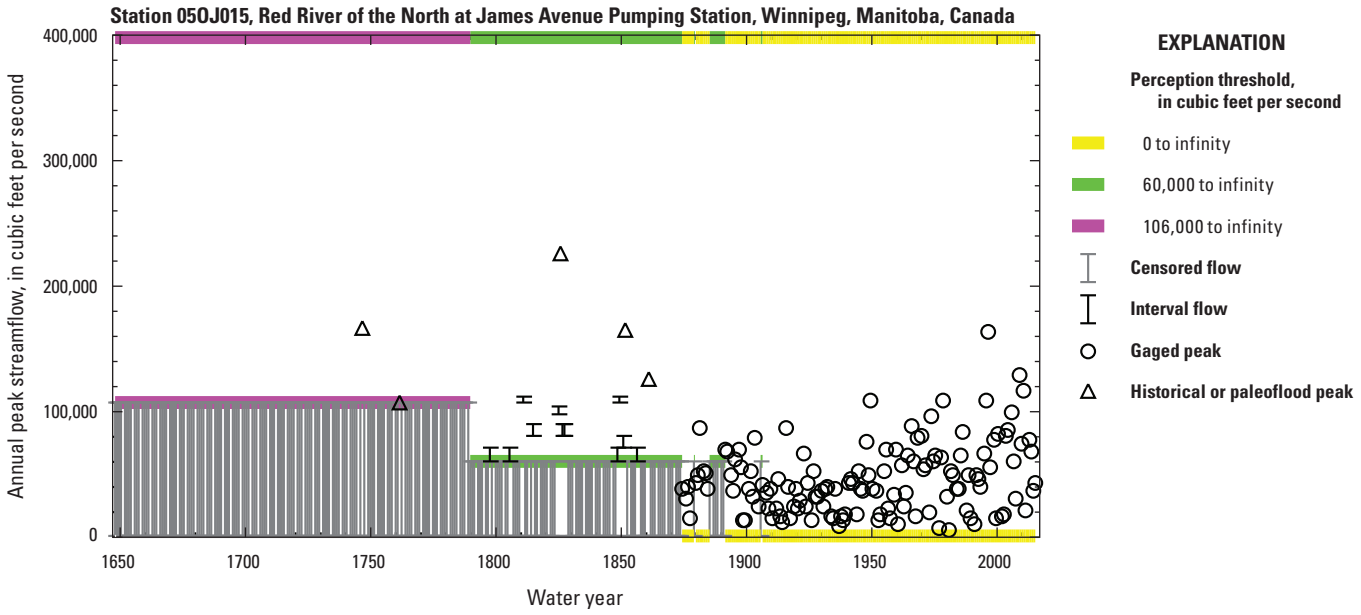

Figure 8. Systematic and historical peaks, paleo-derived peaks, and historical and paleo-derived thresholds used for flood-frequency analysis scenarios 9 and 10 for streamgage station 05OJ015, Red River of the North at James Avenue Pumping Station, Winnipeg, Manitoba, Canada.

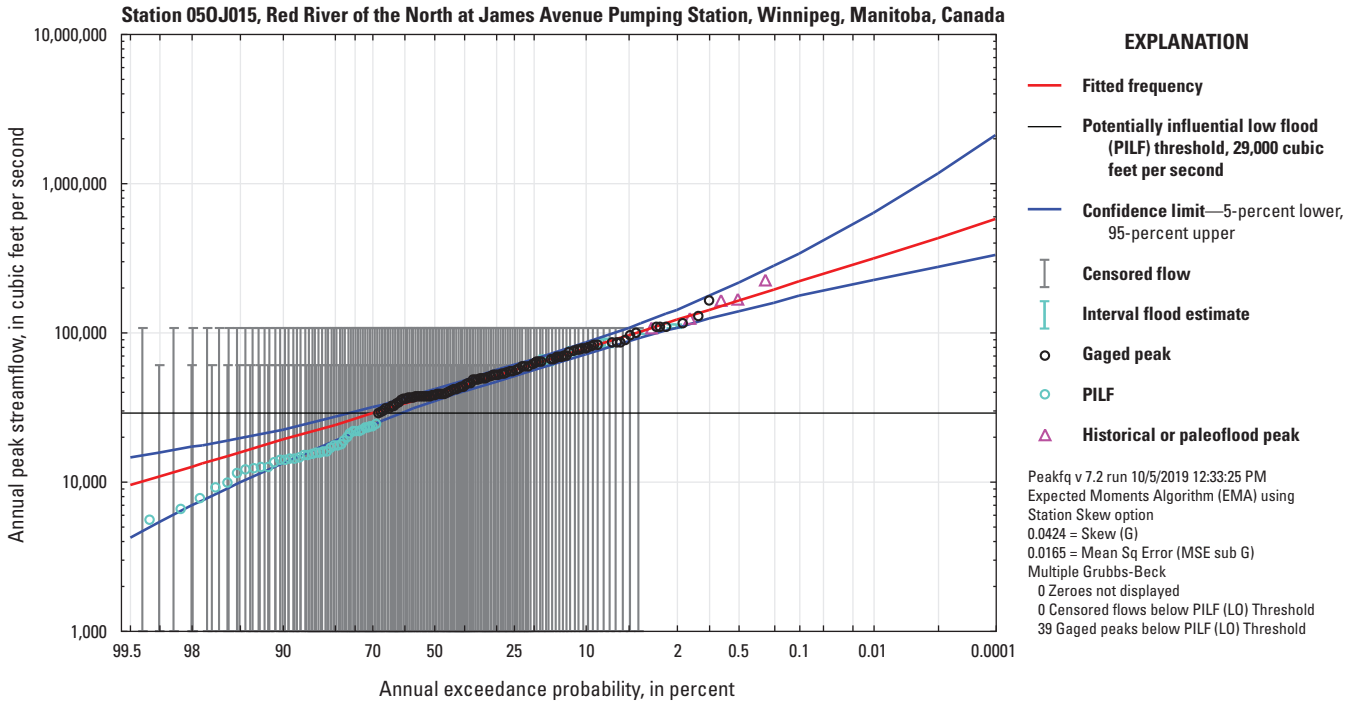

Figure 9. Annual exceedance probabilities for streamgage station 05OJ015, Red River of the North at James Avenue Pumping Station, Winnipeg, Manitoba, Canada, with the input data depicted in figure 8 and at-site skew (scenario 9).

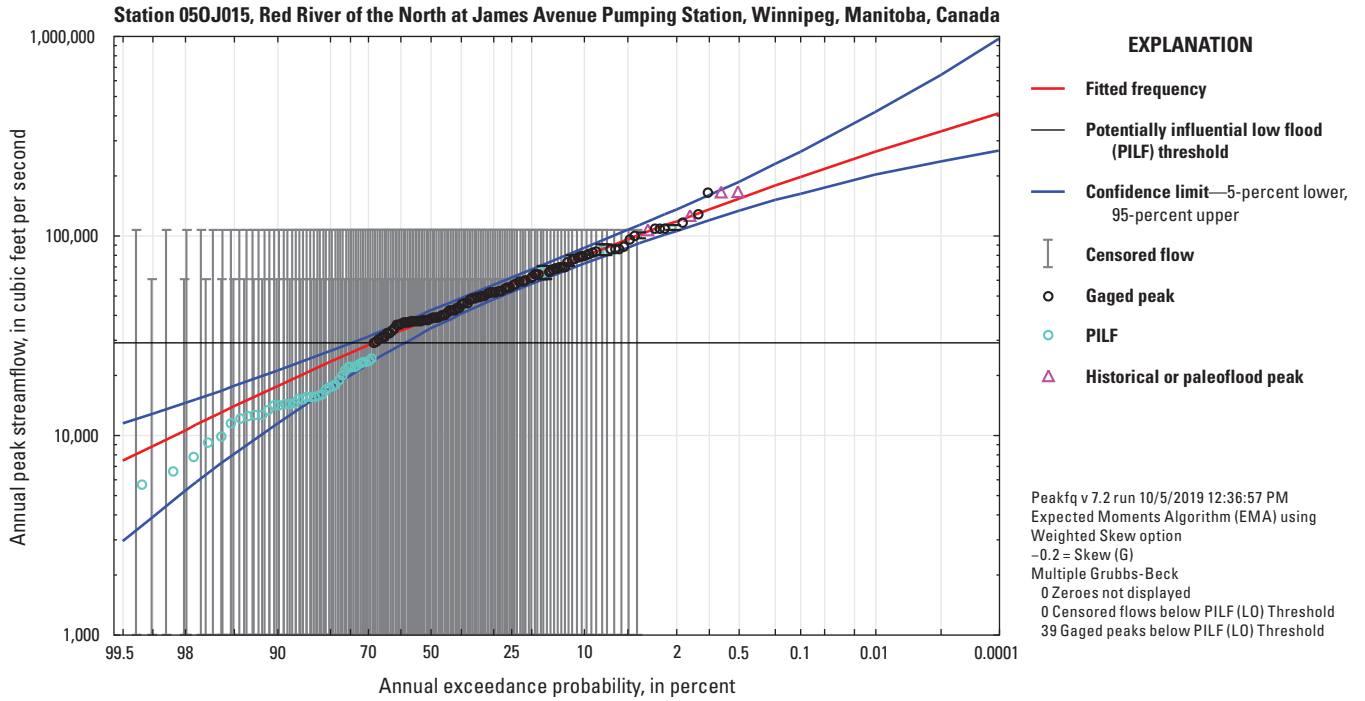

Figure 10. Annual exceedance probabilities for streamgage station 05OJ015, Red River of the North at James Avenue Pumping Station, Winnipeg, Manitoba, Canada, with the input data depicted in figure 8 and weighted skew (scenario 10).

be the best estimate of skew for the Red River at Winnipeg because the regional skew is based in many streamgages that have much smaller peaks and shorter periods of record.

All scenarios are aligned along a single x-axis in figures 11–16 to compare the point estimates and 95-percent confidence intervals for the AEPs derived from PeakFQ. These figures have an added vertical line that indicates the mean of the point estimates. This line is not meant to indicate an ensemble mean or other recommendation of a "best" estimate; it is simply a way to vertically compare the point estimates. Figures 12–16 feature an added vertical line indicating the point estimate for the largest flood found to have occurred in over 350 years, 225,000 ft^3/s in 1826. Figure 12 also shows point estimates from other studies discussed in the next section.

Comparisons to Other Flood-Frequency Methods

Burn and Goel (2001) published flood-frequency analysis for the Red River at Winnipeg using the gaged record through 1998 (naturalized by Manitoba Water Stewardship as was the data we used), the three historical peaks from the Canada Department of Resources and Development (1953), and historical peaks from Rannie (1998). Burn and Goel's methods did not incorporate interval estimates; therefore, they converted the interval estimates to point estimates selected to "span the range of flood events identified by Rannie" (Burn and Goel, 2001, p. 356; see also table 2 of Burn and Goel, 2001). Burn and Goel (2001) found STP (lag-one serial correlation) and LTP (significant Hurst coefficient) in the Red River record and published flood-frequency analyses using several different distributions (generalized extreme value, PE3, and 3-parameter lognormal) and estimation methods (method of moments, MLE, and L-moments). (See Asquith and others [2017] for details about the effect of distribution and estimation choices on flood-frequency analysis.) Burn and Goal also used a mixed-noise model (Booy and Lye, 1989) that generated serially correlated data and compared it to an analysis with an independent dataset, focusing on floods with an AEP of 0.01 (their results have been included in table 4 for comparison to PeakFQ estimates; scenarios 11–21).

Harden (1999) reported flood-frequency results using the PE3 distribution fitted with the method of moments for several AEPs (an AEP of 0.01 is the only one in common with this study). Flood-frequencies were reported under five scenarios, three of which were included in table 4 (scenarios 22–24). Those three include using the gaged record, the gaged record plus four historical peaks, and the gaged record plus four historical peaks and Rannie's interval peaks converted to the midpoint of Rannie's range. Three of the historical peaks were those determined by the Canada Department of Resources and Development (1953) and used in our study, as well as the study by Burn and Goel (2001). The fourth event was described in 1776 (Rannie, 1998) but has a great deal of uncertainty surrounding it. Harden (1999) used a value that was slightly higher than the 1826 flood. However, the 1776 flood does not appear in the tree-ring record and, therefore, was not used in this study.

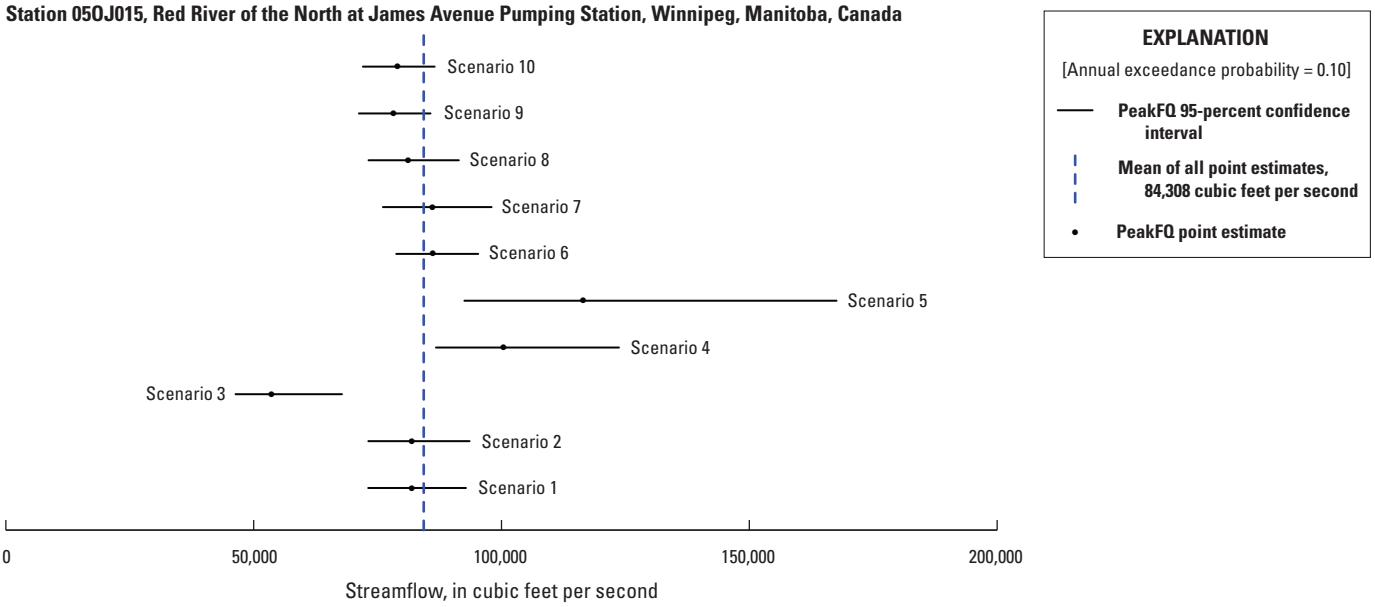

Figure 11. Point and interval estimates for streamgage station 05OJ015, Red River of the North at James Avenue Pumping Station, Winnipeg, Manitoba, Canada, floods with annual exceedance probability of 0.10, calculated using U.S. Geological Survey PeakFQ software (Veilleux and others, 2014) version 7.2 under 10 different scenarios. See table 4 for descriptions of the scenarios and the numeric values.

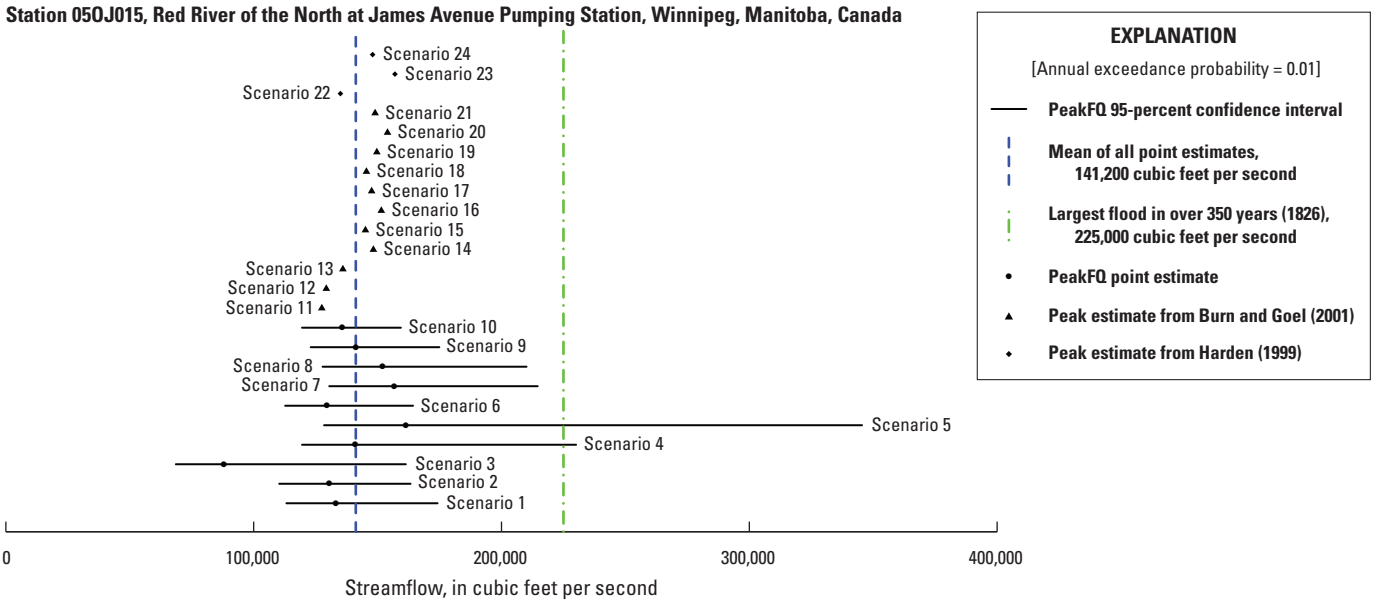

Figure 12. Point and interval estimates for streamgage station 05OJ015, Red River of the North at James Avenue Pumping Station, Winnipeg, Manitoba, Canada, floods with annual exceedance probability of 0.01, calculated using U.S. Geological Survey PeakFQ software (Veilleux and others, 2014) version 7.2 under 10 different scenarios and 13 additional point estimates from other flood-frequency studies (Burn and Goel, 2001; Harden, 1999). See table 4 for descriptions of the scenarios and the numeric values.

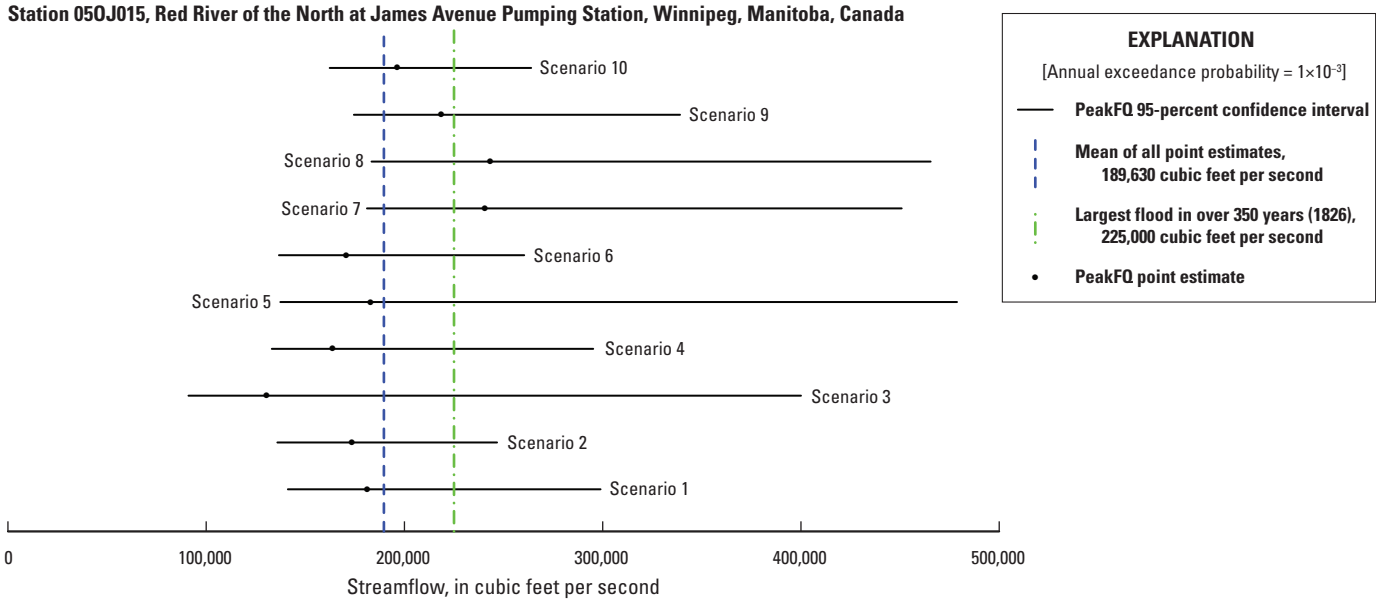

Figure 13. Point and interval estimates for streamgage station 05OJ015, Red River of the North at James Avenue Pumping Station, Winnipeg, Manitoba, Canada, floods with annual exceedance probability of 1×10^{-3}, calculated using U.S. Geological Survey PeakFQ software (Veilleux and others, 2014) version 7.2 under 10 different scenarios. See table 4 for descriptions of the scenarios and the numeric values.

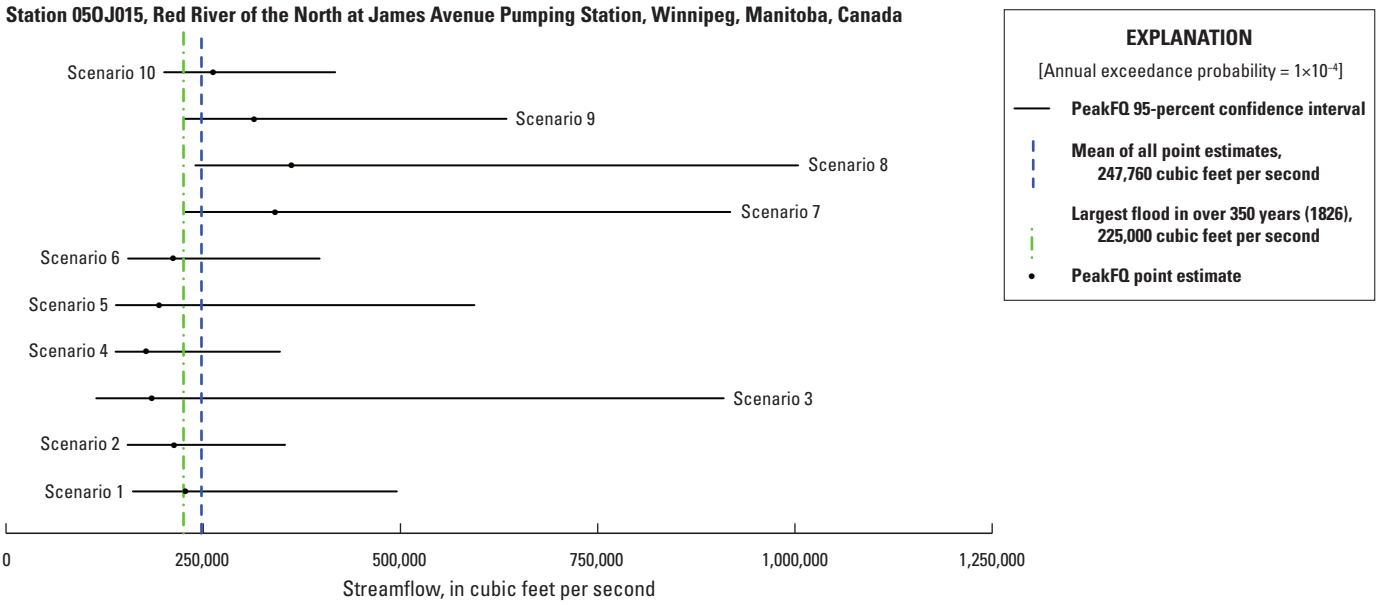

Figure 14. Point and interval estimates for streamgage station 05OJ015, Red River of the North at James Avenue Pumping Station, Winnipeg, Manitoba, Canada, floods with annual exceedance probability of 1×10^{-4}, calculated using U.S. Geological Survey PeakFQ software (Veilleux and others, 2014) version 7.2 under 10 different scenarios. See table 4 for descriptions of the scenarios and the numeric values.

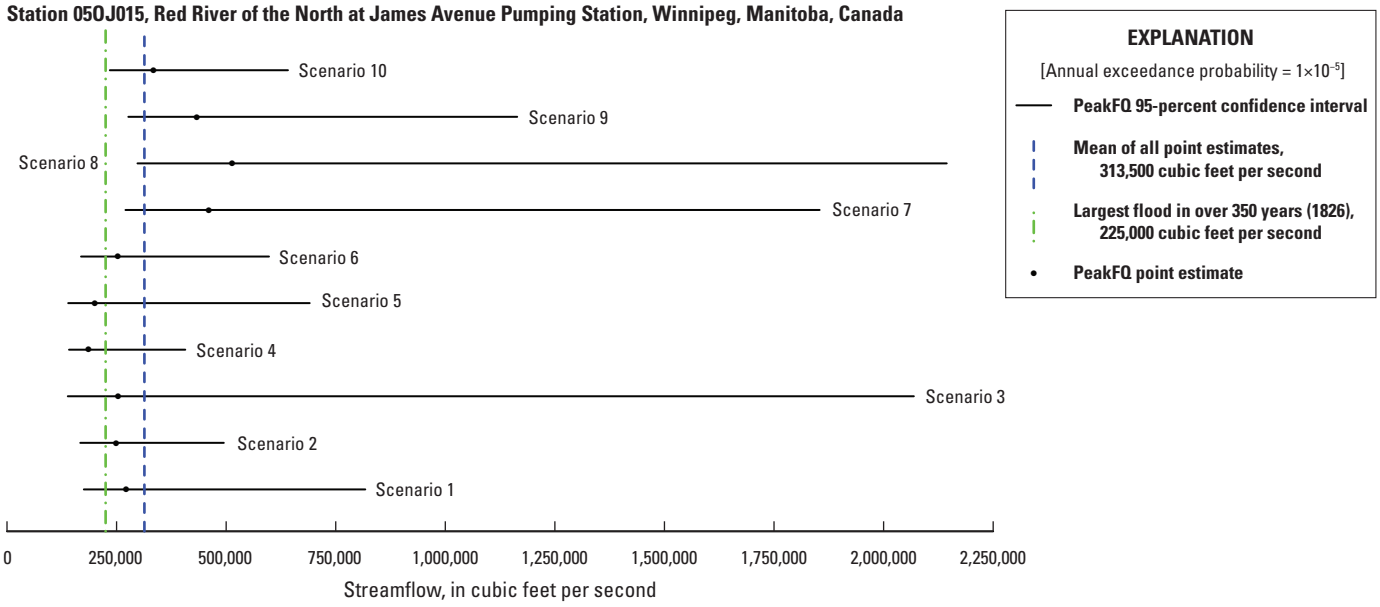

Figure 15. Point and interval estimates for streamgage station 05OJ015, Red River of the North at James Avenue Pumping Station, Winnipeg, Manitoba, Canada, floods with annual exceedance probability of 1×10^{-5}, calculated using U.S. Geological Survey PeakFQ software (Veilleux and others, 2014) version 7.2 under 10 different scenarios. See table 4 for descriptions of the scenarios and the numeric values.

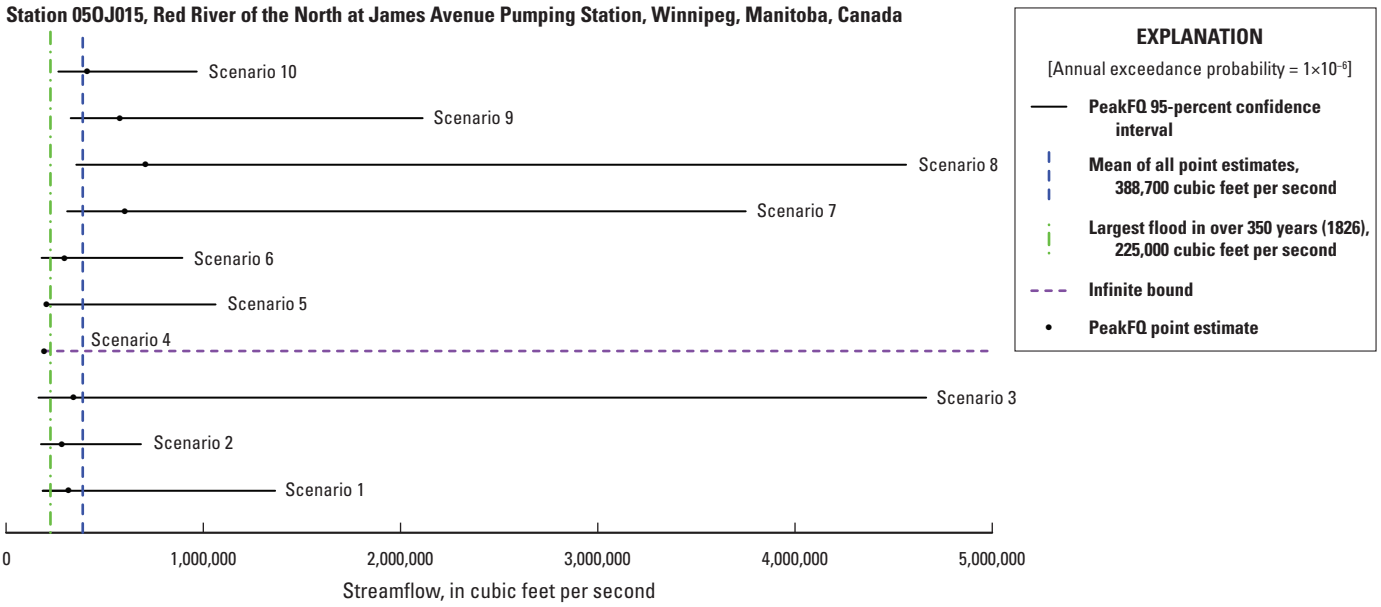

Figure 16. Point and interval estimates for streamgage station 05OJ015, Red River of the North at James Avenue Pumping Station, Winnipeg, Manitoba, Canada, floods with annual exceedance probability of 1×10^{-6}, calculated using U.S. Geological Survey PeakFQ software (Veilleux and others, 2014) version 7.2 under 10 different scenarios. See table 4 for descriptions of the scenarios and the numeric values.

Summary

The peak-flow record for the Red River at Winnipeg exhibits autocorrelation, a change point, and a monotonic trend. These are all nonstationarities, and Federal guidance does not yet exist for how to deal with these. Major implications for the autocorrelation include that trend analysis may report incorrect *p*-values and that there is redundancy in the record. When the MKT was modified to deal with serial correlation, the trend was still significant. When historical and paleoflood information is added to the record, this extends the record and provides additional information for the upper end of the distribution, offsetting the shortening of the effective record from autocorrelation. The identification of PILFs decreases the effect of some of the peaks in the drier period, which helps to address the change point.

The addition of regional information by using a skew weighted with regional information did not improve the fit of the distribution to the low AEP floods. Regional skew may not be the best estimate of skew for this site because the regional skew is based in many streamgages that have much smaller peaks and shorter periods of record. Historical and paleoflood data add information to the upper end of the flood-frequency distribution and provide more information for estimating very low AEP floods.

For AEPs of 0.10 (fig. 11 and table 4), compared to the full systematic record (scenarios 1 and 2), adding historical and paleoflood data and associated thresholds (scenarios 9 and 10) slightly decreases the flood estimates and the widths for the confidence bounds. Scenario 5 (using the most recent 30 years of record, assuming it is indicative of future conditions) has a much larger point estimate than the other scenarios and much wider confidence bounds. This is likely because of the serial correlation in the data, resulting in a record of less than 30 years and a great deal of uncertainty.

The graphical depiction of the estimates for the AEP of 0.01 (fig. 12) highlights differences in the estimates and confidence interval widths as more information is added to the analysis and different periods are used. Compared to using the systematic record with at-site skew (scenario 1), the addition of paleoflood and historical estimates and thresholds increases the 0.01 AEP estimates and decreases the confidence interval widths (scenario 9), showing the precision benefit of including additional information about flood magnitude and frequency. The largest point estimates, in decreasing order, are the most recent 30 years with EMA–PE3 (scenario 5, 161,000 ft^3/s), Harden's 1999 analysis using the systematic record plus historical peaks (scenario 23, 157,000 ft^3/s), the systematic peaks plus historical peaks (scenario 7, 156,000 ft^3/s), and Burn and Goel's 2001 mixed-noise model (scenario 20, 154,000 ft^3/s). Confidence bounds are not available for the other studies but for those determined with EMA–PE3 (scenarios 1–10), scenario 5 is noticeable for wide confidence bounds. Two scenarios, 7 and 23, show how adding historical peaks (without longer term paleoflood data) has the potential to bias the flood estimate up. Scenario 23 was based on the addition of four large historical peaks (one of them with a great deal of uncertainty) and no paleoflood data, so it is reasonable to think of this as potentially being biased high.

Scenarios 9 (systematic, historical, and paleoflood with at-site skew), 10 (systematic, historical, and paleoflood with weighted skew), and 20 (Burn and Goel, 2001; mixed-noise model that addresses the correlation in the series) seem the most realistic. Booy and Morgan (1985) used a fractional-noise model and Bayesian updating to show that the clustering of floods in the Red River record results in underestimates of flood risk for Winnipeg when the series is analyzed with methods that assume independence. The estimate from scenario 20 that address the correlation is within the confidence intervals for scenarios 9 and 10 (fig. 12). For this site, the addition of historical and paleoflood peaks and thresholds extend the record, offsetting the loss of information in a correlated series.

Figure 13 shows a distinct difference between those scenarios that have historical or paleoflood information (scenarios 7–10) and those that do not (scenarios 1–6), with the mean estimates for an AEP of 1×10^{-3} being above the overall mean point estimate for scenarios 7–10 and below the overall mean for scenarios 1–6. Adding only the historical peaks and thresholds results in large estimates with wide confidence intervals. Providing additional magnitude and frequency information with additional paleoflood data reduces the point estimates and the width of the confidence intervals. According to scenario 9 (systematic, historical, and paleoflood with at-site skew), the 1826 flood has an AEP of approximately 1×10^{-3}. If only the systematic data were used (scenario 1), figure 14 indicates that the 1826 flood would have an approximate an AEP of 1×10^{-4}.

Figures 15 and 16 further emphasize the differences in point estimates generated using systematic data or generated with systematic data and historical or paleoflood data. The figures also highlight some dramatic differences in confidence bounds for an AEP of 1×10^{-5} and 1×10^{-6}. If one desires to extend the record with estimates of peaks beyond the systematic record, historical and paleoflood data seem necessary to produce more precise confidence intervals.

Comparison of methods and AEPs in figures 15 and 16 shows that there is a great deal of variability among estimates, depending on the period of record used, on whether historical and paleoflood data are used, on the AEP being estimated, and on the skew used. Using the dry period only (scenario 3) underestimates the potential flood, and as the AEP becomes smaller, the dry period estimate has wider confidence bounds. Using the most recent 30 years of data (scenario 5) seems to bias the flood to the larger end when the AEP is 0.10 or 0.01 and results in huge confidence intervals as AEPs become smaller, which is understandable given 30 years of record is too short to reliably estimate very low AEP floods. The flood-frequency analysis that incorporated the mean-shifted dry period (scenario 6) has narrower confidence intervals than many of the other estimates, which is logical in that the shift reduced the variability in the underlying data. Adding historical peaks and thresholds (scenarios 7 and 8) to the systematic record tends to increase the confidence interval, which is

reasonable given that historical peaks are usually biased large and would affect the flood-frequency curve. However, by adding paleoflood peaks and thresholds (scenarios 9 and 10) that provide a longer-term description of the occurrence of very large floods, the confidence interval can narrow. The choice of skew also makes a significant difference in the point estimates and the width of the confidence intervals. For this case study and the given set of the data, the weighted skew generally gives lower point estimates and narrower confidence intervals than at-site skew; however, on the basis of visual inspection of the fit, at-site skew produces a distribution that better fits the peaks at the upper end of the distribution.

The effects of moving from an analysis with the systematic record to an analysis with a record that includes historical and paleoflood peaks and thresholds (including regional information in the form of a weighted skew) are shown in figures 17 and 18. Figure 17 shows the point and interval estimates, for a range of annual exceedance probabilities, resulting from flood-frequency analysis with the systematic record only using at-site (scenario 1; fig. 17*A*) and weighted skew (scenario 2; fig. 17*B*; table 4). Figure 18 shows the point and interval estimates, for a range of annual exceedance probabilities, resulting from flood-frequency analysis with systematic and historical peaks, historical and paleo-derived estimates, and paleo-derived thresholds, using at-site (scenario 9; fig. 18*A*) and weighted skew (scenario 10; fig. 18*B*; table 4). Again, the systematic record indicates the 1826 flood has an AEP of approximately 1×10^{-4}. However, when additional historical and paleoflood information is added, the 1826 flood becomes more likely with an AEP of approximately 1×10^{-3}. Using weighted skew reduces the point estimates for all flood quantiles except those with AEPs of 0.10 and results in more precise confidence bounds for the lowest AEPs.

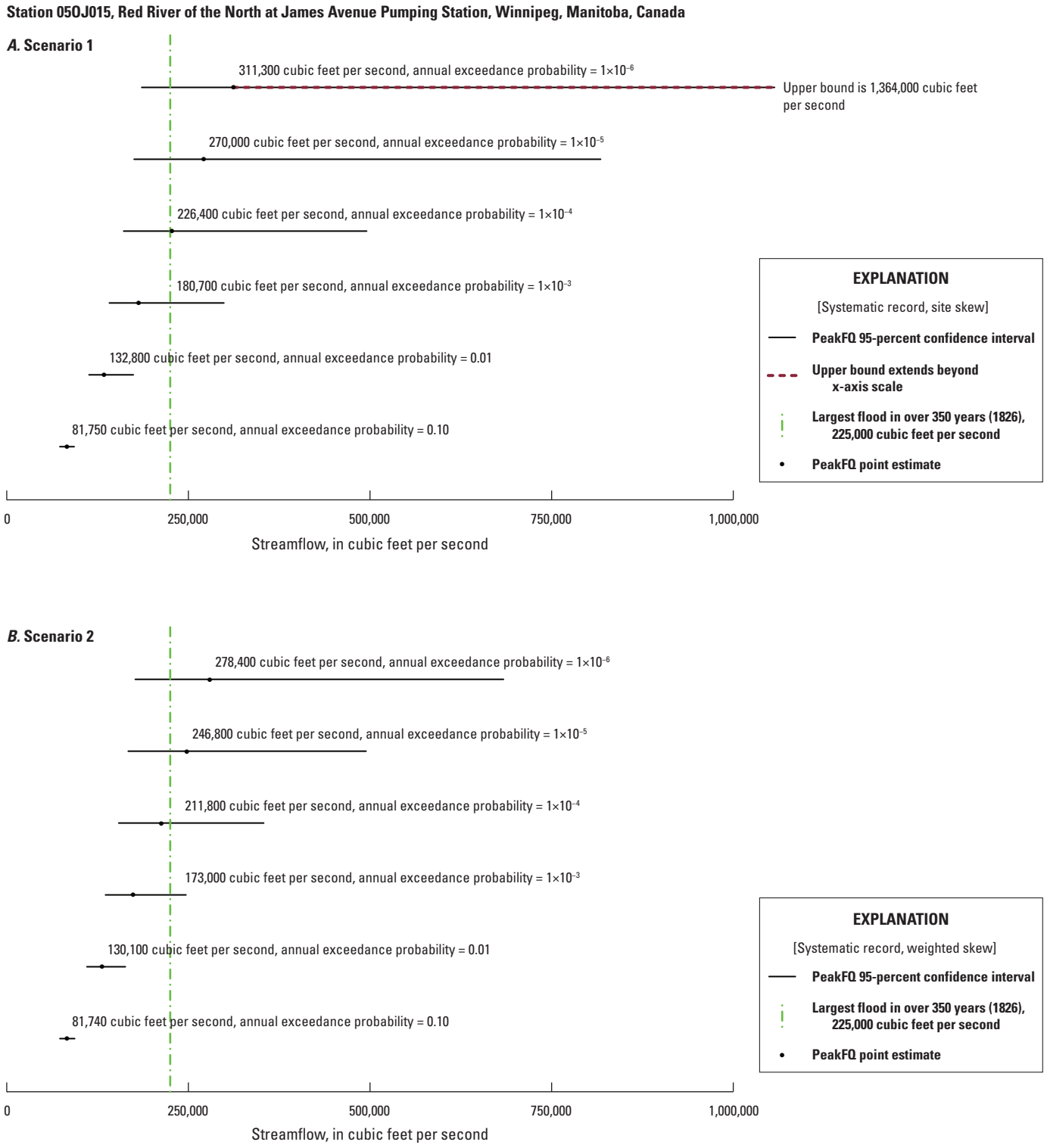

Figure 17. Point and interval estimates for a range of annual exceedance probabilities for streamgage station 05OJ015, Red River of the North at James Avenue Pumping Station, Winnipeg, Manitoba, Canada, floods, calculated using U.S. Geological Survey PeakFQ software (Veilleux and others, 2014) version 7.2, with *A*, at-site and *B*, weighted skew and the systematic record only. This depicts analysis results for *A*, scenario 1 and *B*, scenario 2 of table 4.

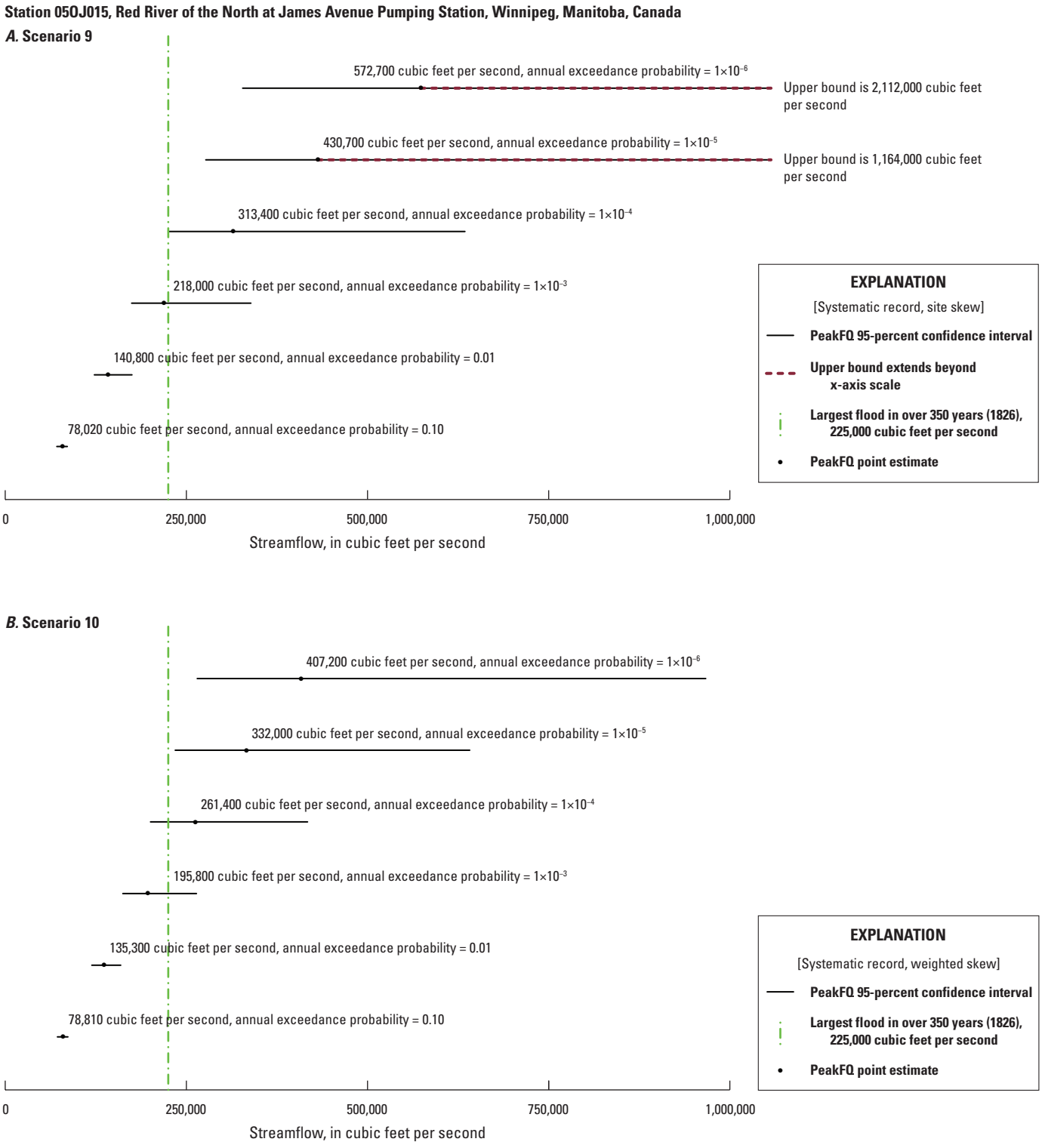

Figure 18. Point and interval estimates for a range of annual exceedance probabilities for streamgage station 05OJ015, Red River of the North at James Avenue Pumping Station, Winnipeg, Manitoba, Canada, floods, calculated using U.S. Geological Survey PeakFQ software version 7.2 with *A*, at-site and *B*, weighted skew and the systematic record plus historical peaks and thresholds and paleo-derived peaks and paleo-derived thresholds. This depicts analysis results for *A*, scenario 9 and *B*, scenario 10 of table 4.

Lower reach, Rapid Creek, South Dakota

The peak-flow record for the lower reach of Rapid Creek is based on streamflow records from multiple streamgages that were compiled and adjusted to be comparable with a paleoflood chronology developed for this reach (Harden and others, 2011). This synthetic record is referred to as a systematic record for consistency with the other case studies because the synthetic record is based on systematic record collection. Some peaks were designated as historical. The historical and systematic peaks are depicted in figure 19.

Initial Data Analysis

For the autocorrelation analysis, only the systemic record (1929–2009) peak series was examined. Figure 20 shows that this site does not have autocorrelation. In figure 21, the change-point algorithm assumes all peaks are consecutive (that is why the historical and paleoflood point estimates were not included) and relabels them 1 to *n*, where *n* is the number of values in the series. Figure 21 shows that the high outlier (1972) peak causes a change point, highlighting the challenge of determining reasonable criteria for change points given outliers. When the historical peaks are included, there is a downward trend in peak flow; however, when those peaks are not included, there is no trend in peak flow (fig. 22).

Flood-Frequency Analysis

Flood-frequency analysis with at-site skew was originally considered, but the fit (not shown) was very poor. Therefore, flood-frequency analysis was analyzed under three scenarios, with comparisons to seven other variations on flood-frequency analysis from a previous study:

1. systematic peaks, with weighted skew;
2. systematic peaks and historical peaks, with weighted skew;
3. systematic data, historical peaks, and paleo-derived interval peaks and thresholds, with weighted skew;

4–10. in addition to the analyses performed for this study, estimates were obtained from another flood-frequency study (Harden and others, 2011) and are presented as comparison scenarios. See table 5 (available for download at https://doi.org/10.3133/sir20205065) for more information.

The historical peaks under 7,000 ft^3/s were designated opportunistic and not included in the flood-frequency analysis. The peaks not designated as historical, but outside a systematic period of record, did not fit the distribution of the other peaks. Therefore, they were treated as opportunistic peaks (Sando and McCarthy, 2018) and removed. Sando (1998) found that the generalized skew coefficient from the map in Bulletin 17B (U.S. Water Resources Council,

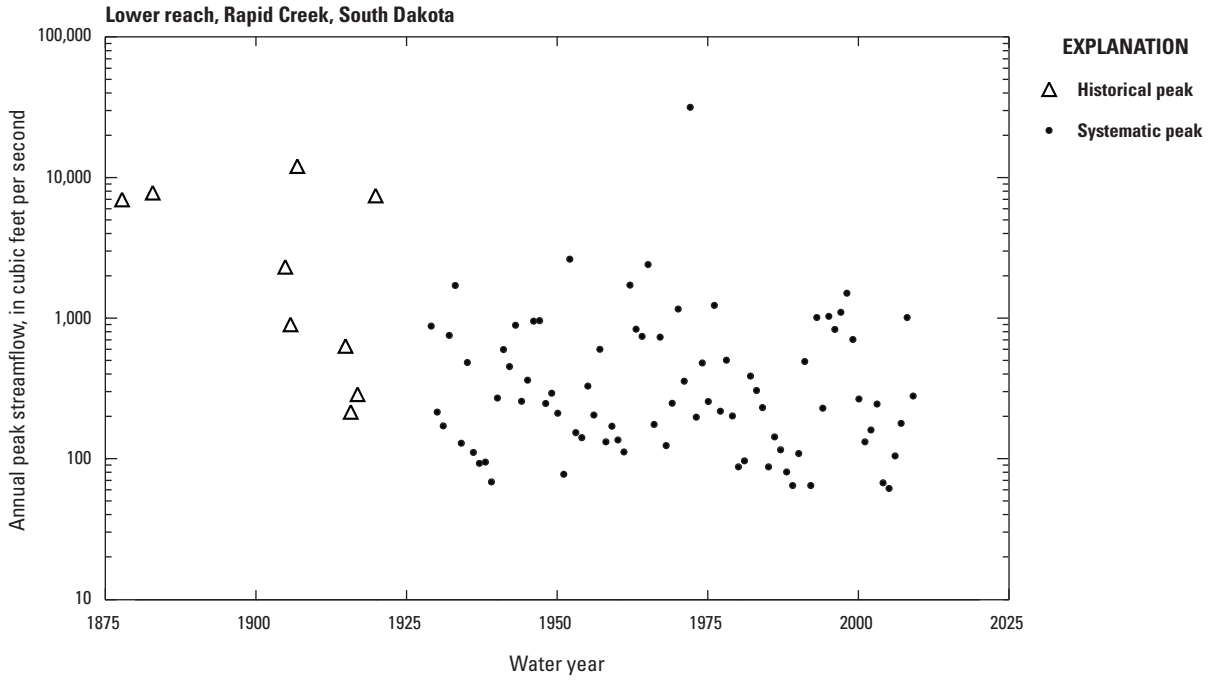

Figure 19. Systematic peaks and historical peaks for lower reach, Rapid Creek, South Dakota (Harden and others, 2011).

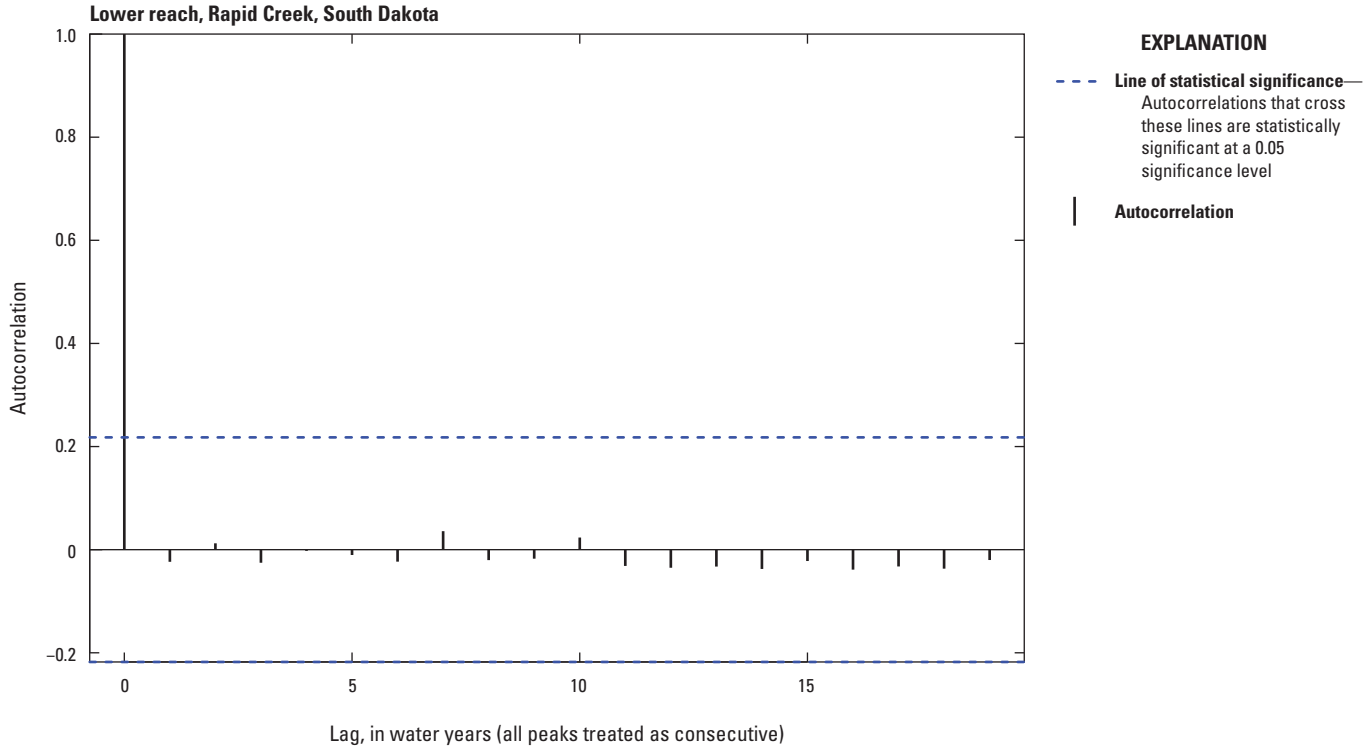

Figure 20. The autocorrelation for peaks in systematic period of record for lower reach, Rapid Creek, South Dakota.

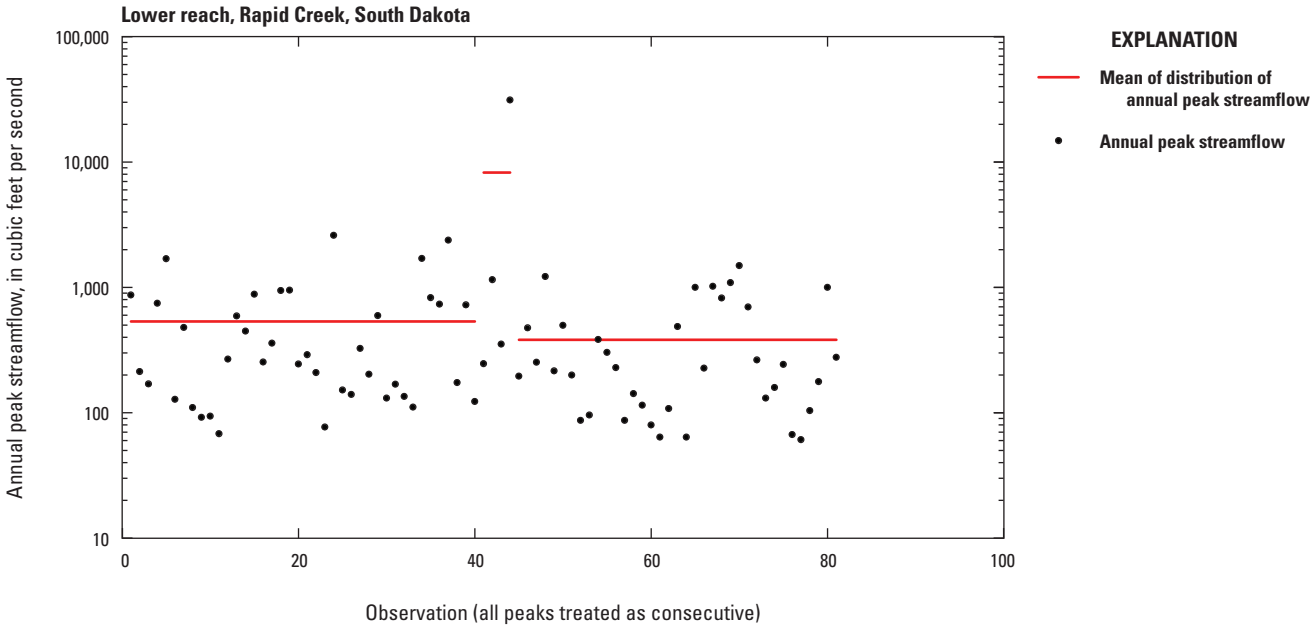

Figure 21. Change points in mean and variance for peaks in systematic period of record for lower reach, Rapid Creek, South Dakota.

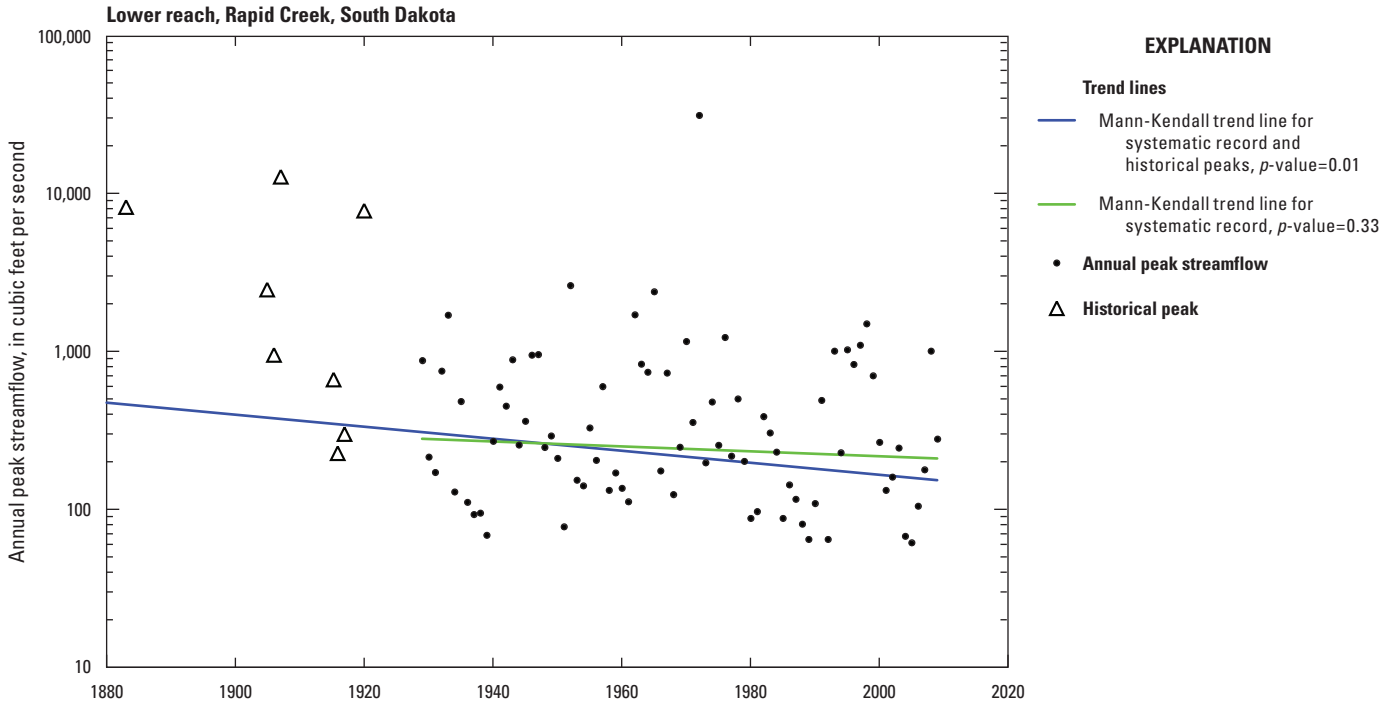

Figure 22. Mann-Kendall test for trend in the peak-streamflow record for lower reach, Rapid Creek, South Dakota.

1976) was adequate for South Dakota streamgages; therefore, the regional skew used was 0.194 with a mean square error of 0.302.

Given the magnitude of the 1972 peak, which was considerably larger than any other peak in the systematic or historical record, the flood-frequency curves for systematic data only and systematic plus historical data did not completely plot in PeakFQ because of the steep slope and extremely large confidence bounds on the very low AEPs and are not shown. The input information and the resulting flood-frequency curve for scenario 3 are shown in figures 23 and 24, and selected AEPs for the three scenarios are shown in table 5.

Comparisons to Other Flood-Frequency Methods

Harden and others (2011) completed flood-frequency analysis with several techniques using the same dataset with the exception that they used the opportunistic peaks in some analyses. As compared to some other flood-frequency methods used for comparisons to results at other sites in this study, the methods used by Harden and others (2011) were able to incorporate paleoflood data, including interval estimates and thresholds, and they provided confidence intervals for their estimates. They used two models that used PE3 distributions: FLDFRQ3 (O'Connell, 1999; O'Connell and others, 2002) and PeakfqSA (Cohn and others, 1997; Cohn and others, 2001; Griffis and others, 2004). FLDFRQ3 uses a Bayesian approach described in O'Connell and others (2002) with MLE. Results from Harden and others (2011) under seven different scenarios are shown in table 5 and designated as scenarios 4–10. Scenarios 4–7 use PeakfqSA and 8–10 use FLDFRQ3.

For an AEP of 0.01, all 10 scenarios are plotted in figure 25 to compare the estimates. Scenarios 1, 4, and 8 are very similar in that they use the same data (except for the opportunistic peaks dropped in this study). Scenarios 4 and 8 have much larger confidence intervals, presumably because of the four extra peaks used that do not fit well with the distribution of other peaks. Scenarios 2, 5, and 9 are also very similar (except for the opportunistic peaks). Scenario 5, using PeaksfqSA, has much larger confidence bounds than scenarios 2 and 9. Scenarios 3, 6, and 10 also use similar data (except for the opportunistic peaks) and produce similar estimates and confidence bounds. Scenario 7 uses top fitting by excluding peak values less than the median and produces the largest estimate for an AEP of 0.01.

Summary

The peak-flow record for the lower reach of Rapid Creek is not autocorrelated. The large 1972 peak causes a change point in the distribution if one uses a fairly short minimum segment length for change points (four in this analysis). This highlights the challenge in defining change points. The 1972 peak would have a large effect on moving means and variances that include this peak; therefore, one may want to treat the 1972 peak as an outlier rather than a change point. Change point detections are not definitive because of the many methods and criteria that can be adjusted. Statistical analysis should include graphical analysis (such as fig. 21) that allow one to place the change point(s) in context with what is known about the hydroclimatology and setting of the streamgage site.

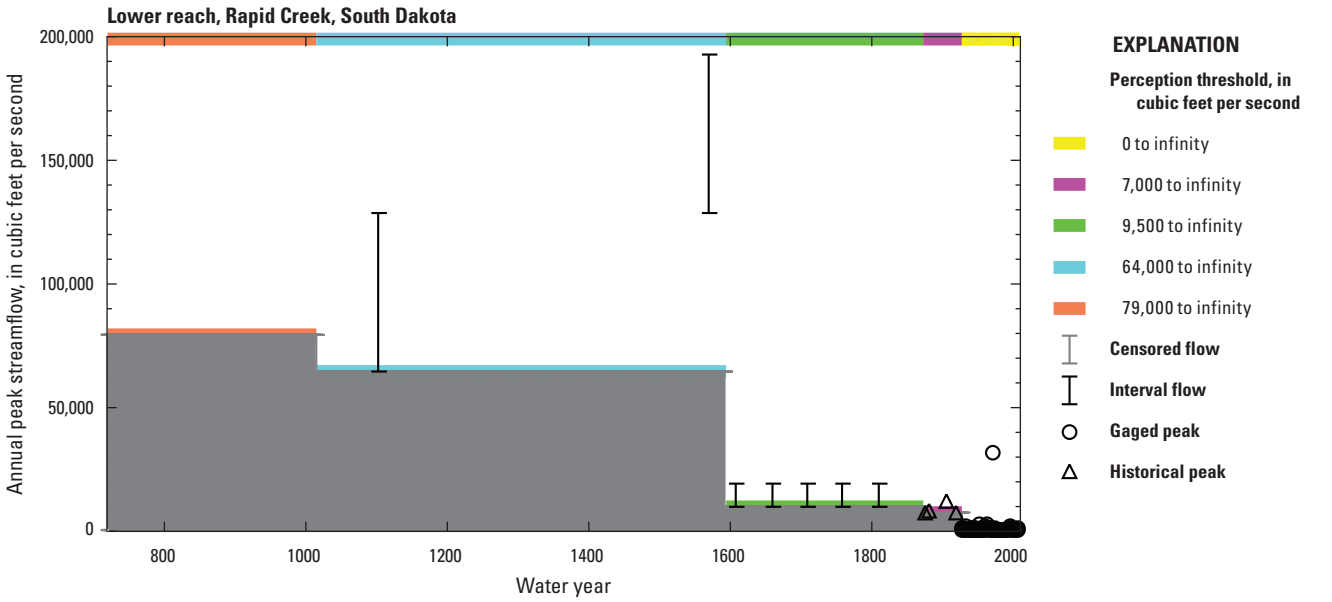

Figure 23. Systematic and historical peaks, paleo-derived interval peaks, and historical and paleo-derived thresholds used as input for flood-frequency analysis with weighted skew (scenario 3), lower reach, Rapid Creek, South Dakota.

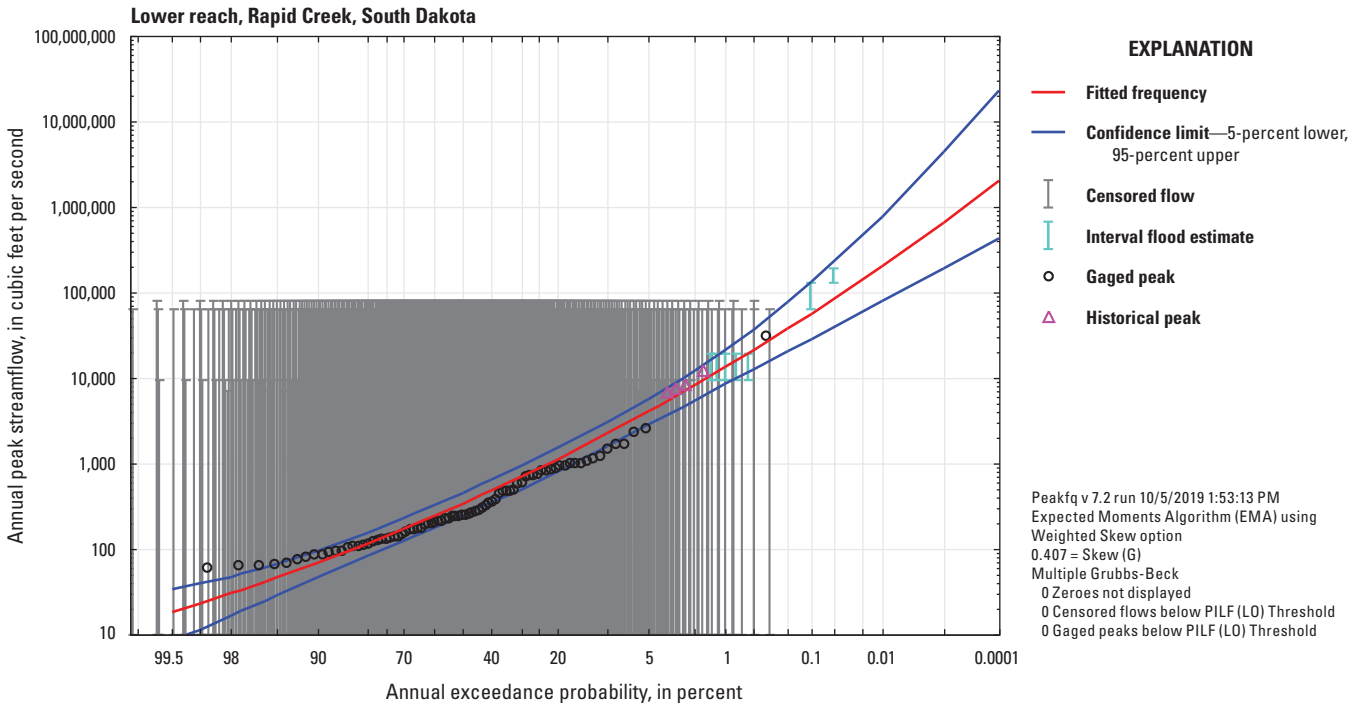

Figure 24. Annual exceedance probability plot and fitted distribution for lower reach of Rapid Creek, South Dakota, using the input data depicted in figure 23 and weighted skew (scenario 3).

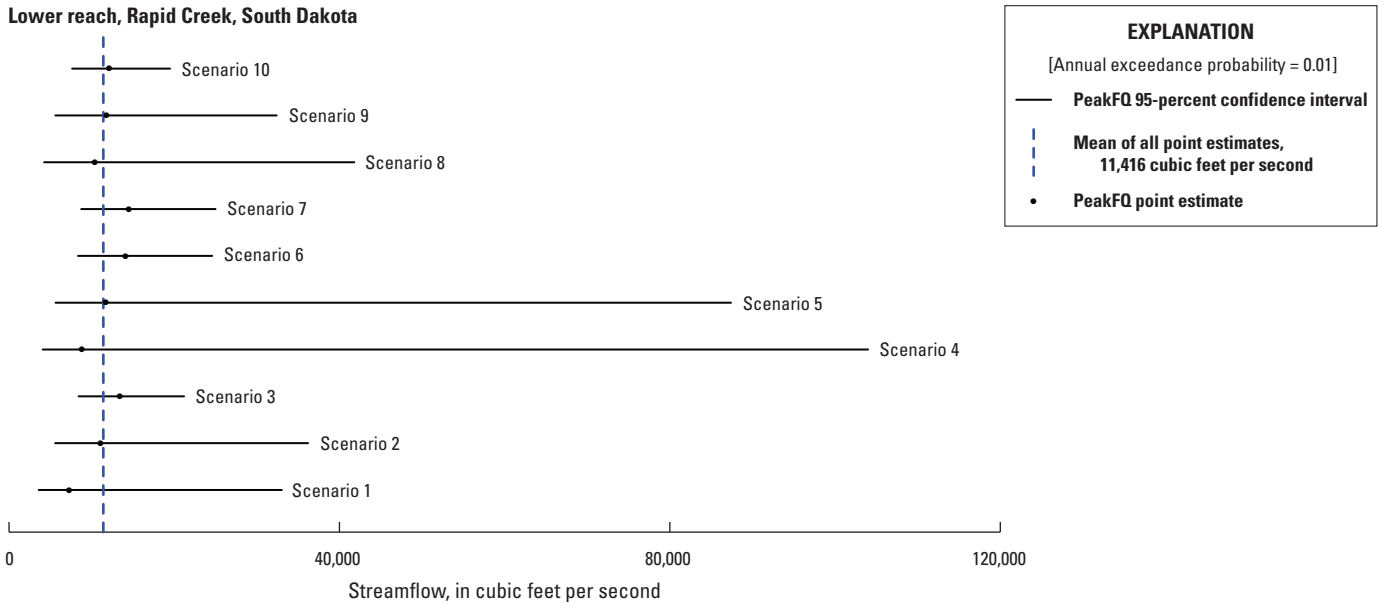

Figure 25. Point estimates and confidence bounds for scenarios using U.S. Geological Survey PeakFQ software (Veilleux and others, 2014) version 7.2 for lower reach of Rapid Creek, South Dakota, for floods with annual exceedance probability of 0.01, calculated under three different PeakFQ scenarios and compared to seven estimates from Harden and others (2011). See table 5 for descriptions of the scenarios and the numeric values.

When including early historical peaks, there is a statistically significant downward trend for the lower reach of Rapid Creek (fig. 22). This means that AEP estimates may be biased high, given current conditions, but cannot be extrapolated to future conditions.

Using a skew weighted with regional information greatly improved the fit of the distribution to the low AEP floods. This site is a special case in that it has a high outlier in the gaged record and large paleoflood peaks. The paleoflood peaks do help provide context for the outlier peak and improve the fit of the distribution. These large peaks result in a steep flood-frequency curve with large error bounds when estimating very low AEPs. Fewer scenario comparisons were plotted for this site than others in the study because the error bounds are so large that it is difficult to graphically compare the results. The complete set of AEPs estimated in this study, along with confidence bounds, are plotted in figures 26 and 27 for the three scenarios that were estimated using EMA–PE3 (scenarios 1–3).

Using paleoflood data results in a substantial reduction in the confidence bounds for very low AEPs; however, the bounds remain large for very low AEPs (less than 0.001). This jointly highlights the value of paleoflood data and the challenge of obtaining precise magnitude estimates for very low AEPs.

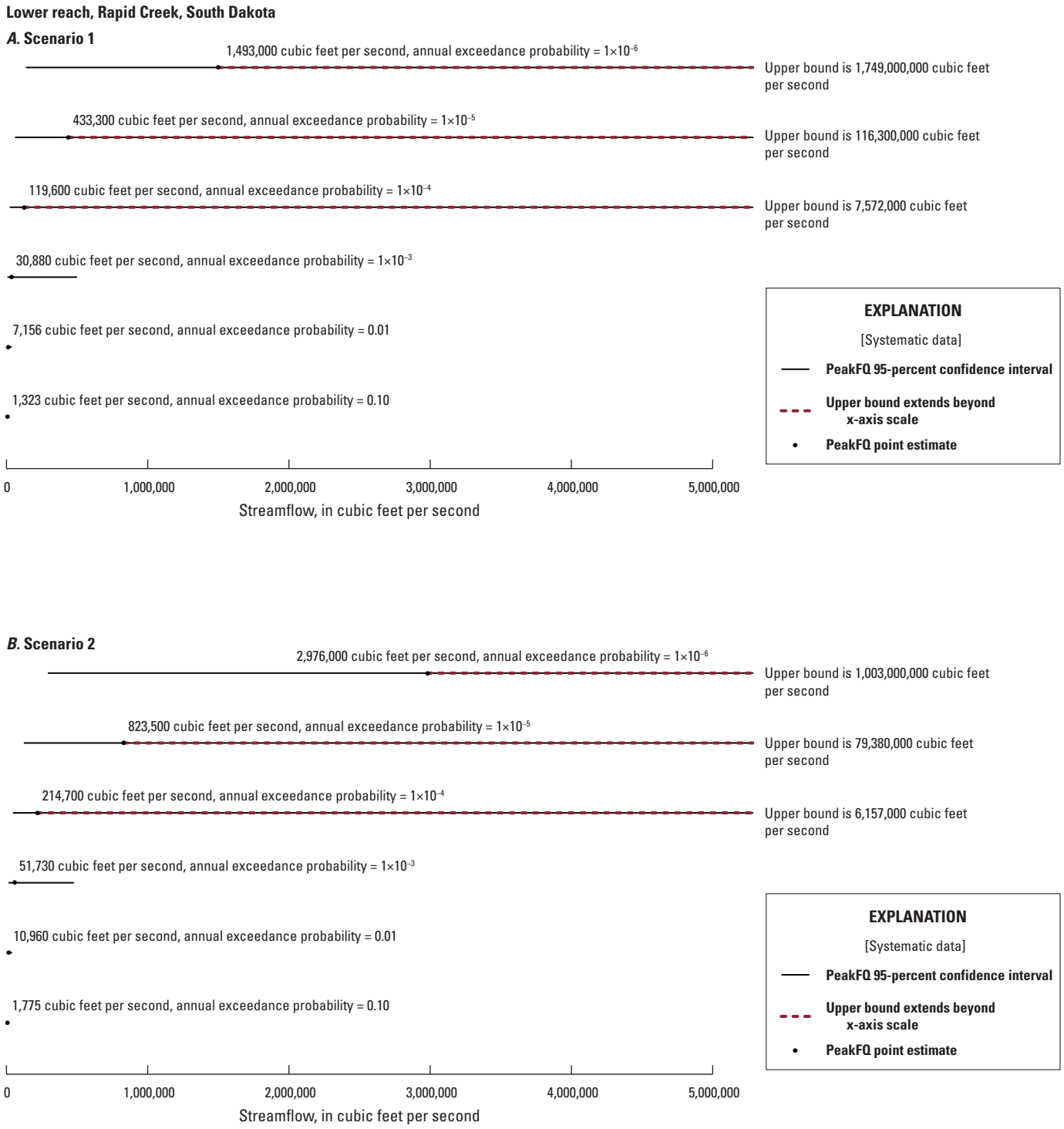

Figure 26. Point and interval estimates for a range of annual exceedance probabilities for lower reach of Rapid Creek, South Dakota, floods, calculated using U.S. Geological Survey PeakFQ software (Veilleux and others, 2014) version 7.2 with *A*, as weighted skew and systematic data and *B*, as systematic plus historical data. This depicts *A*, as scenario 1 and *B*, as scenario 2 of table 5.

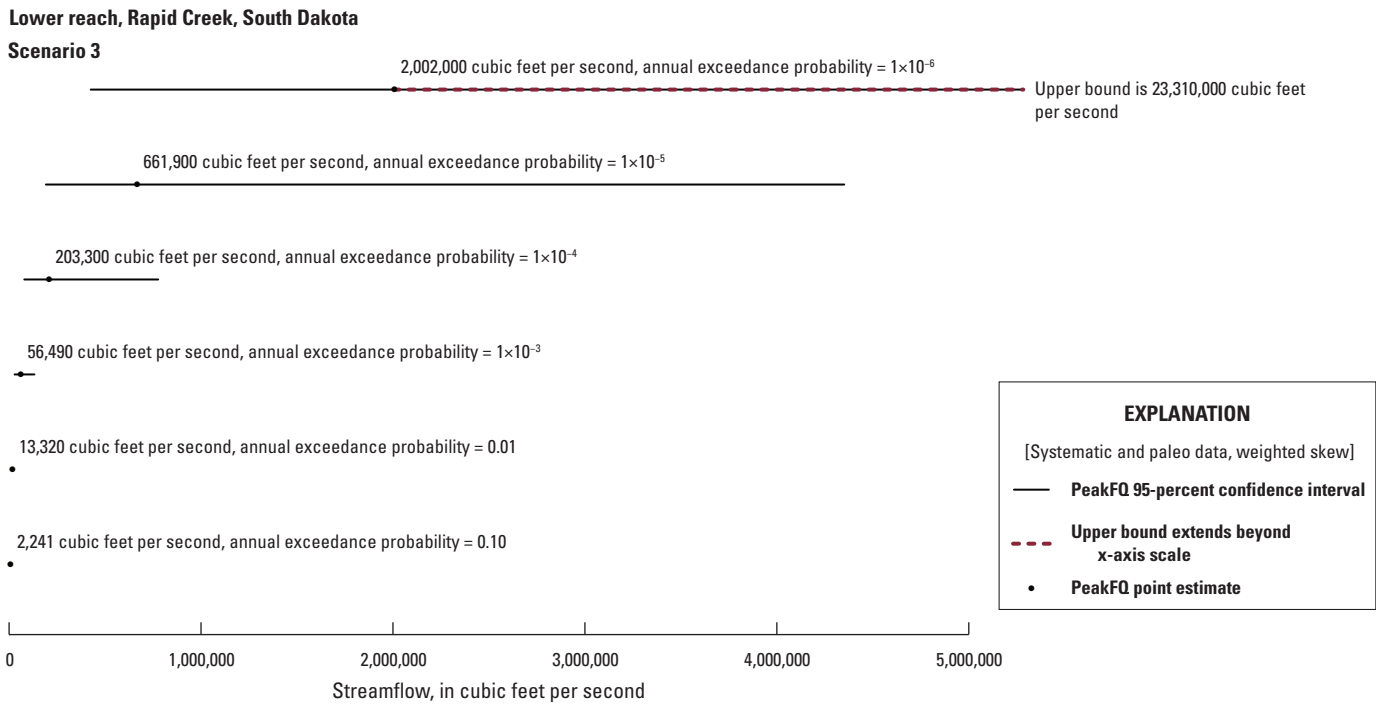

Figure 27. Point and interval estimates for a range of annual exceedance probabilities for lower reach of Rapid Creek, South Dakota, floods, calculated using U.S. Geological Survey PeakFQ software (Veilleux and others, 2014) version 7.2, with weighted skew and systematic, historical, and paleoflood data. This depicts scenario 3 of table 5.

Spring Creek, South Dakota

The peak-flow record for Spring Creek is based on streamflow records from multiple streamgages that were compiled and adjusted to be comparable with a paleoflood chronology developed for this reach (Harden and others, 2011). This synthetic record is referred to as a systematic record for consistency with the other case studies because the synthetic record is based on systematic record collection. More information about this site and the paleoflood data is available in Harden and others (2011).

Initial Data Analysis

The systematic peaks were examined for autocorrelation, change points, and a trend. There is no autocorrelation at this site (fig. 28), but there a several change points in the mean and variance (fig. 29). Most notable is the largest flood in the record (the 1972 flood), which causes a change in the mean and variance. Despite changes in mean and variance, there is no trend over the period of systematic record (fig. 30).

Flood-Frequency Analysis

Flood-frequency analysis with at-site skew was originally considered, but the fit (not shown) was very poor. Therefore, flood-frequency analysis was performed under three scenarios, with comparisons to two other variations on flood-frequency analysis from a previous study:

1. systematic peaks, with weighted skew;
2. systematic peaks with paleo-derived peaks and thresholds, with weighted skew;
3. systematic peaks with predicted paleo-derived peaks and thresholds on the basis of paleofloods in the nearby lower reach of Rapid Creek, with weighted skew;

4–5. in addition to the analyses performed for this study, estimates were obtained from another flood-frequency study (Harden and others, 2011) and are presented as comparison scenarios. See table 6 (available for download at https://doi.org/10.3133/sir20205065) for more information.

There were peaks in Harden and others (2011) outside a systematic period of record but not designated as historical. Given their occurrence outside the systematic period of record, they should be designated as historical using guidelines in Ryberg and others (2017). However, it was not clear whether

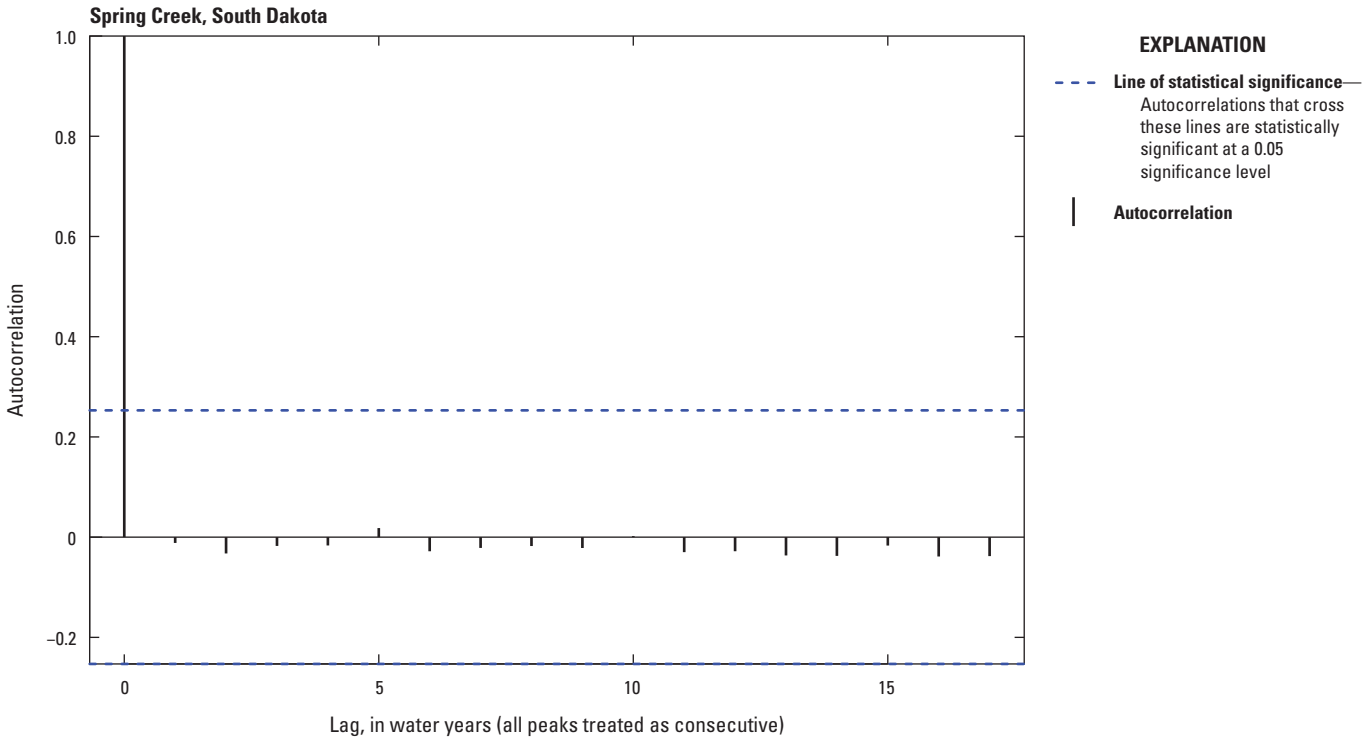

Figure 28. The autocorrelation for peaks in systematic period of record for Spring Creek, South Dakota.

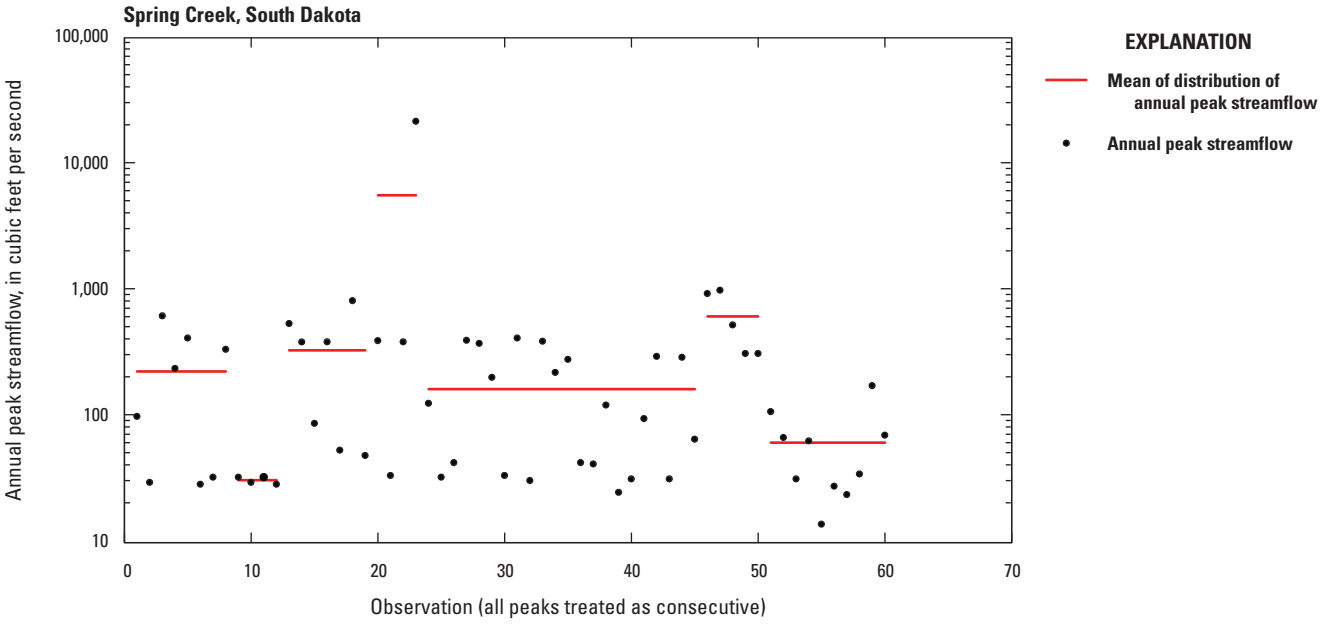

Figure 29. Change points in mean and variance for peaks in systematic period of record for Spring Creek, South Dakota.

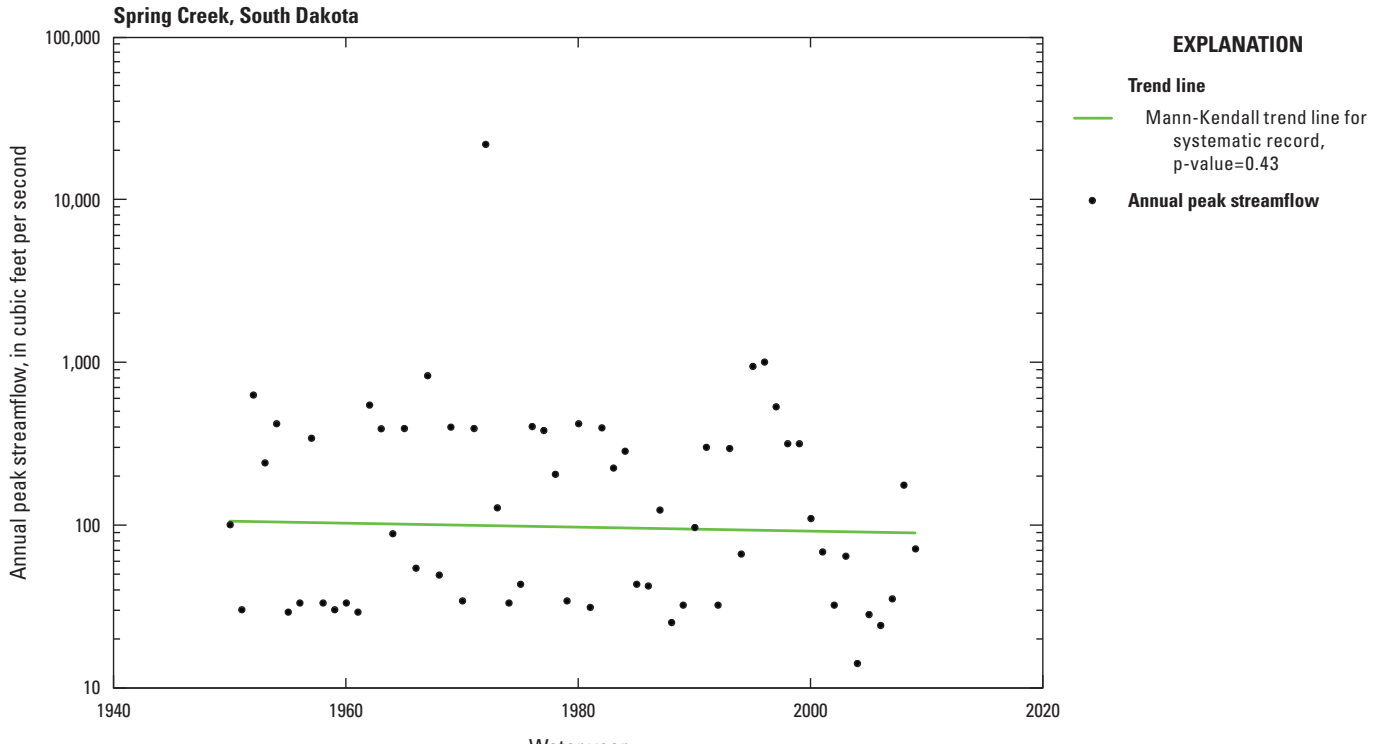

Figure 30. Mann Kendall test for trend in the peak-streamflow record for Spring Creek, South Dakota.

they were historical or opportunistic peaks. That is, it was not clear that there was a particular threshold above which all peaks would be recorded during the historical period. The historical peaks are below the perception threshold for large peaks based on the paleoflood data and provide no additional information to the analysis; therefore, the historical peaks were treated as opportunistic peaks (Sando and McCarthy, 2018) and removed from the analysis. Sando (1998) found that the generalized skew coefficient from the map in Bulletin 17B (Interagency Advisory Committee on Water Data, 1982) was adequate for South Dakota streamgages; therefore, the regional skew used was 0.194 with a mean square error of 0.302.

In all three EMA–PE3 scenarios, the fit of the flood-frequency curve was not as good as desired. PeakFQ did not identify any PILFs, but a PILF threshold of 40 was manually entered on the basis of visual inspection of the distribution and user expertise in order to focus the analysis on the upper end of the distribution.

For scenario 1, the flood-frequency curves for systematic data only did not completely plot in PeakFQ. This is because of the magnitude of the 1972 peak at the upper end of the distribution. It was considerably larger than any other peak in the systematic record and results in a steep flood-frequency curve slope and extremely large confidence bounds for the very low AEPs. The estimates for selected AEPs are shown in table 6.

The input data for scenario 2 are shown in figure 31. The resulting flood-frequency curve is shown in figure 32. The fit is not ideal, in part, because the paleoflood peaks and the gaged peak from 1972 are so large that they are a separate, much larger group of peaks than the rest. The estimates for selected AEPs are shown in table 6.

For scenario 3, the systematic and paleoflood records for Spring Creek and the lower reach of Rapid Creek were analyzed for correlation using Kendall's tau. The two sites are significantly correlated. Methods development was beyond the scope of this study, and MOVE.3 does not provide interval estimates (as described earlier); therefore, a simple non-parametric relation was developed using a Theil-Sen slope estimator (Sen, 1968; Theil, 1992) and the Conover equation (Conover, 1999) for the intercept. The resulting prediction equation is shown in equation 1. The relation was developed using the EnvStats package for R (Millard, 2013), which provides the functionality for confidence intervals, but not prediction intervals. Confidence intervals are better than point estimates, but are narrower than prediction intervals would be; however, because methods development was beyond the scope of this study, the confidence intervals were used for proof of concept.

$$SpringCreekPeak = 0.2939 \times LowerReachRapidCreekPeak + 55.5747 \quad (1)$$

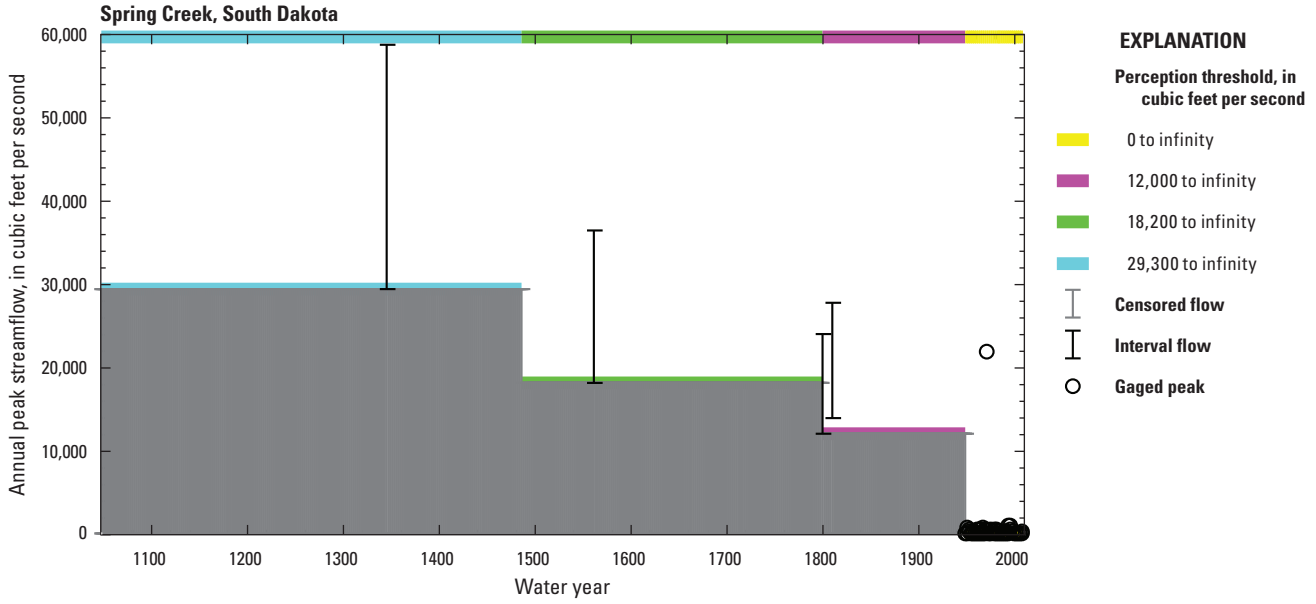

Figure 31. Systematic and paleo-derived interval peaks and thresholds used as input for flood-frequency analysis with weighted skew, Spring Creek, South Dakota.

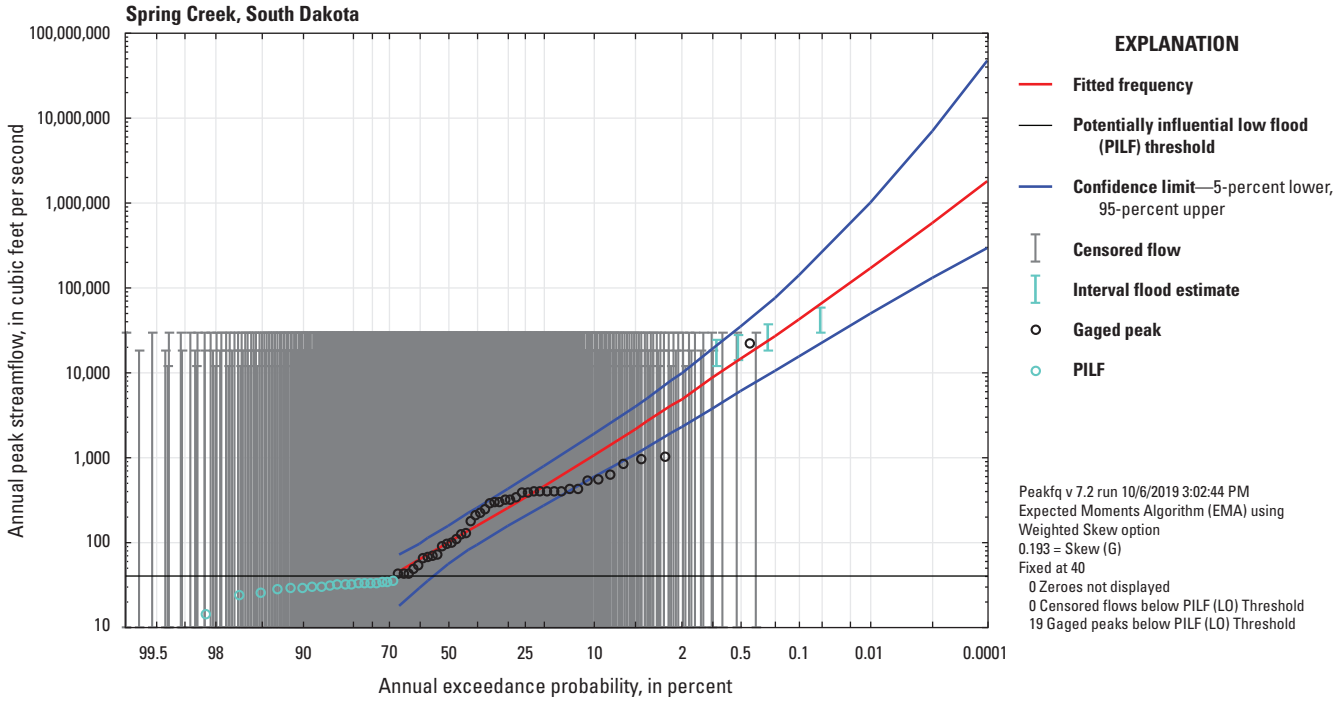

Figure 32. Annual exceedance probability plot and fitted distribution for Spring Creek, South Dakota, analyzed with the input data depicted in figure 31 and weighted skew.

where

SpringCreekPeak is the peak-flow estimate for Spring Creek; and

LowerReachRapidCreekPeak is the peak flow from the lower reach of Rapid Creek.

The paleoflood peaks were removed from the Spring Creek dataset, then from the beginning of the Rapid Creek paleoflood record, 1103, to 1949, the last year in the Spring Creek record before the systematic period, anytime there was a lower reach Rapid Creek peak, one was predicted for Spring Creek with 95-percent confidence limits. To use the lower reach Rapid Creek paleoflood peaks for prediction, the value for the magnitude of the peak was taken from table 6 of Harden and others (2011). The input information and the resulting flood-frequency curve for scenario 3 are shown in figures 33 and 34, and selected AEPs are shown in table 6.

Predicting paleoflood peaks at Spring Creek using lower reach Rapid Creek peaks had the effect of lowering the threshold at which a peak might be detected. Predicting paleoflood peaks this way filled in the record of peak magnitude between the systematic peaks and the group of larger peaks that included the 1972 peak. The confidence bounds for the very low AEPs narrowed as well. Despite the cautions about this type of transfer discussed earlier, it appears that it could be effective in some cases.

Comparisons to Other Flood-Frequency Methods

Harden and others (2011) completed flood-frequency analysis with several techniques using the same dataset with the exception that they used the opportunistic peaks in some analyses. They used two models that used PE3 distributions: FLDFRQ3 (O'Connell, 1999; O'Connell and others, 2002) and PeakfqSA (Cohn and others, 1997; Cohn and others, 2001; Griffis and others, 2004). Results from Harden and others (2011), under two different scenarios that used all available data (paleoflood, historical/opportunistic, and systematic), are shown in table 6 and are designated as scenarios 4 and 5. Scenario 4 uses PeakfqSA, and scenario 5 uses FLDFRQ3.

For an AEP of 0.01, all five scenarios are plotted in figure 35 to compare the estimates. Scenario 1, systematic data only, analyzed with PeakFQ has large confidence bounds as the distribution is affected by the single outlier in 1972. The rest of the scenarios use paleoflood data. Results for scenarios 2, 4, and 5 are similar because much of the same data and the same probability distribution, PE3, are used. Scenario 3 has the predicted paleoflood peaks, which resulted in more paleoflood peaks in the record. Including the predicted paleoflood peaks results in more information about the theoretical distribution and narrower confidence bounds.

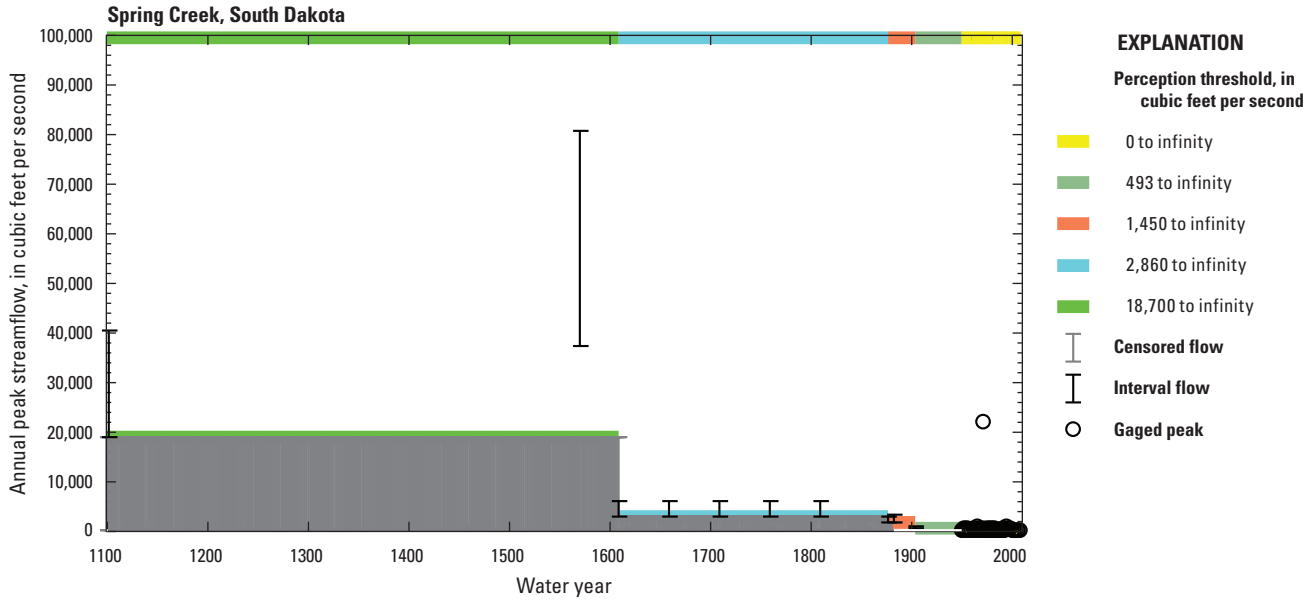

Figure 33. Interval peaks predicted from lower reach Rapid Creek, thresholds, and systematic data used as input for flood-frequency analysis with weighted skew, Spring Creek, South Dakota.

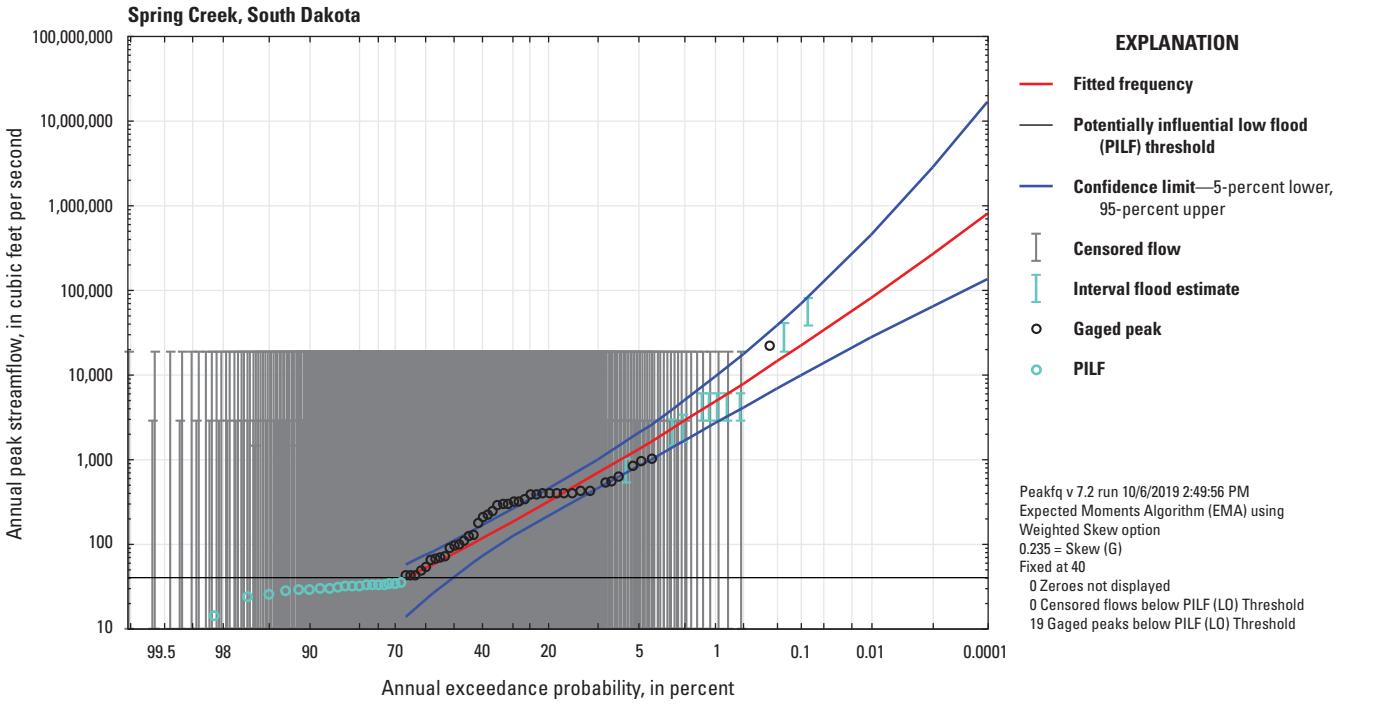

Figure 34. Annual exceedance probability plot and fitted distribution for Spring Creek, South Dakota, analyzed with the input data depicted in figure 33 and weighted skew.

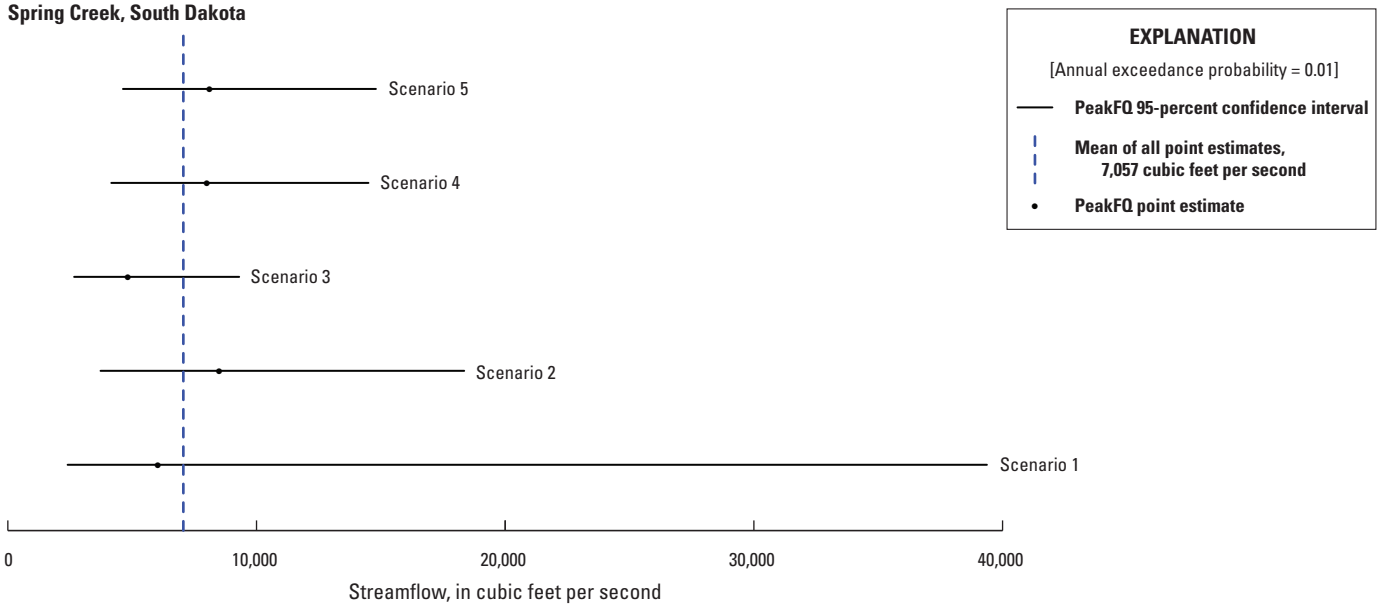

Figure 35. Point estimates and confidence bounds for PeakFQ scenarios for Spring Creek, South Dakota, for floods with annual exceedance probability of 0.01, calculated under three different scenarios using U.S. Geological Survey PeakFQ software (Veilleux and others, 2014) version 7.2 and compared to two estimates from Harden and others (2011). See table 6 for descriptions of the scenarios and the numeric values.

Summary

The lower reach, Rapid Creek peak-flow record is not autocorrelated and does not have a trend. However, several change points were identified. The same change-point methodology was used for all site analyses in this report, but this example shows that an analyst might want to adjust the settings on a case-by-case basis depending on their degree of concern about change points. The large 1972 peak also causes a change point in the distribution, as it does for the lower reach of Rapid Creek. Again, this shows that change-point detections are not definitive and should be accompanied by graphical analysis.

The use of regionally weighted skew greatly improved the fit of the distribution to the very low AEP floods. Like the lower reach of Rapid Creek, this site has a high outlier in the gaged record, a peak in 1972, and large paleoflood peaks. The paleoflood peaks provide context for the 1972 gaged peak and improve the fit of the distribution. The inclusion of regional information by estimating peaks based on paleoflood peaks from the lower reach of Rapid Creek added more information to the statistical distribution, resulting in a better fit. However, there are methodological issues that would need to be worked out before such estimations could be made in practice (see Regression Methods section).

Peaks outside the systematic period of record need to be examined carefully to determine whether they are opportunistic peaks, which do not provide additional information about appropriate thresholds for missing periods, or whether they are large peaks from which a threshold can be derived. Although helpful in determining very low AEPs, paleoflood data can raise concerns if they appear to come from a different, larger population than the peaks in the systematic record. Ideally, the range of paleoflood peaks should have some overlap with the observed range to provide a smooth transition of the distribution.

The AEPs under the three PeakFQ scenarios are plotted in figures 36 and 37. Estimating very low AEPs at this site without paleoflood data results in an upper bound for an AEP of 1×10^{-6} that is into the billions. Adding paleoflood information dramatically reduces the error bounds (fig. 36). Having a large set of paleoflood peaks, when they were predicted, continues to increase the precision of the estimates, although error bounds for an AEP of 1×10^{-5} and 1×10^{-6} are still very large.

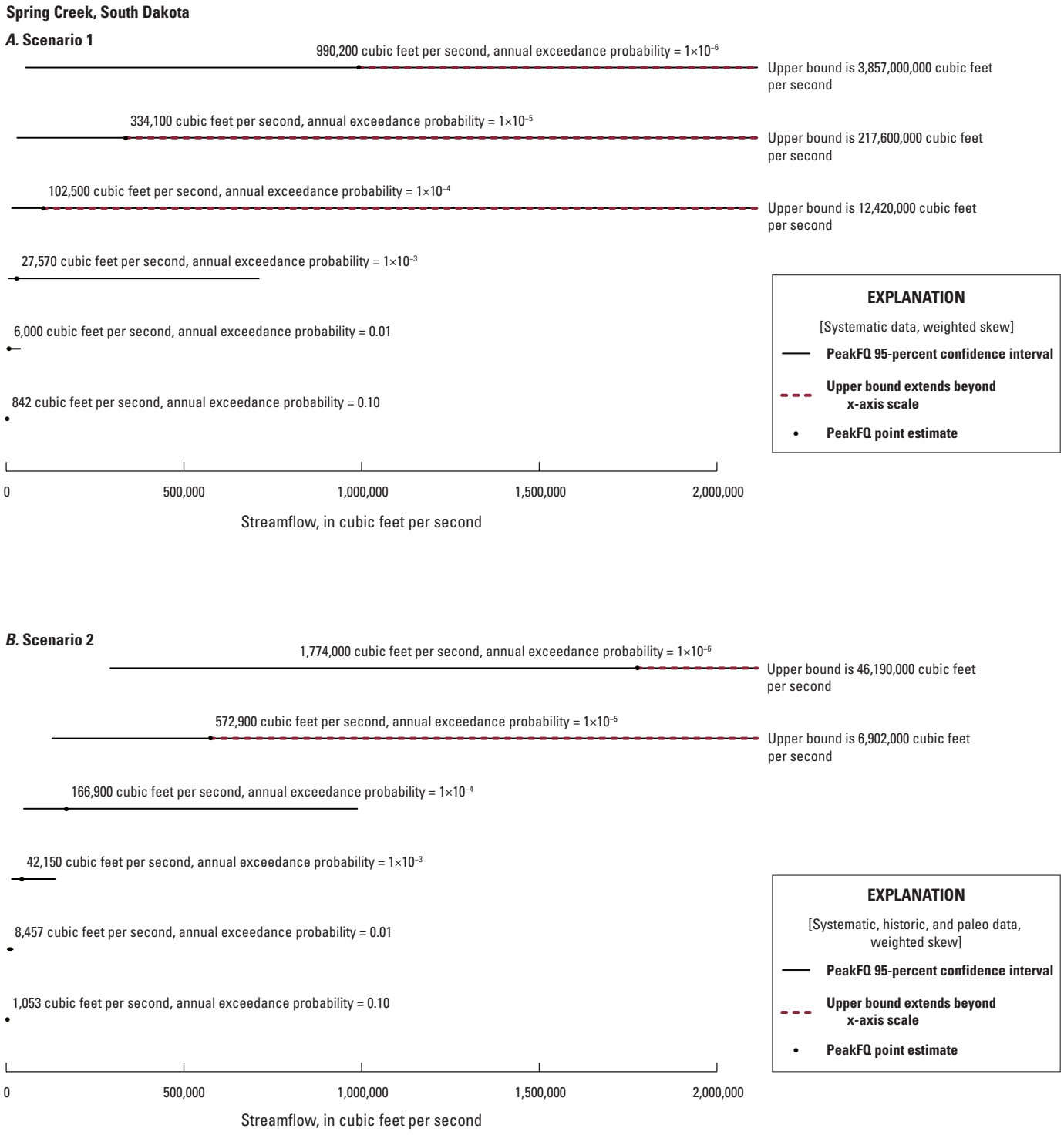

Figure 36. Point and interval estimates for a range of annual exceedance probabilities for Spring Creek, South Dakota, floods, calculated using U.S. Geological Survey PeakFQ software (Veilleux and others, 2014) version 7.2, with *A,* as weighted skew and systematic data and *B*, as systematic plus paleoflood data. This depicts analysis results for *A*, scenario 1 and *B*, scenario 2 of table 6.

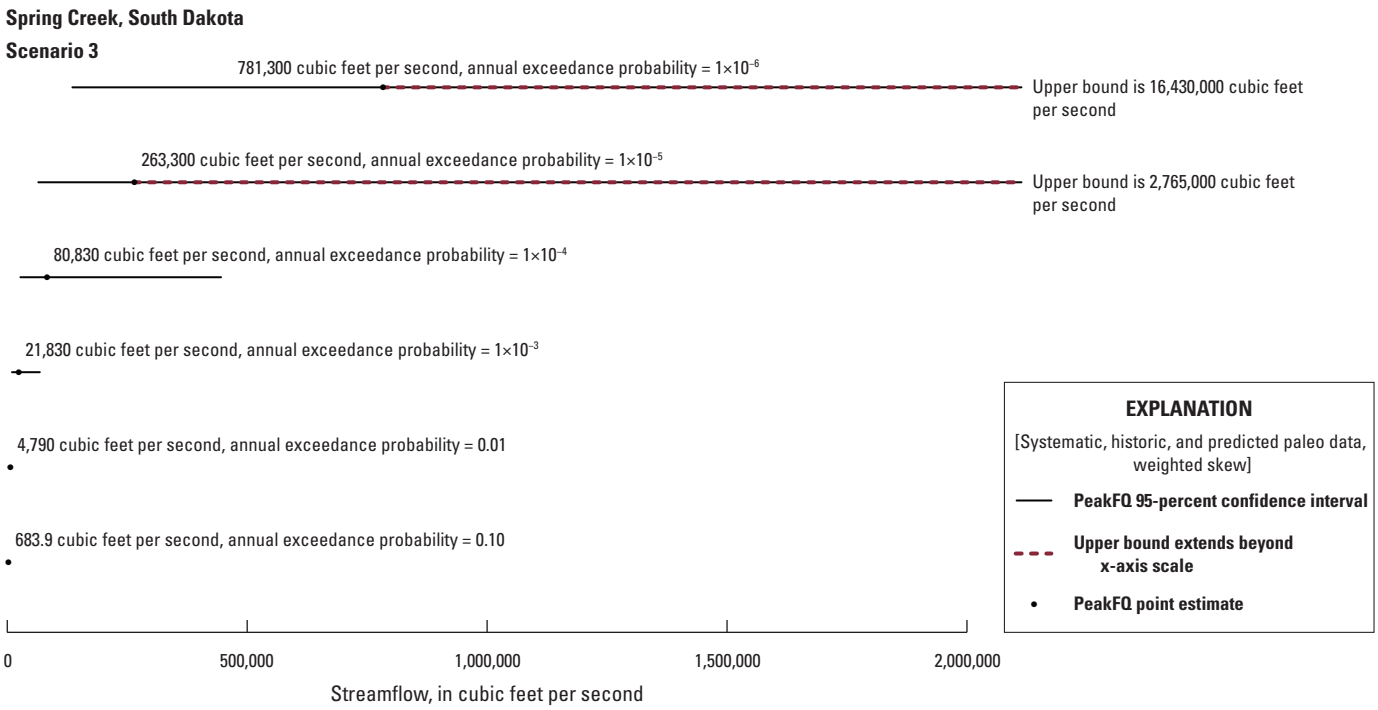

Figure 37. Point and interval estimates for a range of annual exceedance probabilities for Spring Creek, South Dakota, floods, calculated using U.S. Geological Survey PeakFQ software (Veilleux and others, 2014) version 7.2, with weighted skew and systematic, historical, and predicted paleoflood data. This depicts analysis results for scenario 3 of table 6.

Cherry Creek near Melvin, Colorado

This site had one historical peak; however, that peak was qualified with a code 3 indicating it occurred because of a dam failure. In 1933, Castlewood Canyon Dam, upstream from the Melvin streamgage (06712500), failed (Jarrett, 2000). That flood left evidence of flood-deposited sediments, and the peak value is available; however, because peak value was the result of a dam failure, the peak was not used in flood-frequency analysis. The paleoflood magnitude was determined using the slope-conveyance method (U.S. Geological Survey, 2019), and the age of the paleoflood deposits was determined using relative-dating methods, including degree of soil development, surface-rock weathering, surface morphology, and boulder development (Jarrett, 2000; Jarrett and Tomlinson, 2000; Kohn and others, 2016). Jarrett (2000) determined that the largest flood in 1,500 to 5,000 years was 2,100 m^3/s (74,161 ft^3/s) and that the flood with an AEP of 1×10^{-4} was approximately 2,200 m^3/s (77,692 ft^3/s).

Initial Data Analysis

The systematic peaks were examined for autocorrelation. Figure 38 indicates that autocorrelation is not a concern. Then the systematic peaks were examined for change points and a change point was found (fig. 39); however, the short period of record makes it difficult to determine whether this change point is a change in the distribution, or it simply breaks the record into periods affected by outliers. It also is difficult to determine what might be considered an outlier in a record this short.

Trend analysis was completed with and without the historical peak. The historical peak, a result of dam failure, was not used in flood-frequency analysis, but likely represented what would have been a large runoff event. The trend test is resistant to outliers, so the historical peak was used for comparison of the trend lines. Visually, one might perceive a downward trend at this site (fig. 40); however, because of the variability in the peaks, there is not a significant trend with or without the historical peak.

Flood-Frequency Analysis

Flood-frequency analysis was completed under two scenarios, comparisons to eight other flood-frequency analysis results using different distributions and a different fitting method:

1. systematic peaks and weighted skew;
2. systematic peaks with paleo-derived peaks and thresholds and weighted skew;

3–10. at-site point estimates for flood magnitudes using the asymmetric exponential power, generalized extreme value, generalized logistic, generalized normal, generalized Pareto, PE3, Wakeby, and Weibull distributions

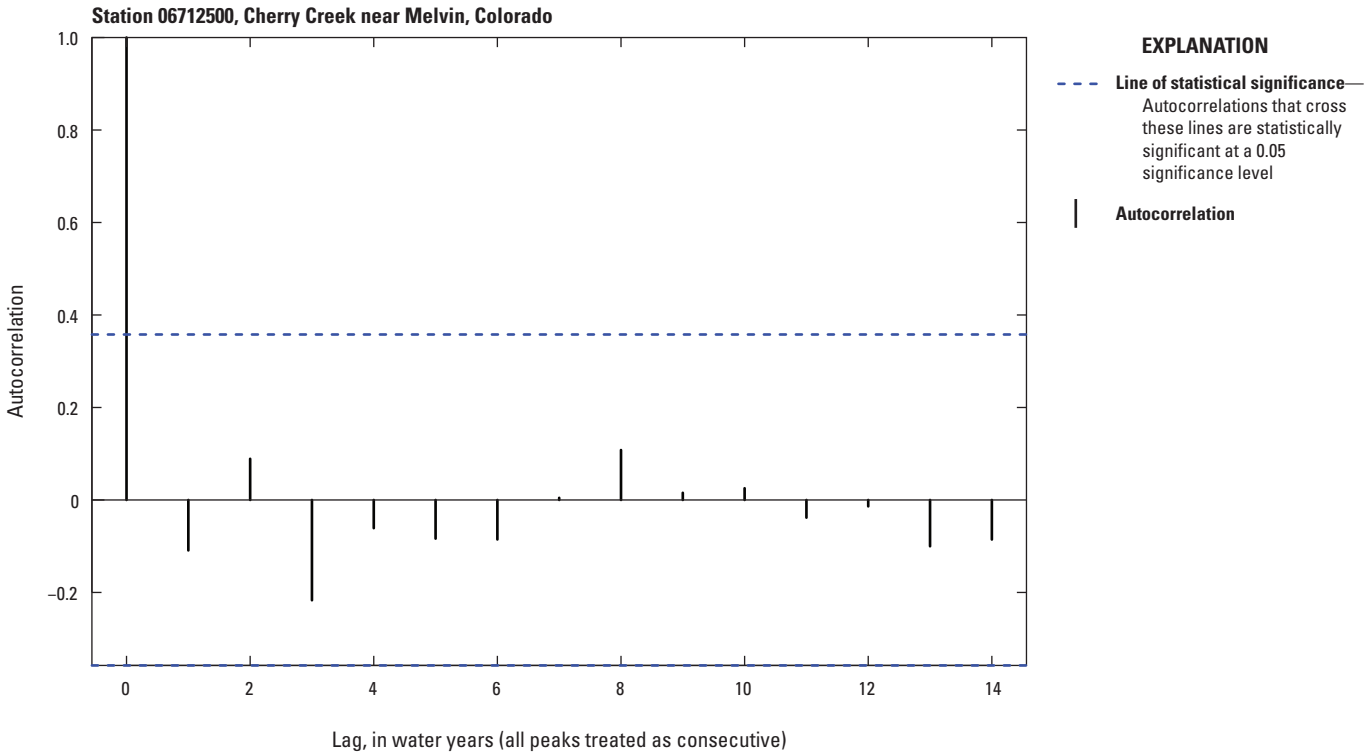

Figure 38. The autocorrelation for peaks in systematic period of record for streamgage station 06712500, Cherry Creek near Melvin, Colorado.

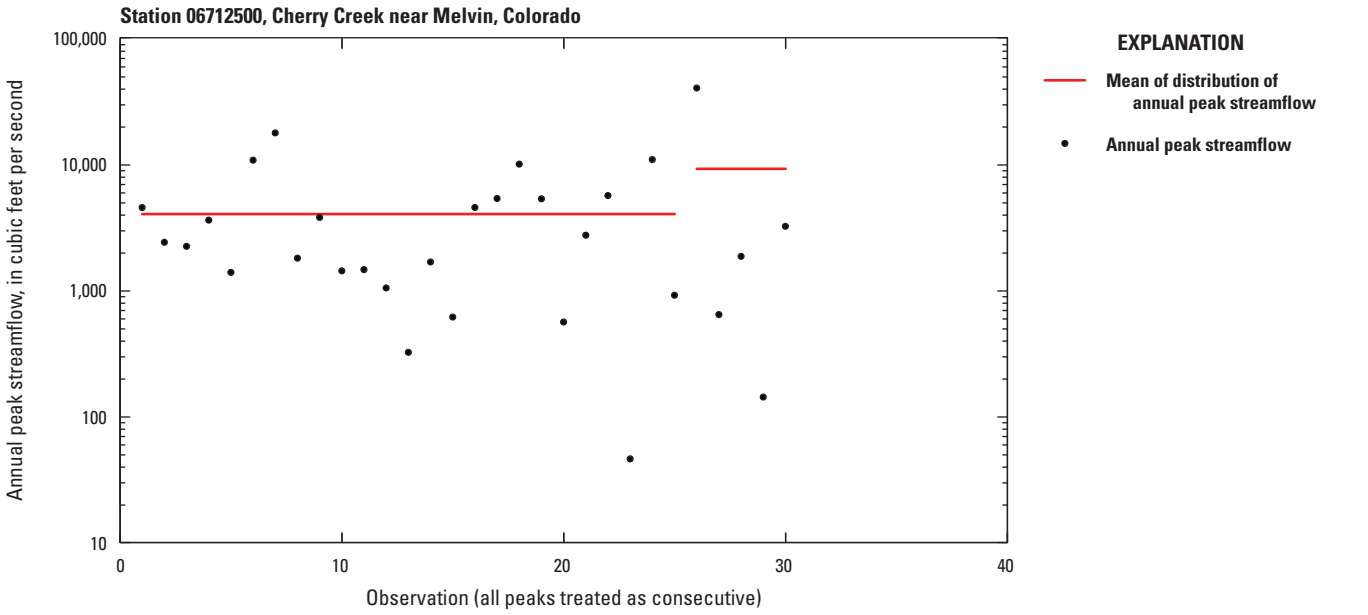

Figure 39. Change points in mean and variance for peaks in systematic period of record for streamgage station 06712500, Cherry Creek near Melvin, Colorado.

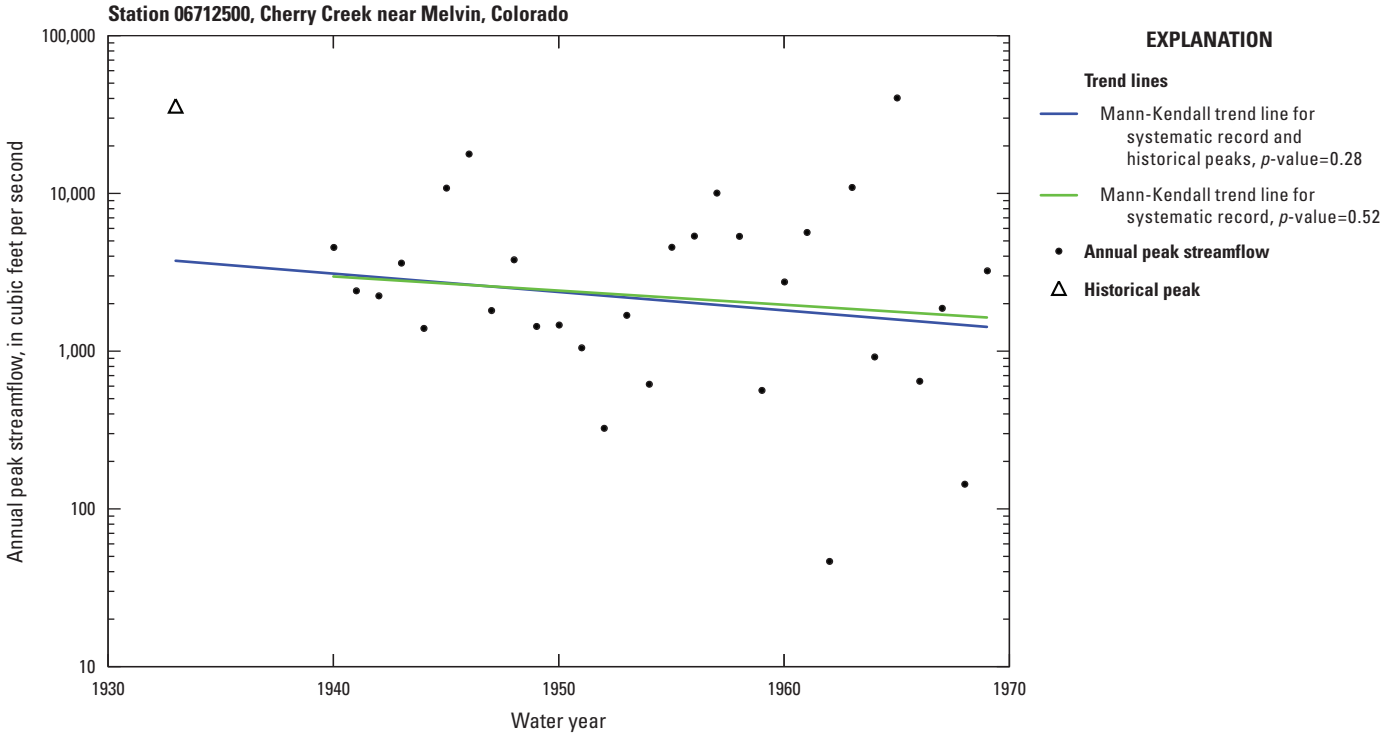

Figure 40. Mann-Kendall test for trend in the peak-streamflow record for streamgage station 06712500, Cherry Creek near Melvin, Colorado.

fitted using the method of L-moments (W. Asquith, written commun., 2017; Asquith and others, 2017) are presented for comparison. See table 7 (available for download at https://doi.org/10.3133/sir20205065) for more information.

In scenarios 1 and 2, the PeakFQ settings used by Kohn and others (2016) were used for flood-frequency analysis, including weighted skew (regional skew=−0.119 and standard error=0.550 from Bulletin 17B; Interagency Advisory Committee on Water Data, 1982, plate I) and threshold values. The difference here is that we used a newer version of PeakFQ (version 7.2) than Kohn and others (2016, version 7.1) with extended output options to obtain estimates of flood magnitude for very low AEPs. The flood-frequency curves for systematic data only and systematic plus paleoflood data are shown in figures 41 and 42, and selected AEPs are shown in table 7.

In figure 42, the largest gaged peak is outside the confidence bounds for the fitted frequency line. This is the same result as in Kohn and others (2016) and was their best estimate of flood frequency at this site. Notably, the inclusion of paleoflood information in the analysis depicted in figure 42 dramatically decreases the width of the confidence interval for very low AEPs. Information about the data used and the numeric flood estimates are provided in table 7.

Comparisons to Other Flood-Frequency Methods

Asquith and others (2017) examined probability distributions applicable to flood-frequency analysis beyond the PE3 distribution and fitting methods other than EMA. Scenarios 3–10 in table 7 present at-site point estimates for flood magnitudes using the asymmetric exponential power, generalized extreme value, generalized logistic, generalized normal, generalized Pareto, PE3, Wakeby, and Weibull distributions fitted using the method of L-moments (W. Asquith, written commun., 2017; Asquith and others, 2017). The mathematics of these distributions in the context of L-moments is described in appendix 5 of Asquith and others (2017).

Examination of table 7 shows that scenario 7, which used the generalized Pareto distribution (Asquith and others, 2017), is not an acceptable fit for the data because its value is almost constant with AEPs from 0.01 to 1×10^{-6}. This was the same result as the analysis of two rivers in the Eastern United States in Asquith and others (2017).

Examination of table 7 shows the effect of paleoflood data in that scenario 1 (systematic data, weighted skew with PeakFQ) has a fit (estimate) of 653,900 ft^3/s for an AEP of 1×10^{-6}, but when paleoflood information is added to the analysis (scenario 2), the AEP of 1×10^{-6} estimate decreases to 170,900 ft^3/s. Scenario 3 (asymmetric exponential power

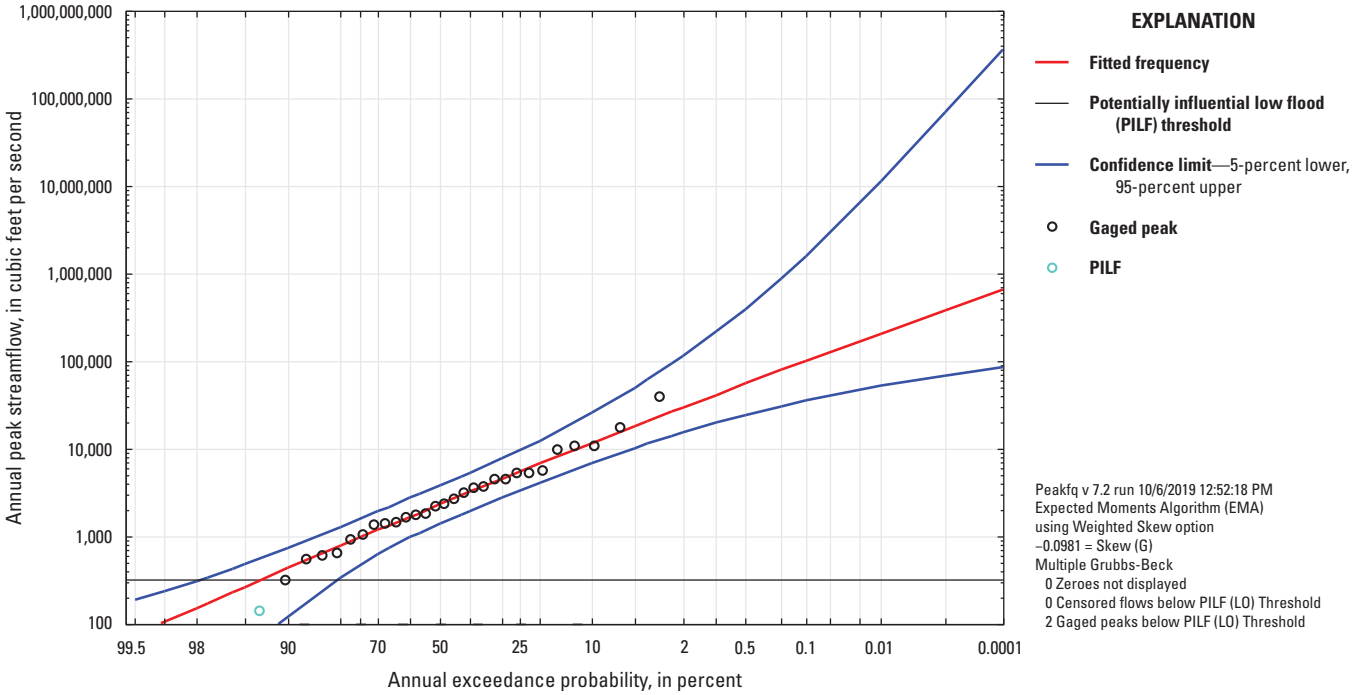

Figure 41. Annual exceedance probability plot and fitted distribution for streamgage station 06712500, Cherry Creek near Melvin, Colorado, using systematic data only and weighted skew (scenario 1).

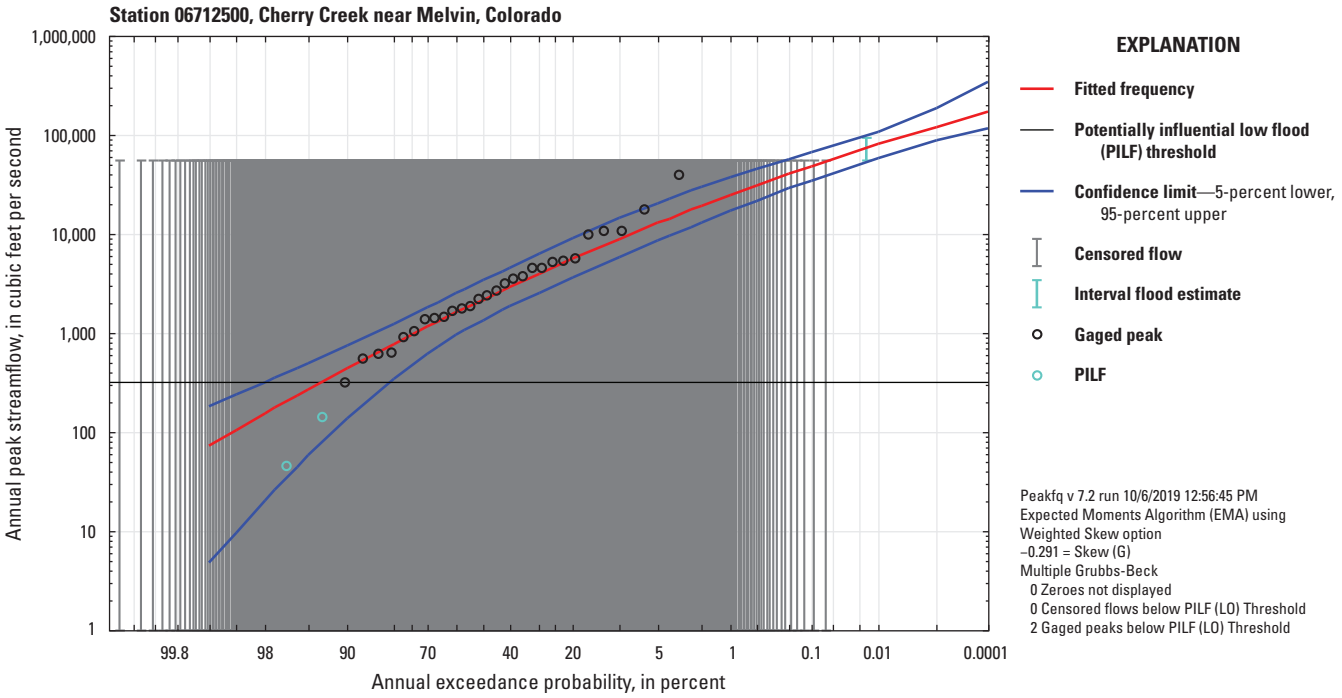

Figure 42. Annual exceedance probability plot and fitted distribution for streamgage station 06712500, Cherry Creek near Melvin, Colorado, using systematic and paleoflood data with weighted skew (scenario 1).

distribution, AEP4 in Asquith and other, 2017) also provides large estimates for an AEP of 1×10^{-3} to 1×10^{-6} with an AEP of 1×10^{-6} of 44,542,802 ft³/s. Scenario 5 (generalized logistic distribution, GLO in Asquith and others, 2017) estimates an AEP of 1×10^{-6} as 1,214,797. All AEPs for scenarios 1, 3, and 5 can be compared to the largest flood in 1,500 to 5,000 years—2,100 m³/s (74,161 ft³/s; Jarrett, 2000)—indicating that they likely overestimate the very low AEPs.

Figures 43–48 provide visual comparisons of the flood estimates for the AEPs listed in table 7. Some values for scenarios 1, 3, and 5 are so large that they are not shown on the plots. The mean of the estimates is shown as a blue dashed line in the plots and is based only on those estimates shown in the plot. For comparison, the largest flood in 1,500 to 5,000 years is shown as a green dashed line in figures 44–48.

Summary

The Cherry Creek site did not have autocorrelation and did not have a statistically significant trend. A change point was found, but it is difficult to determine whether this is a statistical artifact (as change-point methods are prone to false positives; Ryberg and others, 2020) or a meaningful change point because of the short period of record. Weighting of the skew with regional skew improved the fit of the statistical distribution for the very low AEP floods.

Paleoflood data are important for estimation of very low AEPs for sites with short periods of record (the definition of a short period of record varies with the characteristics of a site, but generally less than 100 years of record). Paleoflood data can diminish the width of the confidence intervals, resulting in a more precise estimate. Figure 49 shows that the PeakFQ flood-frequency estimates with paleoflood data result in reasonable estimates for floods for AEPs of 1×10^{-3} and 1×10^{-4}, because the largest paleoflood in the last 1,500 to 5,000 years, falls in between these estimates. The accuracy of the estimates for AEPs of 1×10^{-3} and lower is harder to judge as there is a great deal of variance in the point estimates depending on distribution and method of fit choices (table 7).

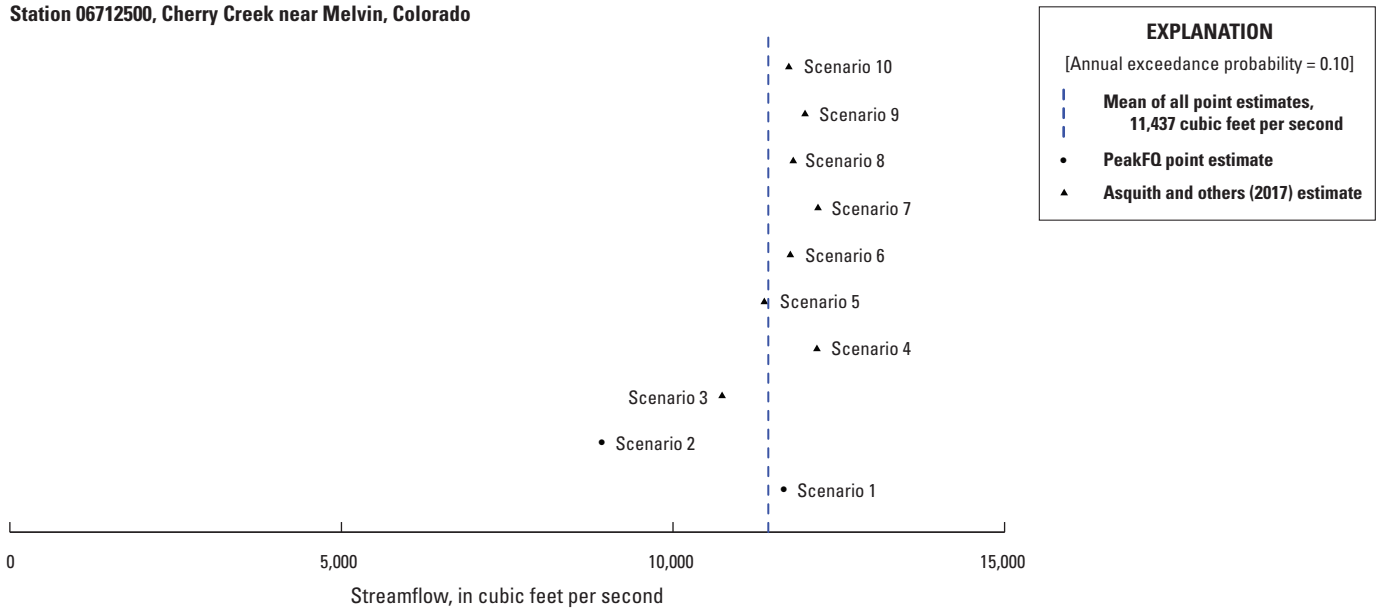

Figure 43. Point estimates for streamgage station 06712500, Cherry Creek near Melvin, Colorado, flood with annual exceedance probability of 0.10, calculated under 10 different scenarios. See table 7 for descriptions of the scenarios and the numeric values.

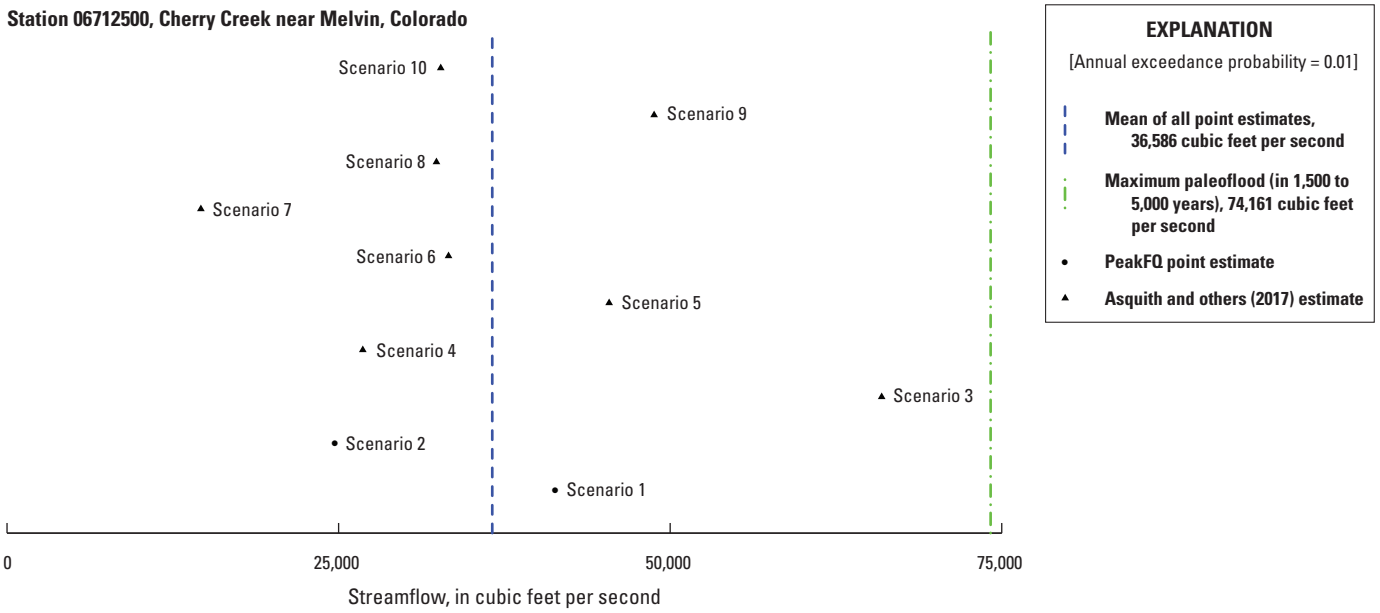

Figure 44. Point estimates for streamgage station 06712500, Cherry Creek near Melvin, Colorado, flood with annual exceedance probability of 0.01, calculated under 10 different scenarios. See table 7 for descriptions of the scenarios and the numeric values.

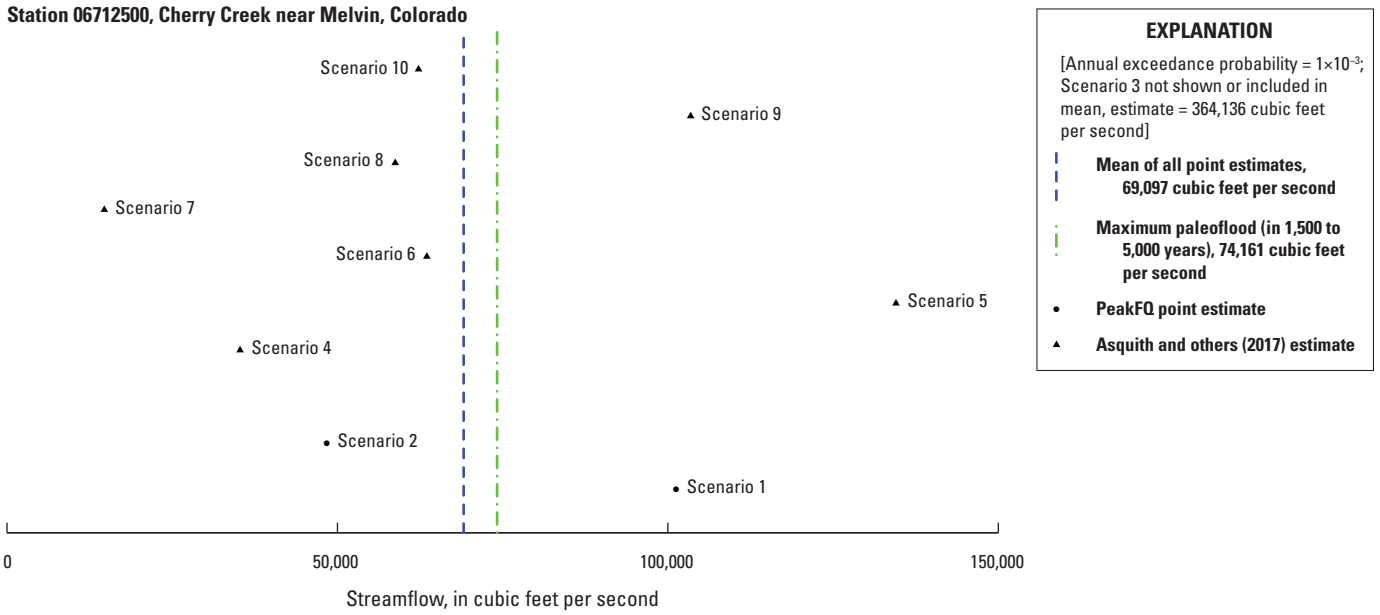

Figure 45. Point estimates for streamgage station 06712500, Cherry Creek near Melvin, Colorado, flood with annual exceedance probability of 1×10^{-3}, calculated under 10 different scenarios. See table 7 for descriptions of the scenarios and the numeric values.

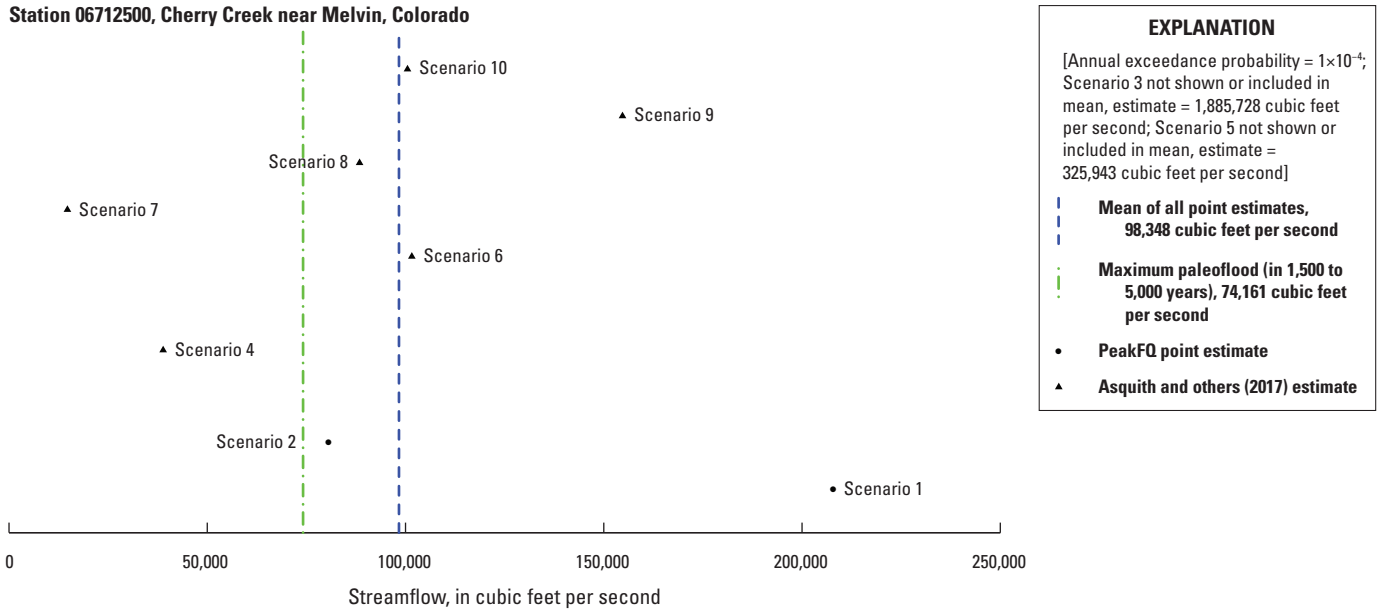

Figure 46. Point estimates for streamgage station 06712500, Cherry Creek near Melvin, Colorado, flood with annual exceedance probability of 1×10^{-4}, calculated under 10 different scenarios. See table 7 for descriptions of the scenarios and the numeric values.

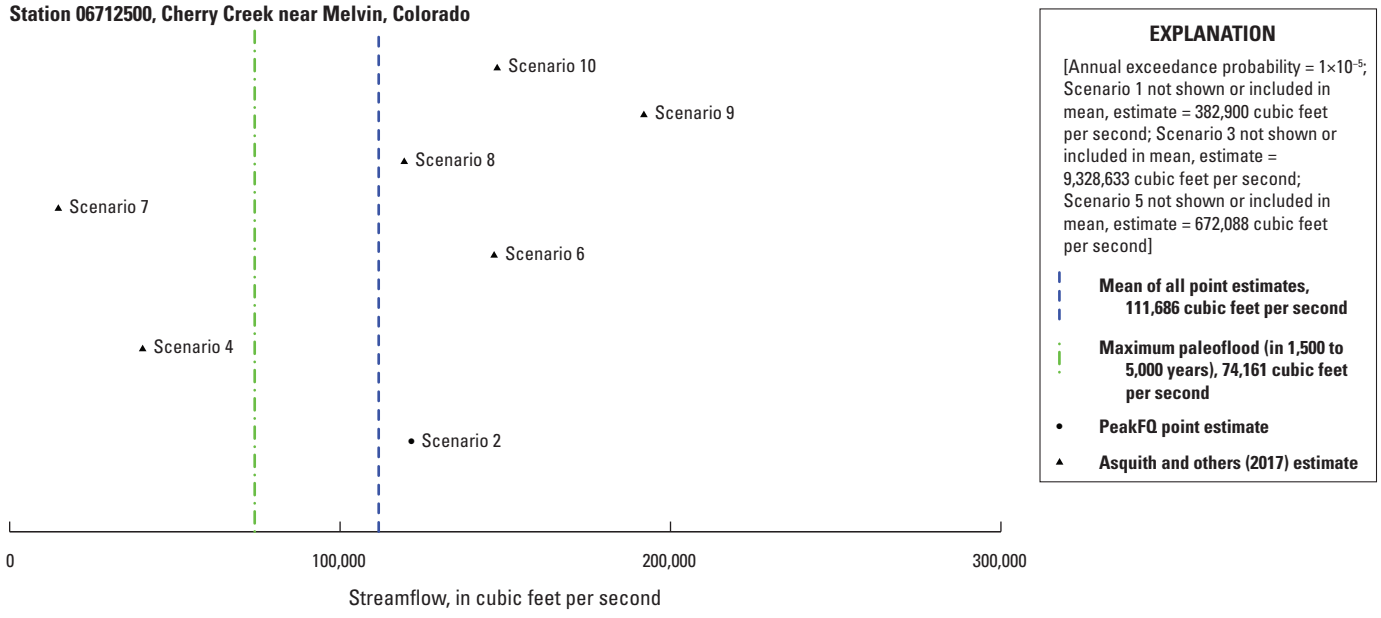

Figure 47. Point estimates for streamgage station 06712500, Cherry Creek near Melvin, Colorado, flood with annual exceedance probability of 1×10^{-5}, calculated under 10 different scenarios. See table 7 for descriptions of the scenarios and the numeric values.

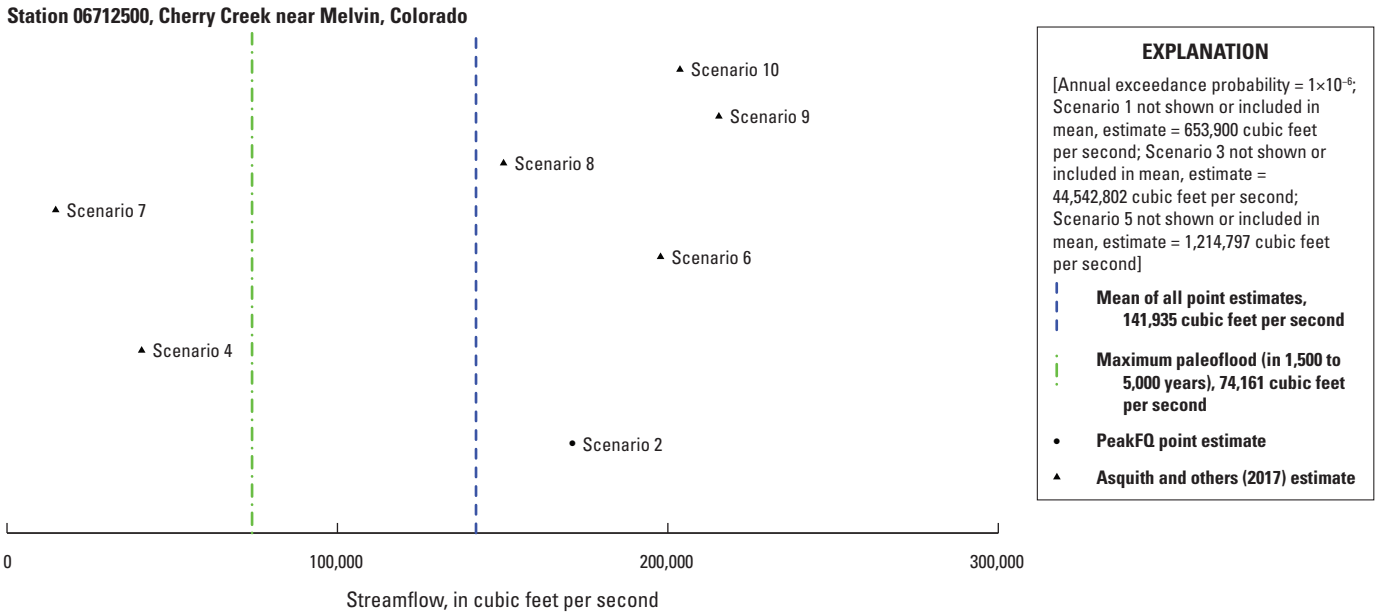

Figure 48. Point estimates for streamflow-gaging station 06712500, Cherry Creek near Melvin, Colorado, flood with annual exceedance probability of 1×10^{-6}, calculated under 10 different scenarios. See table 7 for descriptions of the scenarios and the numeric values.

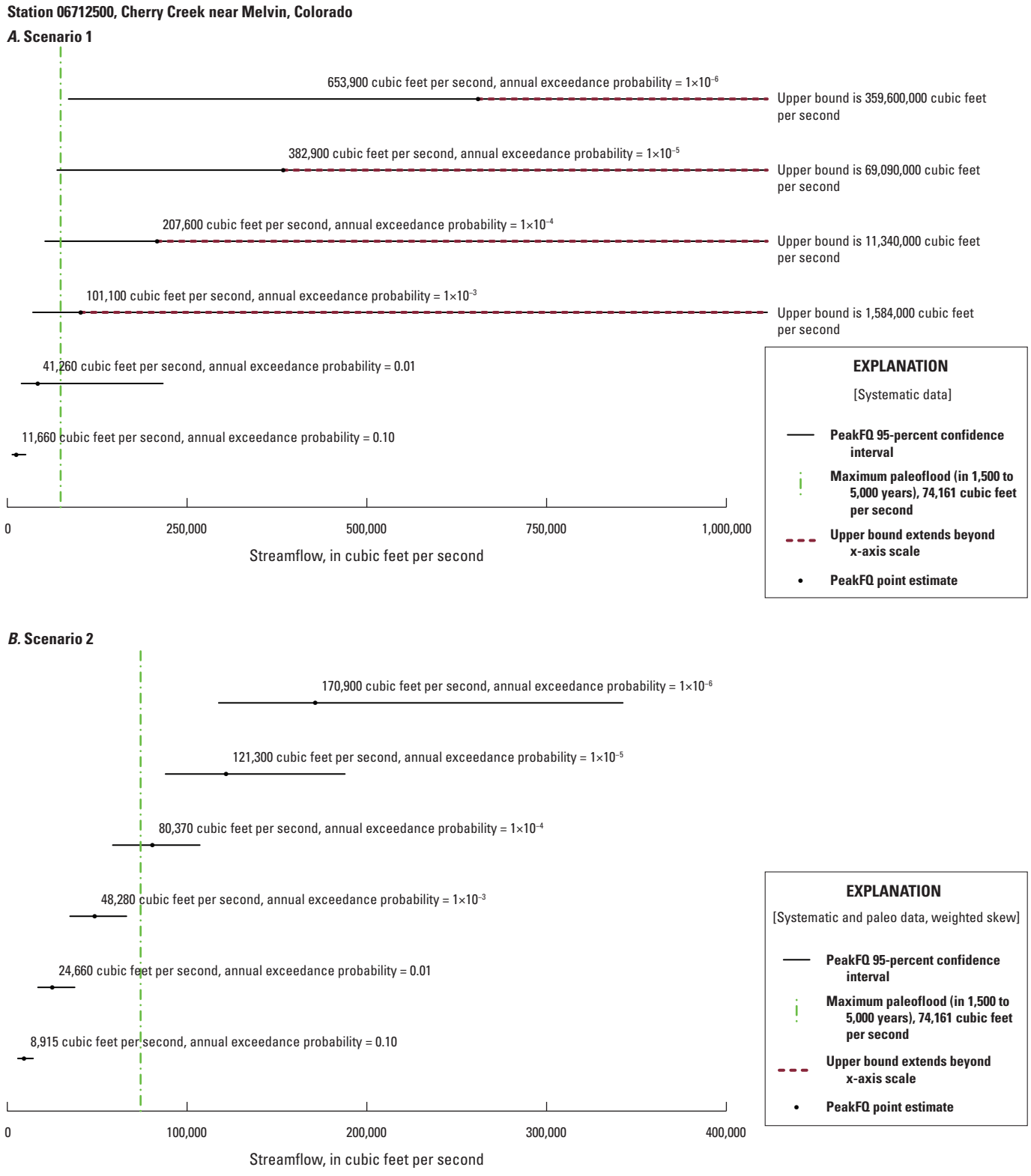

Figure 49. Point and interval estimates for a range of annual exceedance probabilities for streamgage station 06712500 Cherry Creek near Melvin, Colorado, floods, calculated using U.S. Geological Survey PeakFQ software (Veilleux and others, 2014) version 7.2, with *A*, as weighted skew and no paleoflood data and *B*, as weighted skew and systematic and paleoflood data. This depicts analysis results for *A*, scenario 1 and *B*, scenario 2 of table 7.

Escalante River near Escalante, Utah

The Escalante River peaks estimated by Webb and others (1988) are historical in that they occurred during settlement, and paleo, in that they were determined by analysis of flood deposits. Webb and others (1988) refer to the peaks they estimated as "historic" peaks. In keeping with terminology used throughout this report, where peaks determined with analysis of flood deposits or tree-rings were referred to as paleo, we call the additional peaks determined by Webb and others (1988) "paleo" peaks. The USGS PFF contains an additional three peaks outside the systematic period of record that occurred in 1910, 1911, and 1912. These are considered historical peaks in this analysis.

Initial Data Analysis

The systematic peaks were examined for autocorrelation in two periods: 1943–55 and 1972–2015. There is no autocorrelation in either systematic period of record at this site (figs. 50 and 51). Then the systematic peaks were examined for change points in the two periods. The first period, 1943–55, is very short for change-point analysis, so no change points were found (fig. 52). Although, visually, the peaks from 1972 to 2015 appear to have a reduction in variance, no change point was found in that period (fig. 53). Statistical and visual inspection are important, and analysts have a great deal of flexibility in using change-point methods more sensitive to changes, if that is a concern. With and without the historical peaks, this site does not have a trend in peak flow (fig. 54).

Flood-Frequency Analysis

Flood-frequency analysis was completed under three scenarios, with comparisons to five other flood-frequency analysis results from previously published studies:

1. systematic peaks, with weighted skew;
2. systematic peaks and three historical peaks, with weighted skew;
3. systematic peaks, three historical peaks, three paleoflood peak point estimates and one paleo interval estimate, and a threshold that indicates the paleoflood peaks were the largest since 1909, with weighted skew.

4–8. in addition to the analyses performed for this study, estimates were obtained from several other flood-frequency studies (Webb and others, 1988; Webb and Rathburn, 1988; Kenney and others, 2008) and are presented as comparison scenarios. See table 8 (available for download at https://doi.org/10.3133/sir20205065) for more information.

A recent Utah flood-frequency study included this site (Kenney and others, 2008) and used a weighted skew based on a regional skew estimated in 2004 (Perica and Stayner, 2004). We, therefore, completed weighted skew analysis with the Perica and Stayner (2004) regional skew of −0.250 and a mean square error of 0.197.

For scenarios 2 and 3, the three historical peaks are not notably large—historical peaks are usually recorded because of their large magnitude. However, a flood in 1909 destroyed the USGS streamgage on August 31 (Freeman and Leighton, 1911). A new streamgage was installed at a site 35 feet upstream from the old streamgage. Peaks were entered in the USGS peak-flow file for 1910, 1911, and 1912 with a qualification code of 7, indicating they were historical and outside the period of systematic record. One could make an argument to treat them as systematic peaks rather than historical because of the efforts to gage the stream in the early 1900s. We kept the historical designation, though, because the estimates of streamflow were considered "very unreliable" in 1909, and these peaks have a higher degree of error than those recorded beginning in 1943. The period 1913–42 is ungaged and an appropriate period to use a threshold value. If the historical peaks were particularly large, we could use the smallest of the three as a threshold value indicating that if a peak occurred above that value from 1913 to 1942, it would have been recorded. We cannot say that though, so the thresholds for the period 1913–42 and 1956–71 were set from negative infinity to infinity (inf and inf in the Lower Bound and Upper Bound fields of PeakFQ) indicating that we do not know anything about this period.

With the additional information gained in scenario 3, we can add a threshold to the periods of missing gage record indicating that if the peak was above 17,700 ft^3/s, it would have been determined in the flood reconstruction of Webb and others (1988). The estimated paleoflood peaks were known to be the largest since 1875 (Webb and others, 1988), so one could extend the threshold period back to 1875. However, the 1909 flood changed the channel (Webb and others, 1988), so the threshold was extended back to 1909 rather than 1875.

The input data for scenario 3 (which includes the input for scenarios 1 and 2) are shown in figure 55. The resulting flood-frequency curves for scenarios 1, 2, and 3 are shown in figures 56–58. The flood magnitudes and confidence bounds are shown in table 8. Figure 56 shows that the upper confidence bound for very low AEPs levels off (in what may be a computational issue) and indicates that the systematic record only does not provide a good error estimate for very low AEPs at this site. With the introduction of the historical and paleoflood peaks, the upper confidence bound estimates behave normally (figs. 57 and 58). The paleoflood information shown in figures 55 and 58 as interval flows, censored flows, and historical peaks are considerably larger than the observed peaks and appear as though they may come from a different population. One might think of this record as three distributions: low runoff years (the nine PILFs and the more typical distribution of floods), the gaged peaks and 1910–1912 peaks,

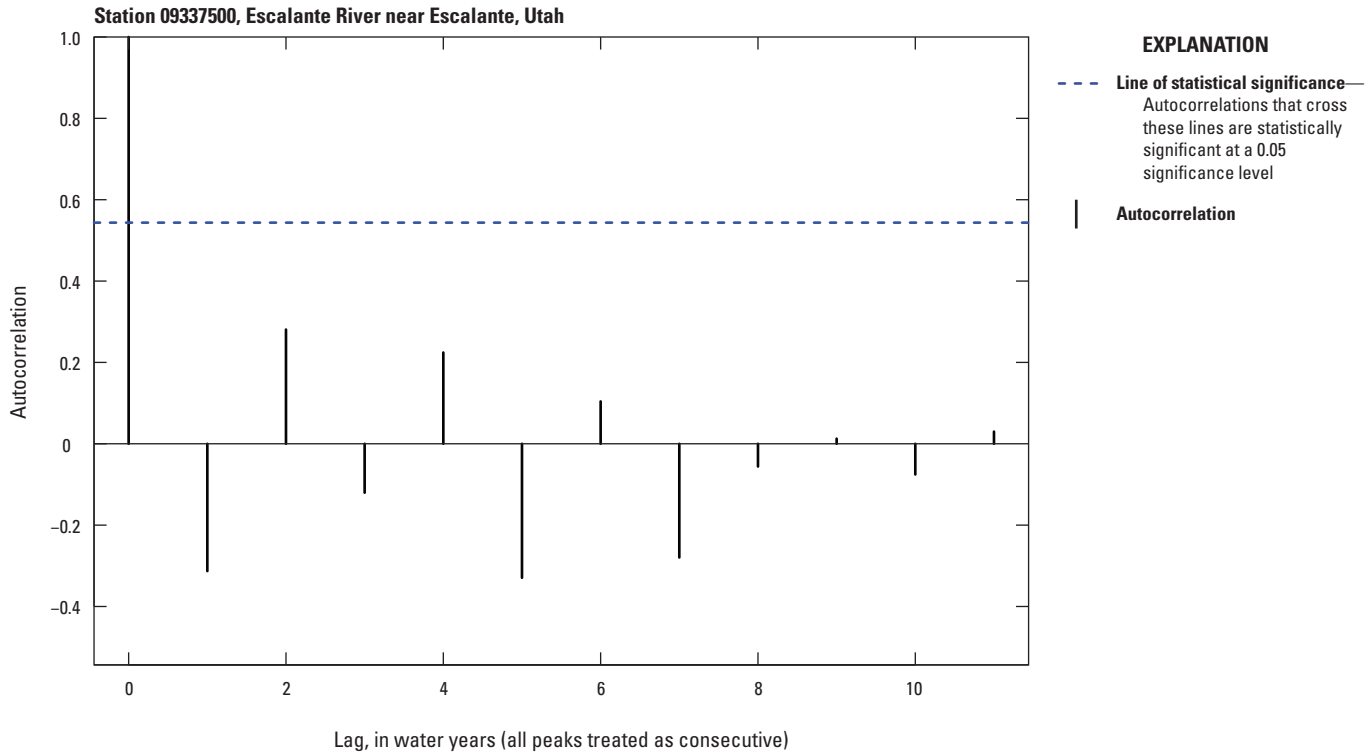

Figure 50. The autocorrelation for peaks in systematic period of record for streamgage station 09337500, Escalante River near Escalante, Utah, 1943–55.

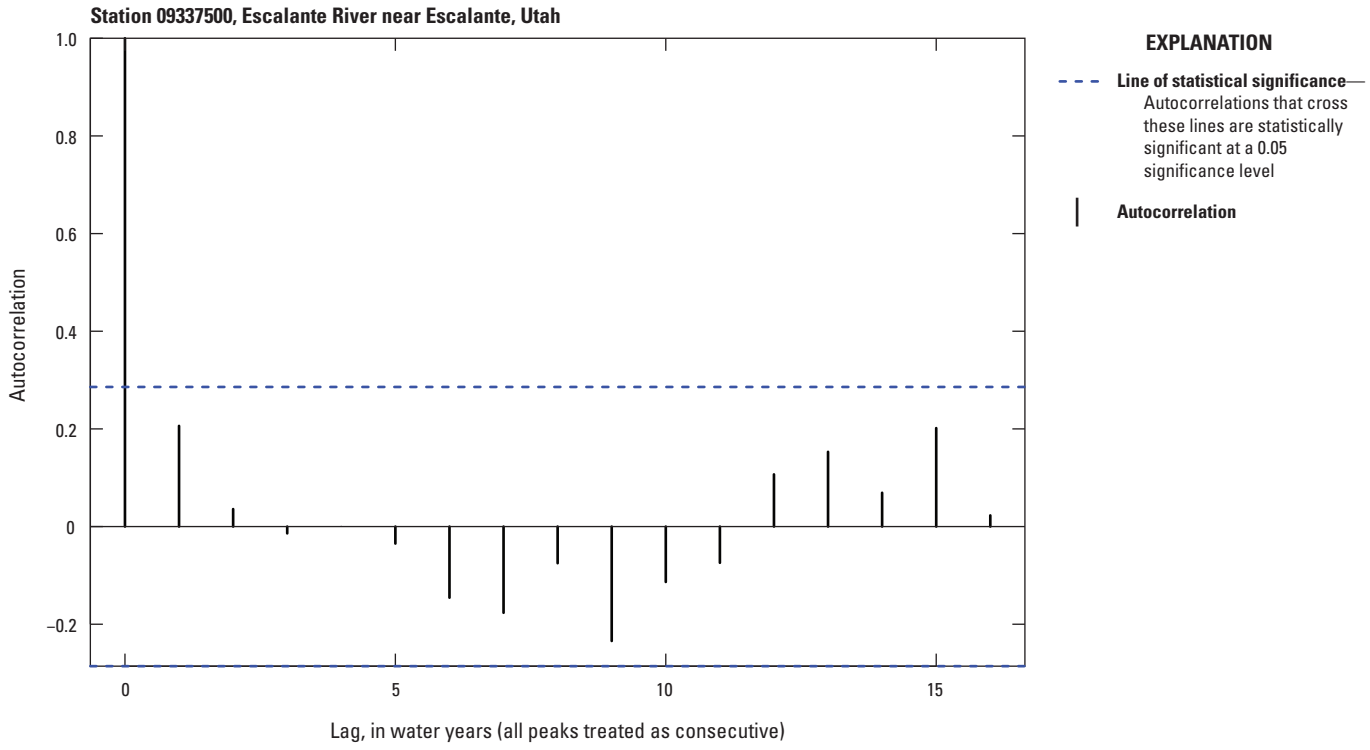

Figure 51. The autocorrelation for peaks in systematic period of record for streamgage station 09337500, Escalante River near Escalante, Utah, 1972–2015.

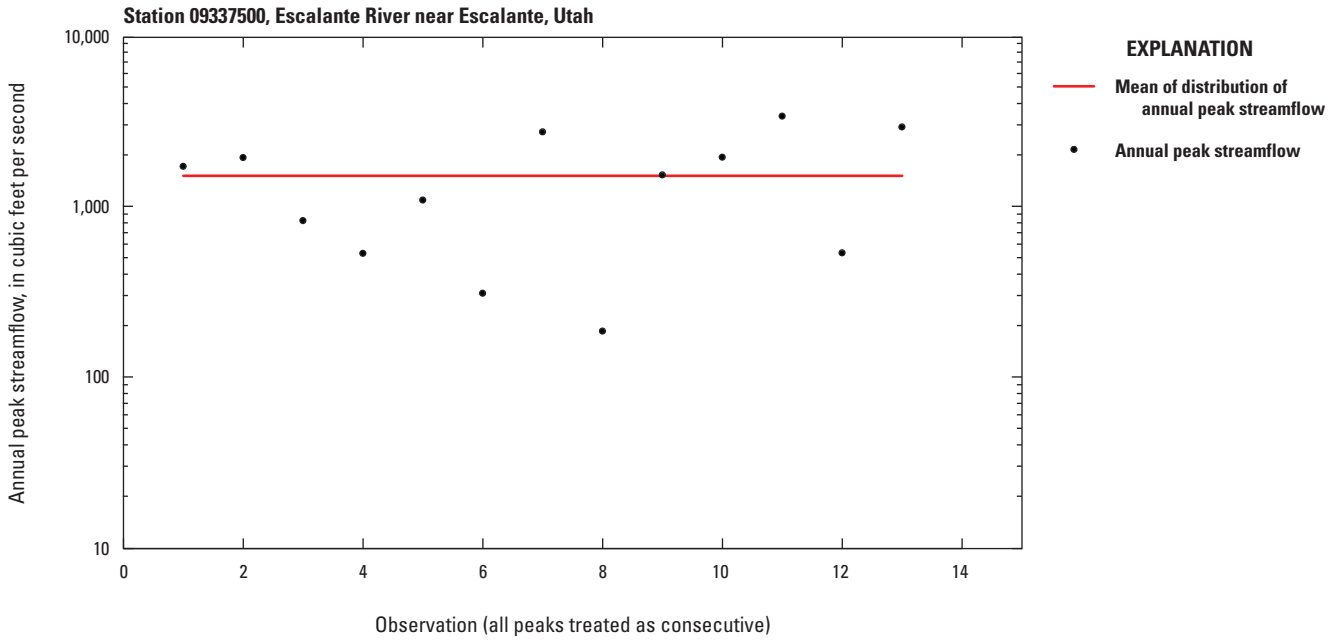

Figure 52. Change points in mean and variance for peaks in systematic period of record for streamgage station 09337500, Escalante River near Escalante, Utah, 1943–55.

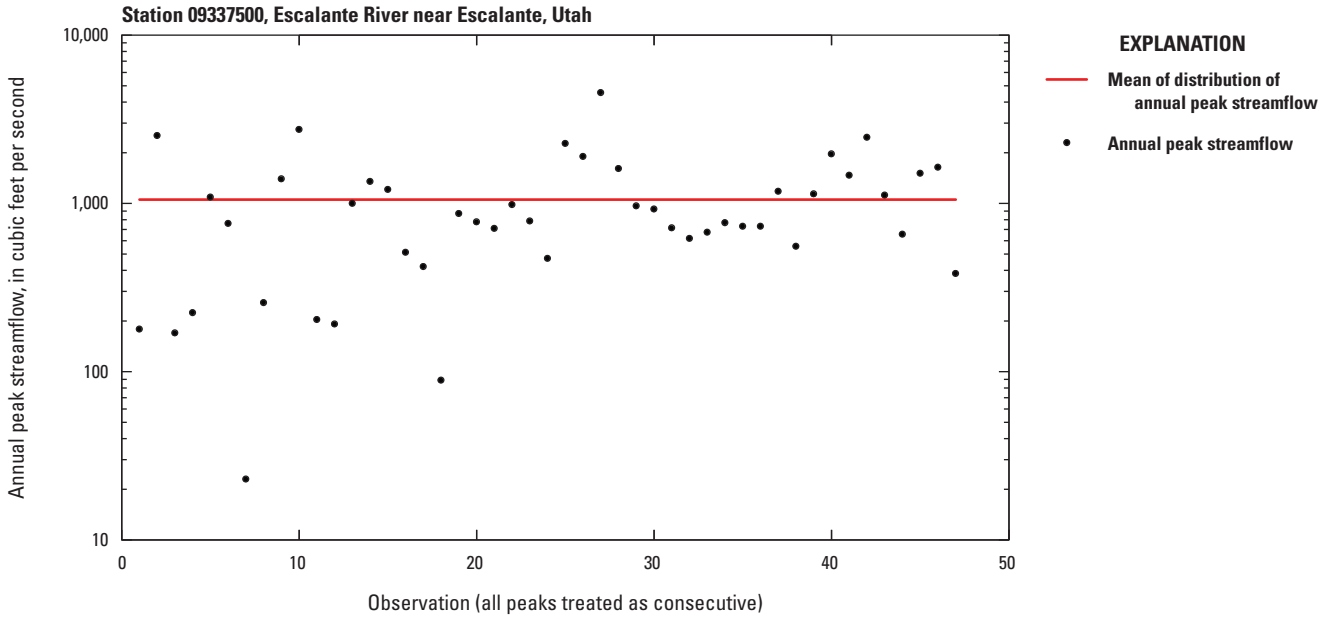

Figure 53. Change points in mean and variance for peaks in systematic period of record for streamgage station 09337500, Escalante River near Escalante, Utah, 1972–2015.

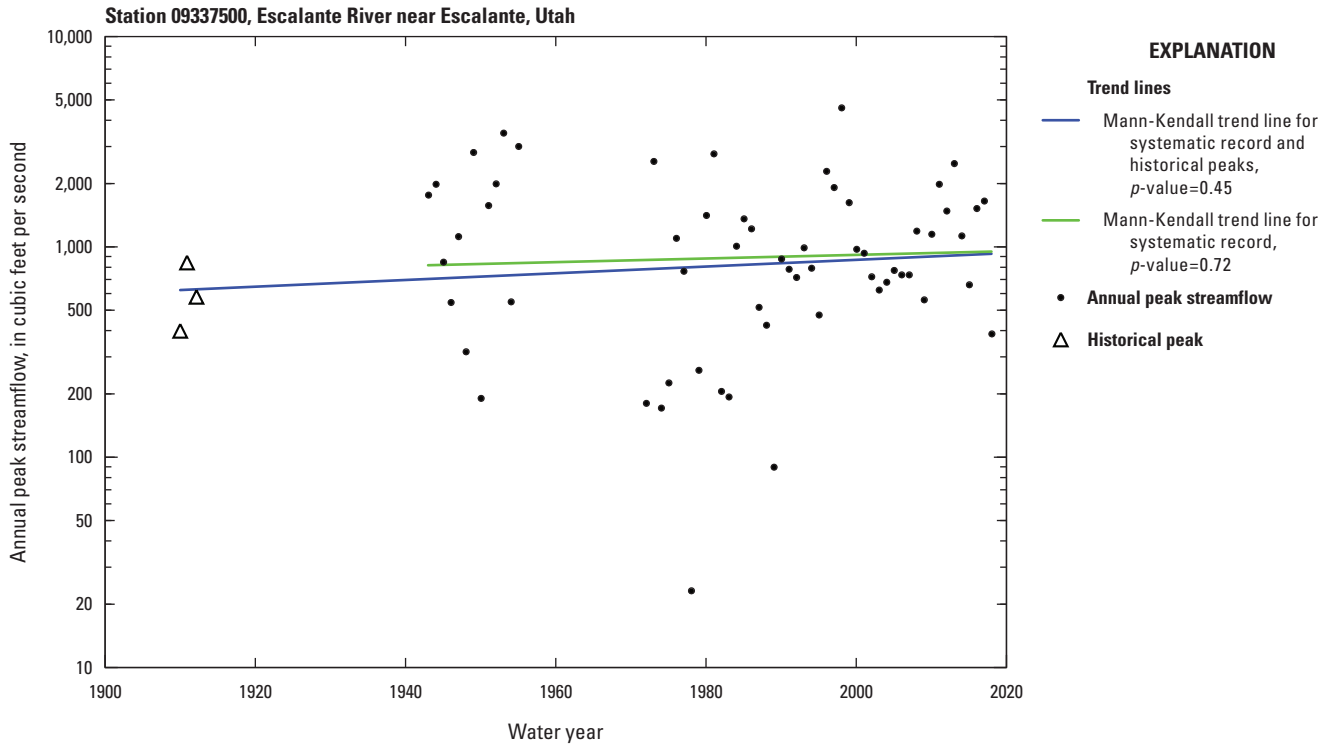

Figure 54. Mann Kendall test for trend in the peak-streamflow record for streamgage station 09337500, Escalante River near Escalante, Utah.

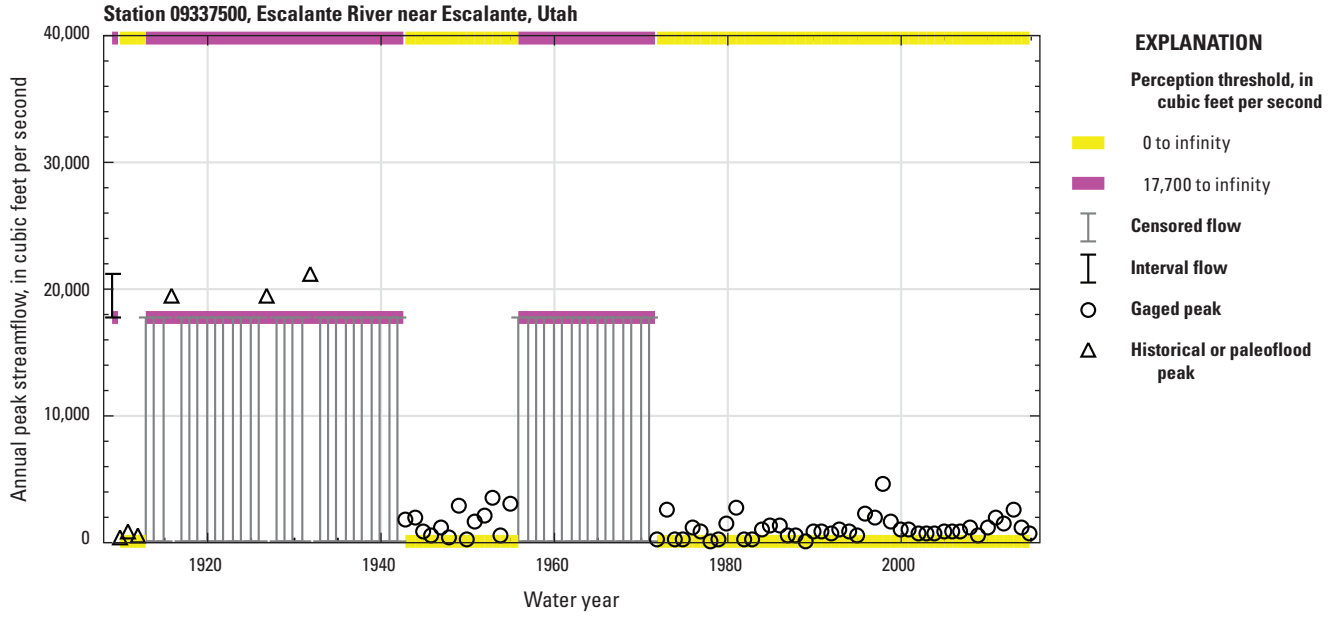

Figure 55. Peaks and thresholds for flood-frequency analysis, Escalante River near Escalante, Utah.

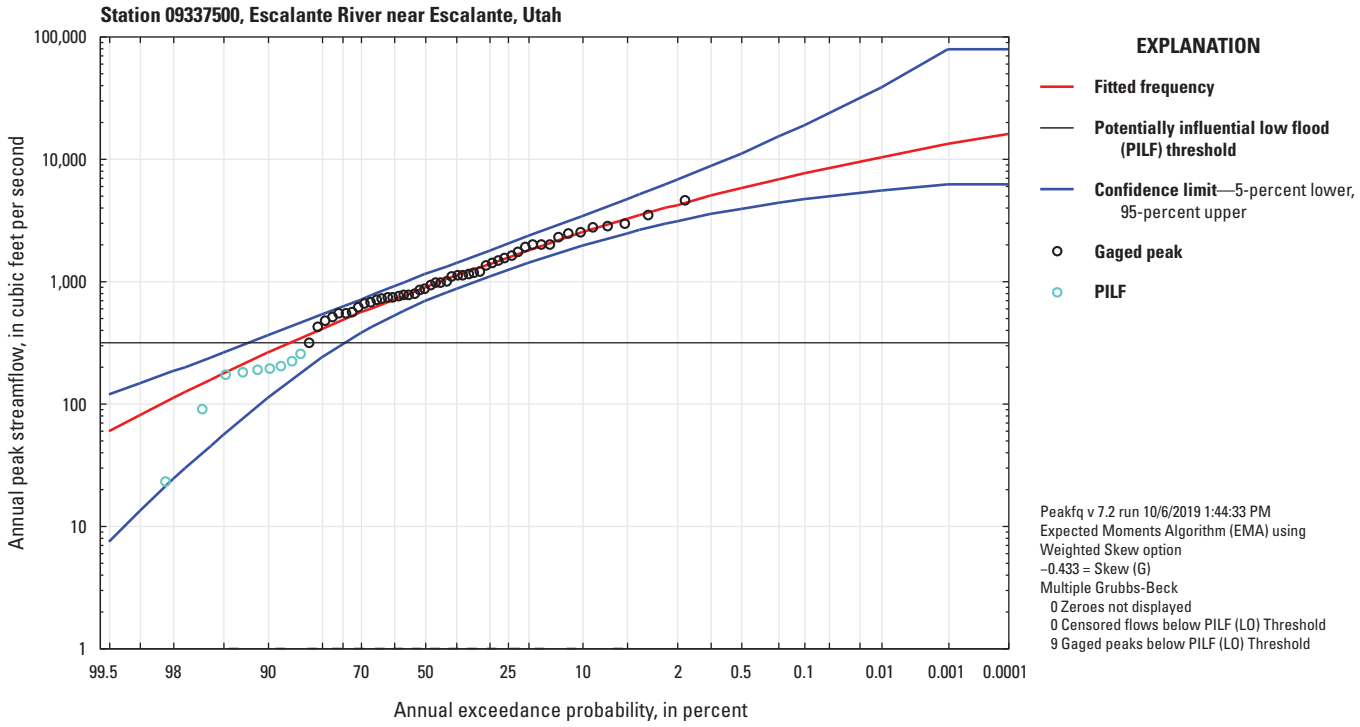

Figure 56. Annual exceedance probabilities for streamgage station 09337500, Escalante River near Escalante, Utah, using the systematic peaks only (scenario 1).

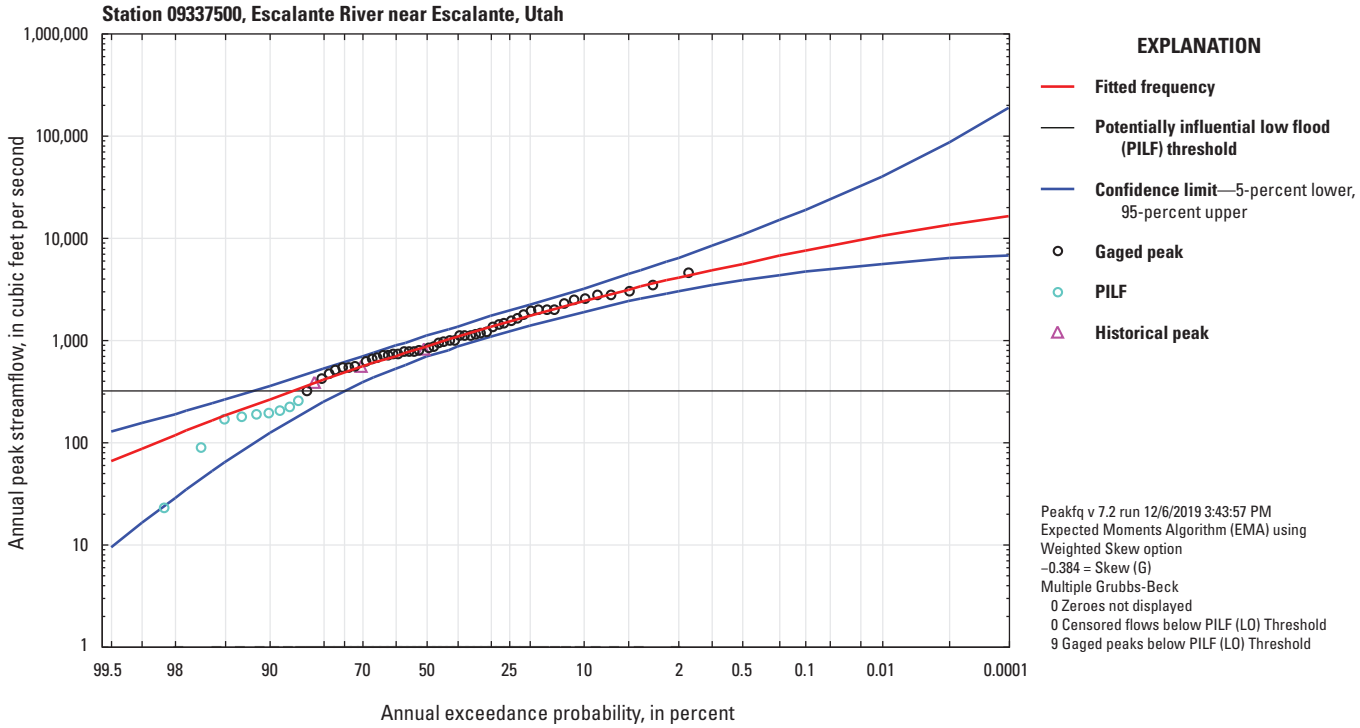

Figure 57. Annual exceedance probabilities for streamgage station 09337500, Escalante River near Escalante, Utah, using the input data depicted in figure 55.

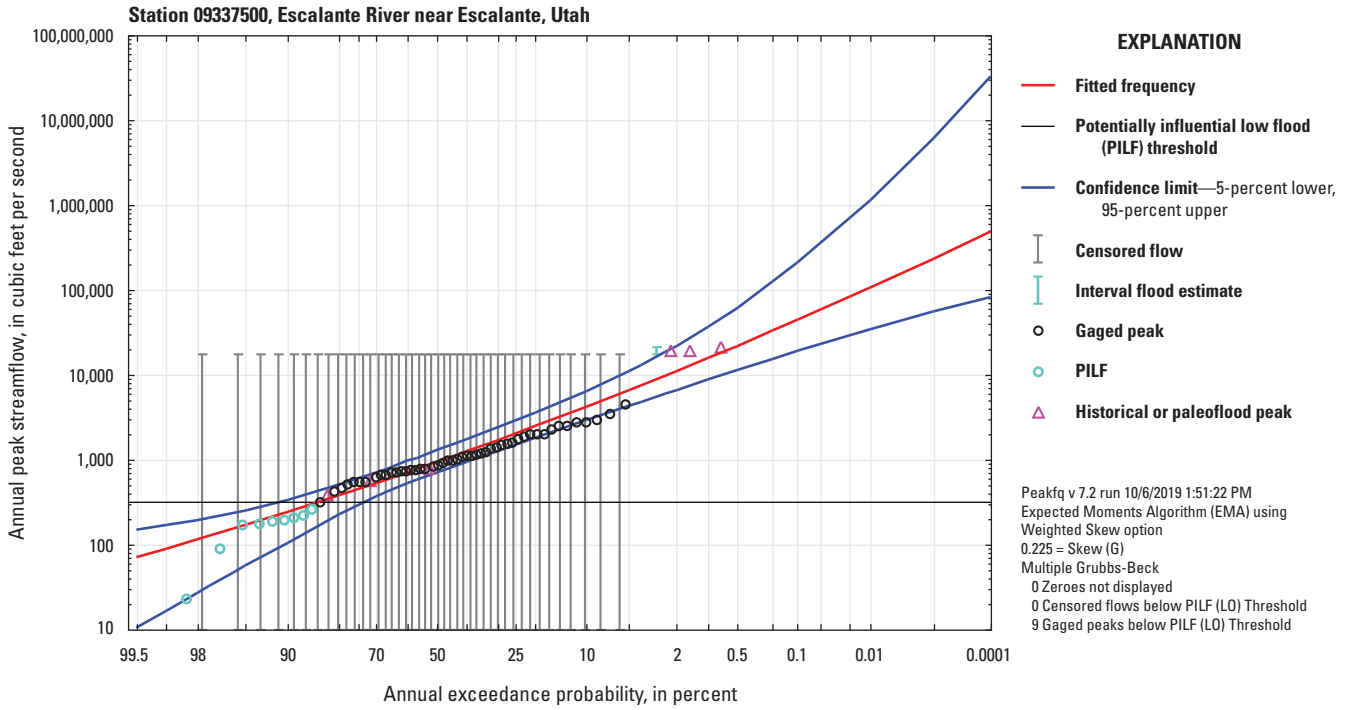

Figure 58. Annual exceedance probabilities for streamgage station 09337500, Escalante River near Escalante, Utah, using systematic, historical, and paleoflood peaks and thresholds.

and the large paleoflood peaks. It is possible the large paleoflood peaks are the result of unique climatic conditions. The flood-frequency analyses of Webb and others (1988) and Webb and Rathburn (1988), completed when the gage record was substantially shorter, show these peaks as standing out from the rest. However, in this study, the paleoflood point estimates fall within the error bounds of the fitted frequency curve and, therefore, magnitudes for very low AEPs were estimated. Inclusion of the large paleoflood peaks dramatically increases the confidence limits for the very low AEPs.

The AEPs calculated under these different scenarios are compared graphically in figures 59–64. Figure 60 also includes point estimates of magnitudes calculated for an AEP of 0.01 in other studies discussed in the next section.

Comparisons to Other Flood-Frequency Methods

Kenney and others (2008) estimated flood frequencies for the Escalante River site using the streamgage data through water year 2005 and the three historical peaks. Their AEP of 0.01 estimate is provided in table 8. The dataset and methodology are comparable to scenario 2 in this study, and their estimate was 5,290 ft^3/s, whereas the estimate in the current study with 10 additional years of gaged record was 4,794 ft^3/s.

Webb and others (1988) used gaged data through 1985; gaged data plus 4 paleoflood peaks; and gaged data, 4 paleoflood peaks, and a threshold indicating that the paleoflood peaks were the largest since 1875. The scenarios using the data from Webb and others (1988) were designated as scenarios 5–7 in figure 60 and table 8. Scenario 5 is like scenario 1 and falls within the confidence bounds for the estimate at AEP of 0.01. It is, however, higher than the estimate in scenario 1, and this shows how the much longer gaged record in scenario 1 reduced the flood magnitude estimate. Scenario 7 is very similar to scenario 3 with slightly different assumptions about the appropriate starting period (1909 for scenario 3 and 1875 for scenario 7). The estimates are similar: 15,730 ft^3/s for scenario 3, with the shorter beginning threshold and longer gaging period, and 17,000 ft^3/s for scenario 7.

Scenario 8 includes nine additional paleoflood peaks described by Webb and Rathburn (1988) as “prehistoric” peaks. They reference Webb and others (1988) for these peaks, but the nine “prehistoric” peaks are not quantified or used in flood-frequency analysis there; however, dates were estimated with considerable uncertainty for floods from approximately A.D. 450 to A.D. 1550. The dates for large floods had uncertainties as much as plus or minus 110 years in strata that had date uncertainties as much as plus or minus 860 years (Webb and others, 1988). Webb and Rathburn (1988) graphically depict these nine floods indicating they had determined interval estimates and selected years for plotting, but those values are not listed. The graphical depiction hints that the Escalante River analysis could be extended even further back in time, but that was not done here because of the date and magnitude uncertainties, as well as indications of significant channel change (Webb and others, 1988). Scenario 8’s estimate of

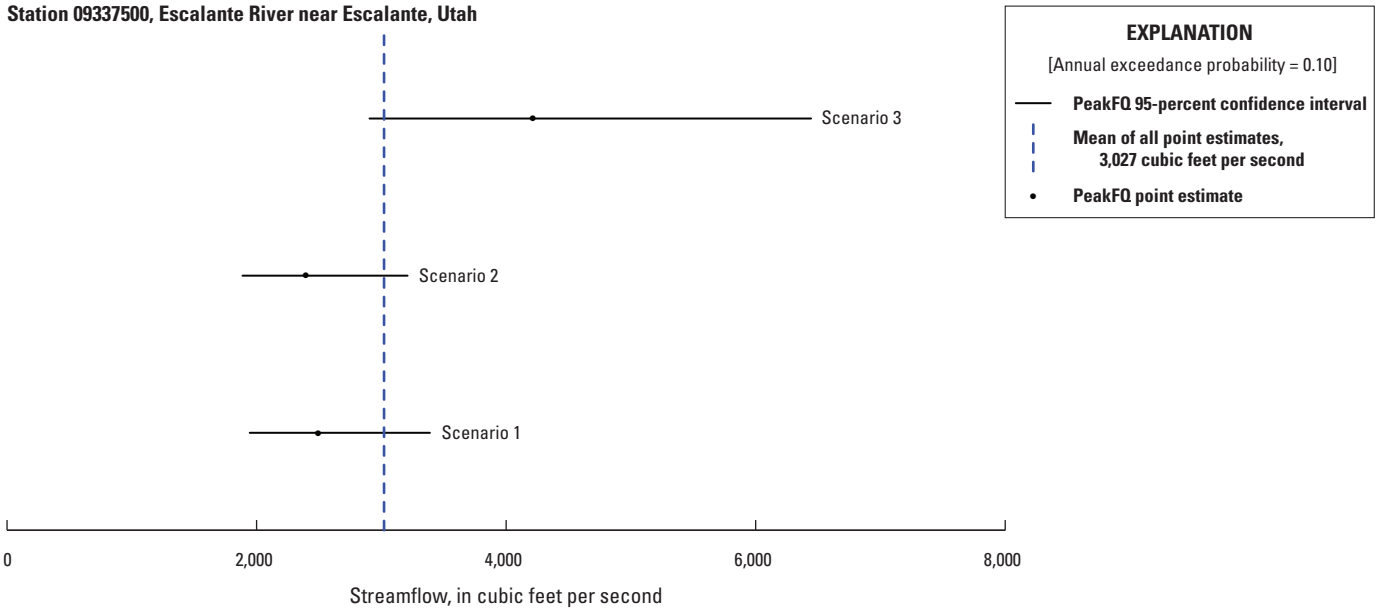

Figure 59. Point estimates and confidence bounds for streamgage station 09337500, Escalante River near Escalante, Utah, floods with annual exceedance probability of 0.10, calculated under three different scenarios using U.S. Geological Survey PeakFQ software (Veilleux and others, 2014) version 7.2. See table 8 for descriptions of the scenarios and the numeric values.

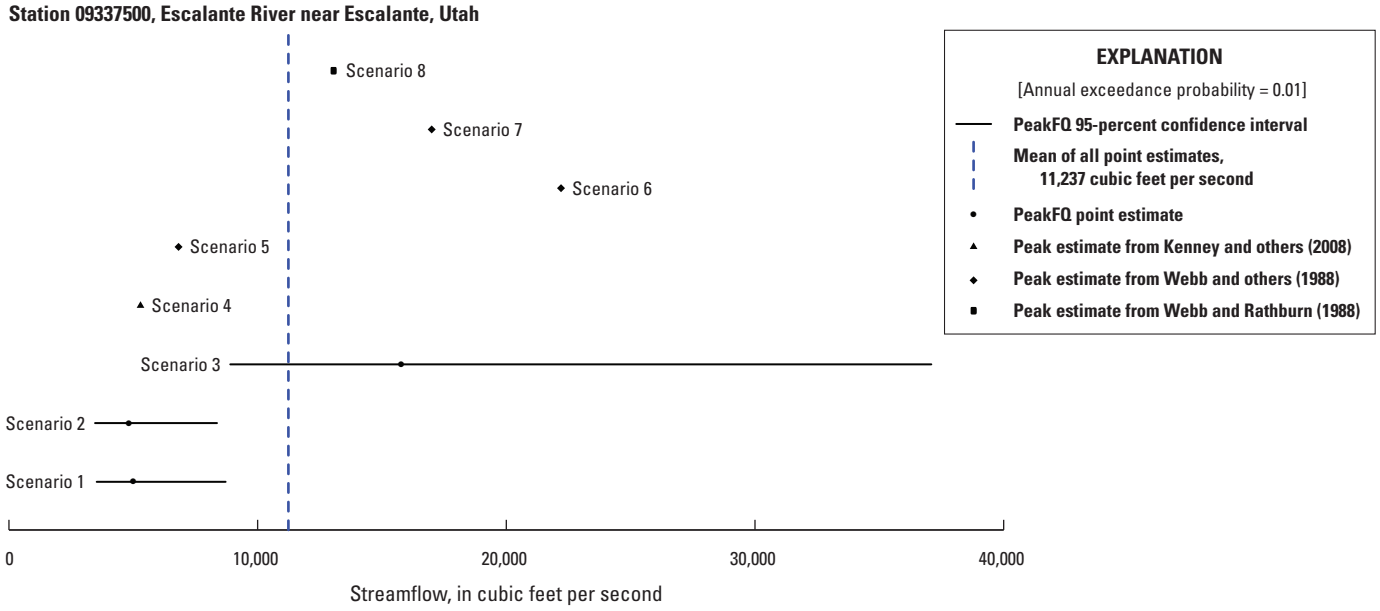

Figure 60. Point estimates and confidence bounds for streamgage station 09337500, Escalante River near Escalante, Utah, floods with annual exceedance probability of 0.01, calculated under three different scenarios using U.S. Geological Survey PeakFQ software (Veilleux and others, 2014) version 7.2 compared to five point estimates from other studies (Kenney and others, 2008; Webb and others, 1988; Webb and Rathburn, 1988). See table 8 for descriptions of the scenarios and the numeric values.

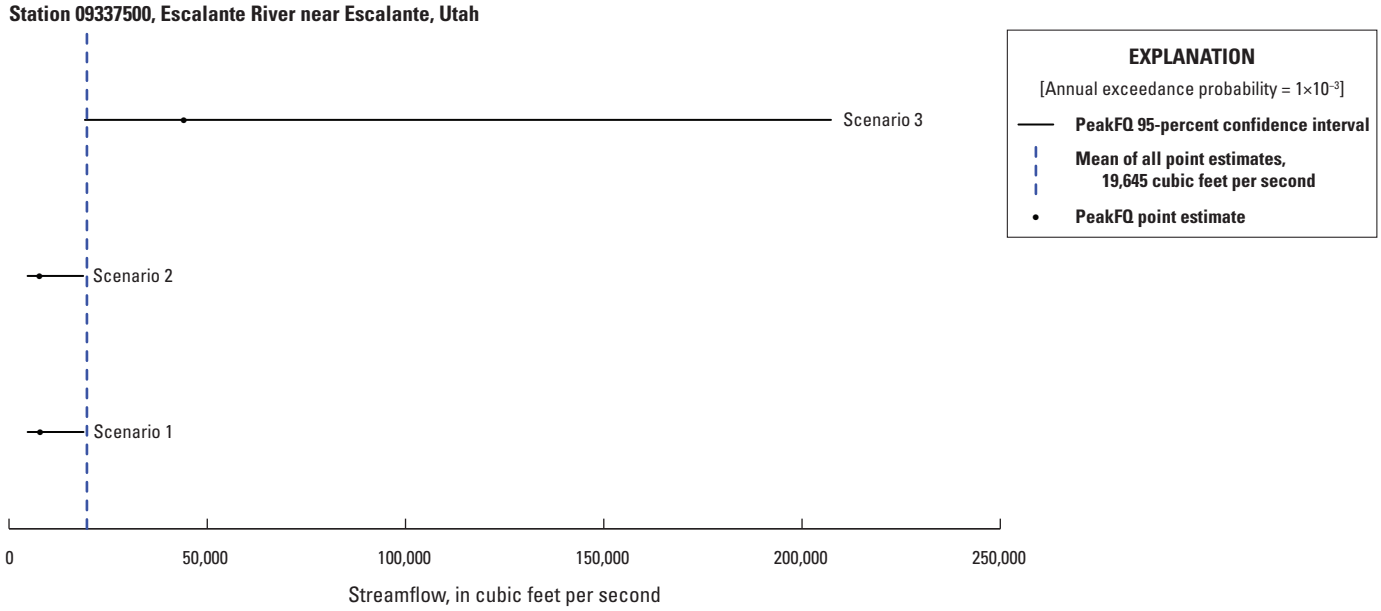

Figure 61. Point estimates and confidence bounds for streamgage station 09337500, Escalante River near Escalante, Utah, floods with annual exceedance probability of 1×10^{-3}, calculated under three different scenarios using U.S. Geological Survey PeakFQ software (Veilleux and others, 2014) version 7.2. See table 8 for descriptions of the scenarios and the numeric values.

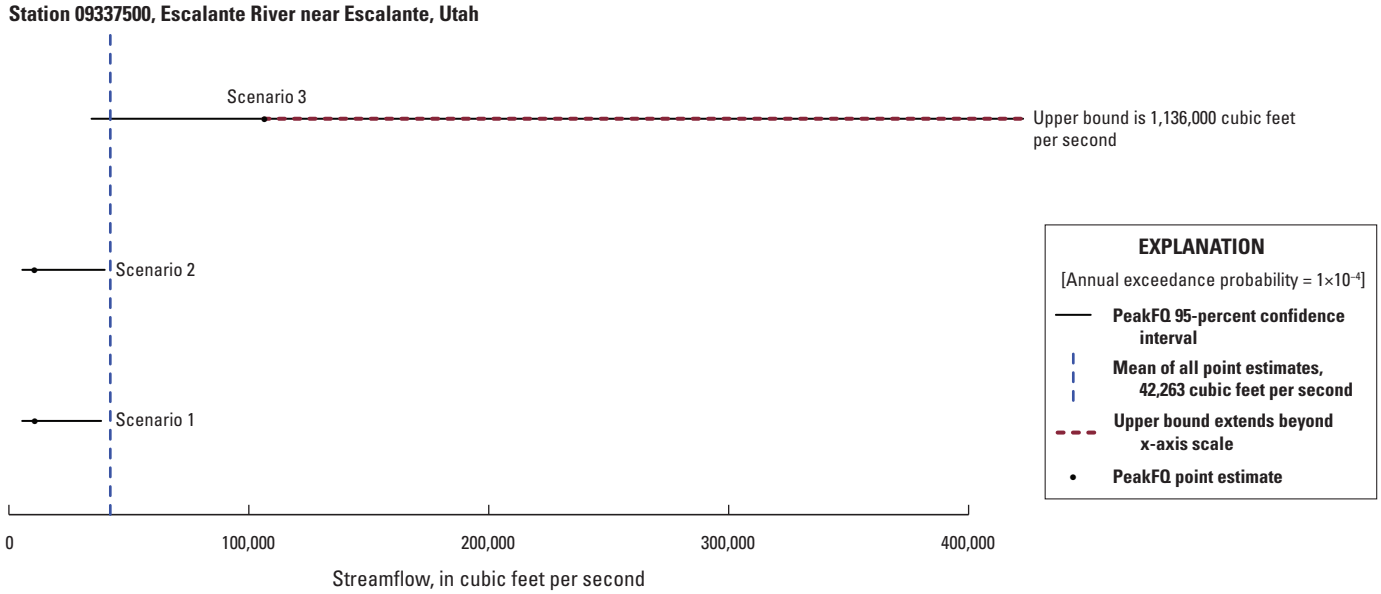

Figure 62. Point estimates and confidence bounds for streamgage station 09337500, Escalante River near Escalante, Utah, floods with annual exceedance probability of 1×10^{-4}, calculated under three different scenarios using U.S. Geological Survey PeakFQ software (Veilleux and others, 2014) version 7.2. See table 8 for descriptions of the scenarios and the numeric values.

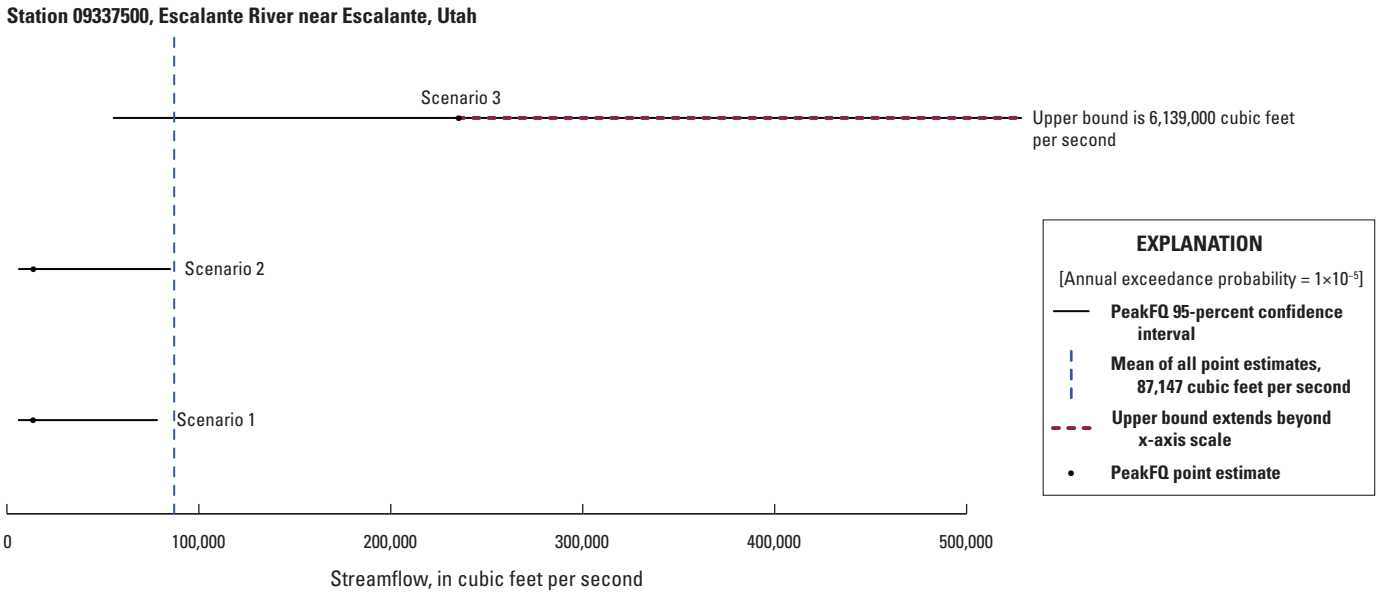

Figure 63. Point estimates and confidence bounds for streamgage station 09337500, Escalante River near Escalante, Utah, floods with annual exceedance probability of 1×10^{-5}, calculated under three different scenarios using U.S. Geological Survey PeakFQ software (Veilleux and others, 2014) version 7.2. See table 8 for descriptions of the scenarios and the numeric values.

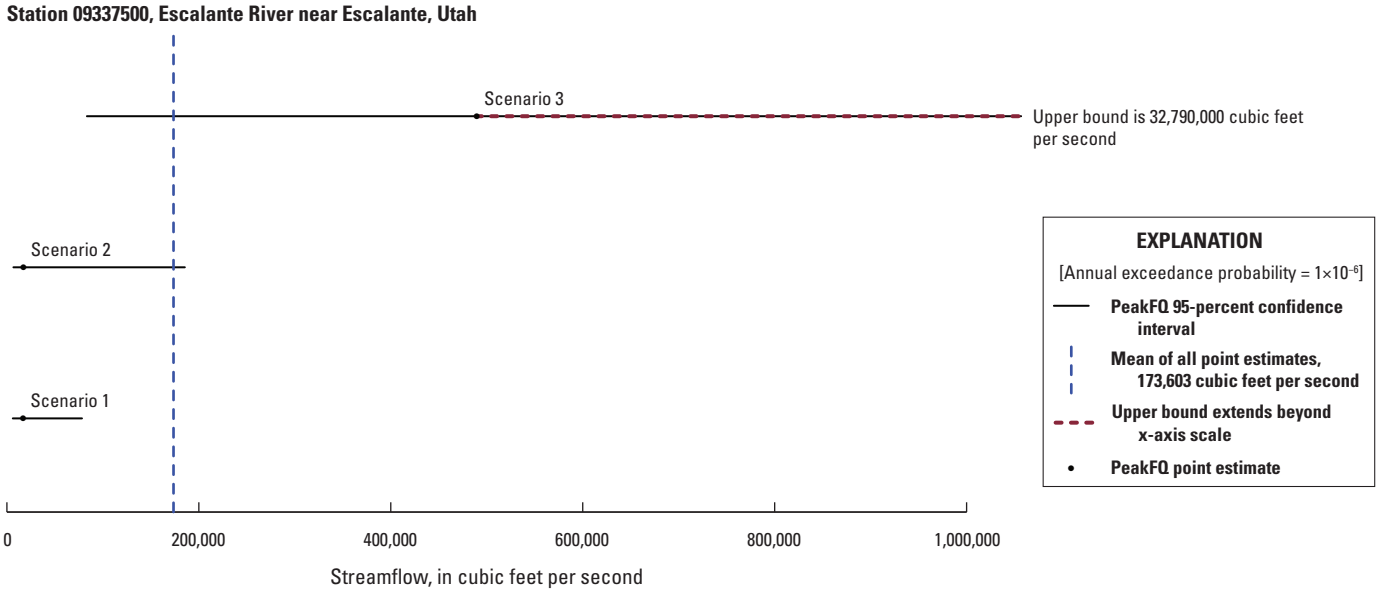

Figure 64. Point estimates and confidence bounds for streamgage station 09337500, Escalante River near Escalante, Utah, floods with annual exceedance probability of 1×10^{-6}, calculated under three different scenarios using U.S. Geological Survey PeakFQ software (Veilleux and others, 2014) version 7.2. See table 8 for descriptions of the scenarios and the numeric values.

an AEP of 0.01 is 13,100 ft^3/s indicating that the addition of paleoflood information going back to A.D. 450 reduced the peak estimate. This estimate is within the confidence bounds for scenario 3 (table 8 and fig. 60).

Summary

The Escalante River had no autocorrelation, no change points, and no trend. This site would seem to be a suitable candidate for extending the record with paleoflood peaks to refine confidence limits for very low AEPs. AEPs calculated under the three PeakFQ scenarios are summarized in figures 65 and 66. The figures show that adding paleoflood information does not always decrease uncertainty. The paleoflood peaks added were very large peaks and increased the uncertainty for very low AEPs, while also increasing the estimated magnitudes. The effect of the addition of paleoflood peaks at this site is similar to the effect at Spring Creek where the paleoflood peaks and single systematic outlier formed their own group at much larger magnitudes than the systematic record. The regional transfer experiment at Spring Creek showed that if the space between the two distributions could be filled in with additional peaks, the fit might improve. Going back much further in time, Webb and Rathburn (1988) added more paleoflood data to their flood-frequency analysis and reduced the estimate for an AEP of 0.01. However, their confidence bounds are unknown, and their exact data were unable to be replicated for this study. To further understand very low AEPs at this site, more study would need to be done on persistent climatic conditions and channel changes over time.

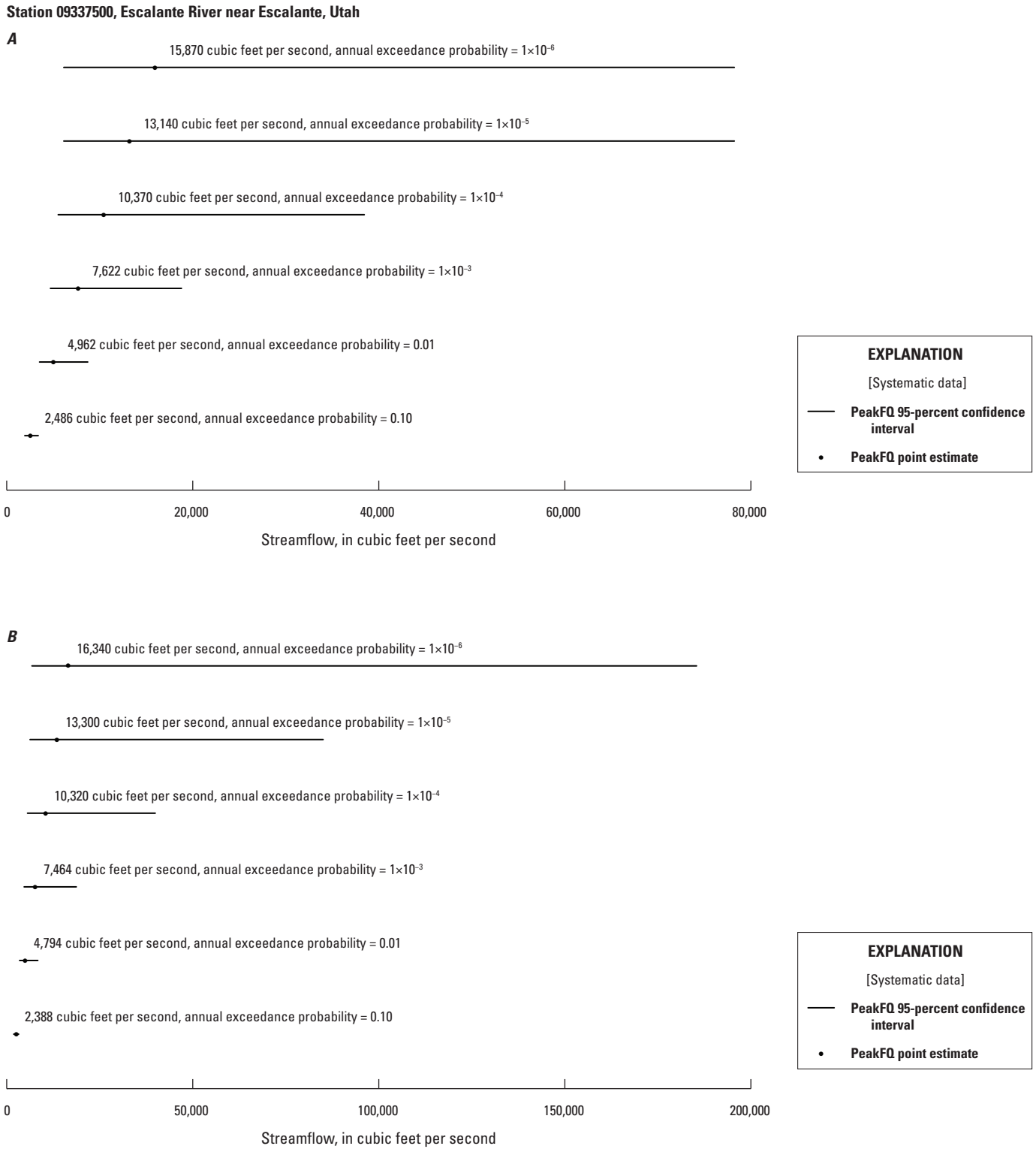

Figure 65. Point and interval estimates for a range of annual exceedance probabilities for streamgage station 09337500, Escalante River near Escalante, Utah, floods, calculated using U.S. Geological Survey PeakFQ version 7.2, with *A*, as weighted skew and systematic data and *B*, as weighted skew systematic plus historical data. This depicts analysis results for *A*, scenario 1 and *B*, scenario 2 of table 8.

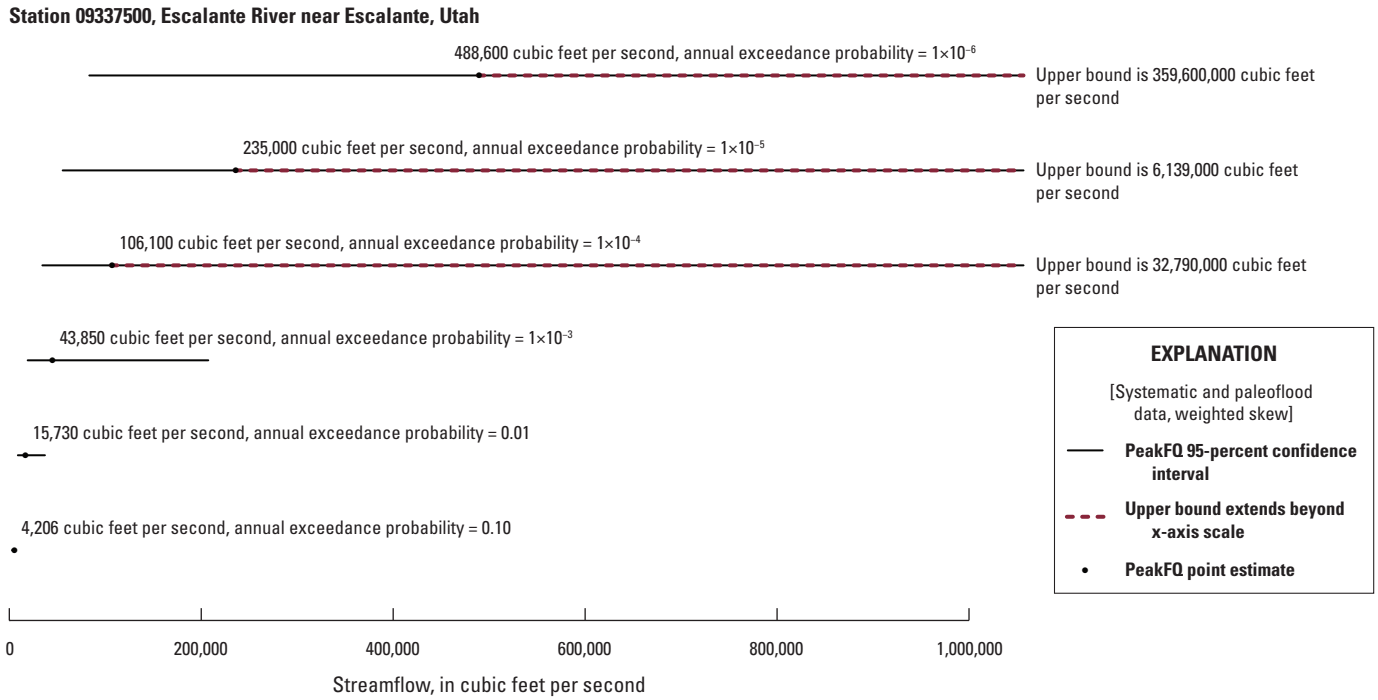

Figure 66. Point and interval estimates for a range of annual exceedance probabilities for streamgage station 09337500, Escalante River near Escalante, Utah, floods, calculated using U.S. Geological Survey PeakFQ version 7.2, with weighted skew and systematic, historical, and paleoflood data. This depicts analysis results for scenario 3 of table 8.

Summary

Very low probability floods may have an annual exceedance probability (AEP) less than 0.001, meaning the mean recurrence interval may be more than 1,000 years. Yet, estimation of these flood frequencies is needed to accurately portray risks to critical infrastructure, such as nuclear powerplants and large dams. Standard methods for statistical estimation of flood frequency rely on the systematic streamflow record, which provides a time series of annual maximum flood peaks. Uncertainties are large when trying to extrapolate magnitudes of very low AEP events from a streamflow record that is much shorter (typically less than 100 years). An additional complication for flood-frequency analysis is the underlying assumption that the flood series is stationary. That is, the peak-flow time series varies around a constant mean within a particular range of values (a defined variance). As the hydrologic community's understanding of natural systems and anthropogenic effects has evolved, it has become clear that the stationarity assumption is sometimes inappropriate. However, there is not a consensus on the appropriate methodology for the computation of flood frequencies for nonstationary systems.

Flood-frequency analysis under nonstationary conditions is an active area of research, and many suggested methods are not yet able to incorporate paleoflood data. However, a literature review was completed to summarize the state of flood-frequency science. The literature review highlights tools available to detect nonstationarities and identify possible attributing factors, and highlights efforts to include external information for detection of nonstationarities. Additionally, the review contributes to the understanding of underlying causes of nonstationarities and potential ways to address nonstationarities, while simultaneously showing that the problem is not easy to address.

Five sites were selected to demonstrate methods for initial data analysis and detection of trends and for incorporation of historical and paleoflood information in flood-frequency analysis. The flood-frequency results should not be considered definitive at any of these sites. The purpose of this analysis was to study the effect of historical and paleoflood data on the flood-frequency distribution. Some subjectivity is inherent in assessing the validity of historical and paleoflood data and in incorporating thresholds for missing periods during the systematic record and for paleo periods. Local or regional experts might make different choices when assessing these sites.

The sites were Red River of the North at James Avenue Pumping Station, Winnipeg, Manitoba, Canada (Red River); lower reach, Rapid Creek, South Dakota (lower reach, Rapid Creek); Spring Creek, South Dakota (Spring Creek); Cherry Creek near Melvin, Colorado (Cherry Creek); and Escalante River near Escalante, Utah (Escalante River). The sites were chosen for geographic diversity and their unique characteristics, which highlighted issues such as autocorrelation, outlier peaks, or short period of record.

The peaks for these sites were all analyzed for indicators of nonstationarity including autocorrelation, change points, and monotonic trends. Detected nonstationarities can be naturally occurring, anthropogenically induced, or can be statistical artifacts in the data. Therefore, it is difficult to say when a nonstationarity disqualifies a site or a period for flood-frequency analysis, and the degree to which one of these issues will affect flood frequency is difficult to assess.

The flood-frequency analysis completed for this study used version 7.2 of the U.S. Geological Survey PeakFQ program with extended output for AEPs as low as 1×10^{-6}. PeakFQ assumes that the peak-flow series follow a log-Pearson type III distribution. This distribution is widely used in hydrology, particularly in the United States, where it is used in Bulletin 17C, which provides guidelines used by some Federal agencies in the determination of flood flow frequencies (under specific recommended assumptions). Applications of the distribution use systematically collected and historical peak-streamflow values to define a frequency distribution based on the sample mean (location), standard deviation (scale), and skew (shape). This study estimates those distribution parameters using the expected moments algorithm. Nonstandard flood data may be used with the expected moments algorithm, including flood interval estimates, as opposed to the standard point estimates and flood thresholds.

When other flood-frequency studies were available, their results were compared to the results here. The comparisons in some cases simply show the effect of additional years of data, whereas other comparisons show results from methods other than PeakFQ that use different probability distributions or fitting methods.

The Red River was chosen because of the availability of well documented historical peaks and paleoflood peaks. The site has autocorrelated peaks; among the implications for this is that 117 peaks on the Red River may have equivalent information to 45 independent peaks. The Red River had a change point in mean and variance. The change point and autocorrelation are related to well documented climatic persistence in this basin. The Red River also has an increasing peak magnitude trend, likely more than just an artifact of climatic persistence at the end of the record. Flood-frequency analysis was completed under 11 different scenarios to show how regional information, in the form of a weighted skew, and incrementally adding data of different types (historical peaks, historical intervals, paleoflood data, and thresholds) affects the flood-frequency analysis. In addition, several other flood-frequency studies were compared so that for an AEP of 0.01, 23 different scenarios were compared numerically and graphically. The addition of peaks and thresholds beyond the systematic record can increase the precision and accuracy of estimates for very low AEPs (less than 0.001); in fact, paleoflood data appear necessary to reduce uncertainty for very low AEPs at this site. When compared to another study that adjusted for correlation, the addition of paleoflood data, creating a much longer record, appears to offset the loss of information caused by correlated data.

The lower reach of Rapid Creek, chosen because of the existence of paleoflood data in a well-documented study, did not have autocorrelation but did have one high outlier peak that affects the fit of the upper end of the distribution when calculating flood frequencies. Paleoflood information helped put the outlier in context; however, very low AEPs at this site still had extraordinarily large confidence bounds.

Spring Creek, chosen because of the existence of paleoflood data in a well-documented study and because it was nearby the lower reach of Rapid Creek for an experiment in information transfer, was like the lower reach of Rapid Creek in that it was uncorrelated and had a single outlier. This site showed that peaks outside the systematic period of record need to be examined carefully to determine whether they are opportunistic peaks, which do not provide additional information about appropriate thresholds for missing periods, or whether they are large peaks from which a threshold can be derived. Although generally helpful in determining very low AEPs, paleoflood data can increase uncertainty or worsen the fit of the upper end of the distribution if they appear to come from a different, larger, population than the peaks in the systematic record. Ideally, the range of paleoflood peaks should have some overlap with the observed range to provide a smooth transition of the distribution. This site was also used as an experiment in transferring regional paleoflood data—transferring information from the lower reach of Rapid Creek to this site. This transfer of information provided more information for the upper end of the distribution. However, the transfer was based on methods that need more development and refinement for future applications.

Cherry Creek was used to compare the results with paleoflood data to results for distributions described in Asquith and others (2017). This showed that the generalized Pareto distribution was not a good distribution for estimating very low AEPs, as Asquith and others (2017) found. The asymmetric exponential power distribution and the generalized logistic distribution generated large estimates for very low AEPs and were not good distributions for this site. Of the remaining distributions, it appears that the best may depend on which AEP is desired. In an analysis that is not exploratory, how to weight the quantiles at given AEPs for the acceptable distributions would need to be determined by subject matter experts.

The Escalante River was chosen because of the existence of paleoflood data and past flood-frequency analyses using these data. Peaks at this site did not have autocorrelation, change points, or a monotonic trend. This river has been the subject of several paleoflood studies and some of the paleoflood data were incorporated here. The paleoflood peaks added were very large peaks and increased the uncertainty for very low AEPs.

The addition of historical peaks, paleoflood peaks and paleoflood thresholds can increase or decrease the magnitude of very low AEP floods, depending on the distribution and length of the systematic period. The additional information can reduce the error bounds on floods with very low exceedance probabilities; however, the effect is not uniform across sites.

References Cited

Abramowitz, M., and Stegun, I.A., eds., 1965, Handbook of mathematical functions with formulas, graphs and mathematical tables: Dover, N.Y., 1046 p.

Acreman, M.C., and Wiltshire, S.E., 1987, Identification of regions for regional flood frequency analysis: Eos (Washington, D.C.), v. 68, no. 44.

Allaby, M., ed., 2008, A dictionary of earth sciences (3d ed.): Oxford University Press, Oxford, United Kingdom, accessed August 4, 2018, at https://www.oxfordreference.com/view/10.1093/acref/9780199211944.001.0001/acref-9780199211944.

Armstrong, W.H., Collins, M.J., and Snyder, N.P., 2012, Increased frequency of low-magnitude floods in New England: Journal of the American Water Resources Association, v. 48, no. 2, p. 306–320. [Also available at https://doi.org/10.1111/j.1752-1688.2011.00613.x.]

Asquith, W.H., 2001, Effects of regulation on L-moments of annual peak streamflow in Texas: U.S. Geological Survey Water-Resources Investigations Report 01–4243, 66 p., accessed July 23, 2018, at https://doi.org/10.3133/wri014243.

Asquith, W.H., 2011, Distributional analysis with L-moment statistics using the R environment for statistical computing: Lubbock, Tex., Create Space Independent Publishing Platform, 360 p.

Asquith, W.H., 2017, lmomco—L-moments, censored L-moments, trimmed L-moments, L-comoments, and many distributions: R package version 2.2.9., accessed February 28, 2017, at https://cran.r-project.org/web/packages/lmomco/index.html.

Asquith, W.H., Kiang, J.E., and Cohn, T.A., 2017, Application of at-site peak-streamflow frequency analyses for very low annual exceedance probabilities: U.S. Geological Survey Scientific Investigations Report 2017–5038, 93 p. [Also available at https://doi.org/10.3133/sir20175038.]

Auger, I.E., and Lawrence, C.E., 1989, Algorithms for the optimal identification of segment neighborhoods: Bulletin of Mathematical Biology, v. 51, no. 1, p. 39–54. [Also available at https://doi.org/10.1016/S0092-8240(89)80047-3.]

Ayalew, T.B., Krajewski, W.F., and Mantilla, R., 2013, Exploring the effect of reservoir storage on peak discharge frequency: Journal of Hydrologic Engineering, v. 18, no. 12, p. 1697–1708. [Also available at https://doi.org/10.1061/(ASCE)HE.1943-5584.0000721.]

Ayalew, T.B., Krajewski, W.F., Mantilla, R., Wright, D.B., and Small, S.J., 2017, Effect of spatially distributed small dams on flood frequency—Insights from the Soap Creek watershed: Journal of Hydrologic Engineering, v. 22, no. 7, 11 p. [Also available at https://doi.org/10.1061/(ASCE)HE.1943-5584.0001513.]

Ballesteros Cánovas, J.A., Eguibar, M., Bodoque, J.M., Díez-Herrero, A., Stoffel, M., and Gutiérrez-Pérez, I., 2011, Estimating flash flood discharge in an ungauged mountain catchment with 2D hydraulic models and dendrogeomorphic palaeostage indicators: Hydrological Processes, v. 25, no. 6, p. 970–979. [Also available at https://doi.org/10.1002/hyp.7888.]

Ballesteros Cánovas, J.A., Trappmann, D., Shekhar, M., Bhattacharyya, A., and Stoffel, M., 2017, Regional flood-frequency reconstruction for Kullu district, Western Indian Himalayas: Journal of Hydrology, v. 546, p. 140–149. [Also available at https://doi.org/10.1016/j.jhydrol.2016.12.059.]

Baranowski, R., and Fryzlewicz, P., 2015, wbs—Wild binary segmentation for multiple change-point detection: R package version 1.3, accessed February 28, 2017, at https://CRAN.R-project.org/package=wbs.

Barendregt, R.W., and Irving, E., 1998, Changes in the extent of North American ice sheets during the late Cenozoic: Canadian Journal of Earth Sciences, v. 35, no. 5, p. 504–509. [Also available at https://doi.org/10.1139/e97-126.]

Barry, D., and Hartigan, J.A., 1993, A Bayesian analysis for change point problems: Journal of the American Statistical Association, v. 35, no. 3, p. 309–319.

Bartles, M., Brunner, G., Fleming, M., Faber, B., and Slaughter, J., 2016, HEC-SSP—Statistical software package version 2.1: U.S. Army Corps of Engineers Computer Program Documentation, 379 p., accessed August 4, 2018, at https://www.hec.usace.army.mil/software/hec-ssp/documentation/HEC-SSP_21_Users_Manual.pdf.

Bayazit, M., 2015, Nonstationarity of hydrological records and recent trends in trend analysis—A state-of-the-art review: Environmental Processes, v. 2, no. 3, p. 527–542. [Also available at https://doi.org/10.1007/s40710-015-0081-7.]

Bayazit, M., and Önöz, B., 2007, To prewhiten or not to prewhiten in trend analysis?: Hydrological Sciences Journal, v. 52, no. 4, p. 611–624. [Also available at https://doi.org/10.1623/hysj.52.4.611.]

Benito, G., Lang, M., Barriendos, M., Llasat, M.C., Francés, F., Ouarda, T., Thorndycraft, V., Enzel, Y., Bardossy, A., Coeur, D., and Bobée, B., 2004, Use of systematic, palaeoflood and historical data for the improvement of flood risk estimation—Review of scientific methods: Natural Hazards, v. 31, no. 3, p. 623–643. [Also available at https://doi.org/10.1023/B:NHAZ.0000024895.48463.eb.]

Beran, J., 1994, Statistics for long-memory processes—Monographs on statistics and applied probability: New York, Chapman & Hall/CRC, 315 p.

Bluemle, J.P., 1996, From the state geologist: North Dakota Geological Survey Newsletter, v. 23, no. 1, p. 1–2.

Booy, C., and Lye, L.M., 1989, A new look at flood risk determination: Water Resources Bulletin, v. 25, no. 5, p. 933–943. [Also available at https://doi.org/10.1111/j.1752-1688.1989.tb05407.x.]

Booy, C., and Morgan, D.R., 1985, The effect of clustering of flood peaks on a flood risk analysis for the Red River: Canadian Journal of Civil Engineering, v. 12, no. 1, p. 150–165. [Also available at https://doi.org/10.1139/l85-015.]

Brath, A., Castellarin, A., Franchini, M., and Galeati, G., 2001, Estimating the index flood using indirect methods: Hydrological Sciences Journal, v. 46, no. 3, p. 399–418. [Also available at https://doi.org/10.1080/02626660109492835.]

Bronaugh, D., and Werner, A., 2013, zyp: Zhang + Yue-Pilon trends package: R package version 0.10-1, accessed February 28, 2017, at https://CRAN.R-project.org/package=zyp.

Buckley, J.J., and Jowers, L.J., 2008, Monte Carlo methods in fuzzy optimization: Berlin, Springer-Verlag, Studies in Fuzziness and Soft Computing, 260 p.

Burn, D.H., 1990a, An appraisal of the "region of influence" approach to flood frequency analysis: Hydrological Sciences Journal, v. 35, no. 2, p. 149–165. [Also available at https://doi.org/10.1080/02626669009492415.]

Burn, D.H., 1990b, Evaluation of regional flood frequency analysis with a region of influence approach: Water Resources Research, v. 26, no. 10, p. 2257–2265. [Also available at https://doi.org/10.1029/WR026i010p02257.]

Burn, D.H., and Goel, N.K., 2001, Flood frequency analysis for the Red River at Winnipeg: Canadian Journal of Civil Engineering, v. 28, no. 3, p. 355–362. [Also available at https://doi.org/10.1139/l00-122.]

Busuioc, A., and von Storch, H.V., 1996, Changes in the winter precipitation in Romania and its relation to the large-scale circulation: Tellus. Series A, Dynamic Meterology and Oceanography, v. 48, no. 4, p. 538–552. [Also available at https://doi.org/10.1034/j.1600-0870.1996.t01-3-00004.x.]

Buttle, J.M., 2011, Streamflow response to headwater reforestation in the Ganaraska River basin, southern Ontario, Canada: Hydrological Processes, v. 25, no. 19, p. 3030–3041. [Also available at https://doi.org/10.1002/hyp.8061.]

Caeiro, F., and Mateus, A., 2014, randtests—Testing randomness in R: R package version 1.0, accessed February 28, 2017, at https://CRAN.R-project.org/package=randtests.

Canada Department of Resources and Development, 1953, Report on investigations into measures for the reduction of the flood hazard in the greater Winnipeg area: Red River Basin Investigation, Water Resources Division, Engineering and Water Resources Branch, 66 p., 8 appendices.

Carslaw, D.C., and Ropkins, K., 2012, openair—An R package for air quality data analysis: Environmental Modelling & Software, v. 27–28, p. 52–61. [Also available at https://doi.org/10.1016/j.envsoft.2011.09.008.]

Castellarin, A., Vogel, R.M., and Matalas, N.C., 2005, Probabilistic behavior of a regional envelope curve: Water Resources Research, v. 41, no. 6, 13 p. [Also available at https://doi.org/10.1029/2004WR003042.]

Chiew, F.H.S., and McMahon, T.A., 1993, Detection of trend or change in annual flow of Australian rivers: International Journal of Climatology, v. 13, no. 6, p. 643–653. [Also available at https://doi.org/10.1002/joc.3370130605.]

Chiew, F., and Siriwardena, L., 2005, TREND—User guide: CRC for Catchment Hydrology, 23 p.

Cohn, T.A., England, J.F., Berenbrock, C.E., Mason, R.R., Stedinger, J.R., and Lamontagne, J.R., 2013, A generalized Grubbs-Beck test statistic for detecting multiple potentially influential low outliers in flood series: Water Resources Research, v. 49, no. 8, p. 5047–5058. [Also available at https://doi.org/10.1002/wrcr.20392.]

Cohn, T.A., Lane, W.L., and Baier, W.G., 1997, An algorithm for computing moments-based flood quantile estimates when historical flood information is available: Water Resources Research, v. 33, no. 9, p. 2089–2096. [Also available at https://doi.org/10.1029/97WR01640.]

Cohn, T.A., Lane, W.L., and Stedinger, J.R., 2001, Confidence intervals for expected moments algorithm flood quantile estimates: Water Resources Research, v. 37, no. 6, p. 1695–1706. [Also available at https://doi.org/10.1029/2001WR900016.]

Cohn, T.A., and Lins, H.F., 2005, Nature's style—Naturally trendy: Geophysical Research Letters, v. 32, no. 23, 5 p. [Also available at https://doi.org/10.1029/2005GL024476.]

Conover, W.J., 1999, Practical nonparametric statistics: New York, John Wiley & Sons, Inc., 584 p.

Cox, D.R., and Stuart, A., 1955, Some quick sign tests for trend in location and dispersion: Biometrika, v. 42, no. 1/2, p. 80–95. [Also available at https://doi.org/10.2307/2333424.]

Crippen, J.R., and Bue, C.D., 1977, Maximum floodflows in the conterminous United States: U.S. Geological Survey Water Supply Paper 1887, 52 p., accessed February 3, 2017, at https://pubs.usgs.gov/wsp/1887/report.pdf.

Curran, J.H., Barth, N.A., Veilleux, A.G., and Ourso, R.T., 2016, Estimating flood magnitude and frequency at gaged and ungaged sites on streams in Alaska and conterminous basins in Canada, based on data through water year 2012: Scientific Investigations Report 2016–5024, 58 p., accessed March 1, 2017, at https://pubs.er.usgs.gov/publication/sir20165024.

Dalrymple, T., 1960, Flood-frequency analyses, manual of hydrology—Part 3: U.S. Geological Survey 1543–A, 80 p., accessed February 3, 2017, at https://pubs.er.usgs.gov/publication/wsp1543A.

Davison, A.C., and Hinkley, D.V., 1997, Bootstrap methods and their application—Cambridge series in statistical and probabilistic mathematics: New York, Cambridge University Press, 594 p. [Also available at https://doi.org/10.1017/CBO9780511802843.]

Dawdy, D.R., Griffis, V.W., and Gupta, V.K., 2012, Regional flood-frequency analysis—How we got here and where we are going: Journal of Hydrologic Engineering, v. 17, no. 9, p. 953–959. [Also available at https://doi.org/10.1061/(ASCE)HE.1943-5584.0000584.]

Dinicola, K., 1996, The "100-year flood": U.S. Geological Survey Fact Sheet 229-96, accessed February 28, 2017, at https://pubs.usgs.gov/fs/FS-229-96/pdf/FS_229-96.pdf.

Douglas, E.M., Vogel, R.M., and Kroll, C.N., 2000, Trends in floods and low flows in the United States—Impact of spatial correlation: Journal of Hydrology, v. 240, no. 1-2, p. 90–105. [Also available at https://doi.org/10.1016/S0022-1694(00)00336-X.]

Dutta, D., Kim, S., Vaze, J., and Hughes, J., 2015, Streamflow predictions in regulated river systems—Hydrological non-stationarity versus anthropogenic water use: Proceedings of the International Association of Hydrological Sciences, v. 371, p. 35–42. [Also available at https://doi.org/10.5194/piahs-371-35-2015.]

Eng, K., Chen, Y.-Y., and Kiang, J.E., 2009, User's guide to the weighted-multiple-linear regression program (WREG version 1.0): Techniques and Methods, book 4, chap. A8, 21 p., accessed September 2, 2018, at https://pubs.er.usgs.gov/publication/tm4A8.

Eng, K., Kiang, J.E., Chen, Y.-Y., Carlisle, D.M., and Granato, G.E., 2011, Causes of systematic over- or underestimation of low streamflows by use of index-streamgage approaches in the United States: Hydrological Processes, v. 25, no. 14, p. 2211–2220. [Also available at https://doi.org/10.1002/hyp.7976.]

Eng, K., Milly, P.C., and Tasker, G.D., 2007, Flood Regionalization—A hybrid geographic and predictor-variable region-of-influence regression method: Journal of Hydrologic Engineering, v. 12, no. 6, p. 585–591. [Also available at https://doi.org/10.1061/(ASCE)1084-0699(2007)12:6(585).]

Eng, K., Tasker, G.D., and Milly, P.C.D., 2005, An analysis of region-of-influence methods for flood regionalization in the Gulf-Atlantic Rolling Plains: Journal of the American Water Resources Association, v. 41, no. 1, p. 135–143. [Also available at https://doi.org/10.1111/j.1752-1688.2005.tb03723.x.]

England, J.F., Jr.; Cohn, T.A.; Faber, B.A.; Stedinger, J.R.; Thomas, W.O., Jr.; Veilleux, A.G.; Kiang, J.E.; and Mason, R.R., Jr., 2019, Guidelines for determining flood flow frequency—Bulletin 17C (ver. 1.1, May 2019): U.S. Geological Survey Techniques and Methods, book 4, chap. B5, 148 p., accessed March 1, 2017, at https://doi.org/10.3133/tm4B5.

Enzel, Y., Ely, L.L., House, P.K., Baker, V.R., and Webb, R.H., 1993, Paleoflood evidence for a natural upper bound to flood magnitudes in the Colorado River Basin: Water Resources Research, v. 29, no. 7, p. 2287–2297. [Also available at https://doi.org/10.1029/93WR00411.]

Erdman, C., and Emerson, J.W., 2007, bcp—An R package for performing a Bayesian analysis of change point problems: Journal of Statistical Software, v. 23, no. 3, p. 1–13. [Also available at https://doi.org/10.18637/jss.v023.i03.]

Eslamian, S., ed., 2014, Handbook of engineering hydrology—Modeling climate change, and variability: New York, CRC Press, 646 p. [Also available at https://doi.org/10.1201/b16683.]

Federal Emergency Management Agency, 2016, Why dams fail: Federal Emergency Management Agency web page, accessed February 28, 2017, at https://www.fema.gov/why-dams-fail.

Filliben, J.J., and Heckert, A., 2012, Maximum likelihood, *in* Croarkin, C., and Tobias, P., eds., NIST/SEMATECH e-Handbook of Statistical Methods: Gaithersburg, Md., National Institute of Standards and Technology, accessed January 24, 2017, at https://www.itl.nist.gov/div898/handbook/eda/section3/eda3652.htm.

Flynn, K.M., Kirby, W.H., and Hummel, P.R., 2006, User's manual for program PeakFQ annual flood-frequency analysis using Bulletin 17B guidelines: U.S. Geological Survey, Techniques and Methods Book 4, Chapter B4, 42 p., accessed January 23, 2017, at https://pubs.usgs.gov/tm/2006/tm4b4/.

Freeman, W.B., and Leighton, M.O., 1911, Surface water supply of the United States, 1909, Part IX, Colorado River basin: Water Supply Paper 269, 247 p., accessed August 24, 2017, at https://pubs.er.usgs.gov/publication/wsp269.

Friedman, D., Schechter, J., Baker, B., Mueller, C., Villarini, G., and White, K.D., 2016, U.S. Army Corps of Engineers nonstationarity detection tool user guide: U.S. Army Corps of Engineers, accessed January 24, 2017, at http://corpsmapu.usace.army.mil/rccinfo/nsd/docs/Nonstationarity_Detection_Tool_User_Guide.pdf.

Friedman, D., Schechter, J., Saint-Miller, A.M., Mueller, C., Villarini, G., White, K.D., and Baker, B., 2018, US Army Corps of Engineers nonstationarity detection tool user guide—Version 1.2—May 2016—User manual update—September 2018: U.S. Army Corps of Engineers, accessed April 22, 2018, at http://corpsmapu.usace.army.mil/rccinfo/nsd/docs/Nonstationarity_Detection_Tool_User_Guide.pdf.

Fryzlewicz, P., 2014, Wild binary segmentation for multiple change-point detection: Annals of Statistics, v. 42, no. 6, p. 2243–2281. [Also available at https://doi.org/10.1214/14-AOS1245.]

Fuller, W.E., 1914, Flood flows, *in* Transactions of the American society of civil engineers v. 77: New York, American Society of Civil Engineers, p. 564–617.

Fulton, R.J., ed., 1989, Quaternary geology of Canada and Greenland: Geological Survey of Canada, Geology of Canada, no. 1, 839 p.

Gado T.A., and Nguyen, Van-Thanh-Van, 2016, Comparison of homogeneous region delineation approaches for regional flood frequency analysis at ungauged sites: Journal of Hydrologic Engineering, v. 21, no. 3, p. 04015068 (1–10).

Gaume, E., Gaál, L., Viglione, A., Szolgay, J., Kohnová, S., and Blöschl, G., 2010, Bayesian MCMC approach to regional flood frequency analyses involving extraordinary flood events at ungauged sites: Journal of Hydrology, v. 394, no. 1–2, p. 101–117. [Also available at https://doi.org/10.1016/j.jhydrol.2010.01.008.]

Gilbert, R.O., 1987, Statistical methods for environmental pollution monitoring: New York, Van Nostrand Reinhold Co., 320 p.

Government of Canada, 2019, Real-time hydrometric data graph for RED RIVER AT JAMES AVENUE PUMPING STATION (05OJ015) [MB]: Government of Canada database, accessed October 10, 2019, at https://wateroffice.ec.gc.ca/report/real_time_e.html?stn=05OJ015.

Grayson, R.B., Argent, R.M., Nathan, R.J., McMahon, T.A., and Mein, R.G., 1996, Hydrological recipes—Estimation techniques in Australian hydrology: Australia, Cooperative Research Centre for Catchment Hydrology, 125 p.

Greenbaum, N., Harden, T.M., Baker, V.R., Weisheit, J., Cline, M.L., Porat, N., Halevi, R., and Dohrenwend, J., 2014, A 2000 year natural record of magnitudes and frequencies for the largest Upper Colorado River floods near Moab, Utah: Water Resources Research, v. 50, no. 6, p. 5249–5269. [Also available at https://doi.org/10.1002/2013WR014835.]

Griffis, V.W., and Stedinger, J.R., 2007, Evolution of flood frequency analysis with Bulletin 17: Journal of Hydrologic Engineering, v. 12, no. 3, p. 283–297. [Also available at https://doi.org/10.1061/(ASCE)1084-0699(2007)12:3(283).]

Griffis, V.W., Stedinger, J.R., and Cohn, T.A., 2004, Log Pearson type 3 quantile estimators with regional skew information and low outlier adjustments: Water Resources Research, v. 40, no. 7, W07503. [Also available at https://doi.org/10.1029/2003WR002697.]

Grover, P., Burn, D., and Cunderlik, J., 2002, A comparison of index flood estimation procedures for ungauged catchments: Canadian Journal of Civil Engineering, v. 29, no. 5, p. 734–741. [Also available at https://doi.org/10.1139/l02-065.]

Haddad, K., and Rahman, A., 2012, Regional flood frequency analysis in eastern Australia—Bayesian GLS regression-based methods within fixed region and ROI framework—Quantile Regression vs. Parameter Regression Technique: Journal of Hydrology, v. 430–431, p. 142–161. [Also available at https://doi.org/10.1016/j.jhydrol.2012.02.012.]

Haddad, K., Rahman, A., and Ling, F., 2015, Regional flood frequency analysis method for Tasmania, Australia—A case study on the comparison of fixed region and region-of-influence approaches: Hydrological Sciences Journal, v. 60, no. 12, p. 2086–2101. [Also available at https://doi.org/10.1080/02626667.2014.950583.]

Hamed, K.H., 2008, Trend detection in hydrologic data—The Mann–Kendall trend test under the scaling hypothesis: Journal of Hydrology, v. 349, no. 3-4, p. 350–363. [Also available at https://doi.org/10.1016/j.jhydrol.2007.11.009.]

Hamed, K.H., and Rao, A.R., 1998, A modified Mann-Kendall trend test for autocorrelated data: Journal of Hydrology, v. 204, no. 1–4, p. 182–196. [Also available at https://doi.org/10.1016/S0022-1694(97)00125-X.]

Harden, N., 1999, Red River flood frequency and risk analysis, *in* Red River Flooding—Decreasing our Risks, Winnipeg, Manitoba, 1999, Proceedings: Winnipeg Manitoba, Canadian Water Resources Association Conference, p. IV1–IV18.

Harden, T.M., and O'Connor, J.E., 2017, Prehistoric floods on the Tennessee River—Assessing the use of stratigraphic records of past floods for improved flood-frequency analysis: U.S. Geological Survey Scientific Investigations Report 2017–5052, 15 p., accessed September 30, 2016, at https://doi.org/10.3133/sir20175052.

Harden, T.M., O'Connor, J.E., and Driscoll, D.G., 2015, Late Holocene flood probabilities in the Black Hills, South Dakota with emphasis on the Medieval Climate Anomaly: Past Hydrological Extreme Events in a Changing Climate, v. 130, p. 62–68.

Harden, T.M., O'Connor, J.E., Driscoll, D.G., and Stamm, J.F., 2011, Flood-frequency analyses from paleoflood investigations for Spring, Rapid, Boxelder, and Elk Creeks, Black Hills, western South Dakota: U.S. Geological Survey Scientific Investigations Report 2011–5131, 136 p., accessed September 30, 2016, at https://pubs.usgs.gov/sir/2011/5131/.

Hazen, A., 1930, Flood flows—A study of frequencies and magnitudes: New York, John Wiley & Sons, Inc., 199 p.

He, W., Wan, S., Jiang, Y., Jin, H., Zhang, W., Wu, Q., and He, T., 2013, Detecting abrupt change on the basis of skewness—Numerical tests and applications: Journal of Climatology, v. 33, p. 2713–2727.

Helsel, D.R., and Hirsch, R.M., 1992, Statistical methods in water resources: New York, Elsevier, 529 p.

Higgins, J.J., 2003, Introduction to modern nonparametric statistics: Pacific Grove, California, Duxbury Press, 384 p.

Hirsch, R.M., 1982, A comparison of four streamflow record extension techniques: Water Resources Research, v. 18, no. 4, p. 1081–1088. [Also available at https://doi.org/10.1029/WR018i004p01081.]

Hirsch, R.M., 2011, A perspective on nonstationarity and water management: Journal of the American Water Resources Association, v. 47, no. 3, p. 436–446. [Also available at https://doi.org/10.1111/j.1752-1688.2011.00539.x.]

Hirsch, R.M., and Ryberg, K.R., 2012, Has the magnitude of floods across the USA changed with global CO2 levels?: Hydrological Sciences Journal, v. 57, no. 1, p. 1–9. [Also available at https://doi.org/10.1080/02626667.2011.621895.]

Hodgkins, G.A., and Dudley, R.W., 2011, Historical summer base flow and stormflow trends for New England rivers: Water Resources Research, v. 47, no. 7, p. 1–16. [Also available at https://doi.org/10.1029/2010WR009109.]

Hodgkins, G.A., Dudley, R.W., Archfield, S.A., and Renard, B., 2019, Effects of climate, regulation, and urbanization on historical flood trends in the United States: Journal of Hydrology, v. 573, p. 697–709. [Also available at https://doi.org/10.1016/j.jhydrol.2019.03.102.]

Hodgkins, G.A., Whitfield, P.H., Burn, D.H., Hannaford, J., Renard, B., Stahl, K., Fleig, A.K., Madsen, H., Mediero, L., Korhonen, J., Murphy, C., and Wilson, D., 2017, Climate-driven variability in the occurrence of major floods across North America and Europe: Journal of Hydrology, v. 552, p. 704–717. [Also available at https://doi.org/10.1016/j.jhydrol.2017.07.027.]

Holmes, R.R., Jr., and Dinicola, K., 2010, 100-Year flood–it's all about chance: U.S. Geological Survey General Information Product 106, 1 p. [Also available at https://pubs.usgs.gov/gip/106/.]

Homer, C., Dewitz, J., Yang, L., Jin, S., Danielson, P., Xian, G., Coulston, J., Herold, N., Wickham, J., and Megown, K., 2015, Completion of the 2011 National Land Cover Database for the conterminous United States—Representing a decade of land cover change information: Photogrammetric Engineering and Remote Sensing, v. 81, no. 0, p. 345–354.

Hosking, J.R.M., and Wallis, J.R., 1986, Paleoflood hydrology and flood frequency analysis: Water Resources Research, v. 22, no. 4, p. 543–550. [Also available at https://doi.org/10.1029/WR022i004p00543.]

Hosking, J.R.M., and Wallis, J.R., 2005, Regional frequency analysis—An approach based on L-moments: New York, Cambridge University Press.

Hosman, K.J., Ely, L.L., and O'Connor, J.E., 2003, Holocene paleoflood hydrology of the lower Deschutes River, Oregon, *in* O'Connor, J.E., and Grant, G.E., eds., A peculiar river—Geology, geomorphology, and hydrology of the Deschutes River, Oregon, (v. 7): American Geophysical Union, Water Science and Application Series, p. 121–146.

Hurst, H.E., 1951, Long-term storage capacity of reservoirs: Transactions of the American Society of Civil Engineers, v. 116, no. 1, p. 770–799.

Interagency Advisory Committee on Water Data, 1982, Guidelines for determining flood flow frequency—Bulletin 17B of the hydrology subcommittee: U.S. Geological Survey Interagency Advisory Committee on Water Data, accessed February 21, 2017, at https://water.usgs.gov/osw/bulletin17b/dl_flow.pdf.

James, N.A., and Matteson, D.S., 2014, ecp—An R package for nonparametric multiple change point analysis of multivariate data: Journal of Statistical Software, v. 62, no. 7, p. 1–25. [Also available at https://doi.org/10.18637/jss.v062.i07.]

Jarrett, R.D., 2000, Paleoflood investigations for Cherry Creek basin, eastern Colorado, *in* Joint Conference on Water Resources Engineering and Water Resources Planning and Management, Minneapolis, Minn., 2000, Proceedings: Minneapolis, Minn., American Society of Civil Engineers, p. 1–10. [Also available at https://doi.org/10.1061/40517(2000)122.]

Jarrett, R.D., and Tomlinson, E.M., 2000, Regional interdisciplinary paleoflood approach to assess extreme flood potential: Water Resources Research, v. 36, no. 10, p. 2957–2984. [Also available at https://doi.org/10.1029/2000WR900098.]

Jarvis, C.S., 1936, Floods in the United States—Magnitude and frequency: U.S. Geological Survey Water Supply Paper 771, 495 p., accessed August 9, 2017, at https://pubs.er.usgs.gov/publication/wsp771.

Javelle, P., Ouarda, T.B.M.J., Lang, M., Bobée, B., Galéa, G., and Grésillon, J.-M., 2002, Development of regional flood-duration–frequency curves based on the index-flood method: Journal of Hydrology, v. 258, no. 1–4, p. 249–259. [Also available at https://doi.org/10.1016/S0022-1694(01)00577-7.]

Jin, M., and Stedinger, J.R., 1989, Flood frequency analysis with regional and historical information: Water Resources Research, v. 25, no. 5, p. 925–936. [Also available at https://doi.org/10.1029/WR025i005p00925.]

Kendall, M.G., 1938, A new measure of rank correlation: Biometrika, v. 30, no. 1–2, p. 81–93. [Also available at https://doi.org/10.1093/biomet/30.1-2.81.]

Kennedy, J.R., Paretti, N.V., and Veilleux, A.G., 2014, Methods for estimating magnitude and frequency of 1-, 3-, 7-, 15-, and 30-day flood-duration flows in Arizona: U.S. Geological Survey Scientific Investigations Report 2014–5109, 45 p., accessed August 9, 2017, at https://pubs.er.usgs.gov/publication/sir20145109.

Kenney, T.A., Wilkowske, C.D., and Wright, S.J., 2008, Methods for estimating magnitude and frequency of peak flows for natural streams in Utah: U.S. Geological Survey Scientific Investigations Report 2007–5158, 28 p.

Khaliq, M.N., Ouarda, T.B.M.J., and Gachon, P., 2009, Identification of temporal trends in annual and seasonal low flows occurring in Canadian rivers—The effect of short- and long-term persistence: Journal of Hydrology, v. 369, no. 1–2, p. 183–197. [Also available at https://doi.org/10.1016/j.jhydrol.2009.02.045.]

Killick, R., and Eckley, I.A., 2014, changepoint—An R package for changepoint analysis: Journal of Statistical Software, v. 1, no. 3, p. 1–19.

Killick, R., Fearnhead, P., and Eckley, I.A., 2012a, Optimal detection of changepoints with a linear computational cost: Journal of the American Statistical Association, v. 107, no. 500, p. 1590–1598. [Also available at https://doi.org/10.1080/01621459.2012.737745.]

Killick, R., Fearnhead, P., and Eckley, I.A., 2016, changepoint—An R package for changepoint analysis: R package version 2.2.1, accessed September 30, 2016, http://CRAN.R-project.org/package=changepoint.

Killick, R., Nam, C.F.H., Aston, J.A.D., and Eckley, I.A., 2012b, The changepoint repository: accessed February 1, 2017, at [Also available at http://changepoint.info.]

Kjeldsen, T.R., and Rosbjerg, D., 2002, Comparison of regional index flood estimation procedures based on the extreme value type I distribution: Stochastic Environmental Research and Risk Assessment, v. 16, no. 5, p. 358–373. [Also available at https://doi.org/10.1007/s00477-002-0104-6.]

Kohn, M.S., Stevens, M.R., Harden, T.M., Godaire, J.E., Klinger, R.E., and Mommandi, A., 2016, Paleoflood investigations to improve peak-streamflow regional-regression equations for natural streamflow in eastern Colorado, 2015: U.S. Geological Survey Scientific Investigations Report 2016–5099, 58 p., accessed September 30, 2016, at https://pubs.er.usgs.gov/publication/sir20165099.

Kolars, K.A., Vecchia, A.V., and Ryberg, K.R., 2016, Stochastic model for simulating Souris River Basin precipitation, evapotranspiration, and natural streamflow: U.S. Geological Survey Scientific Investigations Report 2015–5185, accessed April 20, 2016, at https://pubs.er.usgs.gov/publication/sir20155185.

Koutsoyiannis, D., 2002, The Hurst phenomenon and fractional Gaussian noise made easy: Hydrological Sciences Journal, v. 47, no. 4, p. 573–595. [Also available at https://doi.org/10.1080/02626660209492961.]

Koutsoyiannis, D., 2003, Climate change, the Hurst phenomenon, and hydrological statistics: Hydrological Sciences Journal, v. 48, no. 1, p. 3–24. [Also available at https://doi.org/10.1623/hysj.48.1.3.43481.]

Koutsoyiannis, D., 2006, Nonstationarity versus scaling in hydrology: Journal of Hydrology, v. 324, no. 1–4, p. 239–254. [Also available at https://doi.org/10.1016/j.jhydrol.2005.09.022.]

Koutsoyiannis, D., and Montanari, A., 2007, Statistical analysis of hydroclimatic time series—Uncertainty and insights: Water Resources Research, v. 43, no. 5, p. 1–9. [Also available at https://doi.org/10.1029/2006WR005592.]

Kundzewicz, Z.W., and Robson, A., 2000, Detecting trend and other changes in hydrological data: Geneva, World Meteorological Organization, World Climate Programme Data and Monitoring WCDMP–45, WMO/TD no. 1013, 158 p.

Kundzewicz, Z.W., and Robson, A.J., 2004, Change detection in hydrological records—A review of the methodology / Revue méthodologique de la détection de changements dans les chroniques hydrologiques: Hydrological Sciences Journal, v. 49, no. 1, p. 7–19. [Also available at https://doi.org/10.1623/hysj.49.1.7.53993.]

Kunsch, H.R., 1989, The jackknife and the bootstrap for general stationary observations: Annals of Statistics, v. 17, no. 3, p. 1217–1241. [Also available at https://doi.org/10.1214/aos/1176347265.]

Lang, M., Renard, B., Sauquet, E., Bois, P., Dupeyrat, A., Laurent, C., Mestre, O., Niel, H., Neppel, L., and Gailhard, J., 2006, A national study on trends and variations of French floods and droughts: Climate Variability and Change, Hydrological Impacts, v. 308.

Law, G.S., and Tasker, G.D., 2003, Flood-frequency prediction methods for unregulated streams of Tennessee, 2000: U.S. Geological Survey Water-Resources Investigations Report 2003–4176, accessed August 2, 2018, at https://pubs.er.usgs.gov/publication/wri034176.

Lins, H.F., and Cohn, T.A., 2011, Stationarity—Wanted dead or alive?: Journal of the American Water Resources Association, v. 47, no. 3, p. 475–480. [Also available at https://doi.org/10.1111/j.1752-1688.2011.00542.x.]

Lombard, F., 1987, Rank tests for changepoint problems: Biometrika, v. 74, no. 3, p. 615–624. [Also available at https://doi.org/10.1093/biomet/74.3.615.]

Malekinezhad, H., Nachtnebel, H.P., and Klik, A., 2011, Comparing the index-flood and multiple-regression methods using L-moments: Hydrological Earth Observatories and Artificial Catchments, v. 36, no. 1–4, p. 54–60. [Also available at https://doi.org/10.1016/j.pce.2010.07.013.]

Mallakpour, I., and Villarini, G., 2015, The changing nature of flooding across the central United States: Nature Climate Change, v. 5, no. 3, p. 250–254. [Also available at https://doi.org/10.1038/nclimate2516.]

Mann, H.B., and Whitney, D.R., 1947, On a test of whether one of two random variables is stochastically larger than the other: Annals of Mathematical Statistics, v. 18, no. 1, p. 50–60. [Also available at https://doi.org/10.1214/aoms/1177730491.]

Martínez-Goytre, J., House, P.K., and Baker, V.R., 1994, Spatial variability of small-basin paleoflood magnitudes for a southeastern Arizona mountain range: Water Resources Research, v. 30, no. 5, p. 1491–1501. [Also available at https://doi.org/10.1029/94WR00065.]

Mazouz, R., Assani, A.A., Quessy, J.-F., and Légaré, G., 2012, Comparison of the interannual variability of spring heavy floods characteristics of tributaries of the St. Lawrence River in Quebec (Canada): Advances in Water Resources, v. 35, p. 110–120. [Also available at https://doi.org/10.1016/j.advwatres.2011.10.006.]

McCabe, G.J., and Wolock, D.M., 2002, A step increase in streamflow in the conterminous United States: Geophysical Research Letters, v. 29, no. 24, 4 p. [Also available at https://doi.org/10.1029/2002GL015999.]

McGilchrist, C.A., and Woodyer, K.D., 1975, Note on a distribution-free CUSUM technique: Technometrics, v. 17, no. 3, p. 321–325. [Also available at https://doi.org/10.1080/00401706.1975.10489335.]

Merz, B., Aerts, J., Arnbjerg-Nielsen, K., Baldi, M., Becker, A., Bichet, A., Blöschl, G., Bouwer, L.M., Brauer, A., Cioffi, F., Delgado, J.M., Gocht, M., Guzzetti, F., Harrigan, S., Hirschboeck, K., Kilsby, C., Kron, W., Kwon, H.-H., Lall, U., Merz, R., Nissen, K., Salvatti, P., Swierczynski, T., Ulbrich, U., Viglione, A., Ward, P.J., Weiler, M., Wilhelm, B., and Nied, M., 2014, Floods and climate—Emerging perspectives for flood risk assessment and management: Natural Hazards and Earth System Sciences, v. 14, no. 7, p. 1921–1942. [Also available at https://doi.org/10.5194/nhess-14-1921-2014.]

Merz, R., and Blöschl, G., 2005, Flood frequency regionalisation—Spatial proximity vs. catchment attributes: Journal of Hydrology, v. 302, no. 1–4, p. 283–306. [Also available at https://doi.org/10.1016/j.jhydrol.2004.07.018.]

Millard, S.P., 2013, EnvStats—An R package for environmental statistics: New York, Springer, 291 p. [Also available at https://doi.org/10.1002/9780470057339.vae043.pub2.]

Milly, P.C.D., Betancourt, J., Falkenmark, M., Hirsch, R.M., Kundzewicz, Z.W., Lettenmaier, D.P., and Stouffer, R.J., 2008, Stationarity is dead—Whither water management?: Science, v. 319, no. 5863, p. 573–574. [Also available at https://doi.org/10.1126/science.1151915.]

Mood, A.M., 1954, On the asymptotic efficiency of certain nonparametric two-sample tests: Annals of Mathematical Statistics, v. 25, no. 3, p. 514–522. [Also available at https://doi.org/10.1214/aoms/1177728719.]

Morris, E.C., 1982, Mixed-population frequency analysis: U.S. Army Corps of Engineers, Institute for Water Resources, Hydrologic Engineering Center Technical Document TD–17, 43 p., accessed August 9, 2017, at www.hec.usace.army.mil/publications/TrainingDocuments/TD-17.pdf.

Nazemi, A., Wheater, H.S., Chun, K.P., Bonsal, B., and Mekonnen, M., 2017, Forms and drivers of annual streamflow variability in the headwaters of Canadian Prairies during the 20th century: Hydrological Processes, v. 31, no. 1, p. 221–239. [Also available at https://doi.org/10.1002/hyp.11036.]

Neter, J., Kutner, M.H., Nachtsheim, C.J., and Wasserman, W., 1996, Applied linear statistical models 4th ed.: New York, WCB McGraw-Hill, 1408 p.

O'Connell, D.R.H., 1999, FLDFRQ3 user's guide, release 1.1. U.S. Bureau of Reclamation, 19 p.

O'Connell, D.R.H., Ostenaa, D.A., Levish, D.R., and Klinger, R.E., 2002, Bayesian flood frequency analysis with paleohydrologic bound data: Water Resources Research, v. 38, no. 5, p. 16–1—16–13. [Also available at https://doi.org/10.1029/2000WR000028.]

O'Connor, J.E., Atwater, B.F., Cohn, T.A., Cronin, T.M., Keith, M.K., Smith, C.G., and Mason, R.R., Jr., 2014, Assessing inundation hazards to nuclear powerplant sites using geologically extended histories of riverine floods, tsunamis, and storm surges: U.S. Geological Survey Scientific Investigations Report 2014–5207, 66 p., accessed March 1, 2017, at https://doi.org/10.3133/sir20145207.

Olsen, J.R., Kiang, J.E., and Waskom, R., eds., 2010, The problem of nonstationarity in water management—Three perspectives, *in* Workshop on nonstationarity, hydrologic frequency analysis, and water management, Boulder, Colo., 2010, Proceedings: Boulder, Colo., Colorado Water Institute Information Series No. 109, 304 p.

Önöz, B., and Bayazit, M., 2012, Block bootstrap for Mann-Kendall trend test of serially dependent data: Hydrological Processes, v. 26, no. 23, p. 3552–3560. [Also available at https://doi.org/10.1002/hyp.8438.]

Oxford University Press, 2017, "Historic" or "historical"?: Oxford University web page, accessed November 3, 2017, at [Also available at https://en.oxforddictionaries.com/usage/historic-or-historical.]

Paretti, N.V., Kennedy, J.R., and Cohn, T.A., 2014, Evaluation of the expected moments algorithm and a multiple low-outlier test for flood frequency analysis at streamgaging stations in Arizona: U.S. Geological Survey Scientific Investigations Report 2014–5026, 61 p., accessed March 1, 2017, at http://pubs.er.usgs.gov/publication/sir20145026.

Parrett, C., Veilleux, A., Stedinger, J.R., Barth, N.A., Knifong, D.L., and Ferris, J.C., 2011, Regional skew for California, and flood frequency for selected sites in the Sacramento-San Joaquin River Basin, based on data through water year 2006: U.S. Geological Survey Scientific Investigations Report 2010–5260, 94 p. [Also available at https://doi.org/10.3133/sir20105260.]

Perica, S., and Stayner, M., 2004, Regional flood frequency analysis for selected basins in Utah—Part II—Weber River Basin: Utah Department of Transportation Research and Development Report UT–04.12, 34 p., accessed August 15, 2017, at http://digitallibrary.utah.gov/awweb/awarchive?type=file&item=31718.

Peterson, T.C., Heim, R.R., Jr., Hirsch, R., Kaiser, D.P., Brooks, H., Diffenbaugh, N.S., Dole, R.M., Giovannettone, J.P., Guirguis, K., Karl, T.R., Katz, R.W., Kunkel, K., Lettenmaier, D., McCabe, G.J., Paciorek, C.J., Ryberg, K.R., Schubert, S., Silva, V.B.S., Stewart, B.C., Vecchia, A.V., Villarini, G., Vose, R.S., Walsh, J., Wehner, M., Wolock, D., Wolter, K., Woodhouse, C.A., and Wuebbles, D., 2013, Monitoring and understanding changes in heat waves, cold waves, floods, and droughts in the United States—State of knowledge: Bulletin of the American Meteorological Society, v. 94, no. 6, p. 821–834. [Also available at https://doi.org/10.1175/BAMS-D-12-00066.1.]

Pettitt, A.N., 1979, A non-parametric approach to the change-point problem: Journal of the Royal Statistical Society. Series C, Applied Statistics, v. 28, no. 2, p. 126–135.

Pohlert, T., 2018, trend—Non-parametric trend tests and change-point detection: R package version 1.1.0, accessed March 23, 2018, at https://CRAN.R-project.org/package=trend.

Pope, B.F., and Tasker, G.D., 1999, Estimating the magnitude and frequency of floods in rural basins of North Carolina: U.S. Geological Survey Water-Resources Investigations Report 99–4114, accessed August 2, 2018, at https://nc.water.usgs.gov/reports/abstracts/wri994114.html.

Portela, M.M., and Dias, A.T., 2005, Application of the index-flood method to the regionalization of flood peak discharges on the Portugal mainland: River Basin Management III, v. 83, 475–485.

Prasad, R., Hibler, L.F., Coleman, A.M., and Ward, D.L., 2011, Design-basis flood estimation for site characterization at nuclear power plants in the United States of America: U.S. Nuclear Regulatory Commission NUREG/CR-7046, [variously paged], accessed October 26, 2016, at https://www.nrc.gov/docs/ML1132/ML11321A195.pdf.

Quessy, J.-F., Favre, A.-C., Saïd, M., and Champagne, M., 2011, Statistical inference in Lombard's smooth-change model: Environmetrics, v. 22, no. 7, p. 882–893. [Also available at https://doi.org/10.1002/env.1108.]

R Core Team, 2019, R—A language and environment for statistical computing: Vienna, R Foundation for Statistical Computing.

Rahman, A., Haddad, K., Kuczera, G., and Weinmann, E., 2016, Regional flood methods, *in* Book 3 of Australian Rainfall and Runoff Guidelines: Barton, Commonwealth of Australia, accessed February 22, 2017, at http://www.arr.org.au.

Rannie, W.F., 1998, A survey of hydroclimate, flooding, and runoff in the Red River Basin prior to 1870: Geological Survey of Canada Open-File Report 3705, 189 p.

Razavi, S., Elshorbagy, A., Wheater, H., and Sauchyn, D., 2015, Toward understanding nonstationarity in climate and hydrology through tree ring proxy records: Water Resources Research, v. 51, no. 3, p. 1813–1830. [Also available at https://doi.org/10.1002/2014WR015696.]

Redmond, K.T., Enzel, Y., House, P.K., and Biondi, F., 2002, Climate variability and flood frequency at decadal to millennial time scales, *in* House, P.K., and others, eds., Ancient floods, modern hazards—Principles and applications of paleoflood hydrology, v. 5: American Geophysical Union, p. 21–45. [Also available at https://doi.org/10.1029/WS005p0021.]

Riggs, H.C., 1982, Regional analyses of streamflow characteristics: U.S. Geological Survey Techniques of Water-Resources Investigations, book 4, chap. B3, 15 p.

Rocky Mountain National Park, [n.d.], Timeline of recent Ice Ages: Rocky Mountain National Park database, accessed January 24, 2017, at https://www.nps.gov/features/romo/feat0001/BasicsIceAges.html.

Roland, M.A., and Stuckey, M.H., 2007, Analysis of flood-magnitude and flood-frequency data for streamflow-gaging stations in the Delaware and North Branch Susquehanna River Basins in Pennsylvania: U.S. Geological Survey Open-File Report 2007–1235, 22 p. [Also available at https://doi.org/10.3133/ofr20071235.]

Ross, G.J., 2015, Parametric and nonparametric sequential change detection in R—The cpm package: Journal of Statistical Software, v. 66, no. 3, p. 1–20.

Ross, G.J., Tasoulis, D.K., and Adams, N.M., 2011, Nonparametric monitoring of data streams for changes in location and scale: Technometrics, v. 53, no. 4, p. 379–389. [Also available at https://doi.org/10.1198/TECH.2011.10069.]

Rougé, C., Ge, Y., and Cai, X., 2013, Detecting gradual and abrupt changes in hydrological records: Advances in Water Resources, v. 53, p. 33–44. [Also available at https://doi.org/10.1016/j.advwatres.2012.09.008.]

Rumsey, B., 2015, From flood flows to flood maps—The understanding of flood probabilities in the United States: Historical Social Research (Köln), v. 40, no. 2, p. 134–150.

Ryberg, K.R., 2008, PFReports—A program for systematic checking of annual peaks in NWISWeb: U.S. Geological Survey Open-File Report 2008–1284, 17 p., accessed November 3, 2017, at https://pubs.usgs.gov/of/2008/1284/.

Ryberg, K.R., 2015, The impact of climate variability on streamflow and water quality in the North Central United States: Fargo, North Dakota State University, Ph.D. dissertation, 277 p.

Ryberg, K.R., Goree, B.B., Williams-Sether, T., and Mason, J., R.R., 2017, The U.S. Geological Survey peak-flow file data verification project, 2008–2016: U.S. Geological Survey Scientific Investigations Report 2017–5119, 61 p., accessed November 6, 2017, at https://doi.org/10.3133/sir20175119.

Ryberg, K.R., Hodgkins, G.A., and Dudley, R.W., 2020, Change points in peak streamflows—Method comparisons and historical change points in the United States: Journal of Hydrology, v. 583, 13 p.

Ryberg, K.R., Lin, W., and Vecchia, A.V., 2014, Impact of climate variability on runoff in the north-central United States: Journal of Hydrologic Engineering, v. 19, no. 1, p. 148–158. [Also available at https://doi.org/10.1061/(ASCE)HE.1943-5584.0000775.]

Ryberg, K.R., Vecchia, A.V., Akyüz, F.A., and Lin, W., 2016, Tree-ring-based estimates of long-term seasonal precipitation in the Souris River Region of Saskatchewan, North Dakota and Manitoba: Canadian Water Resources Journal/Revue canadienne des ressources hydriques, v. 41, no. 3, p. 412–428.

Sagarika, S., Kalra, A., and Ahmad, S., 2014, Evaluating the effect of persistence on long-term trends and analyzing step changes in streamflows of the continental United States: Journal of Hydrology, v. 517, p. 36–53. [Also available at https://doi.org/10.1016/j.jhydrol.2014.05.002.]

Sando, S.K., 1998, Techniques for estimating peak-flow magnitude and frequency relations for South Dakota streams: U.S. Geological Survey Water-Resources Investigations Report 98–4055, 48 p.

Sando, S.K., Driscoll, D.G., and Parrett, C., 2008, Peak-flow frequency estimates based on data through water year 2001 for selected streamflow-gaging stations in South Dakota: U.S. Geological Survey Scientific Investigations Report 2008–5104, 367 p. [Also available at https://doi.org/10.3133/sir20085104.]

Sando, S.K., and McCarthy, P.M., 2018, Methods for peak-flow frequency analysis and reporting by the U.S. Geological Survey Wyoming-Montana Water Science Center based on data through water year 2015: U.S. Geological Survey Scientific Investigations Report 2018–5046, 39 p. [Also available at https://doi.org/10.3133/sir20185046.]

Santander Meteorology Group, 2012, fume—FUME package for R: R package version 1.0: accessed December 13, 2016, at https://CRAN.R-project.org/package=fume.

Scott, A.J., and Knott, M., 1974, A cluster analysis method for grouping means in the analysis of variance: Biometrics, v. 30, no. 3, p. 507–512. [Also available at https://doi.org/10.2307/2529204.]

Sen, P.K., 1968, Estimates of the regression coefficient based on Kendall's Tau: Journal of the American Statistical Association, v. 63, no. 324, p. 1379–1389. [Also available at https://doi.org/10.1080/01621459.1968.10480934.]

Sen, A., and Srivastava, M.S., 1975, On tests for detecting change in mean: Annals of Statistics, v. 3, no. 1, p. 98–108. [Also available at https://doi.org/10.1214/aos/1176343001.]

Sharma, S., Swayne, D.A., and Obimbo, C., 2016, Trend analysis and change point techniques—A survey: Energy, Ecology & Environment, v. 1, no. 3, p. 123–130. [Also available at https://doi.org/10.1007/s40974-016-0011-1.]

Smith, A., Sampson, C., and Bates, P., 2015, Regional flood frequency analysis at the global scale: Water Resources Research, v. 51, no. 1, p. 539–553. [Also available at https://doi.org/10.1002/2014WR015814.]

St. George, S., 2010, Dendrohydrology and extreme floods along the Red River, Canada, *in* Stoffel, M., and others, eds., Tree-ring reconstructions in natural hazards research—A state-of-the-art: Springer, p. 277–279.

St. George, S., and Nielsen, E., 2002, Hydroclimatic change in southern Manitoba since AD 1409 inferred from tree rings: Quaternary Research, v. 58, no. 2, p. 103–111. [Also available at https://doi.org/10.1006/qres.2002.2343.]

St. George, S., and Nielsen, E., 2003, Palaeoflood records for the Red River, Manitoba, Canada, derived from anatomical tree-ring signatures: The Holocene, v. 13, no. 4, p. 547–555. [Also available at https://doi.org/10.1191/0959683603hl645rp.]

Stedinger, J.R., and Griffis, V.W., 2008, Flood frequency analysis in the United States—Time to update: Journal of Hydrologic Engineering, v. 13, no. 4, p. 199–204. [Also available at https://doi.org/10.1061/(ASCE)1084-0699(2008)13:4(199).]

Stoa, R.B., 2015, Droughts, floods, and wildfires—Paleo perspectives on disaster law in the Anthropocene: Georgetown International Environmental Law Review, v. 27, no. 3, p. 393–446.

Swain, R.E., England, J.F., Bullard, K.L., and Raff, D.A., 2004, Hydrologic hazard curve estimating procedures: U.S. Department of Interior, Bureau of Reclamation Research Report DSO-04–08, 80 p., accessed January 30, 2017, at https://www.usbr.gov/ssle/damsafety/TechDev/DSOTechDev/DSO-04-08.pdf.

Tan, X., and Gan, T.Y., 2014, Nonstationary analysis of annual maximum streamflow of Canada: Journal of Climate, v. 28, no. 5, p. 1788–1805. [Also available at https://doi.org/10.1175/JCLI-D-14-00538.1.]

Tao, H., Gemmer, M., Bai, Y., Su, B., and Mao, W., 2011, Trends of streamflow in the Tarim River Basin during the past 50 years—Human impact or climate change?: Journal of Hydrology, v. 400, no. 1–2, p. 1–9. [Also available at https://doi.org/10.1016/j.jhydrol.2011.01.016.]

Tasker, G.D., Hodge, S.A., and Barks, C.S., 1996, Region of influence regression for estimating the 50-year flood at ungaged sites: Journal of the American Water Resources Association, v. 32, no. 1, p. 163–170. [Also available at https://doi.org/10.1111/j.1752-1688.1996.tb03444.x.]

Theil, H., 1992, A rank-invariant method of linear and polynomial regression analysis, *in* Raj, B., and Koerts, J., eds., Henri Theil's contributions to economics and econometrics: Dordrecht, Netherlands, Springer, p. 345–381. [Also available at https://doi.org/10.1007/978-94-011-2546-8_20.]

Thomas, B.E., Hjalmarson, H.W., and Waltemeyer, S.D., 1997, Methods for estimating magnitude and frequency of floods in the southwestern United States: U.S. Geological Survey Water Supply Paper 2433, 195 p., accessed October 9, 2019, at http://pubs.er.usgs.gov/publication/wsp2433.

Tregoning, R., Abramson, L., and Scott, P., 2008, Estimating loss-of-coolant accident (LOCA) frequencies through the elicitation process—Main report: U.S. Nuclear Regulatory Commission NUREG-1829, v. 1, 231 p., accessed October 10, 2019, at https://www.nrc.gov/docs/ML0806/ML080630013.pdf.

Tyralis, H., 2016, HKprocess—Hurst-Kolmogorov process: R package version 0.0-2: accessed December 14, 2016, at https://CRAN.R-project.org/package=HKprocess.

U.S. Army Corps of Engineers, 2013, ICI-RAFT—Regional analysis of frequency tool—Version 1.1: U.S. Army Corps of Engineers, accessed March 1, 2017, at https://www.iwr.usace.army.mil/Portals/70/docs/software/ICIRAFT/Quick%20ICI-RAFT%20Guide.pdf.

U.S. Army Corps of Engineers, 2016, Nonstationarity detection tool—Version 1.1: U.S. Army Corps of Engineers database, accessed February 1, 2017, at http://corpsmapu.usace.army.mil/cm_apex/f?p=257:10:0:NO.

U.S. Environmental Protection Agency, 2013, Primary distinguishing characteristics of level III ecoregions of the continental United States: U.S. Environmental Protection Agency online document, accessed October 3, 2019, at ftp://newftp.epa.gov/EPADataCommons/ORD/Ecoregions/us/Eco_Level_III_descriptions.doc.

U.S. Geological Survey, 2014, First USGS streamgage records 125 years of measuring New Mexico's vital water resources: U.S. Geological Survey web page, accessed October 3, 2019, at https://www.usgs.gov/news/first-usgs-streamgage-records-125-years-measuring-new-mexico%E2%80%99s-vital-water-resources.

U.S. Geological Survey, 2017, USGS water data for the Nation: U.S. Geological Survey National Water Information System database, accessed January 20, 2017, at https://doi.org/10.5066/F7P55KJN.

U.S. Geological Survey, 2019, Introduction to the slope-conveyance methods [Megan Poff, videographer]: U.S. Geological survey video, 00:05:28., accessed October 4, 2019, at https://www.usgs.gov/media/videos/introduction-slope-conveyance-method#targetText=A%20slope%2Dconveyance%20is%20one%20of%20the%20simpler%20methods%20of,to%20a%20single%20cross%20section.&targetText=Hydraulic%20radius%20(R)%20is%20just%20the%20area%20of%20the%20channel,divided%20by%20the%20wetted%20perimeter. [Posted June 12, 2019.]

U.S. Task Force on Federal Control Policy, 1966, A unified national program for managing flood losses: U.S. Government Printing Office No. 465, 47 p., accessed August 9, 2017, at https://www.loc.gov/law/find/hearings/floods/floods89-465.pdf.

U.S. Water Resources Council, 1976, Guidelines for determining flood flow frequency: U.S. Water Resources Council, Hydrology Committee, Bulletin #17 [variously paged].

U.S. Water Resources Council, 1977, Guidelines for determining flood flow frequency: U.S. Water Resources Council, Hydrology Committee, Bulletin #17A [variously paged].

Vecchia, A.V., 2008, Climate simulation and flood risk analysis for 2008–40 for Devils Lake, North Dakota: U.S. Geological Survey 2008–5011, 28 p., accessed August 8, 2017, at https://pubs.er.usgs.gov/publication/sir20085011.

Veilleux, A.G., Cohn, T.A., Flynn, K.M., Mason, R.R., and Hummel, P.R., 2014, Estimating magnitude and frequency of floods using the PeakFQ 7.0 program: U.S. Geological Survey Fact Sheet 2013–3108, 2 p., accessed September 30, 2016, at https://doi.org/10.3133/fs20133108.

Veilleux, A.G., Stedinger, J.R., and Lamontagne, J.R., 2011, Bayesian WLS/GLS regression for regional skewness analysis for regions with large cross-correlations among flood flows, *in* World Environmental and Water Resources Congress 201—Bearing knowledge for sustainability, Palm Springs, Calif., 2011, Proceedings: Palm Springs, Calif., American Society of Civil Engineers, 11 p.

Viglione, A., Hosking, J.R.M., Laio, F., Miller, A., Gaume, E., Payrastre, O., Salinas, J.L., N'guyen, C.C., and Halbert, K., 2014, nsRFA—Non-supervised regional frequency analysis: R package version 0.7-12, accessed December 19, 2016, at https://CRAN.R-project.org/package=nsRFA.

Viglione, A., Merz, B., Viet Dung, N., Parajka, J., Nester, T., and Blöschl, G., 2016, Attribution of regional flood changes based on scaling fingerprints: Water Resources Research, v. 52, no. 7, p. 5322–5340. [Also available at https://doi.org/10.1002/2016WR019036.]

Villarini, G., Serinaldi, F., Smith, J.A., and Krajewski, W.F., 2009, On the stationarity of annual flood peaks in the continental United States during the 20th century: Water Resources Research, v. 45, no. 8, 17 p. [Also available at https://doi.org/10.1029/2008WR007645.]

Villarini, G., and Smith, J.A., 2010, Flood peak distributions for the eastern United States: Water Resources Research, v. 46, no. 6, 17 p. [Also available at https://doi.org/10.1029/2009WR008395.]

Vogel, R.M., and Stedinger, J.R., 1985, Minimum variance streamflow record augmentation procedures: Water Resources Research, v. 21, no. 5, p. 715–723. [Also available at https://doi.org/10.1029/WR021i005p00715.]

Vogel, R.M., Tsai, Y., and Limbrunner, J.F., 1998, The regional persistence and variability of annual streamflow in the United States: Water Resources Research, v. 34, no. 12, p. 3445–3459. [Also available at https://doi.org/10.1029/98WR02523.]

Vogel, R.M., Yaindl, C., and Walter, M., 2011, Nonstationarity—Flood magnification and recurrence reduction factors in the United States: Journal of the American Water Resources Association, v. 47, no. 3, p. 464–474. [Also available at https://doi.org/10.1111/j.1752-1688.2011.00541.x.]

Wang, L., and Leigh, D.S., 2012, Late-Holocene paleofloods in the Upper Little Tennessee River valley, southern Blue Ridge Mountains, USA: The Holocene, v. 22, no. 9, p. 1061–1066. [Also available at https://doi.org/10.1177/0959683612437863.]

Wang, X.L., and Swail, V.R., 2001, Changes in extreme wave heights in northern hemisphere oceans and related atmospheric circulation regimes: Journal of Climate, v. 14, no. 10, p. 2204–2221. [Also available at https://doi.org/10.1175/1520-0442(2001)014<2204:COEWHI>2.0.CO;2.]

Wang, X., Erdman, C., and Emerson, J.W., 2015, bcp—Bayesian analysis of change point problems: R package version 4.0.0 web page, accessed March 23, 2018, at https://cran.r-project.org/package=bcp.

Water Resources Council, 1967, A uniform technique for determining flood flow frequencies: U.S. Water Resources Council Hydrology Committee Bulletin No. 15, accessed January 23, 2017, at https://water.usgs.gov/osw/bulletin17b/Bulletin_15_1967.pdf.

Webb, R.H., O'Connor, J.E., and Baker, V.R., 1988, Paleohydrologic reconstruction of flood frequency on the Escalante River, south-central Utah, *in* Baker, V.R., Kochel, R.C., and Patton, P.C., eds., Flood geomorphology: New York, Wiley-Interscience, p. 528.

Webb, R.H., and Rathburn, S.L., 1988, Paleoflood hydrologic research in the southwestern United States: Transportation Research Record: Journal of the Transportation Research Board, no. 1201, p. 9–21.

Williams-Sether, T., 2015, Regional regression equations to estimate peak-flow frequency at sites in North Dakota using data through 2009: U.S. Geological Survey Scientific Investigations Report 2015–5096, 12 p., accessed September 3, 2017, at https://doi.org/10.3133/sir20155096.

Wirth, S.B., Glur, L., Gilli, A., and Anselmetti, F.S., 2013, Holocene flood frequency across the Central Alps—Solar forcing and evidence for variations in North Atlantic atmospheric circulation: Quaternary Science Reviews, v. 80, p. 112–128. [Also available at https://doi.org/10.1016/j.quascirev.2013.09.002.]

Working Group 4 Flood Frequency Estimation Methods and Environmental Change, 2013, A review of applied methods in Europe for flood-frequency analysis in a changing environment: Centre for Ecology & Hydrology, 170 p., accessed February 6, 2017, at http://www.wmo.int/pages/prog/hwrp/publications/Floodfreq_report.pdf.

Yang, L., Smith, J.A., Wright, D.B., Baeck, M.L., Villarini, G., Tian, F., and Hu, H., 2013, Urbanization and climate change—An examination of nonstationarities in urban flooding: Journal of Hydrometeorology, v. 14, no. 6, p. 1791–1809. [Also available at https://doi.org/10.1175/JHM-D-12-095.1.]

Yue, S., Pilon, P., Phinney, B., and Cavadias, G., 2002, The influence of autocorrelation on the ability to detect trend in hydrological series: Hydrological Processes, v. 16, no. 9, p. 1807–1829. [Also available at https://doi.org/10.1002/hyp.1095.]

Yue, S., and Wang, C., 2004, The Mann-Kendall test modified by effective sample size to detect trend in serially correlated hydrological series: Water Resources Management, v. 18, no. 3, p. 201–218. [Also available at https://doi.org/10.1023/B:WARM.0000043140.61082.60.]

Zarriello, P.J., Ahearn, E.A., and Levin, S.B., 2012, Magnitude of flood flows for selected annual exceedance probabilities in Rhode Island through 2010 (ver. 1.2, revised March 27, 2013): U.S. Geological Survey Scientific Investigations Report 2012–5109, 81 p., accessed July 1, 2016, at http://pubs.er.usgs.gov/publication/sir20125109.

Zeileis, A., Leisch, F., Hornik, K., and Kleiber, C., 2002, strucchange—An R package for testing for structural change in linear regression models: Journal of Statistical Software, v. 7, no. 2, p. 1–38. [Also available at https://doi.org/10.18637/jss.v007.i02.]

Zhang, N.R., and Siegmund, D.O., 2007, A modified Bayes Information Criterion with applications to the analysis of comparative genomic hybridization data: Biometrics, v. 63, no. 1, p. 22–32. [Also available at https://doi.org/10.1111/j.1541-0420.2006.00662.x.]

Zrinji, Z., and Burn, D.H., 1994, Flood frequency analysis for ungauged sites using a region of influence approach: Journal of Hydrology, v. 153, no. 1–4, p. 1–21. [Also available at https://doi.org/10.1016/0022-1694(94)90184-8.]

Zrinji, Z., and Burn, D.H., 1996, Regional flood frequency with hierarchical region of influence: Journal of Water Resources Planning and Management, v. 122, no. 4, p. 245–252. [Also available at https://doi.org/10.1061/(ASCE)0733-9496(1996)122:4(245).]

Appendix 1. Data, Settings, and Output for Each Site and Scenario

The following files are provided for documentation and reproducibility. Each zipped file represents the analysis for a particular site and scenario (except for those scenarios that were results from other studies) and contains three types of files, *.txt, *.psf, and *.PRT. The file called RedRiverScenario1.zip, therefore, contains the *.txt, *.psf, and *.PRT files (described below) for the analysis of streamgage station 05OJ015, Red River of the North at James Avenue Pumping Station, Winnipeg, Manitoba, Canada (Mark Lee, written commun., 2014 and 2016), under scenario 1, as described in this report.

For flood-frequency analysis in PeakFQ, peak-flow data must be supplied in a standard WATSTORE text formatted file (Flynn and others, 2006). The WATSTORE format is thoroughly defined in appendixes B.2, B.3, and B.4 of Flynn and others (2006) and is presented here as text files, *.txt.

The PeakFQ user specifies processing options interactively or by supplying a program specification file, *.psf (Veilleux and others, 2014). The specification file is defined in appendix B.1 of Flynn and others (2006). The specification file includes settings related to perception thresholds, historical peaks not in the USGS peak-flow file (PFF) database that is available as part of the U.S. Geological Survey (USGS) National Water Information System at https://nwis.waterdata.usgs.gov/usa/nwis/peak (U.S. Geological Survey, 2017), and perception thresholds.

Results of the flood-frequency analyses are provided in PRT files, *.PRT. The PRT files include processing options, a summary of the input data, including perceptible ranges and flow intervals; diagnostic message and potentially influential low flood (PILF) results; annual frequency curve parameters (mean, standard deviation and skew); numerical values for streamflows at selected exceedance probabilities; a listing of the input data; and Expected Moments Algorithm (EMA) presentation of the data; and other details. Additional resources for PeakFQ are available on the USGS PeakFQ website, https://water.usgs.gov/software/PeakFQ/ (U.S. Geological Survey, 2018).

Each of the following files is a link to the online files associated with this report.

RedRiverScenario1.zip
RedRiverScenario2.zip
RedRiverScenario3.zip
RedRiverScenario4.zip
RedRiverScenario5.zip
RedRiverScenario6.zip
RedRiverScenario7.zip
RedRiverScenario8.zip
RedRiverScenario9.zip
RedRiverScenario10.zip
RapidCreekScenario1.zip
RapidCreekScenario2.zip
RapidCreekScenario3.zip
SpringCreekScenario1.zip
SpringCreekScenario2.zip
SpringCreekScenario3.zip
CherryCreekScenario1.zip
CherryCreekScenario2.zip
EscalanteRiverScenario1.zip
EscalanteRiverScenario2.zip
EscalanteRiverScenario3.zip

References Cited

Flynn, K.M., Kirby, W.H., and Hummel, P.R., 2006, User's manual for program PeakFQ—Annual flood-frequency analysis using Bulletin 17B guidelines: U.S. Geological Survey Techniques and Methods, book 4, chapter B4, 42 p., accessed January 23, 2017, at https://pubs.usgs.gov/tm/2006/tm4b4/.

U.S. Geological Survey, 2017, USGS water data for the Nation: U.S. Geological Survey National Water Information System database, accessed January 20, 2017, at https://doi.org/10.5066/F7P55KJN.

U.S. Geological Survey, 2018, PeakFQ—Flood frequency analysis based on Bulletin 17C and recommendations of the Advisory Committee on Water Information (ACWI) Subcommittee on Hydrology (SOH) Hydrologic Frequency Analysis Work Group (HFAWG): U.S. Geological Survey Water Resources of the United States web page, accessed October 10, 2019, at https://water.usgs.gov/software/PeakFQ/.

Veilleux, A.G.; Cohn, T.A.; Flynn, K.M.; Mason, R.R., Jr.; and Hummel, P.R., 2014, Estimating magnitude and frequency of floods using the PeakFQ 7.0 program: U.S. Geological Survey 2013–3108, 2 p., accessed September 30, 2016, at https://doi.org/10.3133/fs20133108.

For more information about this publication, contact:

Director, USGS Dakota Water Science Center
821 East Interstate Avenue, Bismarck, ND 58503
1608 Mountain View Road, Rapid City, SD 57702
605–394–3200

For additional information, visit:
https://www.usgs.gov/centers/dakota-water

Publishing support provided by the
Rolla and Madison Publishing Service Centers

ISSN 2328-0328 (online)
https://doi.org/10.3133/sir20205065